Multicolour interphase cytogenetics in human sperm and embryos: Chromosome copy number and the relevance of nuclear address

A thesis submitted to the University of Kent for the degree of

DOCTOR OF PHILOSOPHY

in the Faculty of

Science, Technology and Medical Studies

2010

Dimitrios Ioannou

Department of Biosciences

Declaration

No part of this thesis has been submitted in support of an application for any degree or qualification of the University of Kent or any other University or Institute of learning.

Dimitrios Ioannou

10 December 2010

Incorporation of published work

This thesis incorporates published work from three papers (see appendix). The text that I contributed to these papers remains intact in the thesis. Where other authors have contributed material, this has been rewritten. I am the author of all other material in the thesis.

Quantum dots as new generation fluorochromes for FISH: an appraisal (Ioannou *et al.* 2009).

Much of the information within this manuscript is contained in Chapter 3. All figures and text on attemps to incorporate QDs in FISH applications are my work. The text on the use of QDs, introduction and conclusions involved other authors, and this material was revised accordingly.

Nanotechnology and molecular cytogenetics: the future has not yet arrived (Ioannou & Griffin 2010b).

This review summarises data from current QD-FISH literature and discusses it in light of my own findings. All figures and text on our experience with QDs are my work. Revised text has been used in the introduction and discussion of this thesis.

Male fertility, sperm aneuploidy, and nuclear organisation (Ioannou & Griffin 2010a).

Much of the information within this review is contained within the introduction of this thesis.

For a full list of publications *et cetera* arising from this thesis refer to Appendix (10).

Acknowledgements

First of all I would like to thank my supervisor and friend Prof. Darren Griffin, for trusting me with a position in his laboratory and for all his continuous help, guidance, support, ideas and critical evaluation of this thesis. Most importantly I thank him for all the opportunities the life-lessons and experiences that I have acquired in these last four years.

Mr Michael Ellis (Digital Scientific) for sponsoring me and for all his help and technical support regarding the fluorescent microscope, where I spent a significant amount of time.

The scientific team at the Bridge Centre in London: Prof. Alan Handyside, Dr Alan Thornhill, and Dr Mira Grigorova, for help with samples, and providing me the opportunity to work in a clinical environment and see direct applications of my research work.

Equally I would like to thank Eric Meershoek and the Kreatech team for assistance with probes used in this thesis, and for allowing me to be part in the developing process of a product.

Ms Dimitra Christopikou, for organising and providing the OAT samples that were used in Chapter 5.

To all the members of the FISH lab; past (in particular Helen for help and support especially in the early days, Ben for his great mind, Martin for stimulating discussions) and present (Katie, Emma, Steve & Bill) for great atmosphere and their friendship.

To my "comrade" Alem with whom I started this journey together. It was great to share all the experiences and enjoy our work through our different perspectives.

To Gothami for all her help in the lab/clinic and for sharing endless capturing time in the microscope.

Acknowledgements would not be complete without thanking:

My family (Michael – Vassiliki – Sophia) for their love incredible support at all levels and sacrifises they have made.This is for you as well!

And my better half, Tatiana for her love, encouragement and support during this adventure but mostly for being perfect for me!

"Hoi sympinontes phronousin homothymadon"
"Οι *συμπίνοντες φρονούσιν ομοθυμαδών*"

Στη μνήμη της γιαγιάς "Αλαγονίας"

Table of Contents

List of Figures

List of Tables

Abbreviations

°C	Celcius
a-CGH	array-Comparative Genome Hybridisation
AMA	Advance Maternal Age
AR	Androgen Receptor
AZF	Azoospermia Factor
BAC	Bacterial Artificial Chromosome
bp or kbp or Mbp	base pair or kilo base pairs or Mega base pairs
BSA	Bovine Serum Albumin
CCD	Charge Coupled Device
CdS	Cadmium Sulphide
CdSe	Cadmium Selenide
CdTe	Cadmium Telluride
CFTR	Cystic Fibrosis Transmembrane conductance Regulator
CNV	Copy Number Variation
CT	Chromosome Territories
CT-IC	Chromosome Territory-Interchromatin Compartment
CVS	Chorionic Villus Sampling
DAPI	4',6-diamidino-2-phenylindole
DAZ	Deleted in Azoospermia
ddH_2O	Double distilled H_2O
df	Degrees of Freedom
DOP- PCR	Degenerate Oligo Primed-Polymerase Chain Reaction
DS	Dextran Sulphate
DSBs	Double Strand Breaks
DTT	Dithiothreitol
EBV	Epstein Barr Virus
EDTA	EthyleneDiamineTetraacetic Acid
erbB/HER	epidermal growth factor receptor family/Human epidermal growth factor receptor
ESHRE	European Society of Human Reproduction
FA	Formamide
FISH	Fluorescent *in situ* hybridisation
FITC	Fluorescein isothiocyanate
g	gram
HCl	Hydrochloric Acid
HFEA	Human Fertilisation and Embryology Authority
HLA	Human Leukocyte Antigen
hrs	hours
Hsa	Homo sapiens
ICD	Inter Chromosomal Domain
ICM	Inner Cell Mass
ICN	Inter Chromatin Network
ICSI	Intracytoplasmic sperm injection
InP	Indium Phosphate
INSL3	Insulin like factor 3
ISH	*In situ* hybridisation
IVF	*In vitro* fertilisation
KS	Klinefelter Syndrome

L or l	Litre or litre
LGR8	Leucine-rich repeat containing G-protein couple Receptor 8
LMNA	Lamin A/C
MI or MII	Meiosis I or Meiosis II
ml	millilitre
mM	milliMolar
N	Normality
NDRDP	Not discernable from random distribution pattern
ng	nanogram
nm	nanometre
NOR	Nucleolus Organiser Region
OAT	OligoAsthenoTeratozoospermia
PBS	Phosphate Buffer Saline
PbSe	Lead Selenide
PCR	Polymerase Chain Reaction
PGD	Preimplantation Genetic Diagnosis
PGS	Preimplantation Genetic Screening
PML	Promyelotic Leukaemia
PR	Perichromatic Region
QD-FISH	Quantum Dot-Fluorescent *in situ* hybridisation
QDs	Quantum Dots
RCT	Randomised Control Trial
RIF	Repeated Implantation Failure
RM	Repeated Miscarriage
ROS	Reactive Oxygen Species
rpm	rotations per minute
RT	Room Temperature
SAv-QDs	Streptavidin-Quantum Dots
SC	Synaptonemal Complex
Smc1β	Structural maintenance of chromosomes 1β
SMF	Severe Male Factor
SN or NSN	Surrounded Nucleus or Not Surrounded Nucleus
SNP	Single Nucleotide Polymorphism
SRY	Sex determining Region Y
SSC	Saline Sodium Citrate
TBE	Tris Borate EDTA
TE	Trophectoderm
TOPO	Trioctylphosphine oxide
u/μl	Units/microlitre
UV	UltraViolet
WHO	World Health Organisation
X-EDMD	X-linked Emery-Dreifuss muscular dystrophy
ZnS	Zinc Sulphide
μg	microgram
μl	microlitre
μM	microMolar

Abstract

Interphase cytogenetics by fluorescent *in situ* hybridisation (FISH) involves the study of chromosome copy number and nuclear organisation in non-dividing nuclei. It has found particular utility in studies of sperm and IVF embryos but would benefit further from multi-target strategies to detect numerous loci in the same nucleus. The purpose of this thesis was to develop such strategies then apply them to study the relationship between aneuploidy, nuclear organisation, male infertility and human preimplantation embryogenesis. Specifically:

- To ask whether novel inorganic nanomaterials Quantum Dots (QDs) could be used for FISH in the place of organic fluorochromes. Results suggest that, in their current form, QDs are sub-optimal for FISH despite some successful experiments.
- To develop alternative approaches using fast hybridising oligonucleotide probes labelled with organic fluorochromes to assess chromosome copy number and nuclear organisation for each human chromosome on the same nucleus. A 24 chromosome FISH method was successfully developed in a four layer sequential experiment and applied to sperm and embryos.
- To use the above approach to test the hypothesis that severely infertile oligoasthenoteratozoospermic (OAT) males display altered nuclear organisation (manifested as different nuclear address of specific loci) compared to their normal counterparts. Results suggested the presence of a "chromocentre" in both fertile and infertile men, with slight alterations of this strict organisation in some OAT males.
- To use the above approach to assess the level of aneuploidy in "spare" human preimplantation embryos following PGS. Results suggested very high levels of abnormality mostly associated with mosaicism, further calling into question the efficacy of FISH for PGS.
- To test the hypothesis that altered nuclear organisation in human preimplantation embryos is related to increased aneuploidy. Differences between two groups, one with multiple abnormalities, the other with relatively few were apparent providing data on nuclear organisation in individual blastomeres and whole embryos.

Insight into the relationship between chromosome abnormalities and nuclear organisation in sperm and embryos is provided. Applications of the methodology involve sperm aneuploidy screening, "follow-up" of embryos, but probably not PGS.

1. Introduction

1.1. Interphase cytogenetics and the FISH technique

1.1.1. Development of FISH and application of interphase cytogenetics

A tentative but nonetheless accurate statement by Tjio and Levan in 1956 about the number of chromosomes in human cells launched in essence the field of human cytogenetics. The impact of determining the correct number of chromosomes found almost immediate application with the realisation that some human disorders result from changes in chromosome number or appearance (reviewed in Trask, (2002)).

The power of cytogenetics was redoubled in the late 1960s by two simultaneous technological advances: First, staining protocols allowing the visualisation of chromosome specific bands termed "the barcodes of chromosome identification" (Caspersson *et al.* 1968; Sumner *et al.* 1971) and second, Pardue and Gall being the first to show that a form of repetitive DNA (satellite) could hybridise to denatured chromosomes *in situ* on glass slides using radioactive labelled DNA probes that were detected by autoradiography (Pardue & Gall 1969). These early ISH (*in situ* hybridisation) attempts suffered from drawbacks (unstable nature of isotopes, low resolution, long exposure time, and hazards from use of radioactive materials) but inspired the development of new techniques (Langer *et al.* 1981). That is isotope DNA/RNA probes gave way to safer, simpler to use, fluorescent labels and the birth of FISH (fluorescent *in situ* hybridisation).

FISH provided a direct link between the microscope and DNA sequence that revolutionised cytogenetics by introducing "molecular cytogenetics". It involves the labelling of a DNA probe with a hapten (e.g. biotin or digoxigenin) that is hybridised *in situ* to chromosome spreads or interphase nuclei. Hybridisations are subsequently detected by an organic fluorescent molecule that has high affinity for the hapten (avidin for biotin, first reported by Pinkel *et al.* (1986) and anti-digoxigenin for digoxigenin as reviewed by Ekong and Wolfe (1998)). Alternatively, the DNA probe can be pre-labelled with a fluorophore enabling hybridisation and detection in a single step (direct approach). Figure 1.1 illustrates the principles and an example of FISH.

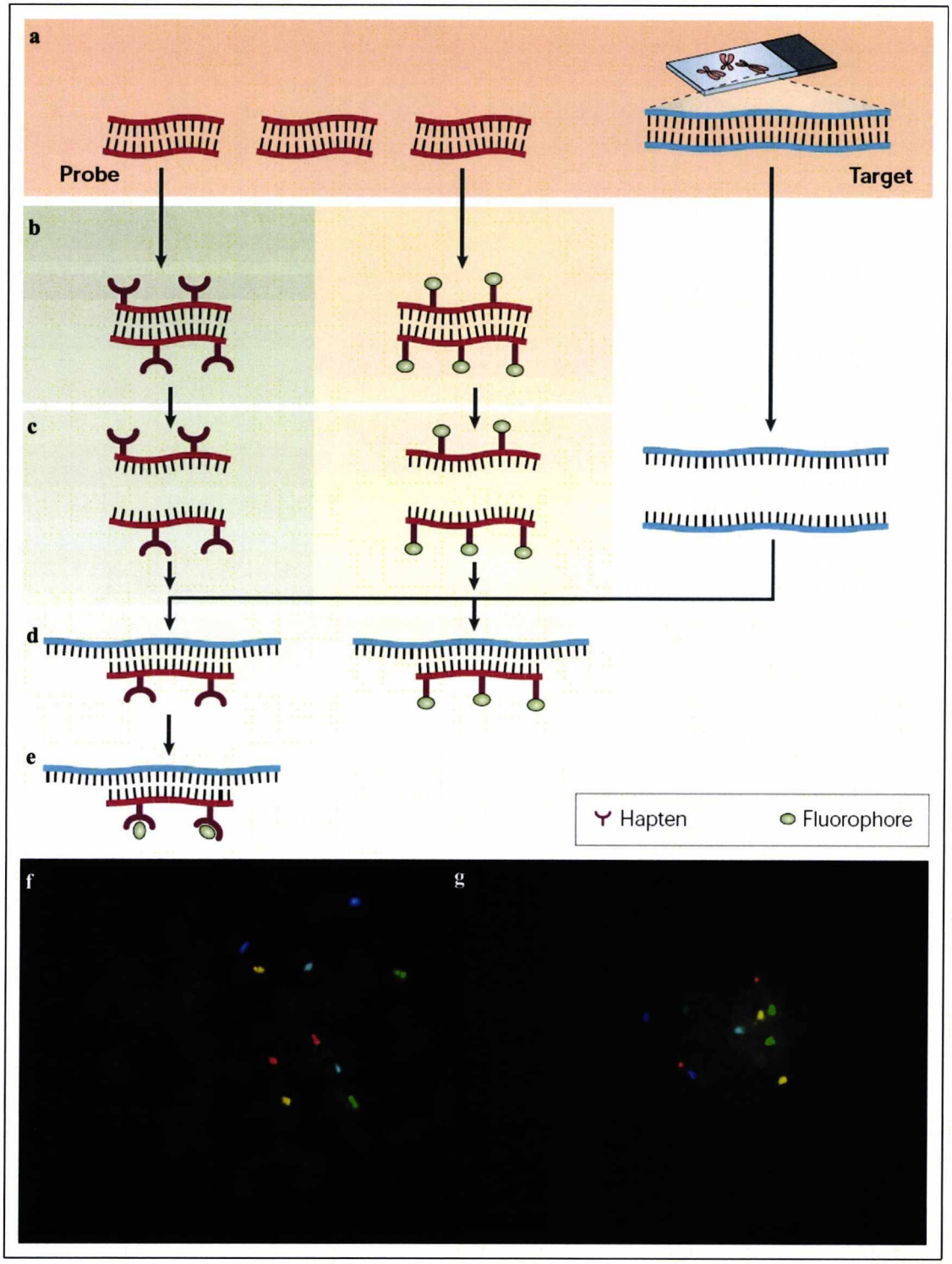

Figure 1.1: The principle of FISH. A probe (a) is a cloned part of the genome recognising a whole or a specific region of a chromosome. Probes are labelled by various means (i.e. nick translation, PCR). Two labelling strategies (b) are commonly used, the indirect (left panel of figure) and the direct (right part of figure). Indirect labelled probes are labelled with a modified nucleotide that contains a hapten (e.g. biotin), whereas in direct labelling the probe is labelled with a fluorophore. The labelled probe and target DNA are denatured (c) and allowed to reanneal for the probe to seek out its complement in the chromosomal DNA (d). An additional step is required in indirect labelling (e) to visualise the non-fluorescent hapten (i.e. antibodies or binding affinity molecules for the hapten with a fluorophore, avidin-Cy3.). (f) Multicolour FISH on metaphase

chromosomes (g) INTERPHASE CYTOGENETICS by FISH, note the copy number of each chromosome is discernable.
Image adapted from http://www.nature.com/scitable/nated/content/35120/10.1038_nrg1692-f1_mid_1.jpg whereas the FISH image has been generated by myself.

Chromosome analyses by FISH have led to marked progress in cytogenetic research, through advancements associated with probes (labelling with distinctive fluorophores, or ratios of different fluorophores for multiplexing) and optics in fluorescence microscopy to resolve multicolour labelling.

FISH opened up the concept of interphase cytogenetics, allowing karyotype analysis to occur in nuclei even of non dividing cells. Conventional cytogenetics requires cells to be arrested in metaphase which is not always feasible (e.g. blastomeres from preimplantation embryos, sperm cells or cells from solid tumours). However with centromeric, or locus specific probes, chromosome enumeration can occur at the interphase level allowing diagnosis of copy number abnormalities (Pinkel *et al.* 1986), revealing structural rearrangements (e.g. translocations and inversions) (Dauwerse *et al.* 1999) or even resolving abnormalities that can only be resolved at the interphase level where DNA is packaged 10,000 fold more loose (e.g. a 1Mb duplication that causes Charcot-Marie tooth syndrome) (Trask 2002). Furthermore interphase FISH allowed the determination of the relative times at which specific DNA sequences are replicated during the S phase of the cell cycle (Trask 2002). The focus of this thesis is in the interphase cytogenetics of human sperm and embryo.

FISH both interphase and metaphase is an extremely powerful diagnostic and research tool with a wide spectrum of applications including: gene mapping (Lichter *et al.* 1993), comparative genomics (Arnold *et al.* 1995) nuclear architecture (Cremer *et al.* 1986) preimplantation (Griffin *et al.* 1991) and prenatal diagnosis (Julien *et al.* 1986) amongst others. However FISH like all techniques has inherent limitations imposed from the use of organic fluorochromes. Prospects with regards the potential use of inorganic fluorochromes (Quantum Dots-QDs) for FISH applications are explored in the following section.

1.1.2. Prospects for inorganic nanocrystals (e.g. Quantum Dots) for FISH

Nanotechnology has hitherto been closely affiliated with engineering since nanomaterials became the major components of computer chips (Chan 2006). Within

the last ten years or so there has been a growing relationship between nanoscience and fluorescent biological imaging (Parak *et al.* 2003). Applications of fluorescent imaging have generated a tremendous drive to develop new probes for tagging molecules, enabling changes in their localisation, concentration and activities to be documented (Jaiswal & Simon 2004). However traditionally used organic fluorochromes face limitations affecting imaging and multicolour detection. A novel class of semiconductor nanocrystals termed Quantum Dots (QDs) (Miller *et al.* 1986; Reed *et al.* 1986) are inorganic fluorophores that provide a promising alternative to their organic counterparts.

QDs are composed of a semi-conductor core such as Cadmium Selenide (CdSe), Indium Phosphate (InP) or Lead Selenide (PbSe) (Lipovskii *et al.* 1997; Invitrogen 2006). This core is coated with a second semiconductor shell (usually zinc sulphide, ZnS) for the purposes of improving the optical properties of the nanocrystal (Michalet *et al.* 2005; Invitrogen 2006). To improve further the utility of QDs an extra polymer coating is attached that serves as a site for conjugation with biomolecule moieties. This brings the total size of the nanocrystal to 10-20nm (a few hundred to few thousand atoms). Figure 1.2 provides a schematic representation of a QD-conjugate.

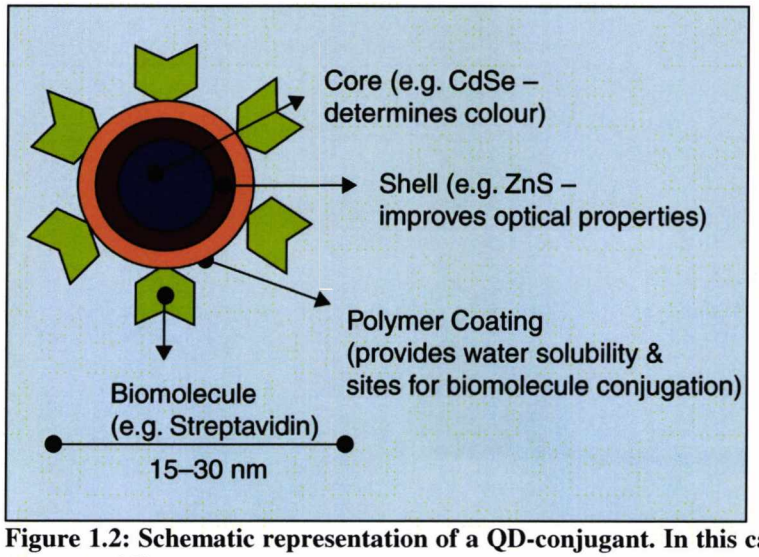

Figure 1.2: Schematic representation of a QD-conjugant. In this case the biomolecule attached is a streptavidin.

The core material is chosen with respect to the required emission wavelength range (e.g. CdS for Ultraviolet-blue, CdSe for the visible spectrum and CdTe for the far red and near infrared) (QuantumDotCorporation 2006). In other words, the QD

fluorescent colour relates to its size, which is controlled during synthesis (Chan *et al.* 2002). Figure 1.3 illustrates this association.

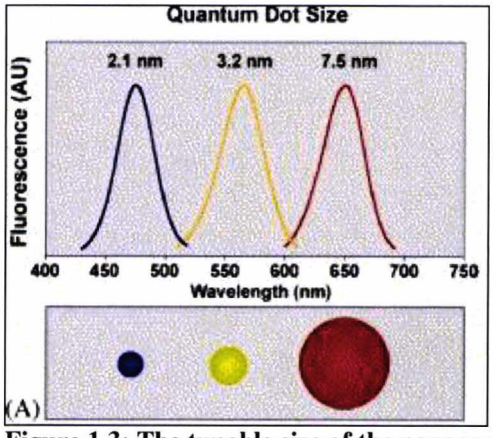

Figure 1.3: The tunable size of the nanocrystals that relates to the colour it emits. Small QDs emit towards the blue and large QDs towards the red. Adapted from a previous publication (Bailey *et al.* 2004).

Synthesis occurs by injecting liquid precursors (dimethyl cadmium and selenium powder dissolved in tributylphosphione) in hot organic solvent (Trioctylphosphine oxide-TOPO) at temperatures reaching 300°C (Murray *et al.* 1993). Nanocrystals initiate formation immediately and the colourless starting mix becomes coloured. The size of the nanocrystals is adjusted by changing the amount of injected precursors and crystal growth time in the hot TOPO mix (Michalet *et al.* 2001; Parak *et al.* 2003). A variety of core shapes can be synthesized, but they require an extra shell of a high band gap semiconductor material, typically ZnS, to stabilise the core and increase the quantum yield [QY-ratio of the amount of light emitted from a sample to the amount of light absorbed by the sample (Fu *et al.* 2005)] up to 80% (Chan *et al.* 2002; Alivisatos *et al.* 2005). The surface layer of the ZnS shell is however hydrophobic and insoluble in aqueous solutions (Michalet *et al.* 2005).

In terms of the optical properties of QDs, they have broad excitation and narrow, symmetric emission spectra. The spectral width of QDs (the full width at half maximum is 12nm), leads to less overlap between absorption and emission spectra (Chan & Nie 1998). Consequently, multicolour nanocrystals of different size can be excited by a single wavelength (excitation source) that is shorter than their emission wavelength (Green 2004; Alivisatos *et al.* 2005; Arya *et al.* 2005). Such an approach cannot be achieved with classical organic fluorophores because they have narrow excitation and broad emission that often results in spectrum overlap or red tailing

(Dabbousi *et al.* 1997). Figure 1.4 compares the absorption and excitation spectra of a QD and an organic fluorochrome.

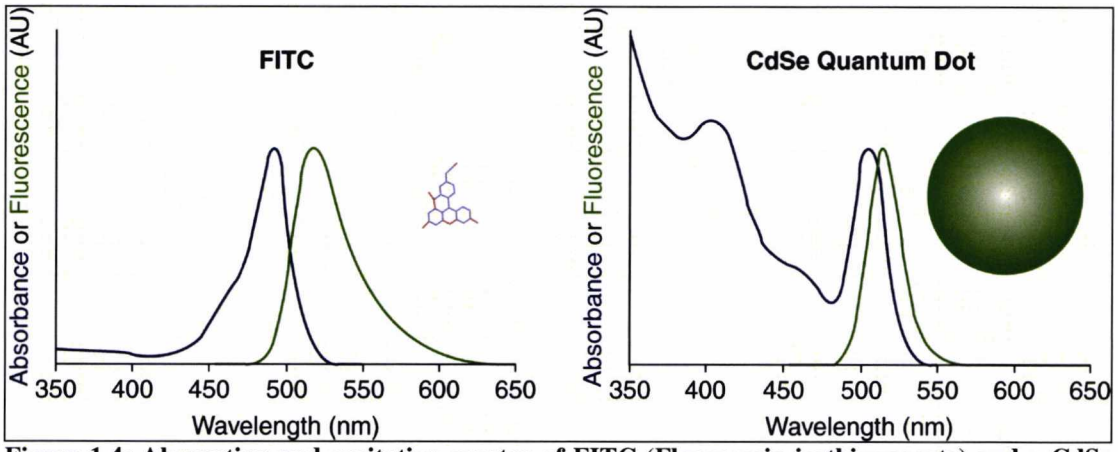

Figure 1.4: Absorption and excitation spectra of FITC (Fluorescein isothiocyanate) and a CdSe QD molecule. The relative size of the two fluorochromes is also illustrated. Adapted from (Bailey *et al.* 2004).

QDs produce significantly brighter fluorescence (2-11 times) (Larson *et al.* 2003) because of the large molar extinction coefficients (10-50 times larger than organic fluorophores) (Gao *et al.* 2005). Due to their inorganic composition they are more resistant to photobleaching than organic fluorophores (Alivisatos 1996; Bruchez *et al.* 1998; Michalet *et al.* 2001; Jaiswal *et al.* 2003; Parak *et al.* 2005). Additionally QDs have a longer fluorescence half-life than typical organic dyes (Lounis *et al.* 2000).

An important photophysical property of QDs is blinking, a phenomenon where the nanocrystals alternate between an emitting (on) and non-emitting (off) state (Michler *et al.* 2000; Pinaud *et al.* 2006). This behaviour has been interpreted according to an Auger ionisation model (Efros & Rosen 1997). Blinking affects single molecule detection applications by saturation of the signal. However blinking suppression strategies have been reported (Hohng & Ha 2004; Lee & Osborne 2009).

Synthesis of QDs renders hydrophobic nanocrystals as it occurs in non-polar organic solvents (Michalet *et al.* 2005). However, for QDs to be useful in biological applications they need to be soluble in aqueous buffers since all experiments involving cells require water soluble conditions (Parak *et al.* 2005; Yu *et al.* 2006). This essentially means that the surface of the QD needs to become hydrophilic. Several strategies have been employed to achieve this and most rely on exchanging

the hydrophobic surfactant molecules with bifunctional molecules that are hydrophobic towards the ZnS shell of the nanocrystal and hydrophilic on the other end (Michalet *et al.* 2005; Parak *et al.* 2005).

Commonly thiols (–SH) are used as the hydrophobic anchoring parts to ZnS and carboxyl (–COOH) as the hydrophilic (Pathak *et al.* 2001; Gerion *et al.* 2002). Alternative approaches include; surface silanisation (Bruchez *et al.* 1998; Gerion *et al.* 2001), coating the QD surface with amphiphilic polymers (Gao *et al.* 2004; Pellegrino *et al.* 2004), or polysaccharides (Osaki *et al.* 2004), phospholipid micelles (Dubertret *et al.* 2002), non charged molecules [i.e. dithiothreitol (Pathak *et al.* 2001)], dendrons (Wang *et al.* 2002), peptides (phytochelatin related) (Pinaud *et al.* 2004) and oligomeric ligands (oligomeric phosphines OPs) (Kim & Bawendi 2003). The effect of surface functionalisation on the optical properties of QDs is difficult to predict. In general however quantum yield and decay behaviour respond to this effect whereas shape and spectral position of absorption and emission are hardly affected (Resch-Genger *et al.* 2008). These strategies allow QDs to be conjugated with a variety of biomolecules including biotin (Bruchez *et al.* 1998), albumin (Gao *et al.* 2002), antibodies (Goldman *et al.* 2002a), avidin (Goldman *et al.* 2002b) and streptavidin (Wu *et al.* 2003; Mason *et al.* 2005). Covalently linked avidin/streptavidin QDs are very popular amongst companies (e.g. Invitrogen, Evident Technologies); they take advantage of the strong affinity that avidin and streptavidin have for biotin, and the plethora of biotinylated reagents (e.g. antibodies, DNA probes) available (Dahan *et al.* 2003).

The unique optical properties of QDs have allowed them to be used both for *in vitro* and *in vivo* applications. With regard to the *in vitro* applications QDs were used in the detection of the cancer marker Her2 on the surface of fixed and live cancer cells (Wu *et al.* 2003) and the identification of the erbB/HER family of transmembrane receptor tyrosine kinases that mediate cellular responses to epidermal growth factor (Lidke *et al.* 2004). QDs have been used as cellular markers because they can be internalised by cells using a receptor (Chan & Nie 1998; Zheng *et al.* 2006) or by non-specific endocytosis (Parak *et al.* 2002). QD cell markers have been used in cell-cell interaction studies by creating unique colour tags for individual cell lines (Mattheakis *et al.* 2004). In addition, QD resistance to photobleaching has enabled 3D optical

sectioning studies of the vascular endothelium (Ferrara *et al.* 2006), applications in cell motility assays for studying actomyosin function (Mansson *et al.* 2004) and phagokinetic tracking of small epithelial cells responsible for 90% of cancers (Parak *et al.* 2002).

Similarly for *in vivo* applications; peptide coated QDs have been used as means to deliver drugs to target molecule sites after injection (Akerman *et al.* 2002) and to study the behaviour of specific cells during early stage embryogenesis in Xenopus and Zebrafish embryos by microinjection of micelle encapsulated QDs (Dubertret *et al.* 2002; Rieger *et al.* 2005). Gao *et al.* (2004) reported *in vivo* cancer targeting and imaging using QDs that were conjugated to an antibody for human prostate cancer and the use of near infra-red QDs have been used as contrast agents during a surgical procedure to map sentinel lymph nodes in the pig and mouse (Kim *et al.* 2004). Despite the challenges for QD technology (e.g. potential cytotoxicity), cancer research has already made extensive use of QD applications for *in vivo* tumour cell imaging (Takeda *et al.* 2008; Ballou *et al.* 2009; Ciarlo *et al.* 2009; Kang *et al.* 2009), surgical oncology (Singhal *et al.* 2010) and metastasis detection (Mahmoud *et al.* 2009).

Given the potentially much-vaunted properties of QDs, they have been proposed as an ideal candidate for the study of chromosomes through adaptations of FISH protocols. It is noteworthy however that a PubMed search using terms such as "Quantum Dots FISH" or "Quantum Dots Fluorescent *in situ* hybridisation" yields few results, of which only 11 are actually QD-FISH studies. For the purposes of this literature review I have summarised (below) the key aspects of these studies.

Initially Xiao and Barker generated biotinylated probes from total genomic DNA and were able to detect it using QD605; they reported much brighter signals with QDs compared to organic fluorochromes, while they highlighted the importance of pH (optimal at 6-7) with regard to the buffer used to dilute the QD streptavidin conjugant (Xiao & Barker 2004b; Xiao *et al.* 2005). Chan *et al.* (2005) used direct labelling strategy to target specific mRNAs in mouse brain sections. This study raised the issue of the multiple streptavidin sites on the QD molecule that could interfere with hybridisation efficiency. Two studies with contradictory results with the use of QDs

in detecting plant chromosomes highlight the importance of the type of QDs used. In the study by Muller *et al.* (2006) commercially available QD streptavidin conjugates were used unsuccessfully, in the plant *Allium Fistulosum* whereas, in the work of Ma *et al.* (2008), successful results were reported with QDs in maize chromosomes due to a different solubilisation strategy used by the authors to reduce the steric hindrance effect. Similar successful results without the use of commercially available QDs were reported by Wu *et al.* (2006) in *Esherichia coli* and by Choi *et al.* (2009) in *Drosophila.*

The importance of quality control test with regard to QD batches was also reported in the first direct QD-FISH study by Bentolila and Weiss (2006). Using analytical grade QD batches for a variety of QD-streptavidin conjugates they formed QD-DNA complexes by incubating biotinylated oligonucleotides at various molar ratios at room temperature for 30 minutes. Complexes were run on an electrophoresis gel and the optimum molar ratio was established. At the same time this assay confirmed binding of the DNA to the nanoparticles because of the motility shift that is caused by the formation of this conjugant. These probes were used to recognise the major (γ) family of mouse satellite DNA. The novel feature in this study was the presentation of a dual colour QD-FISH using QD592 and 655 against centromere associated sequences (satellites). Reading between the lines of this paper however, data was presented only from two out of the five different QDs that were tried, probably due to technical difficulties or hybridisation failure of the remaining constructs. Nevertheless this was an important breakthrough for multicolour QD-FISH. In a recent study by Muller *et al.* (2009) a combination or organic and inorganic fluorochromes were used to increase multiplexing and the authors report also a batch variability regarding QD-conjugates arguing that further progress is anticipated in from the manufacturer's point of view to increase QD robustness and reliability.

Thus although QDs are promising candidates for FISH applications, the number of available QD-FISH studies does not reflect their potential. In Chapter 3 of this thesis, various attempts to incorporate QDs in FISH either through indirect or direct detection, with a view to benefit from their optical properties, through multiplexing, are reported.

1.2. Chromosome aneuploidy in the human gametes and infertility

1.2.1. Gametogenesis - brief overview

Meiosis is the most essential stage in gamete formation for all sexually reproducing organisms. It is characterized by two divisions (one reductional, one equational) that produce diverse haploid products (the gametes). Faithful execution is essential for fertility, for maintaining the integrity of the genome and normal development of the offspring (for most recent reviewed see the following: (Handel & Schimenti 2010)).

A pre-meiotic DNA replication round generates the initial gametocytes (with diploid chromosomal complement – primary spermatocyte vs. primary oocyte). During prophase I, homologous chromosomes pair and exchange genetic material through synapsis. Once this process is completed they are held together via their crossovers. The end of the first meiotic division separates the homologous chromosomes and produces secondary gametocytes (two secondary spermatocytes vs. one secondary oocyte and a polar body). The second meiotic division separates the sister chromatids and produces four haploid spermatids in males and a haploid oocyte and another polar body in females.

Two extremely important differences should be considered with regard to male and female gametogenesis. In females, meiotic prophase is arrested before birth and is resumed in small oocyte populations at periodic intervals after puberty (until the supply or primarily oocytes is depleted), whereas in males there is continuous sperm production during the reproductive life span.

Furthermore, the second meiotic division is also different in timing and the end products. In males it occurs immediately after the end of the first division, with the production of the haploid spermatids, whereas in females, the timing of the division is coordinated with ovulation and fertilisation to yield the haploid oocyte (egg). Figure 1.5 illustrates the mammalian meiosis, incorporating the concept of gametogenesis.

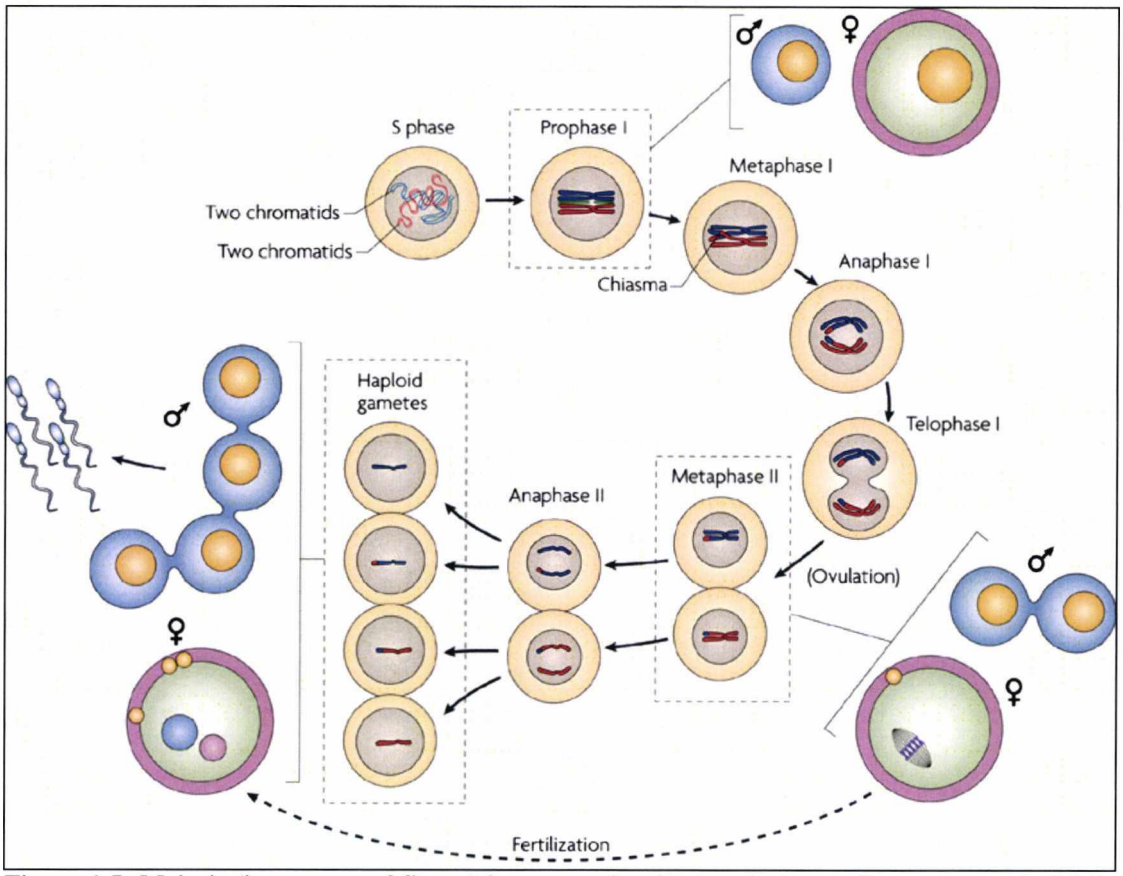

Figure 1.5: Meiosis (inner part of figure) in mammals with key features of gametogenesis. Male germ cells are depicted with blue and female with pink. Results of the first meiotic division are shown in bottom right (two secondary spermatocytes vs. one secondary oocyte and a polar body-yellow sphere in pink germ cell). The products of the second meiotic division are shown at the left of the figure with 4 spermatids (blue circles with yellow spheres) for male (that differentiate to spermatozoa), whereas meiosis II for females completes upon fertilisation so that the fertilised egg can contain the two haploid pronuclei (bottom left pink circle with blue and pink spheres). Adapted by (Handel & Schimenti 2010).

Thus both spermatogenesis and oogenesis are complex processes with crucial differences in timing and highly differentiated end products. After introducing the concept of aneuploidy, its incidence in both gametes is discussed before focusing on male infertility.

1.2.2. Aneuploidy

Aneuploidy can be defined as the presence of an extra or missing chromosome in a nucleus. Most aneuploid conceptuses perish *in utero*, making aneuploidy the leading cause of pregnancy loss, nevertheless some survive to term making aneuploidy also the most common cause of mental retardation (Hassold & Hunt 2001).

As illustrated in section 1.2.1 meiosis is the process to generate haploid gametes through two rounds of division. In the first division the homologous chromosomes

align, exchange genetic material (through crossovers) and segregate to opposite poles whereas in the second division the sister chromatids segregate generating the haploid chromosomal complement. Errors in either of the divisions result in abnormal patterns of segregation (non-disjunction) and aneuploid gametes as shown in Figure 1.6.

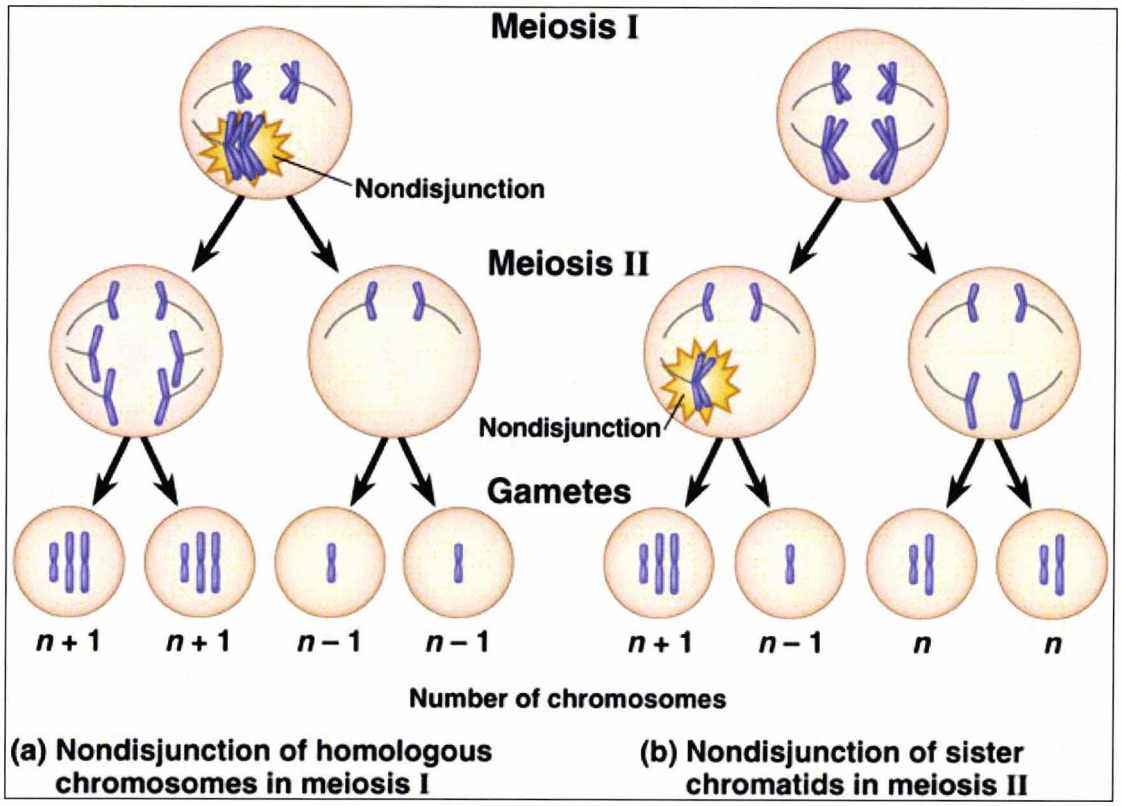

Figure 1.6: Chromosome non-disjunction and resulting aneuploid patterns in the gametes, occurring from MI (left panel) or MII (right panel). Image from: http://www.bio.miami.edu/~cmallery/150/mendel/c8.15x13.nondisjunction.jpg

1.2.2.1. Aneuploidy in sperm

Early attempts to study aneuploidy in sperm were carried out by fusing human sperm into hamster oocyte and karyotype the condensed sperm chromosomes (Martin *et al.* 1991). Cumulative data from these experiments estimates that aneuploidy in spermatozoa of normal controls is 1-2% (Hassold *et al.* 1996). However the frequency of structural abnormalities seems to be higher with an average of 6-7% (Martin 2008). With the advent of FISH technology specific probes could be generated to assess chromosome aneuploidy in sperm in large numbers (interphase cytogenetics). Distribution of aneuploidy revealed that most autosomes had a disomy frequency of 0.1%, whereas there was a significant increase for disomy 21 (0.29%), 22 and sex disomy (0.43%) (Martin 2006). Thus aneuploidy can occur for all chromosomes;

however the particular susceptibility of the chromosomes 21, 22 and the sex chromosomes has specific etiology. These chromosomes have one crossover (21 & 22 due to their small size) and sex chromosomes due to restricted recombination in the pseudoautosomal region (Martin 2005, 2006, 2008). Failure of this single chiasma formation would not ensure proper segregation of chromosomes to opposite poles. Two early reports state that reduced XY recombination was observed in paternally derived XXY patients (Hassold *et al.* 1991; Lorda-Sanchez *et al.* 1992). Actual recombination frequencies between normal and disomy sperm cells were measured using PCR and markers to determine frequency of recombination. A significant decrease was observed for the disomic sperm (Shi *et al.* 2001).

The aforementioned results originate from studies in normal (fertile) males. However with the advent of intracytoplasmic sperm injection (ICSI) (Palermo *et al.* 1992) studies in males with fertility issues could be generated to test hypotheses of higher rates of chromosome abnormalities.

Moosani *et al.* (1995) were the first to report a higher degree of chromosomal abnormalities in men with impaired fertility compared to controls. The general trend from studying males with different types of infertility (e.g. oligo–, astheno–, terato–, zoosperia) is that they have an increased frequency of chromosome abnormalities varying from 2 to 10 times higher that control males (Martin 2005). In an elaborate review by Tempest and Griffin (2004) interphase cytogenetics results for all chromosomes have been summarised (between normal and infertile males) and the consensus for a correlation of sperm aneuploidy and male infertility despite inter-study differences is highlighted. Since reduced recombination has been linked with increased aneuploidy, the same principle could be studied for infertile males for a possible link between reduced recombination and infertility. Using new immunocytogenetic techniques that allow the analysis of recombination foci during prophase I in the synaptonemal complex (SC – the protein structure that links chromosomes during prophase I) Sun *et al.* (2005) reported reduced mean frequencies of recombination and increased frequencies of chromosomes without any recombination site in infertile males. This study has prompted more to investigate the relationship between reduced meiotic recombination and aneuploid gametes and

several lines point towards an association; however research in the same individuals is required to further establish a firm causal link (Sun *et al.* 2008).

Finally a handful of studies have tried to establish a link between lifestyle habits (e.g. smoking, caffeine consumption), and disomy frequency but no consistent association has been found (Shi & Martin 2000; Martin 2003, 2006). The same applies to geographical differences. Furthermore, evidence for a small effect of increased paternal age on sex chromosome aneuploidy has been reported involving 2-fold difference between the oldest and youngest groups (cited in Martin (2008)).

1.2.2.2. Aneuploidy in OAT (OligoAsthenoTeratozoospermia) males

A specific category of males with increased number of studies in literature are the OAT males. According to Pang (1999) OATs are the patients with sperm concentration of less than 15 million per ml, motility of less than 41%, and normal morphology of less than 4.4%. Pang conducted one of the first interphase cytogenetics studies to compare aneuploidy for 12 autosomes and the sex chromosomes in OATs males undergoing ICSI and controls. An increased level (up to 30-fold) of aneuploidy (disomy, diploidy, nullisomy) for all chromosomes was found (Pang *et al.* 1999) in OATs which contributed probably to their infertility. The trend of higher incidence of aneuploidy in OAT males has been observed in other studies (Bernardini *et al.* 1997) (9 OATs with higher sex chromosome disomy), (Storeng *et al.* 1998) (4 OATs with higher sex chromosome disomy), (Pfeffer *et al.* 1999) (10 OATs with higher aneuploid rates for 1, 13, 18, 21, X, Y), (Ushijima *et al.* 2000) (8 OATs with higher disomies for chromosomes 13, 21, X, Y), (Gole *et al.* 2001) (5 OATs with higher sex disomy), (Zhang & Lu 2004) (10 OATs with higher aneuploid levels for 18, X, Y). The largest OAT cohort study was performed recently (Durakbasi-Dursun *et al.* 2008) where 30 OATs and 10 normal controls were studied for aneuploidy in 5 chromosomes (13, 18, 21, X, Y) using a multicolour probe set. Increased rates of disomy for 13, 21, XY, YY, were reported for OATs compared to controls. Also total aneuploidy was significantly higher in OATs (Durakbasi-Dursun *et al.* 2008). The risk that these men have when undergoing ICSI was highlighted in all of the above studies. Moroever, since there has been a link between sperm chromosome abnormalities and the embryonic complement from infertile 46,XY and 47,XYY males (Rodrigo *et al.* 2009), sperm aneuploidy screening could be used as a

prognostic test for couples undergoing ICSI (Petit *et al.* 2005) and are in the high risk categories (e.g. oligospermic, or OAT males) (Durakbasi-Dursun *et al.* 2008; Sanchez-Castro *et al.* 2009). This could improve genetic counselling.

Further to the evidence of higher chromosomal abnormalities in OAT males, two studies implicate functional defects in spermatozoa from OAT men. Corrales *et al.* (2000) suggested abnormal distributions of glycosidase proteins (important in fertilisation) in OAT sperm. Liu *et al.* (2004) purported greater DNA fragmentation and mitochondrial dysfunction in OAT sperm, highlighting the importance of selecting good quality sperm in ICSI for oocyte injection. Finally Plastira *et al.* (2007) argue for an age effect in OAT patients contributing to DNA fragmentation, poor chromatin packaging as well as a decline in semen volume, morphology and motility.

From the above information it is reasonable to argue that, since a high level of aneuploidy is observed in OAT patients, that is linked to infertility, it seems prudent to examine other chromosomally-related perturbations e.g. any relationship between altered nuclear organisation and infertility (see Chapter 5).

1.2.2.3. Aneuploidy in oocytes

When considering aneuploidy in oocytes, there are several timepoints in the oogenesis process that are implicated in the genesis of aneuploidy: First, the mitotic divisions of the germ cells before entering meiosis which imposes the first risk of chromosomal errors. Then during prophase I of meiosis where chromosomes recombine and exchange genetic material however this process halts until puberty, where on average one oocyte per month completes meiosis I and proceeds to meiosis II only if a sperm fertilises it. Failure of chromosome segregation during MI or MII impose further risks of chromosomal error (Delhanty 2005; Hassold & Hunt 2009).

The incidence of chromosome abnormalities in oocytes is around 20% with regard to numerical abnormalities and 1% for structural abnormalities (Martin 2008). The fact that oocytes remain suspended in prophase for many years is probably key to understanding why increased aneuploidy is related to female age (Hunt 1998). Indeed the association between advanced maternal age and aneuploidy was recognised almost 80 years ago by Penrose (Hassold *et al.* 1996). Numerous studies have confirmed the

association estimating that in women under 25 years about 2% of clinically recognised pregnancies are trisomic, (Hunt 2006) whereas this value rises to approximately 35% in women over 35 years (Martin 2008). With regard to the presence of the extra chromosome in trisomies, most studies suggest that it is the result of maternal meiosis errors, with MI errors being more common than MII errors (Hassold *et al.* 2007). However recently results from specific trisomies argue for patterns of non-disjunction; patterns that apply to all groups of chromosomes, patterns for a specific group of chromosomes (e.g. trisomies for acrocentric chromosomes originate from MI with recombination failure), patterns for specific chromosomes (e.g. trisomy 16 originates from MI but with no failure of recombination) (Hassold & Hunt 2009). Evidence from a pioneer study by Sherman and colleagues for trisomy 21 found that 95% originates from maternal MI errors (Freeman *et al.* 2007).

As with errors occurring in sperm, reduced recombination seems to be associated with maternally derived cases of trisomy for 15, 16, 18, 21 and the sex chromosomes. Reduced recombination can lead to achiasmate homologues that are prone to mis-segregation (Delhanty 2005; Farfalli *et al.* 2007; Martin 2008). Furthermore, studies in foetal oocytes have revealed unusual crossover configurations conferring chromosome specific routes to age independent or dependent non-disjunction due to events occurring in foetal oogenesis (Cheng *et al.* 2009). Recently, Hulten and colleagues proposed a different hypothesis on maternal age effect on trisomy 21, by postulating that trisomy 21 oocytes have a delayed development in the pool of growing follicles and could be ovulated later in life than normal oocytes. If this hypothesis holds true then the age effect could be happening as a result of events occurring before oocytes enter meiosis (Hulten *et al.* 2008).

On a molecular level considerable attention has focused on the cohesion protein Smc1β and whether age dependent aneuploidy could reflect the degeneration of cohesion complex components either because of lack of protein turnover or due to insufficient synthesis of replacement proteins during oocyte growth (Hunt & Hassold 2008).

In sections 1.2.2.1 and 1.2.2.3, an overview of aneuploidy in human gametes was presented and Table 1.1 summarises the incidence of chromosome abnormalities.

Gamete	Numerical %	Most common aneuploidy	Structural %	Total %
Oocytes	20	21, 22, 16	1	21
Sperm	1-2	21, 22, X, Y	~7	~9

Table 1.1: Incidence of chromosome abnormalities in the human gametes. The % of numerical aneuploidy in oocytes originates from studies using surplus material from women with maternal age ranging from 22-42 (Martin *et al.* 1991) or 19-46 years (Pellestor *et al.* 2002). Adapted from (Martin 2008).

1.3. Male infertility

Infertility is defined as the inability to conceive after at least a year of unprotected coetus, and accounts for one in six couples (15%) wishing to start a family in the western world (Shah *et al.* 2003). In a multicentre study conducted by the World Health Organisation (WHO) it was concluded that in 20% of infertile couples, male factor was the predominant cause, 38% was originating from female, whereas both partners contributed in the 27% of cases (Seli & Sakkas 2005).

The causes of infertility can be divided to genetic, hormonal, age, lifestyle related; a result of surgery, or associated with abnormalities in semen parameters (Shah *et al.* 2003). Genetic causes account for about 15% of male and 10% of female infertility, while there is a 15-20% of infertility which is unexplained (idiopathic) (Seli & Sakkas 2005; Ferlin *et al.* 2007).

1.3.1. Genetic causes of male infertility (numerical & structural)

With regard to the genetic causes, they can be further subdivided to numerical, structural abnormalities, but also causes inducing sperm DNA damage. As discussed in section 1.2.2.3 most numerical autosomal anomalies originate during maternal meiosis I. Males with trisomy 21 are azoospermic or severely oligospermic and they do not reproduce due to physical and psychosocial limitations (Egozcue *et al.* 2000). The most frequent chromosome aneuploidy regarding sex chromosomes in males is Klinefelter syndrome (KS), present in 5% of severe oligospermic and in 10% of azoospermic males (Ferlin *et al.* 2007). The syndrome causes arrest of spermatogenesis at the primary spermatocyte stage although occasionally later stages of sperm development are possible; and exists in two forms nonmosaic (47,XXY) and mosaic 47,XXY/46,XY (O'Flynn O' Brien *et al.* 2010). The extra X chromosome

originates in paternal meiosis I from non-disjunction of the XY bivalent (>50%), or from maternal meiosis I or II (40%) and post-zygotically in the remainder (Griffin & Finch 2005). The advent of ICSI has enabled KS patients to father children (54 normal births from 122 KS patients) but the risk of producing offspring with chromosome aneuploidies is significant due to elevated disomies in their sperm (Ferlin *et al.* 2007).

Present in 1 in 1000 males is 47,XYY, with fertility ranging from normozoospermia to near azoospermia. The origin of the extra Y chromosome seems to be from paternal meiotic II non-disjunction and causes aberrant hormonal balance in the gonadal environment affecting normal chorionic gonadotrophin function (Shah *et al.* 2003).

Reciprocal translocations affect fertility by imposing a constraint mechanism to the meiotic process through the formation of a pairing cross between the translocated chromosomes. They further reduce the chances of conception by the production of unbalanced gametes from unbalanced disjunction of the pairing cross (Griffin & Finch 2005). Autosomal translocations are found 4-10 times more in infertile men compared to normal (O'Flynn O' Brien *et al.* 2010). Robertsonian translocations, occur when two acrocentric chromosomes fuse and can affect fertility by impairing gametogenesis or by producing gametes with an unbalance combination of the parental rearrangements (Ferlin *et al.* 2007). In addition the frequency of reciprocal carriers in oligo-, and azoospermic males is seven times higher from newborns (Ferlin *et al.* 2007). Similar to translocations, inversions (rearrangement of a chromosome segment, thus changing the sequence of genes), can cause infertility, by imposing pressure on the meiotic time machinery by the formation of a pairing loop (thus impeding meiosis), through reduced recombination in the pairing loop or when recombination occurs within the loop leading to the generation of abnormal gametes (Griffin & Finch 2005).

1.3.2. Y microdeletions and specific gene mutations

Other important genetic causes of infertility are associated with microdeletions in the long arm of Y and specific gene mutations.

Chromosome Y is a small largely heterochromatic chromosome that has retained through the course of evolution important genes for spermatogenesis, plus the all important SRY gene which is responsible for testis development (Ellis & Affara 2006). Yq microdeletions are observed with a prevalence of 10-15% in non-obstructive azoospermic patients and 5-10% in severe oligospermic males (Ferlin *et al.* 2007; O'Flynn O' Brien *et al.* 2010). A particular area of Y is involved in deletions associated with infertility termed AZF (azoospermia factor), which contains vital genes for spermatogenesis (Shah *et al.* 2003). Three subregions (AZF a-b-c) comprise AZF and most deletions occur in areas AZFb and AZFc (Shah *et al.* 2003; Ferlin *et al.* 2007; O'Flynn O' Brien *et al.* 2010) (Figure 1.7).

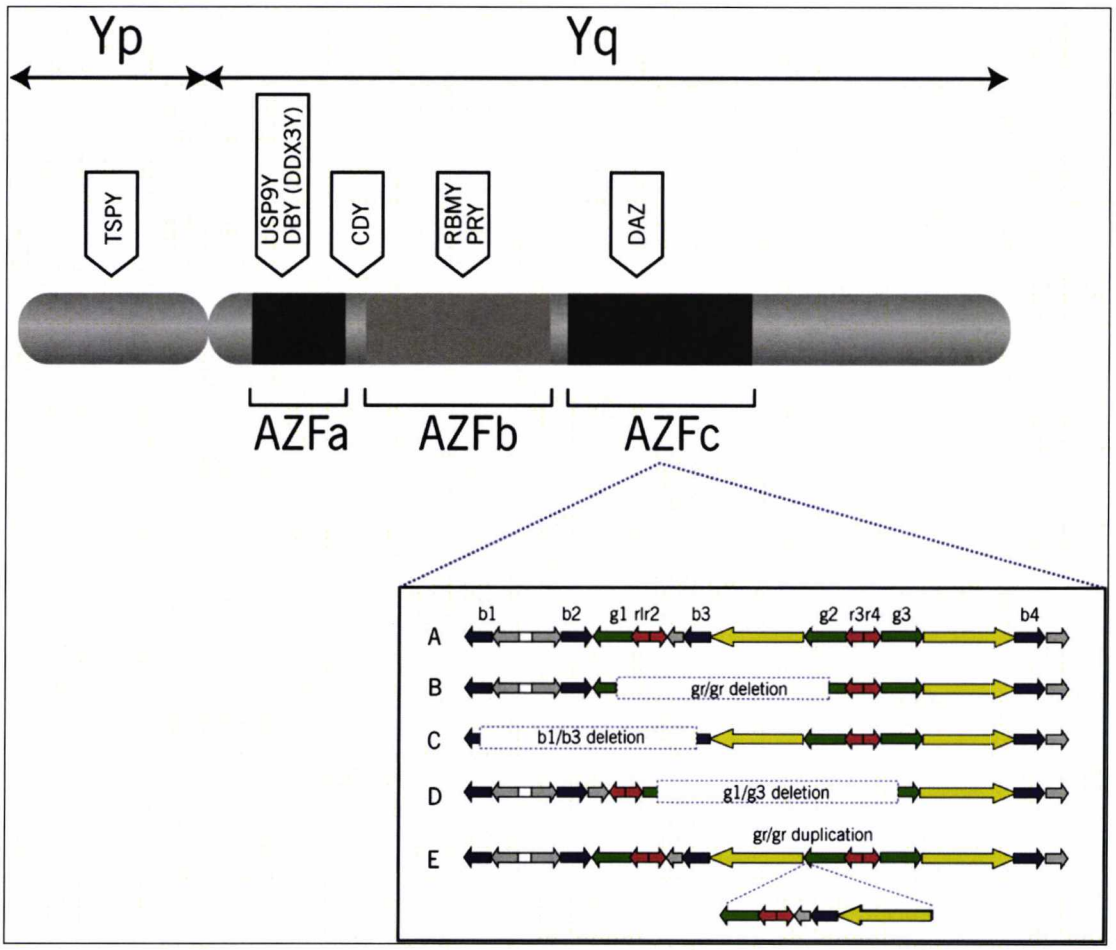

Figure 1.7: Y chromosome illustrating AZF regions with associated genes. The enlarged part illustrates common microdeletions in AZFc region. Adapted from (O'Flynn O' Brien *et al.* 2010).

Most of the microdeletions are generated by intrachromosomal homologous recombination between repeated sequence blocks that are organised as palindromic structures (Ferlin *et al.* 2007; Li *et al.* 2008). The complete deletion of AZFc removes

8 gene families including DAZ (involved in spermatogenesis), which is the strongest candidate for the azoospermic phenotype of AZFc, whereas deletions in the AZFa region lead to Sertoli cell-only syndrome and complete deletions of AZFb or AZfb+c lead to azoospermia associated with Sertoli cell-only syndrome or pre-meiotic spermatogenic arrest (Ferlin *et al.* 2007). Several studies have tried to assess the infertility risk of a specific partial AZFc deletion termed gr/gr and the conclusion is not clear as out of the 15 studies, eight have shown an association with infertility or testicular cancer whereas seven have failed to show a link (Ravel *et al.* 2009).

Overall studies of the ART outcome in patients with AZFc deletion suggest a tendency towards decreased fertilisation rates but not a significant change in overall pregnancy and delivery rates compared to controls (Seli & Sakkas 2005).

Many genes have been studied for potential links to male infertility. A few of the clinically important ones include the CFTR (cystic fibrosis transmembrane conductance regulator) gene, the androgen receptor (AR), the INSL3 (insulin like factor 3) and LGR8 (leucine-rich repeat containing G-protein couple receptor 8) (Ferlin *et al.* 2007). Details of other candidate genes are reviewed in (Shah *et al.* 2003) and more recently in (O'Flynn O' Brien *et al.* 2010). Table 1.2 summarises the roles of the aforementioned four genes in male factor infertility.

Gene	Location	Role in infertility	Treatment for patients
CFTR	Chromosome 7	Mutation causes CBAVD (congenital bilateral absence of vas difference)- a form of obstructive azoospermia	ICSI (as long the female partner does not carry CFTR mutation) or PGD
AR	Chromosome X	Mutation causes what is collectively known as AIS (androgen insensitivity syndrome) Mild AIS patients-infertile, Mutation also implicated in case of cryptorchidism, gynaecomastia	Hormone replacement therapy
INSL3	Chromosome 19	Linked to cryptorchidism Also possible link to Testicular Dysgenesis Syndrome	Surgery (usually in infancy)
LGR8	Chromosome 13	Linked to cryptorchidism (more evidence is required though)	Surgery

Table 1.2: Common genes implicated in infertility. Table shows the location of each gene, its potential role in infertility and possible treatments. Table compiled using information from the following: (Ferlin *et al.* 2007; O'Flynn O' Brien *et al.* 2010).

1.3.3. Sperm DNA damage and infertility

A handful of reviews argue for possible links of sperm DNA damage (in the ejaculate) and male infertility (Zini & Libman 2006; Aitken & De Iuliis 2007; Varghese *et al.* 2008; Delbes *et al.* 2009).

Three major mechanisms seem to be involved in DNA damage although they are not mutually exclusive. These involve chromatin remodelling by topoisomerase, oxidative stress and abortive apoptosis (Tarozzi *et al.* 2007; Aitken & De Iuliis 2009).

Normally during the chromatin remodelling in sperm (histones to protamines), naturally occurring breaks by topoisomerase II relief the torsional stresses as DNA is compacted and subsequently are resealed (Tarozzi *et al.* 2007). Alteration to this machinery of break and repair can cause altered chromatin structure and residual breaks in the DNA of sperm (Tarozzi *et al.* 2007).

Sperm DNA damage has been associated with high levels of reactive oxygen species (ROS); detected in the semen of 25% of infertile men (Zini & Libman 2006). The susceptibility to ROS damage stems from the presence of unsaturated fatty acids in the plasma membrane, necessary for membrane fluidity which is required in the acrosome reaction during fertilisation (Aitken & De Iuliis 2009). The only defence mechanism against ROS is the antioxidant ability of the seminal plasma, and the sperm chromatin compactness (Tarozzi *et al.* 2007). However free radicals can be produced both by defective spermatozoa and semen leukocytes thus inducing sperm damage and conferring to male subfertility (Zini & Libman 2006; Tarozzi *et al.* 2007; Aitken & De Iuliis 2009). The time of damage is still under debate but it is probably during the epididymal maturation as that is the longer exposure time that spermatozoa have to ROS (Tarozzi *et al.* 2007).

Furthermore, sperm DNA damage has been associated with a form of selective apoptosis that, under normal conditions, regulates the production of abnormal sperm in spermatogenesis and limits the population of germ cells to a number that can be supported by the Sertoli cells (Zini & Libman 2006; Tarozzi *et al.* 2007; Varghese *et al.* 2008). Over-expression of this process could lead to oligo- or azoospermia

whereas under-expression could give rise to abnormal sperm, which could impair fertilisation (Varghese *et al.* 2008). Using a marker for apoptosis (Fas) it was found that less than 10% of apoptotic sperm exist in normospermic men whereas approximately 60% of oligospermic men have more than 10% of apoptotic sperm (Varghese *et al.* 2008). It has also been postulated that advancing age and cancer therapies are associated with reduced apoptosis and increase of DNA damaged spermatozoa (Zini & Libman 2006; Varghese *et al.* 2008).

Other factors implicated in sperm DNA damage and thus affecting the integrity of the sperm are presented in the following table.

Factors	Effect	Review
Age	Spermatozoa with higher % of DNA damage in men older than 37 years	Aitken & De Iuliis (2007)
Obesity	Reduce quality of the semen	Varghese *et al.*(2008)
Smoking	Decrease in sperm counts, motility and increase in DNA damage	Zini & Libman (2006) Calogero *et al.*(2009)
Cancer treatment	Impair spermatogenesis	Zini & Libman (2006)
Environmental (air pollution, pesticides)	Increase sperm DNA damage	Zini & Libman (2006) Aitken & De Iuliis (2007) Varghese *et al.*(2008) Barratt *et al.*(2010)

Table 1.3: Other factors implicated in sperm DNA damage and reviews where they are discussed.

The emerging message from clinical studies with regard to sperm DNA damage is it has a detrimental effect on reproductive outcomes (lower IntraUterine Insemination pregnancy rates, higher pregnancy loss following IVF/ICSI) and that infertile men possess substantially more spermatozoa with DNA damage (Zini & Libman 2006; Barratt *et al.* 2010). Further examination is required to fully define the impact of sperm damage on reproductive outcomes and similarly to provide more information on the aetiology of infertility to be able to develop new treatments designed to help individuals with fertility problems.

1.4. The cytogenetics of human preimplantation development and ARTs (Assisted Reproduction Techniques)

1.4.1. Background

New life begins with the union of the haploid sperm and egg during fertilisation leading to the formation of the diploid zygote. The single cell zygote undergoes mitotic divisions (cleavage divisions) and forms a differentiated population of cells at the blastocyst stage: The inner cell mass (ICM) that will give further rise to the foetus, and the trophectoderm (TE) that will form the placenta. Parturition at full term occurs after 40 weeks of ovulation (Figure 1.8).

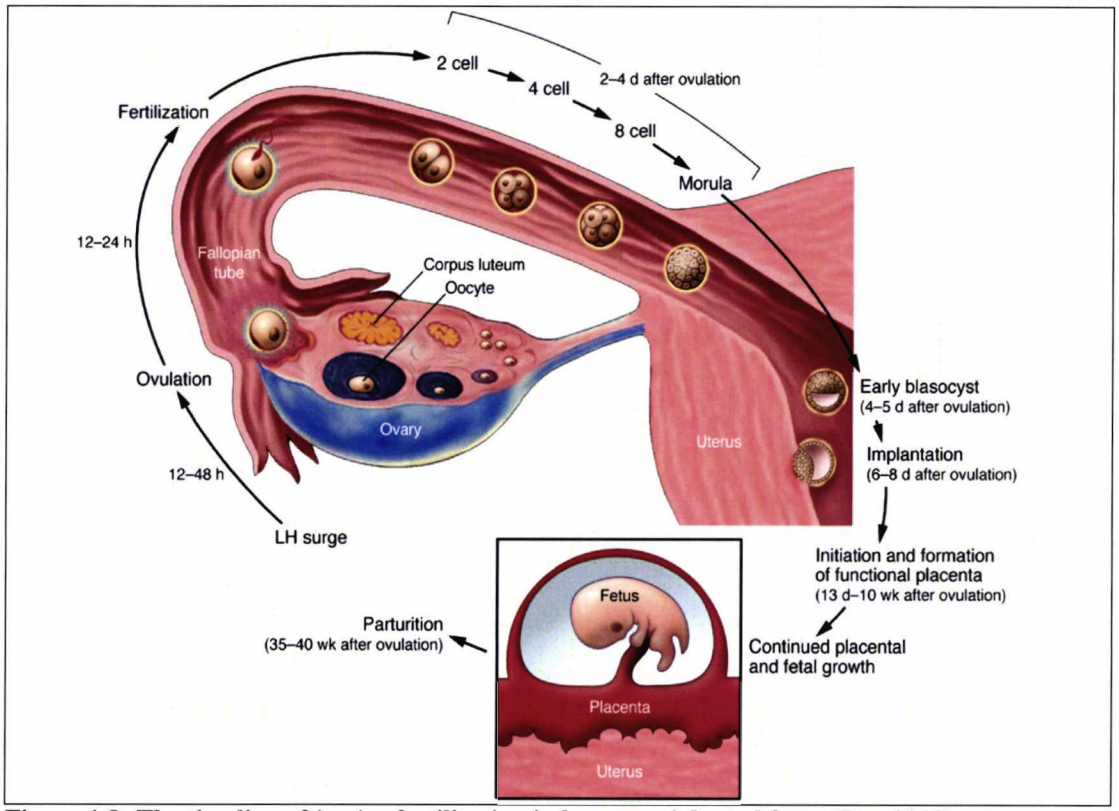

Figure 1.8: The timeline of *in vivo* fertilisation in humans. Adapted from (Dey 2010).

Human fertilisation however is relatively inefficient since around 30% of pregnancies result in spontaneous losses. In addition despite the growing of the human population (projected to be 9 billion by 2050), 15% of couples worldwide are childless because of infertility (Dey 2010). However with the advent of assisted reproduction techniques (ARTs) couples facing problems conceiving naturally are able to start a family. Central to this has been IVF, pioneered by Steptoe and Edwards; the 25th July of 2010

marked the 32nd birthday of the first IVF baby Louise Brown at Oldham General Hospital (Steptoe & Edwards 1978). Since then an exponential increase in the number of IVF cycles has occurred (4,308 in 1985 vs. 46,829 in 2007-987% increase – HFEA published data) leading to 11,091 successful births in 2007 alone, only in the UK (HFEA) and more than 3 million around the world (1978-2006 – data from ivf.net).

1.4.2. IVF (*In vitro* Fertilisation)

The IVF procedure can be divided to 3 phases. First, through the use of a hormone (FSH-Follicle Stimulating Hormone) there is hyper-stimulation of the ovaries in order to produce a large number of eggs. During this treatment (could be up to 12 days) the progress is monitored using vaginal ultrasound scans and blood tests. The second phase is the collection of the eggs by ultrasound guidance under sedation and the use of a needle. The eggs are then mixed with the partner's sperm *in vitro* and allowed to develop for 16-20 hours. In the third phase, eggs that have been fertilised (embryos) are removed from the culture medium and those that fit certain criteria (as determined by the embryologist) are transferred back to the uterus (number depends on maternal age) in the hope of establishing a pregnancy. Remaining embryos may be frozen to be used in another IVF cycle if suitable. The first published guidelines for IVF practise were published by Giannaroli *et al.* (2000) and an update was recently issued by Magli *et al.* (2008). Figure 1.9 illustrates the procedure of IVF.

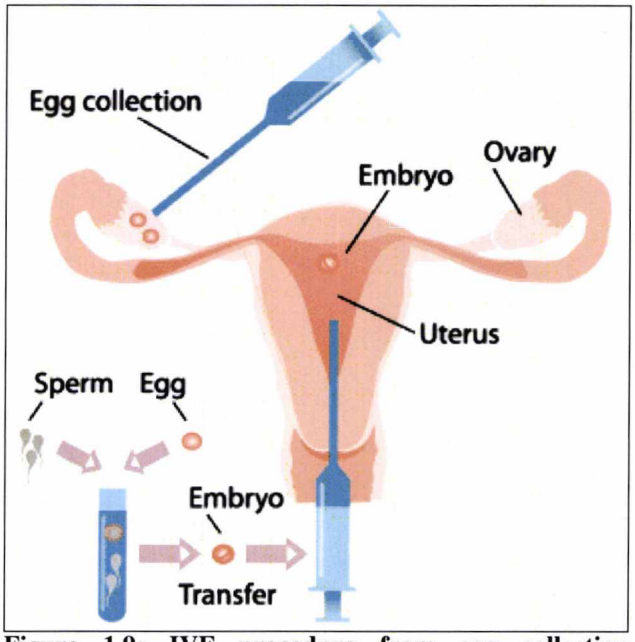

Figure 1.9: IVF procedure from egg collection to embryo transfer. Adapted from http://www.babble.com/CS/blogs/strollerderby/ivf.gif

1.4.3. ICSI (IntraCytoplasmic Sperm Injection)

ICSI was developed in Belgium by Palermo *et al.* (1992). It involves the injection of a single sperm into an egg (that has produced through IVF) using a micropipette 1/14 of the size of a human hair (Sutcliffe 2000). Sperm can be either obtained from the ejaculate or after aspiration from the testis or epididymis. Figure 1.10 illustrates the concept of ICSI.

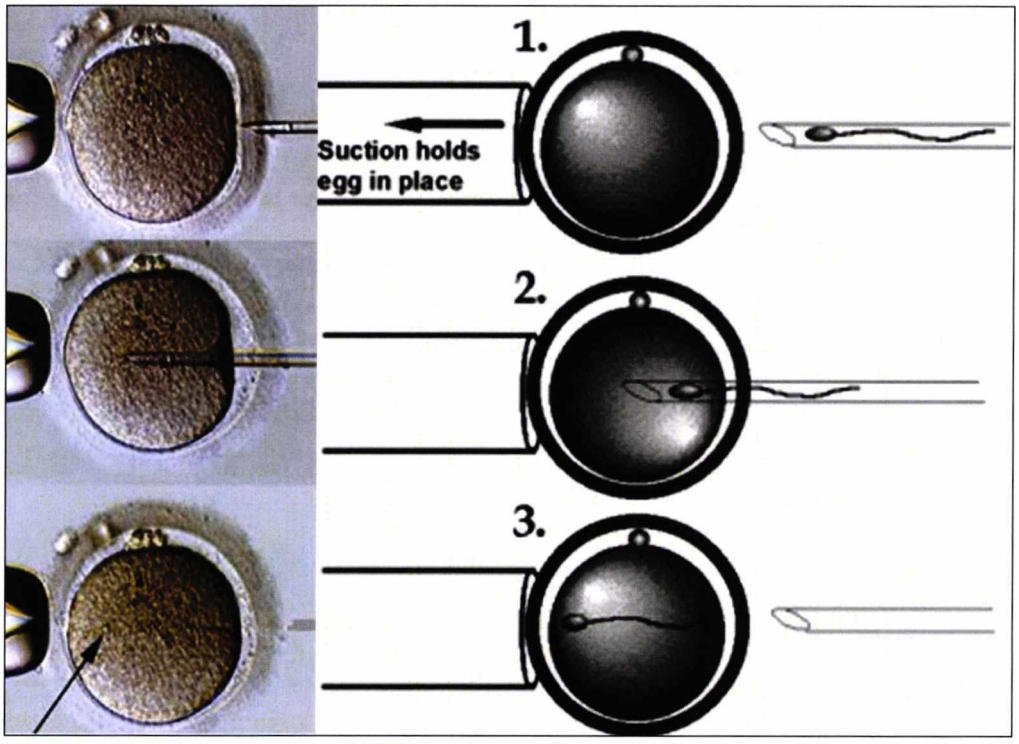

Figure 1.10: The procedure of ICSI using a real case (left) and a cartoon representation (right). Adapted from http://www.vermesh.com/images/art_03.jpg and http://www.pacificfertilitycenter.com/images/lab_icsi_process_fig3.gif

The growing number of babies born after the combined use of IVF/ICSI is presented in the following figure. In 2006 only in the UK 12,589 births from IVF/ICSI have been reported accounting for 1.5% of the babies born in the UK each year, whereas the worldwide estimate is 2 million (HFEA published data up to 2006).

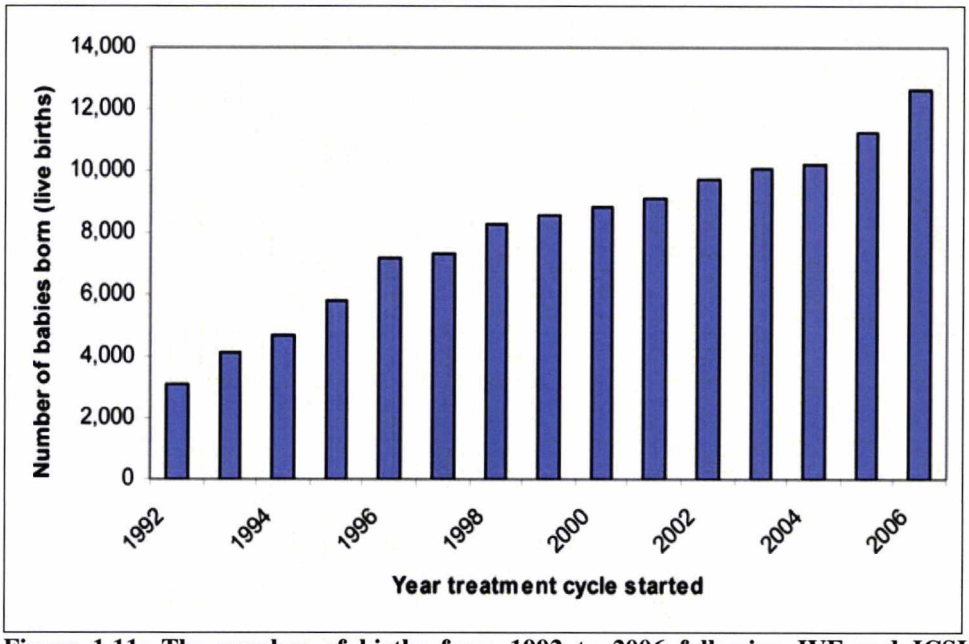

Figure 1.11: The number of births from 1992 to 2006 following IVF and ICSI treatments. Adapted from http://www.hfea.gov.uk/2588.html#3042

ICSI is recommended to men with impaired semen parameters. The World Health Organisation (WHO) published in 1992 a set of guidelines for the classification of normal semen parameters, and Table 1.4 shows what is considered to be normal values.

Semen Parameter	Normal Value
Volume	2.0 ml of more
pH	7.2-7.8
Concentration	$20x10^6$/ml
Total count	$40x10^6$/ml
Motility	50% or more with forward progression
Morphology	30% or more with normal morphology
Vitality	75% or more live
White blood cells	Less than $1x10^6$/ml

Table 1.4: Normal semen parameter classification based on the WHO criteria. Information has been adapted from: http://www.gfmer.ch/Endo/Lectures_09/semen_analysis.htm

Based on the above criteria men with impaired semen parameters can be classified into one of the following categories (Table 1.5).

Category	Definition
Normozoospermia	All parameters (Table 1.4) with normal values
Aspermia	No ejaculate
Asthenozoospermia	Less than 50% with forward progression
Azoospermia	No spermatozoa in the ejaculate
Oligoasthenoteratozoospermia	<20x10^6/ml, <50% motile, <30% normal morphology
Oligozoospermia	Concentration less than 20x10^6/ml
Teratozoospermia	Less than 50% sperm with normal morphology

Table 1.5: Classification of semen parameters. Adapted information from http://www.gfmer.ch/Endo/Lectures_09/semen_analysis.htm

Despite the benefits from the use of ICSI in severe male infertility cases, concerns have been raised due to the possible high risk of chromosomal aneuploidies from paternal origin as natural selection is bypassed using ICSI. These concerns have been confirmed by reports highlighting higher incidence of sex chromosomal aneuploidies and structural *de novo* chromosomal abnormalities in children conceived after ICSI compared to normal population (Durakbasi-Dursun *et al.* 2008).

1.4.4. Preimplantation genetic diagnosis (PGD) techniques

The discovery of Down syndrome caused by a chromosomal defect sparked a close association between cytogenetics and the emerging new discipline of medical genetics during 1960s with the introduction of prenatal diagnosis performed for chromosome abnormalities and metabolic disorders (Ferguson-Smith 2008). Currently the two mainstream prenatal techniques are amniocentesis and chorionic villus sampling (CVS). These are both invasive procedures, offered to couples with a high risk of transmitting a genetic disorder and the probability of miscarriage following amniocentesis is around 0.5%, whereas for CVS is 1-2% (Wells & Delhanty 2001). Despite the technical difficulties that prenatal diagnosis techniques face, there are also emotional and ethical questions if an unfavourable diagnosis is made, as the prospective parents have to make a decision where to terminate pregnancy.

The alternative is offered by PGD, a method used to provide a genetic diagnosis in embryos or oocytes generated by IVF before a pregnancy has been established. Thus it enables identification and transfer of only unaffected embryos without the need to terminate a pregnancy (Kanavakis & Traeger-Synodinos 2002). PGD is offered to

patients that are at a high risk of transmitting a genetic disorder or in couples where the female is of advance maternal age (>36), or couples with recurrent miscarriages (RM), repeated implantation failure (RIF) (Munne 2003; Thornhill *et al.* 2005).

Patients requiring PGD undergo IVF first so that many embryos can be generated, thus increasing the chances to identify a disease free embryo. Three days post-fertilisation one or two cells (blastomeres) are biopsied from the 8-cell stage and are either placed in a tube so that PCR can be applied to test for monogenic disorders (e.g. Cystic Fibrosis) or are fixed on a glass slide and FISH is performed to detect copy number or structural abnormalities. Figure 1.12 illustrates the principle of PGD.

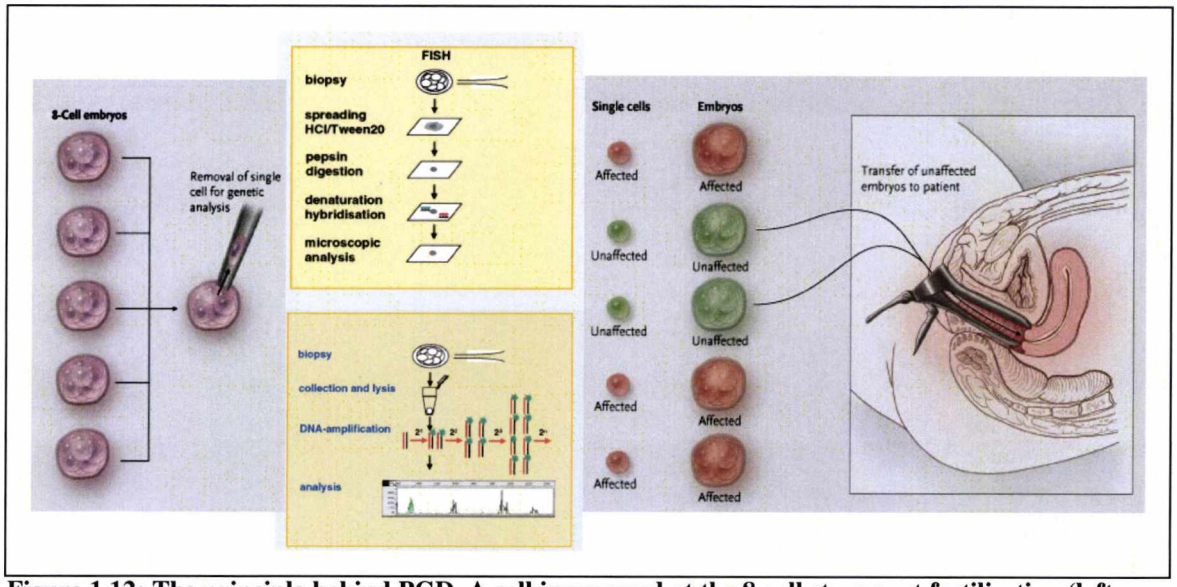

Figure 1.12: The principle behind PGD. A cell is removed at the 8-cell stage post fertilisation (left panel) and FISH (top middle) or PCR (top bottom) is performed to provide a diagnosis. Unaffected embryos are transferred back to the uterus (right panel) with the hope to establish a pregnancy. Adapted from (Braude 2006; Geraedts & De Wert 2009).

The first application of PGD using PCR was performed by Handyside *et al.* (1990) who applied sex selection in two couples with a risk of transmitting X-linked disorder, whereas the first interphase cytogenetics application of PGD was performed by Griffin *et al.* (1993) similarly to prevent risk of X-linked disorder. Further uses of PGD include; detection of monogenic disorders (e.g. Cystic Fibrosis), stem cell transplantation (HLA matching), mitochondrial disorders, translocations, numerical chromosome abnormalities (Geraedts & De Wert 2009) and social sexing at least in some countries (Egozcue 1993).

Other possible sources of genetic material for PGD testing are the first and second polar bodies (however this provides only information from the maternal side) and cells from the blastocyst stage on day 5 post-insemination. A drawback here is that less than 40% of embryos survive *in vitro* to this stage and time constraints as embryos need to be transferred no later than day 6 (Geraedts & De Wert 2009). If analysis does not occur within this point then embryos need to be cryopreserved so that they can be used in a subsequent cycle. However freezing and thawing reduces significantly the chance for a successful pregnancy (Geraedts & De Wert 2009). The newly developed vitrification techniques could help overcoming this issue (Loutradi *et al.* 2008; Rezazadeh Valojerdi *et al.* 2009; Zhang *et al.* 2009). Furthermore, blastocyst biopsy receives more attention as the optimal stage for diagnosis due to the self-correction of aneuploid or mosaic embryos that seems to be happening in that stage of development (Barbash-Hazan *et al.* 2008).

To organise and collate the data from PGD in 1997 the European Society of Human Reproduction (ESHRE) PGD consortium was formed and since 1999 nine data collections with regard to PGD have been published. From this data it is clear that most PGD techniques have been performed to study chromosome aneuploidies or PGS (Preimplantation Genetic Screening) in preimplantation embryos. Figure 1.13 presents the evolution of PGD treatments. The latest data (2008) presented in this year's ESHRE meeting (Rome), showed that PGS still dominates the world of PGD with 60% of all cycles (Harper *et al.* 2010b).

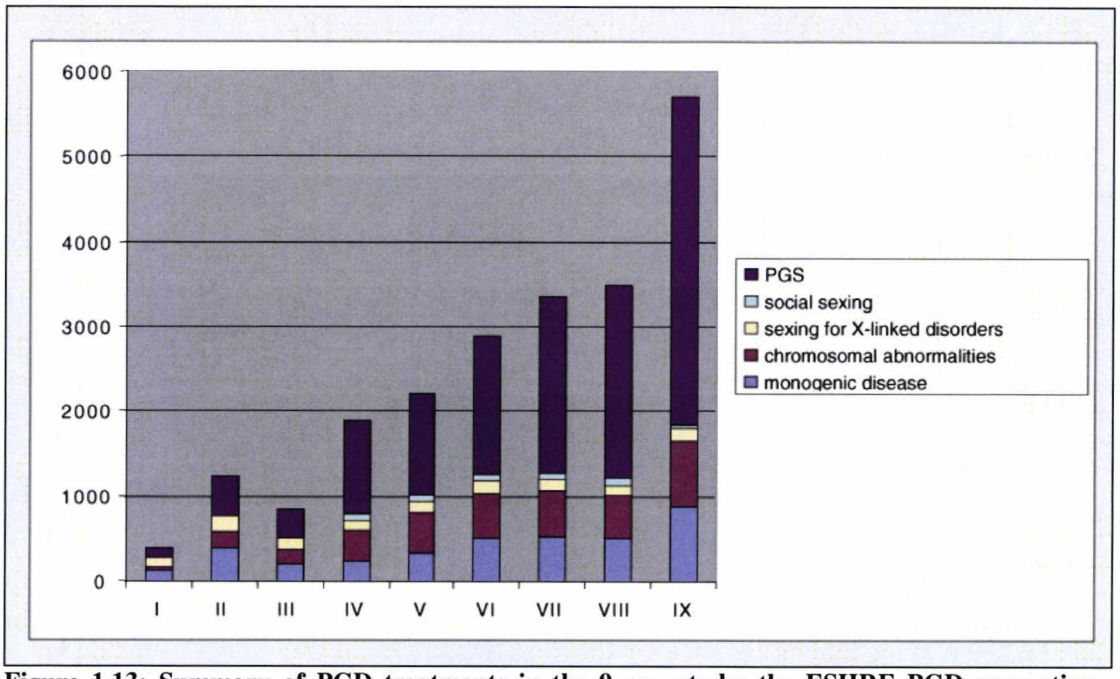

Figure 1.13: Summary of PGD treatments in the 9 reports by the ESHRE PGD consortium. Adapted from (Geraedts & De Wert 2009).

Thus PGS is considered in the next section, in the context of the recent debate as to whether it helps improving pregnancy rates.

1.4.5. PGS (Preimplantation Genetic Screening) and controversy

The main rationale for PGS is to increase the chance of a healthy pregnancy in sub-fertile patients undergoing IVF by screening for chromosome abnormalities. This is based on the fact that patients undergoing IVF with poor prognosis generate embryos with a high incidence of numerical abnormalities (60-70%) (Donoso *et al.* 2007). Thus if abnormal embryos can be identified and excluded and normal ones can be selected for embryo transfer, an improved pregnancy outcome should be expected at least in women with a high risk of chromosome aneuploidy (Fritz 2008).

The main indications for PGS are advance maternal age (AMA – over 37 or 38 years), repeated implantation failure (RIF – 3 or more failed implantation attempts), repeated miscarriage (RM – at least 3 attempts in normal karyotype patients) or severe male factor (SMF – abnormal semen parameters) (Munne 2003; Donoso *et al.* 2007; Harper *et al.* 2010a).

PGS enables the assessment of the numerical chromosome copy number in cleavage stage embryos through the use of interphase cytogenetics. Although karyotype

analysis of banded chromosomes would be ideal, cells would have to be arrested in metaphase and this is time consuming, has a low success rate and could lead to chromosome loss and thus misdiagnosis. Therefore interphase FISH in blastomeres has been the technique of choice because multiple chromosome specific probes can be labelled with different fluorochromes and used in the diagnosis of interphase nuclei (Griffin 1994; Handyside & Delhanty 1997).

The selection of probes predominantly used in the clinics is based on the incidence of chromosome abnormalities in spontaneous abortions and live births. Chromosomes 13, 15, 16, 18, 21, 22, X and Y are the most widely used, enabling the detection of an estimated 72% of abnormalities found in spontaneous abortions (Donoso *et al.* 2007).

Over the years, PGS has become very popular with 75% of the PGD related procedures in the USA being PGS and 65% in Europe (Hernandez 2009). In the most recent ESHRE PGD consortium report this steady increase has been highlighted with 3,900 cycles in 2007 alone compared to 116 in 1997-98 (Goossens *et al.* 2009).

Early studies using PGS reported an increase in implantation rates and at the same time, a reduction in trisomic offspring and spontaneous abortions (Munne 2003; Harper *et al.* 2008). However criticisms of these early reports focus on the fact that they were non-randomised, had poor experimental design, inadequate control groups few or no reports on delivery rates and relatively small patient numbers (Harper *et al.* 2008). The first randomised controlled trial (RCT) that cast some doubts on the efficacy of PGS was by Staessen *et al.* (2004) where no difference in embryo implantation and pregnancy rates was reported between control and PGS patients.

However the RCT study that initiated a huge debate with regard to the efficacy of PGS was published by Mastenbroek *et al.* (2007). The authors reported a significant *decrease* in pregnancy rates and live births following PGS in women of advanced maternal age. The study was however criticised (Cohen & Grifo 2007; Handyside & Thornhill 2007; Munne *et al.* 2007b; Munne *et al.* 2007c; Wilton 2007; Simpson 2008; Sermondade & Mandelbaum 2009) on many levels. First the biopsy procedure and the high rate of biopsy failure (3%) was criticised. For instance, the large percentage of undiagnosed embryos (20%) that were used for transfer, resulted in 6%

implantation in patients compared to 14% in the control group, showing a potentially detrimental effect of the biopsy itself (Cohen & Grifo 2007; Munne *et al.* 2007b; Wilton 2007; Simpson 2008). The need for safer biopsy was also underlined by Handyside and Thornhill (2007). Furthermore the number of embryos per patient seemed to be low judging from the average number of biopsied cells (4.8) indicating that many patients must have had 2 or 3 embryos, which is much smaller from the minimum number of embryos for biopsy (6-8) required to detect any increase in live birth rates after PGS (Munne *et al.* 2007c). Finally the exclusion of probes for chromosomes 15 and 22 in embryo selection (that account for 10% of abnormalities in human IVF embryos) was another reason for criticism (Munne *et al.* 2007b). This study prompted more RCTs (Chiamchanya *et al.* 2008; Hardarson *et al.* 2008; Jansen *et al.* 2008; Mersereau *et al.* 2008; Staessen *et al.* 2008; Twisk *et al.* 2008; Debrock *et al.* 2009; Garrisi *et al.* 2009; Schoolcraft *et al.* 2009b) and the following table summarises the general result from each them.

Study	Sample	Referral reason	Outcome
Jansen *et al.* (2008)	Blastocysts	Young infertile women (median 33.5 years)	Study was terminated prematurely when no PGS advantage was shown
Twisk *et al.* (2008)	Blastomeres	AMA (35-41 years)	No benefit of PGS over standard IVF/ICSI
Mersereau *et al.* (2008)	Blastomeres	Young infertile patients (average 35.2 years)	No statistically significant advantage of PGS, however slight improvement of live birth rates
Hardarson *et al.* (2008)	Blastomeres	AMA (>38 years)	Significantly lower clinical pregnancy rates with PGS-study stopped prematurely
Staessen *et al.* (2008)	Blastomeres	Infertile females <36 years	No difference in delivery rates between controls and PGS group
Debrock *et al.* (2009)	Blastomeres	AMA (>35 years)	No difference between controls and PGS group
Chiamchanya *et al.*(2008)	Blastomeres	Two age subgroups 32-39 years vs. over 40 years (for both partners)	No control group used. PGS pregnancy rate was associated with high abortion rate.
Schoolcraft *et al.*(2009b)	Blastomeres	AMA (>38 years)	No improvement with PGS in pregnancy rates, trend towards decrease of spontaneous abortion in patients
Garrisi *et al.* (2009)	Blastomeres	RPL (>35 years)	Improved pregnancy outcome with PGS

Table 1.6: Summary of RCT studies with regard to PGS after the RCT from Mastenbroek *et al.* (2007). Note: AMA (Advanced Maternal Age), RPL (Recurrent Pregnancy Loss).

Thus from Table 1.6 it is clear that according to the current RCT data there is no evidence for a benefit of PGS and this statement was confirmed by a meta-analysis study of the RCTs. That is Checa *et al.* (2009) concluded that, in women with poor prognosis or undergoing IVF, aneuploidy screening by PGS is associated with lower pregnancy and live birth rates.

There are several reasons as to why PGS has failed to show a positive outcome in the RCTs that have been performed. They can be categorised as either technical or biological. It is understandable that, because PGS is an invasive technique, biopsy is a key feature. Technically experienced embryologists should be able to perform biopsy of a cell in less than a minute when the embryos are in the biopsy dishes. Extended times of biopsy should be avoided (Cohen *et al.* 2009). A report on children born after blastomere biopsy suggests no added risk factors from biopsy compared to IVF/ICSI children without embryo biopsy (Liebaers *et al.* 2009). Furthermore, another important element associated with biopsy is the culture medium used. Beyer *et al.* (2009) found that, as a result of culture medium change improved PGS success rates could be observed in patients aged less than 40 years. The more complex medium contained components to help embryo osmoregulation and maintain its homeostasis and the authors argue that these compounds could mitigate some of the metabolic stress caused by the abscence of calcium and magnesium in the biopsy medium (Beyer *et al.* 2009). Although more studies are clearly required to further validate these statements, they highlight the importance of technical skills required for embryo biopsy, culture selection and fixation.

Once the biopsy has been performed the blastomere has to be fixed on a glass slide before analysis by interphase cytogenetics can occur. Two methods exist in order to prepare the blastomere, Tween:HCl and fixation using methanol:acetic acid. Both methods require a high degree of expertise and if performed poorly can result in difficulties when diagnosing with FISH ("not real" signals, or dirt) (Wilton *et al.* 2009). In a recent review it was argued that methanol:acetic acid method enables better blastomere fixation, with subsequently less overlapping FISH signals and fewer errors than by other methods (Cohen *et al.* 2009).

FISH, like any laboratory technique faces a number of limitations. First the number of available fluorochromes that are within the visible spectrum is limited; also hybridisation can be subject to failure if the target DNA is inappropriately prepared or not fully denatured. In addition some probes (or fluorescent dyes) can demonstrate cross-hybridisation to sites on other chromosomes (or filters if it is a fluorescent dye) so it is essential for this information to be documented (Wilton *et al.* 2009) and prior validation of probes should be performed to record any undesired properties such as cross hybridisation. Also in cases where multicolour probes are used, it is important to analyse each signal under a dedicated filter to be able to distinguish overlapping from true signals. Overlapping signals can be a source of misdiagnosis especially for monosomies but this applies more to ratio labelled probes, rather than probes with individual fluorochromes per chromosomes (Donoso *et al.* 2007; Cohen *et al.* 2009; Wilton *et al.* 2009). Another difficulty, and source of misdiagnosis associated with FISH, is the interpretation of adjacent signals that are labelled with the same fluorochrome. Chromosome target DNA can alter its conformation leading to a "split signal" and it is occasionally difficult to differentiate between a split signal representing one copy of a chromosome and two signals representing two copies for that chromosome (Wilton *et al.* 2009). One possible solution is the introduction of a criterion in which separate signals need to be one signal's diameter apart (Wilton *et al.* 2009). In addition, poor quality embryos have a higher probability of having degenerate interphase chromatin, apoptotic cells or cytoplasm that can interfere with FISH signals (Uher *et al.* 2009).

Despite the aforementioned technical difficulties regarding PGS the most important factor that could be responsible for the missing efficacy of PGS seems to be that of chromosome mosaicism.

The presence of mosaicism at cleavage stage embryos on day 3 has been reported to be as high as 57% (Donoso *et al.* 2007). These embryos are the consequence of mitotic errors post-zygotically and a major source of misdiagnosis in PGS, especially if one blastomere is analysed only (and gives an abnormal result), as it may not be representative of the remaining embryo (Donoso *et al.* 2007; Fauser 2008; Fritz 2008; Hernandez 2009). The high percentage of mosaicism in the 8-cell stage is reduced to 30% in miscarriages, 20% in still births and 0.3% in newborns, indicating that during

the process of development the embryo undergoes self-correction mechanisms based on cell cycle checkpoint control and apoptosis (Hernandez 2009). These mechanisms have been documented in the blastocyst stage but not during the early cleavage stage (Los *et al.* 2004; Hernandez 2009). This has been one of the reasons for arguing in favour of blastocyst biopsy, rather than cleavage stage biopsy and recently a pregnancy following trophectoderm biopsy has been reported (Krieg *et al.* 2009).

Despite the above disadvantages of PGS, there are still certain advantages. The identification of aneuploid embryos that are not transferred prevents high risk patients from having a miscarriage or a viable abnormal pregnancy. The same applies to trisomic conceptions and thus it helps patients with high frequency of aneuploid embryos to choose alternative options (e.g. donor gametes) to achieve a pregnancy (Harper *et al.* 2008).

Also studies that have followed the birth of children from PGS have shown similar prenatal and postnatal growth and health outcome in the first two years of life compared to ICSI children (Desmyttere *et al.* 2009). Recently a study examined the effect of PGS on neurodevelopmental outcome in children. The sample size was small nevertheless the conclusion was that PGS is not associated with a less favourable neurological outcome (Middelburg *et al.* 2010). With regard to the future of PGS, the investigation of new technologies (array based) alternative biopsy timing (polar body or blastocyst) and complete chromosome screening are the major goals. A multicentre RCT using polar body biopsy and array CGH has been proposed by the ESHRE PGD consortium for AMA patients and is underway (Geraedts *et al.* 2009; Harper *et al.* 2010a). Initial results are encouraging (Fragouli *et al.* 2009; Schoolcraft *et al.* 2009a). Recently a novel diagnostic test (Karyomapping) that uses state of the art SNP (single nucleotide polymorphism) technology provides great promise to unify all PGD diagnostic tests (monogenic disorders, copy number variants) in a single platform (Handyside *et al.* 2009).

1.4.6. PGS and Interphase Cytogenetics

As seen in section 1.4.5, FISH for interphase cytogenetics has been used widely in the screening of embryos for aneuploidy. This usually involved the use of 9 probes in a two layer experiment (Thornhill *et al.* 2005). Screening for more chromosomes could

provide a more comprehensive diagnosis in the detection of aneuploid embryos and provide both a clinical and a research benefit. Baart and colleagues showed the added value of aneuploidy detection by screening for 15 chromosomes in cryopreserved day 4 and 5 embryos using three rounds of hybridisation (Baart *et al.* 2007). They used a mix of centromeric and locus specific probes in the first and third round, whereas the second layer comprised of centromeric probes only. They suggested that investigating 6 extra chromosomes allowed them to detect mainly chromosome aberrations of mitotic origin leading to a higher percentage of mosaic embryos (Baart *et al.* 2007). In another study with research interest FISH was used to diagnose whole embryos and compare the diagnosis with the single cell embryos from day 3 that were found abnormal and thus were not transferred (DeUgarte *et al.* 2008). Out of 198 abnormal embryos 164 were confirmed when the whole embryo was analysed by FISH giving a positive predictive value of 83% signifying that 17% of embryos are misdiagnosed as abnormal on day 3 when they are in fact normal (DeUgarte *et al.* 2008). This could be very interesting as it would provide another means of confirming the high level of mosaicism in cleavage stage embryos and thus provide insight into how representative is the single cell with regard to the whole embryo. In this regard, a hitherto undemonstrated 24 chromosome FISH-based interphase cytogenetics screen would be of incredible value and this is one of the aims of this thesis (see Chapters 4 and 6).

Another study that showed the potential for increased number of chromosome screening was by Colls *et al.* (2009). Using three rounds of hybridisation and a mix of centromeric and telomeric probes in the last round, they screened for 12 chromosomes and they found that embryos diagnosed as normal for the initial chromosome panel (9 chromosomes) had extra abnormalities that would not have been found without extended screening. They postulate however that due to the use of telomeric probes to the end and suboptimal conditions, the error rate was slightly higher from the percentage found for the 9 chromosomes alone (Colls *et al.* 2009). Thus the extended screening can be important in revealing other "non-common" abnormalities found in preimplantation embryos.

In the most recent study a 12-chromosome screen was used in blastocysts to compare screening efficiency between FISH and CGH, aCGH and SNP microarrays (Munne *et al.* 2010). Using a 10 and 12 probe panel the efficiency of detecting aneuploid

blastocysts was 89 and 91% respectively compared to the 100% (in theory) that the comprehensive chromosome screen allows. However these methods have other drawbacks as high cost (double from FISH) and require blastocyst freezing to provide a diagnosis (Munne *et al.* 2010). Hence improved FISH tests can be tailored to different subgroups of patients and be price competitive with SNP arrays and CGH, although these techniques will eventually substitute interphase cytogenetics as the method of choice for PGD once technical optimisation is achieved and reagents drop significantly (Munne *et al.* 2010).

Thus although in terms of PGD, FISH will, most likely be eventually replaced in the future, research-wise it is still a valid cytogenetic tool. Using a complete chromosome screen in preimplantation embryos it would be possible to gain insight into the types of abnormalities occurring (e.g. monosomies, trisomies), the level of mosaicism from analysis of all chromosomes, and the relationship between nuclear organisation and chromosome abnormalities.

1.4.7. The future of PGD and Cytogenetics

Since its first application in 1993 for PGD by Griffin *et al.* (1993) to prevent X-linked disorders FISH has been a valuable diagnostic tool for almost 20 years. The limits imposed by the current number of chromosomes tested, the number of available fluorophores and the biology behind the current diagnosis platform (i.e. blastomere, mosaicism) are some of the reasons that the future of PGD (and PGS) are moving towards higher resolution techniques like array CGH.

Array CGH (aCGH) essentially scans the genome for gains or losses of chromosomal material through comparative hybridisation of a patient (usually labelled in green) DNA and a control DNA (usually labelled in red) into a selected set of pre-spotted genomic fragments (array). If the intensities of red and green are the same for one spot, then this region of the patient DNA is interpreted as normal or balanced. If the intensity of green has reached a threshold then duplication (gain) for that part of the patient DNA is suspected or inversely a deletion (loss) when the red has reached an appropriate threshold (de Ravel *et al.* 2007). With the advent of whole genome amplification technology (WGA), aCGH can be applicable to low quantities of DNA

reaching the single cell level and used in detecting chromosome copy number and also copy number variations (CNVs).

However the future holds another challenge, to be able to have a single test that would allow detection of single gene disorders, copy number variants and the incidence and origin of chromosomal abnormalities simultaneously. A new diagnostic test currently receiving great attention is Karyomapping (Handyside *et al.* 2009). Karyomapping uses SNP genotype analysis (300,000 SNPs) of parents and offspring and allows the mapping of crossovers between parental haplotypes and the construction of a "Karyomap" which identifies the independent segregation patterns of parental chromosomes and also the recombination patterns. Hence at the same time information regarding a gene disorder, chromosome abnormalities (structural, numerical) and aneuploidy can be offered simultaneously through analysis of informative SNPs. Figure 1.14 shows the progress from low resolution to high resolution diagnostics.

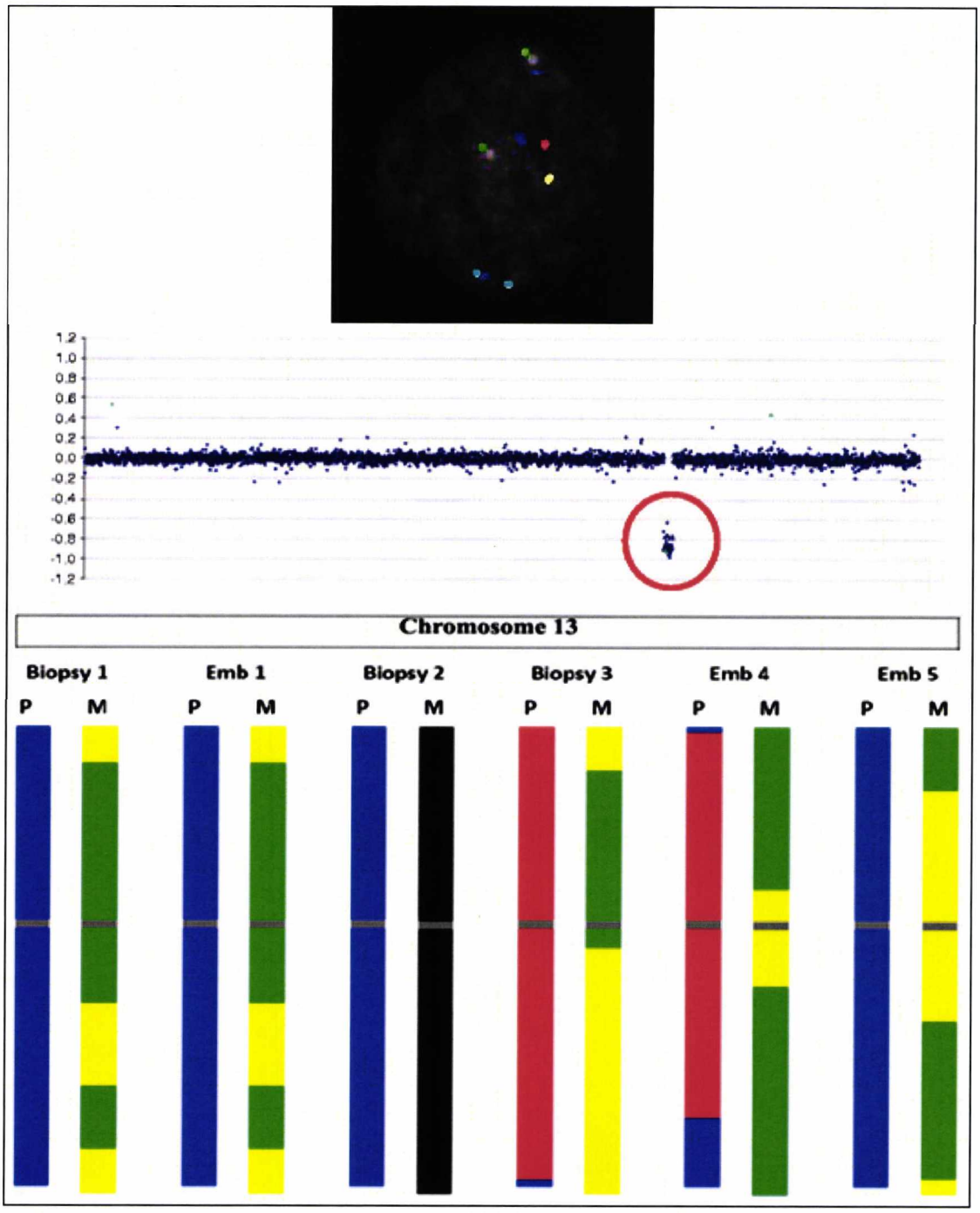

Figure 1.14: The progress in single cell diagnostics. At the top a blastomere from PGS with FISH showing monosomy for chromosome 13 (1 red signal). Information about copy number is offered for 5 chromosomes (5 different fluorophores). aCGH data analysis (middle) for all chromosomes showing a loss for chromosome 13 (red circle). A karyomap output (bottom) from 5 blastomeres for chromosome 13. Aneuploidy information (e.g. Monosomy 13-embryo 2, Trisomy 13-embryos 3 and 4) origin of aneuploidy (e.g. Maternal-Biopsy 2, Paternal-Biopsy 3, 4) can be deduced immediately Karyomaps like that are produced for all chromosomes providing a complete diagnosis. Adapted from (de Ravel *et al.* 2007) for the aCGH data and (Handyside *et al.* 2009) for Karyomap data.

1.4.8. Aneuploidy in human preimplantation embryos

Embryo development begins at fertilisation, which triggers completion of MII in the oocyte and subsequent fusion of male and female pronuclei in the zygote. Paternal and maternal genomes replicate and the zygote undergoes mitotic divisions (cleavage) until the fourth day when it compacts to form the morula and begins to differentiate with the formation of the trophectoderm and inner cell mass of the blastocyst (Ambartsumyan & Clark 2008).

The incidence of chromosomal abnormalities is approximately 0.6% in newborns, 6% in stillbirths and 60% in spontaneous abortions (Martin 2008). Most abnormalities are lethal and do not survive to term, however certain chromosomal abnormalities do survive and the following table shows the major numerical abnormalities and incidence per 10,000 births.

Syndrome	Abnormality	Incidence per 10,000 births	Lifespan of affected individual
Down	Trisomy 21	15	40
Edward	Trisomy 18	3	<1
Patau	Trisomy 13	2	<1
Turner	Monosomy X	2 (female births)	30-40
Klinefelter	XXY	10 (male births)	Normal
XXX	XXX	10 (female births)	Normal
XXY	XYY	10 (male births)	Normal

Table 1.7: Major copy number abnormalities that survive to term. Adapted from http://genome.wellcome.ac.uk/doc_wtd020854.html

With the advent of *in vitro* fertilisation (IVF) and interphase cytogenetics in determining copy number of individual chromosomes in a PGD setting, it was possible to study the aneuploidy rates at this early stage of development (early studies reviewed by Griffin (1996)). Munné *et al.* (2004) analysed 2000 embryos using probes for 14 chromosomes and found that the most frequently involved chromosomes in aneuploidy were 22, 16, 21 and 15, whereas the least involved were 14, X, Y. They also reported higher rates of monosomy rather than trisomy. Another important finding from studies in embryos is that the predominant type of mosaicism affecting preimplantation embryos is the diploid aneuploid type arising from one of the first three division (probably first or second) (Delhanty *et al.* 1997; Daphnis *et al.* 2005). In a recent study by Daphnis *et al.* (2008), embryos were compared to

investigate the evolution of chromosome abnormalities between the cleavage and blastocyst stages The drawn conclusion was that a normal blastomere on day 3 is more likely to give rise to blastomeres with the correct chromosome complement on day 5, whereas an abnormal cell on day 3 suggests for a poor outcome on day 5.

To summarise the above, three trends seem applicable for aneuploidy in human preimplantation embryos (Munne *et al.* 2007a):

1. Aneuploidy increases in cleavage stage embryos with maternal age, irrespective of embryo morphology.
2. Post meiotic abnormalities (mosaicism, polyploidy, haploidy) increase with decreasing embryo development and increase dysmorphism.
3. Post meiotic abnormalities are the most frequent type of abnormalities.

On a molecular level a model for maintaining genomic integrity of preimplantation embryos suggest that human embryos inherit an elevated level of mitotic and cell cycle proteins from the oocyte to ensure that these factors are enough during cleavage stage (Ambartsumyan & Clark 2008). When these factors are limited and aneuploidy occurs the cell cycle checkpoint is not activated. The result of this is the accumulation of aneuploid cells. Upon lineage differentiation the cell cycle and mitotic checkpoint resume and severely aneuploid cells are eliminated. The outcome of this mechanism would be translated as spontaneous abortion or birth defects. However if aneuploid cells are completely removed upon differentiation then a possible euploid embryo might develop (Ambartsumyan & Clark 2008).

A 24 chromosome screen for human embryos would allow a number of these investigations to be taken a step further and address the issues of aneuploidy on a chromosome by chromosome basis. Moreover, it would allow the study of a hitherto under-explored area in preimplantation genetics – that of nuclear architecture (or nuclear organisation) which is commonly assayed by determing the nuclear address of FISH signals in interphase nuclei.

1.5. Interphase cytogenetics and nuclear architecture

The nucleus is a highly complex and compartmentalised organelle that accommodates a wide spectrum of actions, such as genome replication, transcription, splicing and DNA repair. The level of organisation can be considered with regard to chromatin (chromosomes), the interchromatin compartment and specialised structures (nucleolus, nuclear matrix). Chromosomes occupy distinct positions within the nucleus termed chromosome territories (CTs) (Cremer & Cremer 2001; Parada & Misteli 2002) and the position they occupy (usually defined radially i.e as "central", "medial" or "peripheral") with respect to the topology of the nucleus is often termed "**nuclear address**." Thus nuclear organisation (for the purposes of this thesis) is defined as the spatial and temporal location of chromosomes in the interphase nucleus. "Nuclear architechture" refers to the organisation of both the chromatin and the nuclear proteins in the nucleus; while "chromosome position" and "nuclear address" are used interchangeably (as is common in the literature) to mean the part of the nucleus that the chromosome territory or specific locus occupies (e.g. central, medial, peripheral). A recurring theme of this thesis is the nuclear address (chromosome position) of loci used to assess aneuploidy in interphase nuclei, specifically to ascertain the relationship between chromosome copy number and nuclear organisation/architechture.

1.5.1. Brief historical perspective

The concept of the territorial organisation of chromosome originates from the late 19th century. It was Carl Rabl (1885) who first suggested it from studying epithelial cells from *Salamandra maculate larvae*. However it was Theodor Boveri (1909) who first coined the term chromosome territory (CT) from studying the roundworm *Ascaris megalocephala*. Boveri argued that each chromosome occupied a distinct part in the nuclear space of the interphase nucleus (Cremer & Cremer 2006a). Despite this early evidence for CTs, the concept fell into disgrace obscurity during the 1950s to the 1970s. That is, it was mostly electron microscopy studies that argued for an unravelling of chromosomes in interphase nuclei into intermingling chromatin fibers with no sign of individual chromosomes (Cremer & Cremer 2006b).

The first experimental evidence for the existence of CTs came in 1977 by Stephen M. Stack, David B. Brown and William C. Dewey where fixed cells from *Allium cepa* and Chinese hamster were treated with acetic acid, air dried, subjected to salt conditions and then Giemsa-stained. This treatment resulted in clumps of condensed chromatin reflecting interphase chromosomes (Stack *et al.* 1977). Furthermore Thomas and Christoph Cremer proved the existence of CTs using laser-UV-micro-irradiation experiments. Using a laser beam they induced local damage to a small part of a diploid Chinese hamster nucleus. If chromosomes had distinct territories only a few would be affected by damage, if the arrangement was random, many would be affected. The former was demonstrated and thus argued for a CT arrangement (Cremer & Cremer 2006b). With the advent of technology (mid 1980s onwards) and especially FISH direct visualisation of CTs was made possible. The generation of chromosomes specific probes, allowed scientists to delineate individual chromosomes in metaphase spreads and their territories in interphase nucleus. Also combination of 3D-FISH and confocal microscopy allowed the spatial reconstruction of CTs (see Cremer & Cremer (2010) for more details on direct evidence of CTs).

Once the concept of CTs was re-discovered, researchers looked for patterns of proximity as these could provide functional advantages and thus were favoured by natural selection. Finding patterns like that and their functional implications constitute one of the major goals in nuclear organisation studies. Two major models that have attempted to address the radial position of chromosome territories are discussed below.

1.5.2. Models of chromosome position/nuclear address - Gene density model

It has been widely accepted that CT position in the interphase nucleus is non-random (Manuelidis 1990; Cremer *et al.* 2001; Marshall 2002; Oliver & Misteli 2005; Khalil *et al.* 2007; Meaburn & Misteli 2007). The first evidence to support a "gene density model" came by Croft *et al.* (1999), where the position of human chromosome 18 and 19 was studied in lymphoblasts and dermal fibroblasts. Although similar in size, these two chromosomes are different in gene density with 18 being gene-poor and 19 gene-rich. Results showed that chromosome 18 was located at the periphery of the nucleus whereas chromosome 19 was located preferentially towards the nuclear interior.

These observations were also confirmed in another study using 3D-FISH by Cremer *et al.* (2003). Additional evidence was presented in a study by Boyle *et al.* (2001), where human chromosome position was studied in lymphoblasts cells from normal and X-linked Emery-Dreifuss muscular dystrophy (X-EDMD) males, where emerin protein was lacking. They found that chromosomes 1, 16, 17, 19, 22 were positioned in the centre of the nucleus whereas chromosomes 2, 4, 13, 18 were more peripherally located and this preference was not altered in mutant cells. Furthermore, Lukasova *et al.* (2002) studied chromosome territory position in lymphocytes and found that the gene rich chromosomes 9, 17 were positioned close to the centre of nucleus, whereas chromosomes 8 and 13 were found close to the nuclear membrane. In the most recent study to support the gene density model, Federico *et al.* (2008) examined chromosome 7 in lymphocytes. This chromosome contains large block of both gene-dense and gene-poor regions. The gene-rich regions were exposed towards the interior, whereas the gene-poorest located towards the periphery.

The gene density model has also been observed in primates, where orthologous sequences to human chromosomes 18 and 19 were used and occupied positions similar to humans (Tanabe *et al.* 2002), in old world monkeys (Tanabe *et al.* 2005), rodents (cited in Cremer and Cremer (2010)), in chicken (however chicken also fits the size model – below) (Habermann *et al.* 2001) and in cattle (Koehler *et al.* 2009). **All of the above point to the notion that individual chromosome territories and loci occupy a specific nuclear "address" which can alter according to the cell type or related to disease**. The concept of nuclear address is one of the core themes of this thesis.

The functional implications of the gene density model are associated with the transcriptional machinery and the separation of the nucleus to transcriptionaly active (gene rich chromosome areas) and transcriptionaly silent (gene poor areas) regions in order to enhance expression or repression (Foster & Bridger 2005; Meaburn & Misteli 2007). Evidence for this is suggested from the movement of specific genes from periphery to interior upon their activation (e.g. β-globin during differentiation of mouse erythroid cells) (Takizawa *et al.* 2008). However this topic is still under debate as there are genes that move towards the periphery upon activation (Takizawa *et al.*

2008) or reports about transcription sites throughout the nucleus (Foster & Bridger 2005).

1.5.3. Models of chromosome position/nuclear address - Chromosome size model

The size model with regard to chromosome position classifies chromosome territories according to their size, with the small chromosomes being close to nuclear interior and large ones towards nuclear periphery. This model initiated from observations in cells undergoing quiescence or senescence. Small chromosomes 13 and 18 were positioned towards the interior (Bridger *et al.* 2000) and large chromosomes X and 4 were at the nuclear periphery (Foster & Bridger 2005).

In a study by Sun *et al.* (2000), in fibroblasts it was demonstrated that q-arms of small chromosomes were positioned in the interior (e.g. 19, 21) whereas q-arms of large chromosomes (e.g.1, 2), were positioned towards the nuclear periphery thus conferring upon a size model for position. Interestingly the authors' postulate that the interior position of chromosome 21 is in concordance with the nucleolus position, since 21 is one of the nucleolus organiser region (NOR) chromosomes (remaining are 13, 14, 15, 22) (Sun *et al.* 2000). Similar evidence is published for chromosomes 13 and 15 (Kalmarova *et al.* 2007). The position of NOR chromosomes with regard to the nucleolus seems to be conserved through mitosis (Kalmarova *et al.* 2008).

Further support for the size model came by a 3D-FISH study by Bolzer *et al.* (2005) in flat-ellipsoid fibroblast and amniotic fluid cell nuclei, where all the chromosomes were studied. This pattern of position was in contrast to the density correlated position seen in the spherical lymphocytes. However gene-density correlated patterns were found when the distribution of Alu sequences were studied (Alu corresponds to GC-richness), with Alu-rich chromatin positioned in the nuclear interior and Alu-poor attached to nuclear envelope (Bolzer *et al.* 2005).

These are the current two models attempting to explain the radial arrangement of chromosomes in interphase nuclei. Each model seems to be cell type specific, although there are some systems where both models fit [e.g. chicken, New World monkeys – (Mora *et al.* 2006)], others were none seems applicable [e.g. murine –

(Meaburn *et al.* 2008)]. Bridger and Foster propose that these two models are not mutually exclusive, but chromosome position depends on the status of the cell and/or chromosome (Foster & Bridger 2005). In a recent review Cremer and Cremer argue that local gene density is a pivotal factor for the radial position of chromatin but also point that other parameters could be involved (e.g. replication timing) (Cremer & Cremer 2010). More studies in a range of organisms can only elucidate any link between radial positioning and functional implications in nuclear architecture.

1.5.4. Further models of nuclear architecture

The chromosome territory-interchromatin compartment (CT-IC) model divides the nucleus into CTs and the space between them, termed interchromatin compartment (IC). Initially the IC concept originated as the ICD (interchromosomal domain) proposed by Lichter *et al.* (1993) The ICD was described as the space expanding around CTs with little penetration into the actual CTs (Branco & Pombo 2007).

This model claims that active genes are located in the periphery of CTs in order to be accessible to transcription and splicing factors that accumulate in the IC. Conversely the inactive genes would be located in the interior of CTs and thus would have limited accessibility to the transcription machinery (Foster & Bridger 2005; Branco & Pombo 2007; Heard & Bickmore 2007). However evidence that genes could be transcribed both inside and outside of CTs adjusted the ICD concept (no penetration of interchromatin domain to CTs) to the IC concept where the "sponge" like CTs are permeated by intraterritorial IC channels (Cremer & Cremer 2010) (Figure 1.15).

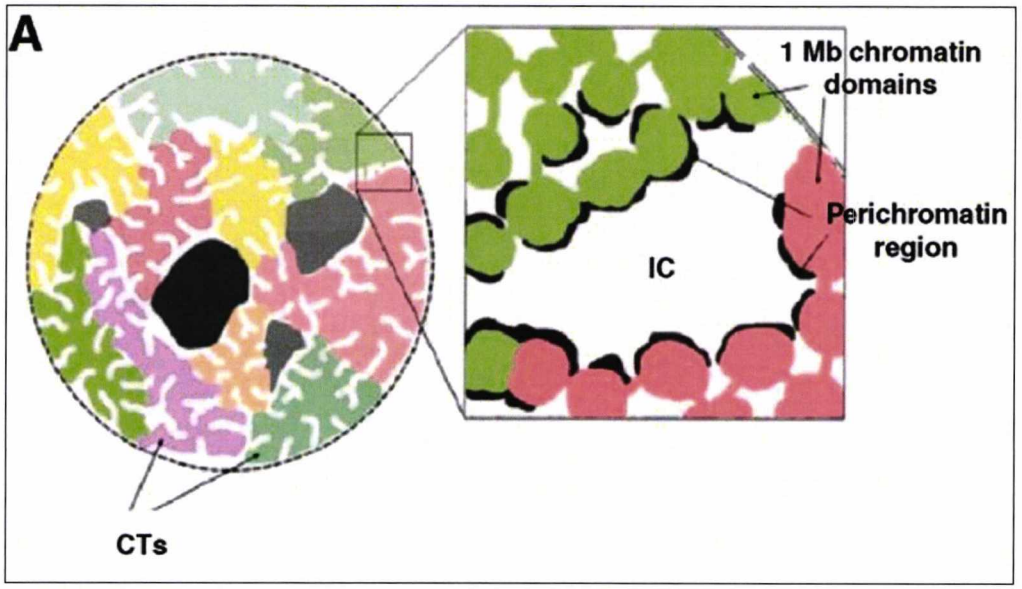

Figure 1.15: The CT-IC nuclear architecture model with CTs being permeated by the IC channels (left side of figure), for more efficient expression. Adapted from (Cremer & Cremer 2010).

Another level of separation between the condense CTs and IC is the perichromatic region (PR) (Figure 1.15 – right side) which seems to be a thin layer of decondensed chromatin which represents the subcompartment where transcription, co-transcriptional RNA splicing and possibly DNA repair occurs (Cremer & Cremer 2010). One important assumption that this model proposes is that small scale loops of 50-200kbp built up the CTs. These are termed ~100kbp loops and their configuration changes depending on the transcriptional status of its genes (Cremer *et al.* 2006).

Another model proposed by Dehghani was based on electron microscopy studies is the lattice model (Figure 1.16), where there is intermingling between adjacent CTs. This intermingling is in the form of 10-30nm chromatin fibers (Branco & Pombo 2007; Heard & Bickmore 2007).

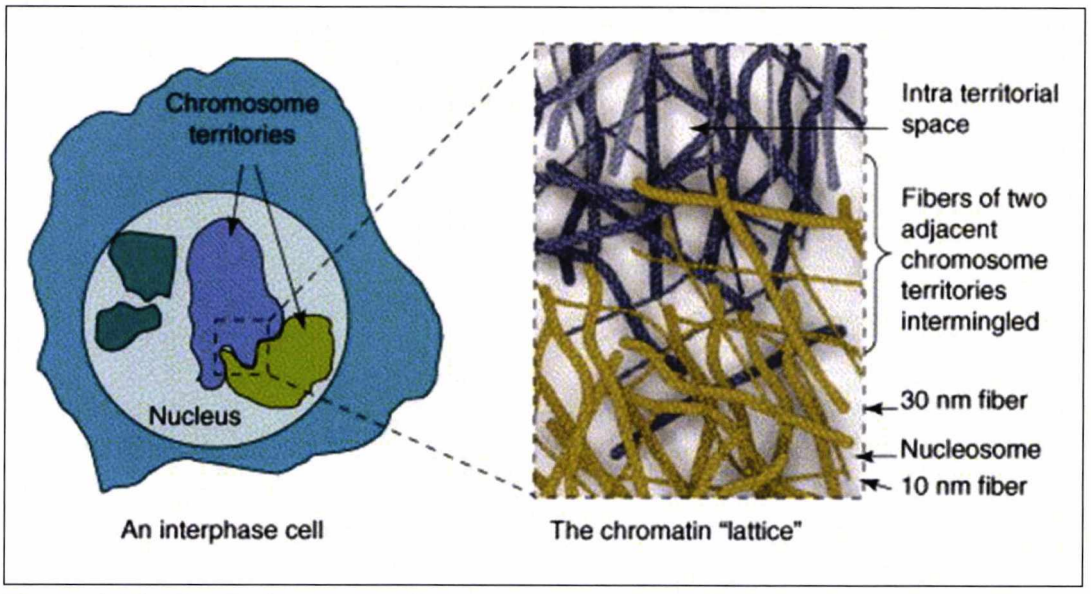

Figure 1.16: The lattice model of nuclear architecture with intermingling in the form of chromatin fibers between neighbouring CTs. Adapted from (Branco & Pombo 2007).

One difference between the lattice and the CT-IC model is that the former argues against the presence of large chromatin free channels, essentially the IC becomes the space within the lattice of 10-30nm fibers (Branco & Pombo 2007).

The interchromatin network (ICN) model was the result of numerous observations of interchromosomal associations (reviewed in Branco and Pombo (2007)). This supports a flexible genome with a high degree of intermingling. The same authors reported intermingling regions reaching 19% of the nuclear volumes with more than one chromosome involved (Branco & Pombo 2006). Thus the ICN proposes that chromatin fibers and loops intermingle in a uniform way either in the interior of individual CTs or between neighbouring CTs (Cremer & Cremer 2010). Also it argues that the nuclear address and conformation will be defined by the tethering of inter or intrachromosomal associations with other nuclear landmarks like the lamina or the nucleolus (Branco & Pombo 2007). Evidence suggests that lamina interacting domains display low gene density and expression levels thus rendering them a chromatin repressive environment (Guelen *et al.* 2008; Reddy *et al.* 2008; Fedorova & Zink 2009). In addition the ICN proposes that double strand breaks (DSBs) formed in regions of intermingling will most probably produce interchromosomal rearrangements whereas DSBs somewhere else in the chromosomes will be responsible for intrachromosomal rearrangements (Branco & Pombo 2006). Figure 1.17 illustrates the ICN model.

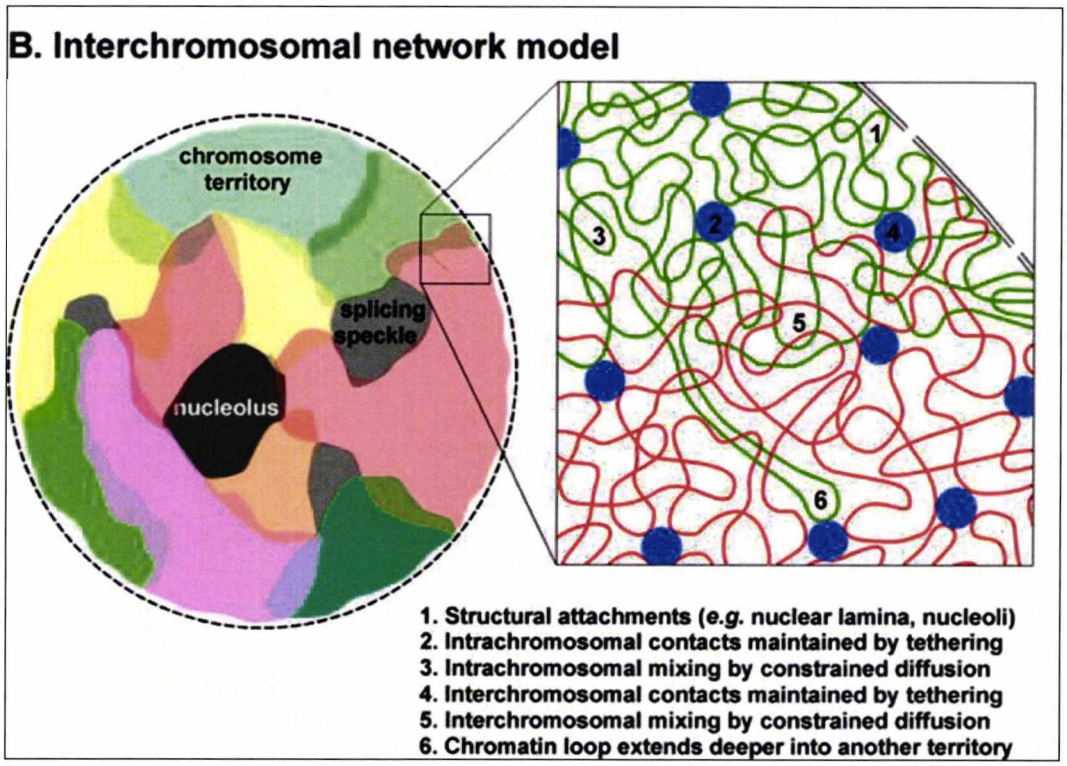

Figure 1.17: The Interchromosomal Network (ICN) model of nuclear architecture. Adapted by (Branco & Pombo 2006).

Despite the three models discussed above, none is fully supported by compelling experimental evidence (Cremer & Cremer 2010). The authors postulate that clarification about the speed and extent of chromatin movement is required and also confirmation or not of the functional tethering between IC and the PR as predicted by the CT-IC model but not by any other. These limitations can be addressed when resolution is improved in light microscopy. Recently a study was published using a technique called Hi-C that allowed mapping of the human genome at a resolution of 1Mbp allowing chromosomes to be visualised as a series of fractal globules (Lieberman-Aiden *et al.* 2009).

1.5.5. Nuclear organisation, nuclear address and cell differentiation

Cell differentiation is a process of specialisation where cells acquire a new phenotype to accomplish specific functions and it is accompanied by activation of a subset of genes and silencing of the remainder (Francastel *et al.* 2000). Thus it becomes a very appealing system in which to study nuclear organisation and gene expression.

Changes in CT or locus position have been observed during differentiation. The immunoglobulin gene cluster repositions from the periphery (in non lymphoid cells) to the centre in pre-B cells, and a similar observation has been described for the Mash1 locus during neural induction (both examples cited in Schneider and Grosschedl (2007)). In both these examples genes tend to localise in the periphery in their inactive state. Furthermore genes like HoxB1 in mouse embryos undergo a shift towards internal location upon activation (Takizawa *et al.* 2008).

The notion seems to be that loci in positions relative to nuclear periphery or heterochromatin domains are linked with gene repression whereas repositioning of loci from nuclear periphery to interior or away from heterochromatin is correlated with gene activation (Takizawa *et al.* 2008; Szczerbal *et al.* 2009). However this suggestion is an oversimplification (it seems to be correlated more for genes whose activity is tightly linked to differentiation) and not universal based on three pieces of evidence: Biallelically expressed genes occupy different radial position in the same nucleus, RNA polymerase II transcription sites are distributed throughout the nucleus (thus transcription is not only occurring internally), and heterochromatin which is largely transcriptionaly silent can be found throughout the nucleus (Takizawa *et al.* 2008). Nevertheless they are based on experiments with the β-globin gene which during its inactive form is in the periphery and remains there until the early stages of activation, and only then repositions towards the interior, it seems that internal position is not a requirement for activity and transcription alone does not drive position of a gene (Francastel *et al.* 2000). Chromosomal neighbourhood seems to be another factor determining whether a locus changes its position. Certain loci show preferred contacts with their neighbours in a phenomenon termed "chromosome kissing" implicated in both transcriptional activation and gene silencing (Cavalli 2007).

Despite this debate with regard to radial position and expression, studies of nuclear architecture in cells undergoing differentiation can still provide important information regarding spatial genome organisation in relation to function. Kuroda *et al.* (2004) studied the relative positions of chromosomes 12 and 16 during adipocyte differentiation and found a close association of these two chromosomes in the differentiated adipocytes. This proximity could influence their involvement in

translocations such as the t (12; 16). Although not a study on differentiation *per se*, Parada *et al.* (2004) studied nuclear position of 6 chromosomes in three different tissues and found considerable differences indicating a tissue-specific genome organisation. Szczerbal *et al.* (2009), found a correlation of gene expression and internal positioning for 6 porcine loci during adipogenesis. Marella *et al.* (2009b) investigated the radial arrangement of chromosomes 18 and 19 during human epidermal keratinocyte differentiation. They found repositioning of chromosome 19 closer to the periphery (compared to chromosome 18) in the differentiated cells, plus a decrease in the interchromosomal associations of these two chromosomes. Recently a striking example of CT organisation was shown by Solovei *et al.* (2009) which seems to offer an advantage to the cells that the pattern is shown. More specifically in mammals adapted to nocturnal life, heterochromatin resides to the interior and euchromatin to the periphery during the differentiation of rod cells, whereas in diurnal animals this reorganisaton does not exist. The inverted pattern in the nocturnal mammals reflects an adaptation to low light conditions. This example shows that under a selective pressure nuclear architecture can be modified to accommodate specific functionality (Cremer & Cremer 2010).

In a very important study by Foster *et al.* (2005) chromosome position was investigated into different stages of spermatogenesis using porcine testes as a model system. It was found that the sex chromosomes repositioned from the periphery to the interior during cell differentiation from spermatocytes to mature sperm. It was argued that this non-random position could have a functional significance in the future expression of the paternal genome during embryo development (Foster *et al.* 2005). The consequences of nuclear organisation in spermatogenesis in humans is one of the topics of this thesis.

1.5.6. Nuclear organisation, nuclear address and disease

The link between the spatial position of a gene and its expression denotes the importance to maintain a stable architecture for proper functionality (Verschure 2004). There is evidence in the literature that nuclear architecture is altered in disease. Cremer *et al.* (2003) reported different patterns of CT position for 18 and 19 in normal and in tumour cell lines. In a more recent study by Marella *et al.* (2009a) they argued for a difference in CT association for chromosomes 4 and 16 in breast cancer

lines compared to normal cells, suggesting that organisation is altered in cancer cells. In addition several studies have highlighted that certain translocations could be generated due to close proximity of the chromosomes involved. An example are the Robertsonian translocations due to the close proximity of the nucleolar associated acrocentric chromosomes (reviewed by Foster and Bridger (2005)).

A report by Petrova *et al.* (2007) analysed chromosome position of X and 1 in human cells having one copy and four copies of X chromosome. In the aneuploid cells (XXXY) the active X is closer to the periphery than in normal XY cells. Also in cells with XXXY the position of chromosome 1 shifts towards the periphery compared to normal XY cells. The authors argue for a possible involvement of nuclear changes induced by the presence of extra chromosomes in the development of diseases related to different polysomies (e.g. Down syndrome, Klinefelter) (Petrova *et al.* 2007). Another change in CT position was noticed for chromosome 17 upon infection of lymphocytes with Epstein-Barr virus (EBV) implying genome instability in host cells (Li *et al.* 2009). Other diseases where a possible perturbed nuclear architecture could be involved although not clear yet are promyelocytic leukaemia (PML), X-linked mental retardation and Huntington's disease (Misteli 2005).

However the most common involvement of perturbed nuclear architecture and disease is found in laminopathies (Foster & Bridger 2005; Misteli 2005). Patients have a mutation in LMNA gene and phenotypes are associated with muscular dystrophy, lipodystrophies, neuropathies and premature ageing disease (Hutchinson-Gilford Progeria) (Misteli 2005). Recently it was shown that, in patients with mutations in the LMNA gene, positions of CT 13 and 18 are more interior than controls (Elcock & Bridger 2010). Possible explanations for the causative mechanisms of the disease purport that mutations in LMNA weaken nuclear integrity by exposing nucleus (more specific nuclear matrix) to mechanical stress or that mutations cause misregulation of genes (Foster & Bridger 2005; Misteli 2005).

If perturbed nuclear architecture is indeed manifested as altered chromosome (and thus gene) position, this could change the local gene environment and the availability of transcription factories thus leading to misregulation or even non-participation of

some genes in transcription (Elcock & Bridger 2010). Further associated studies of gene position and expression will be able to confirm or refute this hypothesis.

One specifc aim of this thesis is to investigate chromosome loci position in sperm cells and preimplantation embryos, and to explore potential association between nuclear organisation with infertility and aneuploidy.

1.5.7. Nuclear architecture in sperm cells

Spermatogenesis can be summed up in three main phases; the mitotic proliferation of spermatogonia to produce spermatocytes, the meiotic divisions to produce round spermatids and spermiogenesis where the early spermatids are maturing to elongated spermatids.

It is during the last stage of spermiogenesis where reorganisation and compaction of the sperm chromatin occurs, as histones are being replaced first by transition proteins (Meistrich *et al.* 2003), followed by protamines (Ward & Coffey 1991). Quantitavely this can be expressed as 15% of chromatin still bound to histones whereas 85% bound by protamines (Wykes & Krawetz 2003). Work by Carrel and colleagues has shown that chromatin is still intact with histones in sperm enriched at important loci important for embryo development (e.g. genes for key embryonic transcription factors) (Carrell & Hammoud 2009). Figure 1.18 shows the compact nature of sperm chromatin.

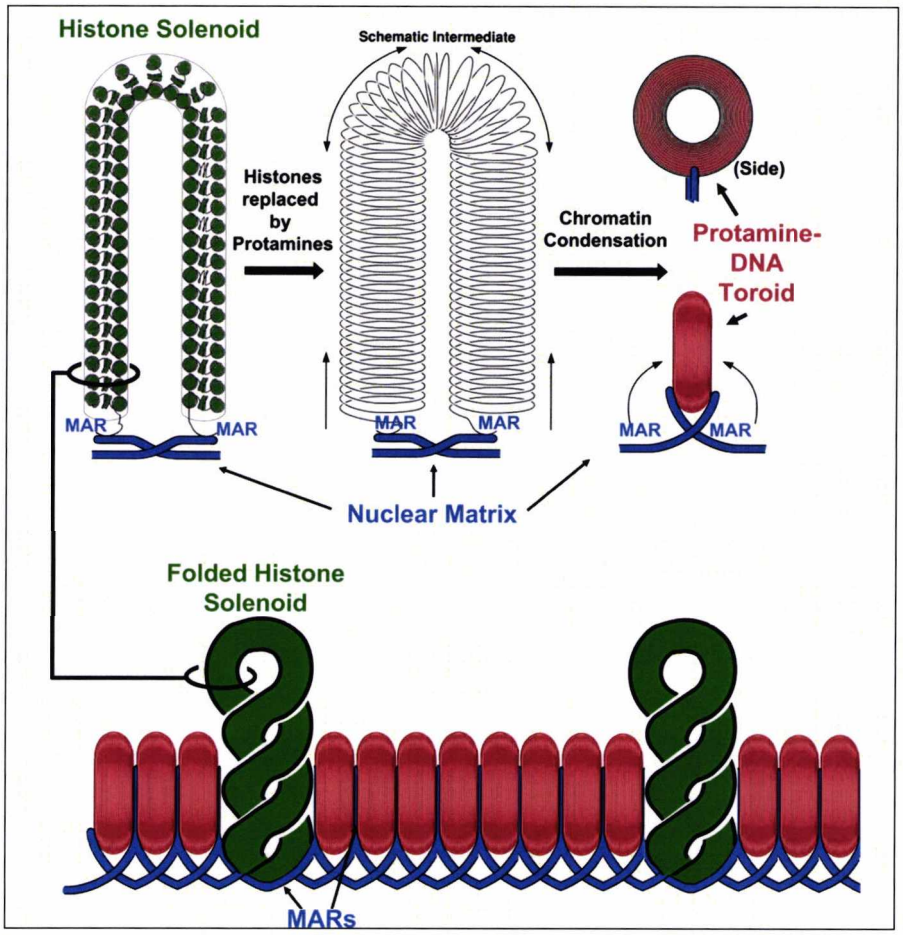

Figure 1.18: Sperm chromatin compaction. The top panel shows replacement of histones by protamines, whereas the bottom shows the arrangement of protamines and remaining histone associated chromatin. Adapted from (Ward 2009).

The major component of protamines is arginine which brings the abundance of positively charged $-NH_3^+$ groups into the protamines (Bjorndahl & Kvist 2009). The functional implication of this is that $-NH_3^+$ groups neutralise the negative charges of the phosphate groups in the DNA backbone allowing a higher degree of compaction of chromatin (Bjorndahl & Kvist 2009). This highly compacted DNA (10^{-6} fold compared to 10^{-5} fold offered by histones) provides an efficient packaging to facilitate proper delivery of the paternal genome to the egg (reviewed in Miller *et al.*(2010)).

The cysteine residues of protamines confer extra stability in the sperm chromatin through intermolecular disulphide cross-links (Ward 2009). Ward also argues that sperm chromatin rearrangement (by protamines) is to ensure proper fertilisation (as a protective agent of the paternal genome) and not for embryonic development. Evidence for this was suggested from experiments where it was shown that

protamines were replaced 2-4hrs post fertilisation by histones thus conferring access to the paternal genome (Ward 2009). Protamines also serve as the silent agents of gene expression during spermiogenesis (Ward 2009).

The nuclear organisation in human sperm has been extensively studied and well defined (Haaf & Ward 1995; Zalensky *et al.* 1995; Hazzouri *et al.* 2000; Tilgen *et al.* 2001; Mudrak *et al.* 2005). The position of the chromosomes is non-random with the chromosomes clustering via the centromeres to form the chromocentre (well inside the nucleus) and the telomeres exposed towards the periphery, where they interact to form dimers (Zalensky *et al.* 1993; 1995; Luetjens *et al.* 1999; Solov'eva *et al.* 2004; Zalenskaya & Zalensky 2004).

Similar spatial organisation seems to be retained in other mammals as it is indicated by data from bovine (Zalenskaya & Zalensky 2004), mouse (Haaf & Ward 1995; Meyer-Ficca *et al.* 1998), pig, horse and rat (Zalenskaya & Zalensky 2004) studies.

The chromocentre was visualised using CENP-A immunolocalisation and FISH using α satellite probes for all chromosomes (Zalensky *et al.* 1993). It seems that the chromocentre is actually pericentric heterochromatin from different chromosomes, which has the tendency to aggregate (Martin *et al.* 2006b). The fact that CENP-A is found in mature spermatozoa [this protein exists in the context of nucleosome structure (Sullivan 2001)] indicates that centromeric DNA exists in both nucleosomal and protamine organisation, and this suggests that these regions of the chromosomes may not need to undergo through dramatic remodelling following fertilisation (Zalensky & Zalenskaya 2007).

With regard to the telomere structure, the dimers are formed between the p and q telomeres of each chromosome, conferring a hairpin loop structure (Figure 1.19) (Solov'eva *et al.* 2004; Mudrak *et al.* 2005). Zalensky and Zalenskaya argue that such a configuration could favour an ordered withdrawal of chromosomes via telomeres through their association with the sperm microtubule machinery (Zalensky & Zalenskaya 2007). The importance of telomeres in fertilisation has been shown in mice, where telomerase knockout disrupts reproductive function (Zalensky & Zalenskaya 2007).

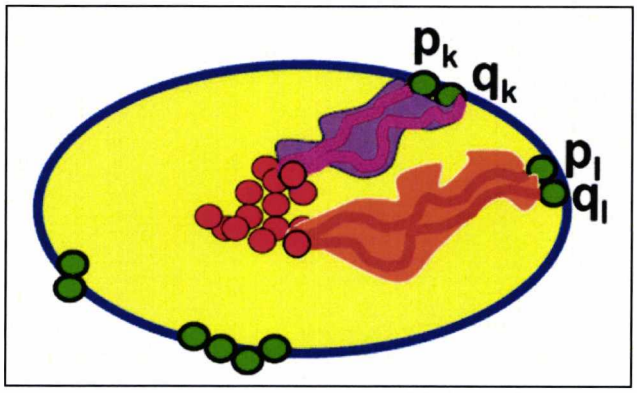

Figure 1.19: The hair-pin loop configuration of human sperm cells, with centromeres (red dots) in the interior and telomere (green dots) in the periphery. Adapted from (Mudrak *et al.* 2005; Zalensky & Zalenskaya 2007).

The positioning of chromosomes in human sperm has been studied both longitudinally and radially. A combination of data (Luetjens *et al.* 1999; Hazzouri *et al.* 2000; Zalenskaya & Zalensky 2004; Mudrak *et al.* 2005) arranges 11 chromosome territories in the following order starting from the acrosome with direction towards the tail: X, 7,[6, 15, 16, 17],1, [Y, 18] 2, 5, whereas chromosome 13 seems to occupy a random position. The functional implication of this could be that the order that chromosomes are being affected by the maternal cytoplasmic environment after fertilisation is specific (Zalensky & Zalenskaya 2007). The above sequence when expressed radially depicts chromosomes 7 and 6 being most peripheral and chromosomes 16 and 18 most internal. The functional implication now would be that the most peripheral chromosomes are first exposed to ooplasm and undergo earlier remodelling from others (Zalensky & Zalenskaya 2007).

It should be emphasized that the positions of the sex chromosomes relative to the acrosome are similar in sperm of all mammals (but not birds) implicating a functional significance with regard to paternal X inactivation (Greaves *et al.* 2003). Another piece of evidence for the significance of preferential location of the sex chromosome comes from Luetjens *et al.* (1999) who suggested that sperm used in ICSI that have not gone through acrosomal reaction, could impair chromatin decondensation located in the apical region (e.g. the sex chromosomes) and thus hinder progression to the first mitotic division of the zygote, hence causing mitotic errors translated as sex chromosome abnormalities in ICSI offspring.

Emerging from these facts becomes the functional significance of the non-random position of chromosomes in human sperm and its possible impact on fertilisation. It has also been generally accepted that sperm of males with compromised fertility contain numerical chromosome abnormalities, malformations or structural rearrangements.

Zalensky and Zalenskaya (2007) argue for a different category of sperm chromosome abnormality with regard to atypical packing of CTs in sperm, aberrant positioning of chromosomes or even disturbed telomere-centromere interactions. Further to that it has long been postulated that sperm with chemically interrupted nuclear matrix (which mediates the attachment sites of compacted sperm chromatin) cannot produce viable offspring (Ward *et al.* 1999). Thus it seems plausible to investigate whether perturbed nuclear organisation in sperm is observed in men with impaired fertility by assaying chromosome position/nuclear address. Only a handful of studies have tried to investigate this possible link.

In a study from Sbracia *et al.* (2002) they investigated the longitudinal nuclear address of the sex chromosomes between normal and oligospermic males going through ICSI without finding a difference. Wiland *et al.* (2008) found inter-individual differences in centromere topology between normal males and reciprocal translocation carriers. Olszewska *et al.* (2008) compared longitudinal positions for chromosomes 15, 18, X and Y between control males and infertile patients without finding a difference in nuclear address. All these studies examined nuclear address in the longitudinal axis and argued that a larger number of individuals and more chromosomes were required. Thus far the only study which examined the radial position for 3 centromeres (X, Y, 18) between normal and infertile males was by Finch *et al.* (2008b) where it was found that all centromeres occupied central positions in normal males but the sex chromosomes showed altered nuclear address in some of the infertile patients (adopting a pattern not discernable to a random distribution). To the best of my knowledge however this phenomenon has not been explored across all chromosomes in the human karyotype. One principal aim of this thesis is therefore to investigate a possible link between altered genome organisation (i.e. nuclear address of specific loci) and infertility by using a larger cohort of patients, by studying all chromosomes (see Chapter 5).

1.5.8. Nuclear architecture in oocytes

As described in section 1.2.1 oogenesis is the process that produces the female haploid gamete. Studies on nuclear architecture in oocytes have been limited probably due to the difficulty in obtaining unfertilised eggs from natural cycles (Delhanty 2005). However a study by Zuccoti *et al.* (2005) looked at nuclear architecture in the developing mouse oocyte. Based on chromatin morphology two types of oocytes exist, the SN (surrounded nucleolus) and NSN (not surrounded nucleolus). Apparently the same morphology exists in human (Zuccotti *et al.* 2005). Three dimensional analysis of centromere position revealed differences in nuclear architecture between NSN (centromeres close to nucleolus) and SN (centromeres juxtaposed forming a ring around nucleolus), thus the authors suggested that nuclear architecture in oocytes is developmentally regulated (Zuccotti *et al.* 2005).

1.5.9. Nuclear architecture in human preimplantation embryos

As the American zoologist F.R.Lillie recognised in 1919 "The elements that unite are single cells, each on the point of death; but by their union a rejuvenated individual is formed, which constitutes a link in the eternal process of Life". Fertilisation is the process that "saves" the sperm and the egg from death by creating the totipotent zygote. Very briefly, sperm binds to the zona pellucida of the egg and undergoes acrosomal reaction to enable it to penetrate zona pellucida and fuse to the egg cytoplasm (Alberts *et al.* 1994). The sperm also provides the centriole, which after replication it allows the chromosomes of both gametes to align in a single metaphase spindle for the first mitotic division of the zygote (Alberts *et al.* 1994; Palermo *et al.* 1997).

A few studies have tried to address the nuclear restructuring during the early developmental stages of embryogenesis in animal model systems. Martin *et al.* (2006a) investigated genome restructuring in early mouse embryo development. They found that at the 2-cell stage pro-chromocentres are formed coinciding with a transcriptional burst. By the blastocyst stage these chromocentres have a definite spatial and temporal organisation and are maintained for proper regulation of differential gene expression (Martin *et al.* 2006a). Mudrak *et al.* (2009) analysed re-modelling of sperm chromatin under the influence of Xenopus egg extracts by localisation of protamines, CENP-A, major α sattelite DNA and CTs. During the

decondensation-recondensation process of sperm chromatin they observed relocalisation of centromeres and remodelling of CTs, arguing that this system could mimic in some aspects human fertilisation (Mudrak *et al.* 2009).

The first study to examine radial position in normal and abnormal human blastomeres using centromeric and locus specific probes was by McKenzie *et al.* (2004). Seven chromosomes were studied (13, 16, 18, 21, 22, X & Y), and nuclear addresses of specific loci in normal blastomeres was observed (13, 18, 21 and X were central; 16, 22, Y favoured more peripheral locations). However in chromosomally aneuploid blastomeres all chromosomes seemed to show a tendency to occupy more peripheral positions. They proposed that localisation of signals in the periphery could be an indication of aneuploid cells undergoing apoptosis or that key functions like transcription of regulatory genes that maintain nuclear architecture has been altered (McKenzie *et al.* 2004). Similarly Diblik *et al.* (2007) studied the same chromosomes in blastomeres and found that, for all but chromosome 18, a random position model was evident in normal and abnormal blastomeres. Chromosome 18 shifted towards the periphery in abnormal blastomeres (Diblik *et al.* 2007). They also argued that the correlation of peripheral position and aneuploidy could be an extra selection criterion for unsuitable embryos for transfer in preimplantation genetic screening (PGS).

The most recent attempt to investigate nuclear organisation in human blastomeres was by Finch *et al.* (2008a). Chromosome radial position was examined for 8 loci (13, 15, 16, 18, 21, 22, X and Y) between committed cells (lymphocytes), normal and abnormal blastomeres. Aneuploid cells showed a similar pattern of organisation with the committed cells, whereas blastomeres with no abnormalities showed a random model of positioning. The authors postulate that this could indicate a unique pattern of organisation for blastomeres with no abnormalities, linked to a more relaxed state of organisation, whereas copy number change is associated with entry into a state of organisation closely related to that of committed cells (Finch *et al.* 2008a). Both studies (Diblik *et al.* 2007; Finch *et al.* 2008a) argue for the use of chromosome loci probes because whole chromosome paints could have a higher risk of signal overlap and splitting plus single loci might illustrate possible positional changes between cell types easier.

Thus from the above data it becomes clear that examining nuclear architecture during early embryogenesis could provide insight into the mechanisms of aneuploidy.

1.6. Thesis aims

1.6.1. Perspectives

As mentioned from the outset, interphase cytogenetics involves the determination of chromosome copy number and assessment of nuclear organisation (through the determination of nuclear address). A "healthy" nucleus clearly requires both correct chromosome copy number and appropriate nuclear organisation however, to the best of my knowledge any relationship between the two has yet to be established.

In order to investigate this, the appropriate tools are required and, as pointed out in section 1.1.1 multicolour approaches would greatly advance the study of nuclear organisation, particularly when cells are scarce such as preimplantation human embryos. One possible solution to this is through inorganic nanomaterials such as quantum dots (see section 1.1.2). Either by nanotechnology or by classical means a 24 chromosome screen would be an excellent tool for asking a number of questions related to chromosome abnormalities in human sperm and preimplantation embryos.

As pointed out in section 1.2.2.1 the relationship between infertility and increased sperm disomy is well established however any link with nuclear organisation is less so. Even in pre-exisiting studies, the number of chromosomes that have been assayed is limited.

Among preimplantation embryos analysis of both chromosome copy number (see section 1.4.6) and nuclear organisation (see section 1.5.9) is limited to an even smaller set of chromosome pairs and thus evaluation of all chromosomes in the human karyotype is essential to further studies in this area. With this in mind, the following specific aims are proposed:

1.6.2. Specific Aims

Given that both aberrant chromosome copy number and aberrant nuclear organisation (nuclear address) can lead to disease phenotypes; the principal objective of this thesis is to exploit whether these two phenomena are linked in human spermatogenesis and preimplantation development. The specific aims of this thesis were therefore as follows:

1. To investigate whether inorganic nanomaterials (quantum dots-QDs) can be used for FISH in place of organic fluorochromes with a view to multiplex experiments.

2. To develop a 24 chromosome aneuploidy screening approach applicable to single nuclei and of use for determining nuclear organisation.

3. To test the hypothesis that nuclear organisation is altered in men with severely compromised semen parameters by assaying loci for all chromosomes.

4. To apply the 24 chromosome FISH strategy to human blastomeres and assay the level of chromosome abnormalities and assess the efficacy of PGS.

5. To apply the 24 chromosome FISH strategy to investigate nuclear organisation in human blastomeres.

Expanding nuclear architecture studies in the whole of human karyotype could have future practical applications of assessing nuclear health and provide better infertility treatments or selection criteria of embryos from a preimplantation diagnosis setting.

2. Materials and Methods

2.1. Samples

2.1.1. Sperm

Informed written consent was obtained from 10 chromosomally normal males from the donor insemination program at the London Bridge, Fertility, Gynaecology and Genetics centre and from 10 chromosomally normal OAT men undergoing male factor IVF treatment at the Embryogenesis Clinic in Athens, Hellas. Research was approved by the Research Ethics Committees of the University of Kent and carried out under the auspices of the treatment licence awarded by the HFEA and Hellenic National Authority of assisted reproduction (EAIYA) to the Bridge and Embryogenesis clinics respectively.

Table 2.1 and Table 2.2 present the information given by the clinics with regard to the semen parameters of the normal donors and males with OAT respectively. Samples are presented according to the order of processing.

		Initial count			Post-thaw		
Sample	**Age**	**[C] 10^6/ml**	**Motility 10^6/ml**	**Progression (Grades 1-3)**	**[C] 10^6/ml**	**Motility 10^6/ml**	**Progression (Grades 1-3)**
N1	37	60	35	2	22	7	2
N2	27	52	33	2-3	32	6	2
N3	33	52	33	2-3	No Post thaw conducted		
N4	44	107	82	2-3	22	5	1-2
N5	41	45	39	2-3	20	4	2
N6	38	54	41	2-3	26	2	2
N7	25	48.6	43.6	2	17.9	5.7	2
N8	23	79	31	2	34	5	2
N9	35	100	90	3	52	16	2
N10	22	43	31	2-3	70	7	2

Table 2.1: Semen parameters for the 10 normal males participating in the donor insemination program at the London Bridge Clinic. Note: with regard to progression; 1-twiching, 2-progressive motility, 3- rapid motility.

Sample	Age	Concentration 10^6/ml	Motility %	Progressive Motility (%)	Abnormal Forms	Previous IVF failed attempts
OAT1	40	18	30	20	90	2
OAT2	29	10	20	10	95	0
OAT3	36	8	10	5	97	0
OAT4	41	6	5	1	98	1
OAT5	37	5	5	2	98	2
OAT6	50	5	5	1	96	4
OAT7	40	2	1	0.1	98	1
OAT8	34	1	5	2	100	1
OAT9	52	3	5	2	99	2
OAT10	48	1.5	2	1	96	3

Table 2.2: Semen parameters for the 10 OAT males undergoing IVF treatment at the Embryogenesis Clinic in Athens, Hellas.

2.1.2. Sperm Sample Preparation

This method can be applied to fresh ejaculate or cryopreserved sperm samples. The sample was then washed in 10mM NaCl/10mM Tris (0.58g NaCl/1.21g Tris per 1L) pH 7.0 sperm wash buffer and then centrifuged for 7 minutes at 1,900rpm (700g). Supernatant was removed and resuspended in sperm buffer. This was repeated 3-5 times depending on the sample quality (pellet size and colour). The sample was then fixed in a drop-wise fashion using 3:1 methanol acetic acid to final volume of 5ml. Again it was centrifuged at 1,900rpm for 7 minutes and after removal of the supernatant the pellet was resuspended in fixative. The process was repeated for up to 5 times (pellet depending). 5 to 20μl of the sample was spread on a Poly-L-lysine coated slide (allows better fixation of cells) and allowed to air dry at room temperature (RT). It was then checked with the aid of a phase contrast microscope for optimal density of cells and area of interest was marked with a diamond pen. Sperm FISH could then be performed as described in section 2.9. Sperm sample could be stored in fixative, like lymphocytes -20°C.

2.1.3. Blastomeres

Human embryos used in this thesis were from patients undergoing PGS for aneuploidy at the London Bridge Fertility Centre and Lister Fertility Clinic. London. Under normal

circumstances, patients that undergo PGS can choose after diagnosis on the single cell level (day 3) whether to have follow up diagnosis on the embryos (whole embryo cultures, day 4 or 5) that were not applicable for transfer. If they opt from having follow-up diagnosis, they can give consent for the use of these embryos in research purposes or for embryologists to train in whole embryo spreading (QC). This was the source of most of the embryos used in this thesis. In addition 8 follow-up whole embryos were obtained from the Abumeliana Clinic, in Libya (embryos 1, 2, 3, 5, 6, 7, 8, 9 – Table 2.3) All patients gave informed consent for the use of their embryos for research purposes and this work was approved under the auspices of the treatments license awarded by the HFEA to London Bridge and Lister Fertility clinics, Libyan Ministry of Health, and the local research and Ethics committee of the University of Kent, all of whom provided approval for this work.

Table 2.3 provides information about the whole embryos used in this thesis. The order that the data is presented follows the processing order as material was becoming available.

Whole embryo	Female Age	Male Age	Day of spread (post-insemination)	Number of blastomeres/whole embryo
1	-	-	-	9
2	-	-	-	25
3	-	-	-	23
4	32	34	5	64
5	-	-	-	No cells found
6	-	-	-	18
7	-	-	-	16
8	-	-	-	11
9	-	-	-	36
10	42	37	6	28
11	42	37	6	12
12	42	37	6	11
13	42	37	6	7
14	42	37	6	21
15	42	53	7	28
16	43	42	5	13
17	44	49	6	28
18	44	49	6	Heavy debris on slide-no analysis
19	44	49	6	16
20	43	45	6	14
21	43	45	6	11
22	33	39	6	12
23	33	39	6	51
24	39	39	5	28
25	39	39	5	29

Table 2.3: Shows information for the whole embryos used in the positional studies in this thesis. Whole embryos within bold lines originate from the same PGS case.

2.1.4. Blastomeres (whole embryo preparation)

Whole embryos were spread using 0.1% Tween/0.01N HCl using a stripper® tip with an inside diameter of 175 microns to transfer whole embryos from the biopsy dish to the spreading solution drop in a clean poly-L-lysine slide. Gentle agitation was used to dissolve the cell membrane. Slides were allowed to dry and the estimated number of blastomeres making up the embryo was recorded. Slides could be stored at 4°C and were usually sent to the University of Kent within a day from spreading. Sequential FISH was

performed immediately in order to prevent embryo quality degradation from prolonged storing.

2.1.5. Lymphocytes

For the purposes of control, lymphocytes from a normal karyotype male (and female for specific experiments) were used from peripheral blood cultures. Research was approved by the Research Ethics Committees of the University of Kent.

2.1.6. Lymphocyte culture preparation from whole blood cultures

Prior to blood process the fume hood was radiated with UV for 20-30 minutes for sterilisation purposes. Blood was taken via standard phlebotomy using heparin tube (6ml maximum) from a healthy karyotyped donor.

Using 25cm^2 tissue culture flasks (CELLSTAR), 1ml of peripheral blood was added with 19ml of PB Max karyotype media (pre-warmed at 37°C) (Invitrogen-12557-039). This mixture was incubated at 37°C for 72 hours vertically in a 37°C incubator with 5% CO_2. Cultures (after 72 hours) were gently mixed to dissolve the red cell layer formed at the bottom. 200µl of demecolcine solution (Sigma-D1925 - 10µg/mL in HBSS liquid, sterile-filtered, AFC Qualified) was added (to arrest cells in metaphase) and cultures were incubated for 40 minutes at 37°C. A KCl (0.075M) solution was allowed to warm at 37°C during demecolcine incubation. Blood cultures were then transferred to 15ml falcon tubes by adding 10ml per falcon (each flask had 20ml of blood/medium in total). The cultures were centrifuged at 1,900rpm for 5 minutes and supernatant was removed. The pellet was resuspended and using the warmed KCl solution it was added in a drop-wise fashion to the resuspended blood pellet (in order to lyse red blood cells) to a maximum of 6ml with a timer of 12 minutes start at the first drop of KCl. Cultures were returned at 37°C for the remaining of the 12 minutes incubation. The next step was to fill tubes with fix (3:1 methanol: acetic acid-freshly made) up to 14ml. Falcon tubes were gently inverted to mix the culture with the fixative. They were then centrifuged for 5 minutes at 1,900rpm. Supernatant was removed leaving around 0.5-1ml of fix to resuspend the pellet. The cells were then fixed in a drop-wise fashion to a volume of 5ml and centrifuged for 5 minutes

at 1,900rpm between each fix step. This can be repeated for 3-5 minutes depending on the pellet and colour. Fixed lymphocyte cultures can be stored at -20°C.

Depending on the size of the pellet after fixing, slides were dropped using 0.5ml of culture. A drop of fix was added on the slides and allowed to air dry. Slides were checked for cells and metaphases before proceeding to FISH, which is decribed in subsequent sections 2.6, 2.7, 2.9, 2.10.

2.2. Probes

For the purposes of the experiments of this thesis different kinds of probes were used. In most of the experiments with QDs chromosome paints for human chromosomes 1, 2, X and Y were tested. In addition a custom made pancentromeric probe (Cambio 1965B-02) was tested together with a biotinylated oligonucleotide probe for chromosome 12 (Sigma Genosys).

In all of the experiments for investigating nuclear architecture (in sperm or pre-implantation embryos) via chromosome position custom made multicolour probes targeting all chromosomes from Kreatech Diagnostics were used. These probes comprised of 4 different multicolour mixes each with sequences for 6 different chromosomes. Three of the mixes were made using centromeric probes, whereas the last mix had unique sequences (BACs) (Chapter 4).

2.3. Generation of biotinylated chromosome paints

2.3.1. PCR amplification (secondary amplification)

Chromosome paints from flow-sorted human chromosomes (sent from Department of Pathology, University of Cambridge) were used as a starting template for amplification. The degenerate primer used was 6MW (5'→3' CCG ACT CGA G NNN NNN ATG TGG). Amplified material with this method was then labeled with biotin via nick translation and used in indirect FISH experiments. The PCR mix (total Volume: 50μl) and amplification conditions are presented in the following table:

Mix component	Amount used (µl)	PCR conditions
5X Buffer D (Invitrogen-K1220-01)	10	**Step1**: (1 Cycle): 94°C for 3 minutes **Step 2**: (30 Cycles): 94°C for 1 minute 62°C for 1minute 72°C for 1.5 minutes **Step 3**: (1 Cycle): 72°C for 8 minutes Store at -20°C
6MW (20µM) (MWG)	5	
dNTPs (2.5µM) (Invitrogen)	4	
Taq polymerase (15u/µl) (HT Biotechnology)	0.2	
ddH_2O	28.8	
DNA	2	

Table 2.4: Showing the PCR amplification mix and conditions followed to amplify the template DNA.

2.3.2. Nick translation of chromosome paints

Amplified DNA material was labeled with biotin using nick translation. The following table shows the reaction components.

Reagent	µl
Buffer NT [500mM Tris-HCl (pH 7.8), 50mM $MgCl_2$, 100µg/ml nuclease-free BSA]	5
B-mercaptoethanol 0.1M	5
dNTPs (2.5mM)	2.5
Biotin 16-dUTP (50nMol – Roche)	2.5
DNA Polymerase I (500u – Fermentas)	1
DNase (1:100) – stock (1mg/ml)	8
DNA (Amplified product)	26

Table 2.5: Nick translation reaction mix.

The mix was incubated at 16°C for 1.5-2 hours. The reaction was then paused by placing the mix on ice. An aliquot was run on an agarose gel (2%). If the fragments were <500bp then 5µl of 0.5M EDTA pH 8 were added to stop the reaction. Ethanol precipitation followed the labelling of the probes immediately after the nick translation reaction was stopped with EDTA.

2.3.3. Agarose Gel preparation

A 2% agarose gel (Invitrogen) was prepared by dissolving 0.6g of agarose in 30ml of 0.5 X TBE (Tris-Borate EDTA buffer - Sigma T4415 10X concentrate). The liquid mix was

microwaved for 40 seconds and 1µl of ethidium bromide (Fisher Scientific) was added. The mix was then poured into the gel tank and allowed to set. The gel was run after each PCR and nick translation to ensure proper work of the reaction. A negative control (water only) was included to check for possible contaminations.

2.3.4. Ethanol precipitation (for 50-100µl reaction)

50µl of 5M ammonium acetate and 250µl of 100% ice cold ethanol were added to the stopped nick translation mix. The mix was vortexed and centrifuged briefly. It was then stored at -80°C overnight to allow DNA precipitation. The mix was then centrifuged at 13,000rpm at 4°C (cold room) for 25 minutes. The supernatant was discarded and 200µl of 70% ice-cold ethanol were added, followed by another centrifugation at 13,000rpm at 4°C for an additional 25 minutes. After the supernatant was discarded tubes were left upside down to air dry, with monitoring in order not to over dry the DNA pellet. 10µl of hybridisation mix [5ml of 100% Formamide (FA), 1ml of 20 X SSC (Saline Sodium Citrate) 2ml of 50% Dextran Sulphate, 2ml of distilled water, for a 10ml volume] were added and the mix was vortexed and centrifuged briefly. The sample was allowed to resuspend by staying at RT (Room Temperature) for 24 hours or incubate in a hot bath at 50°C for 2 hours or 55°C for 90 minutes. The probes were then ready to FISH and could be stored at -20°C.

2.4. Quantum Dot (QD) samples used

In the course of experiments with QDs, commercially available streptavidin-conjugated QDs (Sav-QDs) were used to detect biotinylated chromosome targets. Throughout the rest of this chapter SAv-QDs will be termed QDs for simplicity. Table 2.6 illustrates the conjugates used.

SAv – QD (1µM)	Company	Colour Description
QD520	Evident Technologies	Amaranth Green
QD585	Invitrogen	Red
QD600	Evident Technologies	Fort Orange
QD620	Evident Technologies	Maple Red Orange

Table 2.6: The SAv-QDs used in this thesis.

2.5. Fluorescent *in situ* hybridisation (FISH)

FISH was the main technique used throughout this thesis. Different versions of FISH were used depending on probes and detection agents. The general metaphase-interphase FISH (for indirect detection-thus probe was not labelled with a fluorochrome) is described below. This protocol was largely used in the QD (indirect) experiments.

2.6. Metaphase – Interphase FISH (indirect approach)

2.6.1. Slide preparation and aging

Superfrost slides (VWR) were used and rinsed with 3:1(methanol:acetic acid) and allowed to air dry. Lymphocyte cultures (already in fix as described in section 2.1.6) were centrifuged for 5 minutes at 1,900rpm to concentrate the cells as a pellet. The volume of fix was reduced (usually from 5ml to 1-2ml) and cells were resuspended. An aliquot of 0.5ml was dropped on slides followed by a drop of fixative to spread the chromosomes. Once slide was air dried it was checked under phase contrast for quality and amount of metaphases (primarily) and nuclei. Good areas were under marked with a diamond pen.

Slides were then allowed to age in a hot block by selecting the following conditions: 75°C for 1 hour or 55-56°C for 2-3 hours or RT for 24 hours or 37°C overnight.

2.6.2. Pre-hybridisation washes

Slides were then dehydrated by washing in ethanol series (70, 80 and 100%) for 5 minutes and then air dried. They were then treated with RNase (Promega – stock 4mg/ml) by adding 100µl of 100µg/ml RNase mix (2.5µl of RNase – 97.5µl 2 X SSC per slide). A 22x50mm coverslip (Menzel-Glaser) was placed and slides were incubated at 37°C for 1 hour.

2.6.3. Probe preparation

35 minutes into the RNase incubation, the DNA probe was prepared by adding 1µl of probe (chromosome paint) with 3µl of hybridisation mix and 1.5µl of human cot^{-1} DNA (Roche). The mix was centrifuged briefly and was denatured at 75°C for 5 minutes. It was

then allowed to re-anneal at 37°C for 30-45 minutes before adding it onto the slide which by then had reached the hybridisation stage.

2.6.4. Denaturing

Once the RNase step was completed, slides were washed twice in 2 X SSC for 5 minutes each wash and passed another ethanol series wash for 2 minutes this time and allowed to air dry. The cells were then denatured at 70°C (in a pre-warmed solution) in 70%FA/2 X SSC (for a 50ml coplin jar this was 35ml of FA and 15ml of 2 X SSC). A digital timer was started once the first slide entered the solution. Slides were then washed with 70% ice cold ethanol for 2 minutes followed by a wash with 80 and 100% (RT) ethanol for 2 minutes each. Slides were then allowed to air dry at RT.

2.6.4.1. Denaturing when using oligonucleotide probe (for centromere 12 – QD indirect experiments)

Chromosome denaturation occurred by adding 125μl of 70%FA/2 X SSC (87.5μl FA – 37.5μl 2 X SSC) per slide that was covered with a 24x50mm coverslip and incubated at 80°C for 2 minutes. This was followed by washing slides with 70% cold ethanol followed by RT ethanol washes (80-100%) for 3 minutes each. Slides were air-dried and 10μl of the oligonucleotide-hybridisation mix was added per area and covered with an 18x18mm coverslip. Slides were incubated for 2 hours at 37°C without rubber cement sealing.

The oligonucleotide-hybridisation mix was made by adding 2μl of working stock of the oligonucleotide probe (cen12) (100ng/μl) in 98μl of oligonucleotide-hybridisation mix (20% FA, 2 X SSC, 10% Dextran sulphate, 60μg of salmon sperm DNA, and 100-200ng of probe).

2.6.5. Hybridisation

Probes were added to the specified marked area, and an 18x18mm coverslip was added (if less amount of probe was added i.e. 4μl a 13x13mm coverslip was used instead). The area was sealed with rubber cement (Fixogum) and slides were placed in a wet chamber (empty tip box with ddH_2O) at 37°C overnight.

2.6.6. Post-hybridisation washes

Once the hybridisation period was over, the glue sealant was removed and slides washed in 2 X SSC to remove the coverslips. Slides were then washed in a pre-warmed (at 37°C) 50%FA/2 X SSC solution (for a 50ml coplin that is 25ml FA plus 25ml 2 X SSC) for 20 minutes. They were then transferred to 2 X SSC 0.1% Igepal for 1 minute at RT to wash out any remaining FA solution. The next step was to wash them in storage buffer (4 X SSC 0.05% Igepal) for 15 minutes (up to 3 days) at RT. Slides were then washed in block buffer [4 X SSC 0.05% Igepal, 2-3% BSA – 18ml of block buffer with 2ml of BSA (Sigma A9647-50g)] for 25 minutes at RT. The purpose of the block buffer was to reduce non-specific binding of the detection agent (in this case Cy3-streptavidin) in the following step.

2.6.7. Post-hybridisation washes when using oligonucleotide probe (for centromere 12 – QD indirect experiments)

Slides were washed three times for 5 minutes (each time) in 20%FA/2 X SSC at 37°C (10ml FA and 40ml of 2 X SSC in a 50ml coplin jar). This was followed by three washes for 5 minutes each in storage at 37°C.

Detection with Cy3-streptavidin was as per subsequent section 2.6.8 whereas detection with QDs was as per subsequent section 2.6.9 but with a different wash after detection incubation.

Slides were washed with storage buffer 3 times for 5 minutes each time, followed by a three-5 minute wash with PBS/0.1% Tween 20 (50µl in 50ml coplin jar) in a shaker in the dark. A water rinse was done after; slides were air-dried and counterstained with DAPI.

2.6.8. Detection (using Cy3-streptavidin)

The detection mix was prepared during the block buffer wash, as decribed in section 2.6.6, and was kept at 4°C for 20-25 minutes and then centrifuged at 13,000rpm for 5 minutes. Detection buffer consisted of 4 X SSC 0.05% Igepal, 1.5% BSA and Cy3-streptavidin. Cy3-streptavidin (Amersham Biosciences) was used at a dilution of 1:200. The amount of detection buffer per slide was 100µl. Thus detection mix (including the

fluorochrome) for one slide was made by adding 50μl of detection and 50μl of block buffer together with 0.5μl of Cy3 streptavidin. A coverslip was added and slides were incubated for 35 minutes at 37°C.

The coverslip was then removed and slides washed in fresh storage buffer (in the dark) for 10 minutes, followed by a brief rinse with ddH_2O. Slides were then air dried and counterstained using vectashield with DAPI (Vector Labs). A coverslip was added and slides were blotted for excess DAPI and stored at 4°C in a box.

2.6.9. Detection using QDs

The same protocol was used, but detection mix consisted of 1μl of QD into 99μl of TNB buffer (0.1M Tris-HCl pH: 7.5, 0.15M NaCl, 0.5% BSA) per slide. A coverslip was placed after detection mix was added and incubation for 1 hour at 37°C ensued. Slides were then washed twice for 3 minutes in 1X PBS in the dark (to prevent photobleaching of the fluorochrome). They were then air dried and counterstained with DAPI.

2.7. Metaphase – Interphase FISH (direct approach)

The direct FISH approach was used following a published method by Bentollila and Weiss (2006). Prior to FISH probes (chromosome paints) had to be amplified using primary DOP-PCR, then labeled with a primer bearing a single biotin molecule and then used in the direct FISH experiment where the biotinylated probe would be incubated with a QD. The primary and secondary PCR amplification is described below followed by the direct FISH protocol.

2.7.1. PCR amplification (primary amplification)

Primary DOP-PCR was used to amplify DNA from the chromosome paints. This method uses 3 DOP primers and the end products (3 reactions one with each DOP primer) were pooled together to increase concentration. The pooled product was then purified with PCR purification protocol, described in subsequent section 2.7.3. The following table presents the three DOP primers used, the PCR reaction mix and conditions.

<table>
<tr><td rowspan="3">DOP primers used</td><td colspan="2">DOP1: 5' CCG ACT CGA GNN NNN NCT AGA 3'</td></tr>
<tr><td colspan="2">DOP2: 5' CCG ACT CGA GNN NNN NTA GGA G 3'</td></tr>
<tr><td colspan="2">DOP3: 5' CCG ACT CGA GNN NNN NTT CTA G 3'</td></tr>
<tr><td>PCR mix component</td><td>Amount Used (µl)</td><td>Conditions</td></tr>
<tr><td>*TAPS2 buffer + BSA + βME</td><td>5</td><td rowspan="9">Step 1: (1 cycle):
94°C – 3 minutes

Step 2: (10 cycles):
94°C – 1.5 minutes
30°C – 2.5 minutes
Ramp at 0.1°C/s to 72°C
72°C – 3 minutes

Step 3: (30 cycles):
94°C – 1 minute
62°C – 1.5 minutes
72°C – 2 minutes

Step 4: (1 cycle):
72°C – 8 minutes

Hold at 12°C</td></tr>
<tr><td>DOP priner (1,2 or 3) - 20µM</td><td>5</td></tr>
<tr><td>dNTPs – 2.5mM</td><td>4</td></tr>
<tr><td>**Brij 58 – 1%</td><td>2.5</td></tr>
<tr><td>Amplitaq (Applied Biosystems) – 5u/µl</td><td>0.5</td></tr>
<tr><td>ddH_2O</td><td>32.5</td></tr>
<tr><td>DNA</td><td>0.5</td></tr>
<tr><td colspan="2">* TAPS2 buffer:
TAPS2 salt solution (final volume: 96 ml):
<table><tr><td>250 mM TAPS (Sigma) pH 9.3</td><td>6.08 g</td></tr><tr><td>166 mM $(NH_4)_2SO_4$</td><td>2.20 g</td></tr><tr><td>25 mM $MgCl_2$</td><td>5 ml of 0.5 M stock solution</td></tr></table>Dissolve salts in 50ml water first. Adjust pH strictly to 9.3 with concentrated KOH. Adjust the volume to 96ml using MilliQ water and UV-sterilise.
Transfer 960µl aliquots into eppendorf tube and store at -20 °C. Prior to use, add BSA (33 µl/ml) and β- ME (7 µl/ml) to the buffer aliquots.
** Brij 58
Make 1% stock solution and UV sterilise.</td></tr>
</table>

Table 2.7: Shows DOP primers used, PCR master mix and conditions for primary amplification of DNA template (chromosome paints) prior to labelling with biotin.

2.7.2. PCR amplification using biotinylated primer (secondary amplification)

Once the template DNA was amplified as described in section 2.7.1 and products were pooled and purified, they were labelled using a 5' biotinylated primer (Invitrogen). Table 2.8 shows the sequence of this primer and the PCR master mix and conditions applied. The labelled DNA was then purified, quantified and used in conjugation with QD.

Primer used:	5' biotin-CCG ACT CGA GNN NNN NAT GTG G 3'	
Mix component	**Amount used (µl)**	**PCR conditions**
5X Buffer D (Invitrogen-K1220-01)	10	**Step1**: (1 Cycle): 94°C for 3 minutes **Step 2**: (30 Cycles): 94°C for 1 minute 62°C for 2 minutes 72°C for 2.5 minutes **Step 3**: (1 Cycle): 72°C for 8 minutes Store at -20°C
5bio6MWDOPINV (20µM) (Invitrogen)	5	
dNTPs (2.5µM) (Invitrogen)	4	
Taq polymerase (15u/µl) (HT Biotechnology)	0.2	
ddH_2O	28.8	
DNA	2	

Table 2.8: Presents primer sequence, PCR master mix and conditions for labelling amplified DNA with a single biotin per primer site.

2.7.3. PCR product purification (QIAquick)

This was the method used to purify amplified DNA (via primary amplification described in section 2.7.1 or biotinylated DNA (via secondary amplification, described in section 2.7.2). The purified biotinylated DNA was conjugated with a QD and used in direct FISH experiments. To the 50µl PCR reaction 250µl of Buffer PBI (Binding Buffer-Cat No: 19066-QIAGEN), as the analogy was 5 volumes of PBI to 1 volume of PCR sample. The colour of the mixture was checked that it was similar to PBI.

A QIAquick spin column was placed in a provided 2ml collection tube and the DNA sample was applied to the QIAquick column and centrifuged for 30-60 seconds at 17,900g (or 13,000rpm). The flow-through was discarded and the QIAquick column was placed back in the same tube. 0.75ml of wash buffer PE (Cat No: 19065-QIAGEN) were added to the column and centrifuged for 30-60 seconds at 17,900g (or 13,000rpm). The flow-through was discarded and an additional centrifuge step was carried to remove any residual ethanol (from buffer PE). The QIAquick column was placed in a clean 1.5ml microcentrifuge tube. DNA was eluted by adding 50µl of buffer EB (Elution Buffer-10mM Tris-Cl, pH 8.5) to the center of the QIAquick membrane and centrifugation of the column for 1 minute at 13,000rpm. A more concentrated DNA was eluted by adding 30µl of EB and allowing the column to stand for 1 minute prior to centrifugation.

Purified DNA could then be run on a 2% agarose gel for analysis as described in section 2.3.3.

2.7.4. Metaphase – Interphase (direct approach) – Pre-hybridisation treatment and QD-DNA complex

Lymphocyte cultures were dropped on slides and washed at 2 X SSC for 30 minutes at RT. During this incubation the QD-DNA construct was being made by using 1μl of 500nM QD with 1μl of 50ng/μl biotinylated probe. The mixes were gently pulsed for 5 seconds and were allowed to incubate at RT for a minimum of 30 minutes. Then formed constructs stayed on ice until usage.

Slides were removed from 2 X SSC and underwent pepsin treatment at 37°C for 4 minutes (49ml ddH_2O with 0.5ml 1N HCl and 0.5ml 1% pepsin). A wash with 2 X SSC for 10 minutes after pepsin was done followed by a cell dehydration step with 3 minute ethanol series wash at RT. Slides were then air-dried.

2.7.5. Purification of QD-DNA complex

The QD-DNA construct was purified (from unbound probe) using S300 columns (Amersham Microspin S-300 HR column Cat # 27-5130-01). A column was taken, the tip was cut and a transparent collection tube was applied at the bottom to collect the liquid. The column was centrifuged for 1 minute at 735g or 3,000rpm to equilibrate it with the buffer it came with, whereas the collection tube was discarded.

48μl of hybridisation mix (25% of deionised FA, 2 X SSC, 200ng/μl Salmon Sperm or Herring Sperm, 5X Denhardt's, 50mM Phosphate Buffer 1mM EDTA) were added to the QD-DNA construct (50μl Total Volume). This diluted down the complex concentration to 1ng/μl (It was 50ng in the QD-DNA prior to hybridisation mix addition). The total amount was added to the top of the column making sure not to touch the resin. The column was centrifuged for 2 minutes at 300rpm and the liquid was collected in a new tube.

At that step QD-DNA complex was checked for fluorescence under a UV transilluminator. The tube was then stored in an ice-bucket until later usage.

2.7.6. Denaturation & Hybridisation

The next step was to prepare the 70% deionised FA/2 X SSC, in order to denature the slides (target sequences). In a 50ml volume that would be 35ml of deionised FA (stored at 4°C), 5ml of 20 X SSC and 10ml of milliQ water. The solution was allowed to warm up at 70°C. Slides were then put in the denaturation buffer for 2 minutes at 70°C. This was followed by an ice-cold 70% ethanol wash and then by an RT 90% and 100% washes. Slides were then air-dried. While slides were air drying the QD-DNA complex was denatured at 65°C for 1 minute and then was briefly centrifuged and placed in the ice bucket. While the QD-DNA was denaturing the moist chamber for hybridisation was prepared by putting tissue paper and making 10ml of 25% deionised FA, 2 X SSC (2.5ml of deionised FA, 1ml of 20 X SSC and 6.5ml of ddH2O). 5ml were placed on each box, by soaking the tissue in it. The QD-DNA complex (15µl) was pipetted to the target area of the slide and a 22x22mm coverslip was placed gently on top. The slides were baked at 80°C for 3 minutes to prevent any reannealing of the DNA strand after denaturation. The slides were then put in the box, and rubber cement was used to seal coverglass. Hybridisation occurred on a 37°C incubator overnight.

2.7.7. Post-hybridisation washes

Rubber cement was carefully removed with tweezers and two coplin jars with 2 X SSC (pH: 7.0) were prepared and placed in a 37°C waterbath. Also TST buffer was prepared. The following table shows the TST composition.

TST buffer (for 500ml)		
0.1M Tris	6.05g/500ml	Add Tris and NaCl and 20 X SSC. Make pH 7.4; fill up to 500 with water. Autoclave. Add tween.
0.15 M NaCl	4.4g/500ml	
0.05% Tween 20	250µl/500ml	
20 X SSC	50ml/500ml + 450ml ddH_2O	

Table 2.9: Preparation of TST for detection.

Slides were put at 2 X SSC to allow coverslips to float off. Then they were transferred to TST buffer for two-10 minute washes at 37°C. Slides were then mounted with 90% glycerol and 10% PBS (40μl per slide). A coverslip was applied together with nail polish in the corners. Slides were ready to be stored or analysed.

2.8. Motility assay to investigate QD-DNA complex formation

To test for QD-DNA constructs formation the following gel was set up. The background was that "naked" DNA runs faster that QD-DNA than QD alone. Attachment of QD to DNA causes a negative charge increase (both DNA and QDs are negatively charged). Also by doing a gel like that the complex could be titrated and optimum QD concentration decided. The initial step was to prepare the following dilutions between QD and DNA (probe) which is presented in Table 2.10.

Lane no	1	2	3	4
QD amount (μl)	0	1	1:2 ratio (1μl of 1μM QD + 1μl H_20)	1:4 ratio (1μl of 1μM QD + 3μl H_20)
DNA amount (50ng/μl)	1	1	1	1
QD concentration	-	1μM	0.5μM	0.25μM

Table 2.10: Showing dilutions prepared between QD and DNA probe for motility gel.

The total volume for each construct was 2μl. They were then allowed to stand at RT for 30 minutes. Once the incubation period had ended 5μl of 0.5 X TBE were added to the 2μl reaction mix together with 2μl loading buffer (3ml of 100% glycerol, 2.5ml of 2 X TBE, 4.5ml of distilled water for a 10ml volume). All the samples were loaded to a 2% agarose gel and a water sample with 1μl of orange G (Sigma) loading buffer (0.5ml of distilled water, 0.25ml 2 X TBE, 0.3ml of glycerol, 0.25g orange G) was run for navigation purposes (to know how far samples had run). 90V was applied and the gel was run for 30 minutes and checked under UV for fluorescence of the QD-DNA complexes.

2.9. Sperm FISH

With regard to QD experiments sperm FISH was used with chromosome paints and a pancentromeric probe. Most importantly sperm FISH was used when the fast hybridising

probes from Kreatech Diagnostics were developed to assess the position of chromosome loci in normal and men with impaired semen parameters. The protocol was similar and follows hereafter. A lymphocyte slide was run parallel as a control.

Following sperm sample preparation, according to section 2.1.2 and optical density observation under a phase contrast microscope; slides were aged for 1 hour at 70°C in a hot block. Sperm cells were then dehydrated with the use of ethanol washes (70-80-100% for 3 minutes each).

Slides were then washed in 10mM DTT 0.1M Tris-HCl (pH: 8.0) (400µl of DTT in 40ml of Tris) to swell the sperm cells, at RT (in the dark) for 20-30 minutes and then rinsed in 2 X SSC. This was followed by pepsin treatment. A pre-warmed at 37°C coplin jar; contained 49ml of ddH_2O and 0.5ml of 1N HCl. Before slides were added to the coplin jar, 0.5ml of 1% pepsin was added. Incubation in pepsin was for 20 minutes. Slides were then washed in ddH_2O followed by rinse in PBS. The next step was to wash slides in a pre-made solution of 1% paraformaldehyde/PBS (1.34ml of 37% paraformaldehyde in 49ml of PBS) at 4°C for 10 minutes. Slides were then rinsed with PBS followed by ddH_2O in RT. Another ethanol series wash, was carried after at RT for 2 minutes each and slides were air dried

2.9.1. Probe preparation

When chromosomal paints were used, probe preparation was the same as described in section 2.3.

When the custom made pancentromeric probe (Cambio-1695-B-02), was used 1µl of this probe was added to 11.5µl of hybridisation mix (Cambio information sheet) without any dextran sulphate (5ml of 100% Formamide (FA), 1ml of 20 X SSC, 4ml of distilled water, for a 10ml volume). The probe/hybridisation mix was denatured for 10 minutes at 85°C and then quickly was placed on ice until it was ready to be applied.

With regard to the fast hybridising probes from Kreatech, the appropriate amount was aliquoted (usually 1-1.3µl) and kept at 4°C until denaturation time.

2.9.2. Denaturation & Hybridisation

During this period slides were used for denaturing sperm cells at 70°C (+1°C for every additional slide, e.g. 3 slides-73°C) for 8 minutes. Denaturing was stopped by washing slides into 70% ice cold ethanol followed by and 80, 100% RT ethanol wash.

Probes were applied (either the chromosome paints or the pancentromeric probe) and coverslips were placed with rubber cement to prevent any probe leaking or drying out. Hybridisation occurred by putting the slides in a moist chamber at 37°C overnight.

2.9.3. Denaturation & Hybridisation using Kreatech probes

Probes were denatured at 73°C for 10 minutes, then added onto the slide and sealed with parafilm®. This was followed by a co-denaturaton with the target cells (sperm or lymphocytes) at 75°C for 90 seconds inside a thermobrite® (Abbott Molecular). This was followed by hybridisation at 37°C for either 15 minutes (for the centromeric probes) or overnight (usually 16 hours) for the layer of probes that had the BAC sequences.

2.9.4. Post-hybridisation washes

For slides that were detected with Cy3-streptavidin post-hybridisation washes, blocking and detection are as described in section 2.6.8.

For slides that were detected with QDs procedure was the same as in section 2.6.9, with the only difference being that a different blocking buffer (PBS/BSA; 18ml PBS-2ml 2-3% BSA) was used to the normal one (4 X SSC 0.05% Igepal, 2-3% BSA).

2.9.5. Post-hybridisation washes using Kreatech probes

Once the hybridisation period was completed, slides were removed from hybrite and parafilm® was carefully removed. Slides were placed in 0.7 X SSC-0.3% Tween 20 (35ml of 20 X SSC, 3ml of Tween 20 and 965ml of ddH_2O) at RT, to allow the coverslips to float off. A pre-warmed waterbath at 72°C had a coplin with the same solution and slides were washed for 3 minutes. They were then transferred to 2 X SSC at RT for 2 minutes. Slides were then briefly washed in ddH_2O and then stained with 0.1ng/ml DAPI in a PBS solution (5ml of 10ng/ml in 45 ml of PBS) for 10 minutes. They were then

mounted with Vectashield only (Vector labs) and a coverslip was placed making sure that excess Vectashield is removed without leaving any bubbles. Slides were stored at 4°C for microscopy analysis.

2.10. Sequential FISH in preimplantation embryos

Once whole embryo slides were prepared as per section 2.1.4, a four layer sequential FISH assay using probes from Kreatech was developed in order to obtain as much information as possible from the blastomeres due to the nature of the material (limited compared to the plethora of sperm available). A lymphocyte slide was run in parallel for control purposes.

2.10.1. Pre-hybridisation treatment

Two solutions were prepared prior to treating slides, to allow them to stay in their respective temperatures for at least half an hour. A coplin jar containing 49ml of ddH_2O with 0.5ml of 0.01N HCl was placed at 37°C and a 1% paraformaldehyde/PBS solution was prepared and placed at 4°C. In addition a vial of 10mg/ml pepsin (0.5ml) was taken out of -20°C to thaw.

Slides with whole embryos were washed in PBS for 3 minutes at RT. This was followed by a round of dehydration in 70-80-100% ethanol for 3 minutes each. Slides were then left to air dry. The thawed pepsin solution was added to the pre-warmed coplin jar at 37°C, followed by the slides. Pepsin treatment was for 20 minutes. This was followed by a rinse in ddH_2O and PBS and then slides were placed in the paraformaldehyde solution at 4°C for 10 minutes. During this incubation probes (for all layers) were aliquoted and left at 4°C until utilisation.

After paraformaldehyde treatment slides were rinsed in PBS followed by two ddH_2O rinses. Another round of dehydration followed and slides were allowed to air dry.

2.10.2. Probe denaturation and hybridisation of the first layer

Probes were denatured as described in section 2.9.3 and allowed to hybridise for 15 minutes (first layer was a centromeric probe).

2.10.3. Post-hybridisation washes and reprobing (second layer)

As described in section 2.9.5 with the only difference being that the wash in 0.7 X SSC, 0.3% Tween 20 at 72°C was for 90 seconds and not 3 minutes (sperm only). Once slides were analysed under the microscope, excess immersion oil was wiped and slides were placed in 2 X SSC to allow the coverslip to float off. Slides were then washed for 30 seconds in a pre-warmed ddH_2O solution at 72°C to strip the current probe layer. This was followed by a dehydration round and the second probe layer was added as per section 2.9.3. The second layer hybridised for 15 minutes.

2.10.4. Remaining layers (third and forth)

A similar post-hybridisation sequence as in section 2.10.3 was followed but this time slides were washed for 50-60 seconds at 72°C in 0.7 X SSC, 0.3% Tween 20. Once slides were analysed, the same protocol for stripping and further reprobing was followed for the third layer. Hybridisation was for 15 minutes. The post-hybridisation sequence was followed as in section 2.10.3, but this time slides were washed for 30 seconds at 72°C in 0.7 X SSC, 0.3% Tween 20. The forth layer was added once slides had been analysed and slides were left to hybridise overnight as that layer contained the unique sequence targets. The same post-hybridisation sequence as per third layer was followed and once slides were analysed for the last layer, were stored at 4°C.

2.11. Microscopy

Slides from all experiments were analysed on an Olympus BX-61 epifluorescence microscope equipped with a cooled CCD camera (by Digital Scientific – Hamamatsu Orca-ER C4742-80) and using the appropriate filters.

With regard to QD work; QD filters were purchased by Chroma and the set included a long pass emission (E500LP) and narrow band pass emission filters at 525, 565, 585 605nm.

With regard to work for assessing chromosome position 7 filters were used to accommodate all fluorochromes required (red, green, aqua, gold, blue, far red and DAPI) through the use of two communicating filter wheels (Digital Scientific UK).

All images were acquired using SmartCapture software (Digital Scientific UK) and exported as .tiff files for further analysis.

2.12. Image Analysis – Chromosome position/nuclear address

To be able to assess chromosome position in sperm 100 images minimum were captured for each chromosome for each patient (control and OAT). However, in preimplantation embryos the number of images analysed varied depending on the available number of cells.

The position of chromosomes with the nucleus was measured using an automated method published by Croft *et al.* (1999).

A macro written for ImageJ (Michael Ellis, Digital Scientific UK) split each image of a nucleus to separate RGB planes (red, green for signals and blue for counterstain) and then converted the blue image (representing the DAPI counterstain) to a binary mask from which concentric regions of interest (rings) of equal area were created (Skinner 2009).

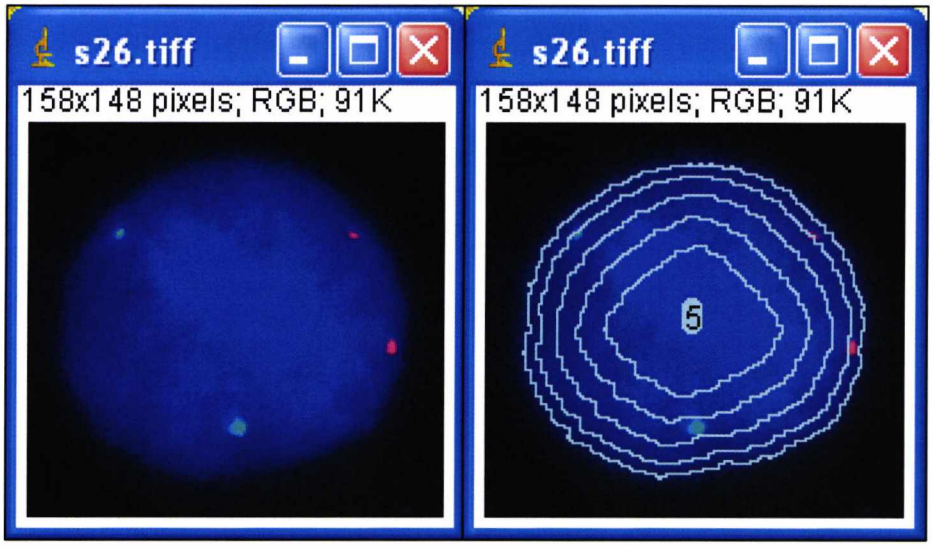

Figure 2.1: A lymphocyte nucleus image converted to RGB planes before the application of the macro (left) and after (right) with the 5 rings of equal area formed.

The proportion of signal in each channel within each ring was measured relative to the total signal for that channel within the area covered by the binary mask (Skinner 2009). The output of these results was pasted to an excel spreadsheet for statistical analysis.

To compensate for the fact that a 3D object is observed under 2D (nucleus flattening) the proportion of signal within each shell was normalised against DAPI density (Boyle *et al.* 2001) and the overall percentage of the normalised signal within each shell was calculated and a χ^2 test was performed to test whether position for that chromosome was significant or random (non-random when $p < 0.05$)

The percentage signal within each shell was used to calculate an 'overall' position for the signal in each nucleus image (Skinner 2009). The median value of the overall positions for all nuclei with a specific probe was taken as the overall position for the probe (Skinner 2009).

Since data appeared to be non-normally distributed thus it was non parametric, median and interquartile ranges were calculated rather than standard error of the mean.

3. Specific aim 1: to investigate whether inorganic nanomaterials (quantum dots - QDs) can be used for FISH in place of organic fluorochromes with a view to multiplex experiments

3.1. Background

As outlined in section 1.1.2 QDs, are a novel class of inorganic fluorochromes composed of nanometre scale crystals made of a semiconductor material. Due, in part, to their inorganic nature, they are much brighter that organic fluorochromes, resistant to photo decay, have narrow emission wavelengths (thus less spectral crosstalk) that can be controlled during particle size synthesis, and thus have great potential for FISH. This is particularly true for multiplexing experiments however only a handful of studies have tried to incorporate the use of QDs in FISH applications and thus the field is under explored.

If QDs could be used in FISH applications they could revolutionise the technique by generating brighter and more photostable probes. In addition multicolour probe sets with low or no spectral overlap could be generated and be used in multicolour experiments. This would be ideal to study chromosome copy number of a large number of targets as well as nuclear architecture, including (as is relevant for this thesis) human sperm and human preimplantation embryos.

3.2. Aims

Given the above rationale, specific aim 1 was broken down into 4 sub-aims thus:

Specific aim 1a: To test the hypothesis that the optical properties of QDs are consistent with the manufacturers claims using simple experiments that involve "spotting" small aliquots on a glass slide.

Specific aim 1b: To investigate whether detection of biotinylated DNA is possible using streptavidin conjugated QDs, also using simple "spotting" experiments.

Specific aim 1c: To ask whether streptavidin conjugated QDs can be used for the detection of biotinylated probes in FISH experiments under a range of conditions ("indirect labelling").

Specific aim 1d: To develop strategies for the direct coupling of QDs to biotinylated probes (including oligonucleotides and chromosome paints) for the use in "direct" FISH experiments.

NB: Only streptavidin conjugated QDs were used in all these experiments and thus the term "QD" will be used throughout to mean "streptavidin QD conjugate" for simplicity and coherence.

3.3. Results

3.3.1. Specific aim 1a: To test the hypothesis that the optical properties of QDs are consistent with the manufacturers claims using simple experiments that involve "spotting" small aliquots on a glass slide

As stated in section 2.4 commercially available QDs were used that emit at different wavelengths. A minute drop was placed on glass slides and QD samples were observed under the bespoke detection filter sets to investigate whether emission was narrow as stated by the manufacturers. The following figure illustrates representative results from this "spotting assay" where several commercially available QDs and an organic fluorochrome (Cy3-streptavidin) were compared.

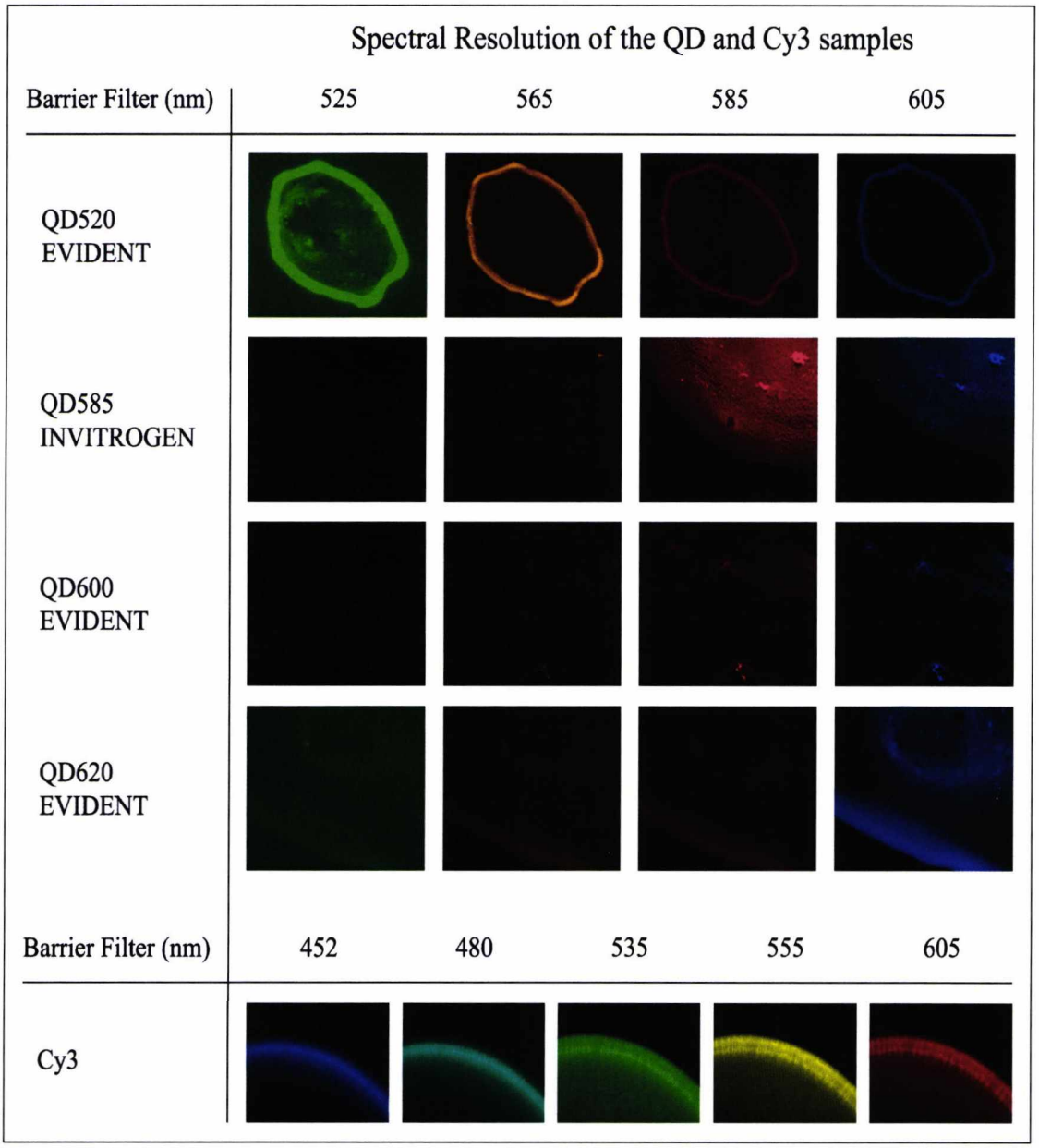

Figure 3.1: Spotting assay to investigate whether QD emission is as narrow as stated by the manufacturers. Samples were irradiated with UV light (from DAPI filter), the dichroic mirror filtered out the UV but let through light above 500nm and different barrier filters were used.

The results showed that QD585 had the narrowest emission spectrum (peaked intensity at 585nm) with limited emission bleedthrough to neighbouring channels. In contrast QD520 peaked at 525nm but showed bleed through to other channels, as did QD620 (brightest signal at 605nm) whereas QD600 hardly fluoresced at all. Cy3 demonstrated significant emission bleedthrough to neighbouring wavelengths confirming that organic fluorochromes are more subject to spectrum overlap. For this reason, most subsequent experiments were continued using QD585 from Invitrogen.

3.3.2. Specific aim 1b: To investigate whether detection of biotinylated DNA is possible using streptavidin conjugated QDs, also using simple "spotting" experiments

Following a similar "spotting" assay, biotinylated DNA was applied to a glass slide and dried and then a layer of streptavidin conjugated QD used to ask whether it could be detected. By dividing the glass slide into areas, different concentrations of probe, QD and FISH conditions could be tested at the same time in order to determine the optimum for later application. Figure 3.2 presents data to determine which QD sample would henceforth be used for a detection of a biotinylated probe in FISH experiments.

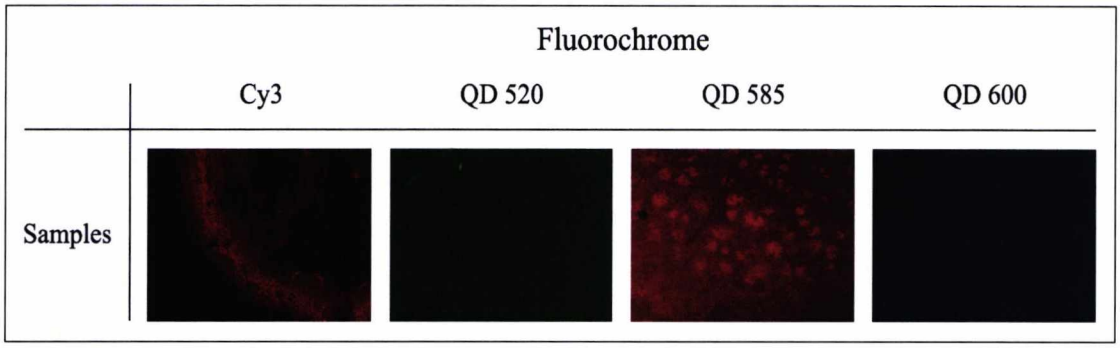

Figure 3.2: Results from a "spotting" experiment for the determination of which QD to use in FISH. QD585 was the only QD that detected the biotinylated DNA in comparison to 520 and 600. Cy3 control also worked well.

Thus, after repeating the experiment up to five times, it became clear that, from the available QD samples, only QD585 could detect the biotinylated DNA in these experiments. This QD was therefore henceforth used alone using the same approach to test further conditions such as the efficacy of a pre-detection block buffer (to reduce non-specific binding of the streptavidin conjugate), incubation time and temperature of detection.

After extensive testing and repeat experiments, results revealed that detection of the biotinylated probe could be achieved regardless of the incorporation of a pre–detection blocking step and that such a step did not appear to increase signal specificity. Detection at 37°C rather than room temperature (RT) improved the brightness of signal which was clear by visual inspection and the optimum time was one hour. Finally, a 1:100 dilution of the stock (1μM) QD solution proved to be the optimum.

Thus the "spotting" assays informed the configuration of FISH conditions and the selection of the most appropriate QD sample to use in the subsequent FISH experiments.

3.3.3. Specific aim 1c: To ask whether streptavidin conjugated QDs can be used for the detection of biotinylated probes in FISH experiments under a range of conditions ("indirect labelling").

Using a biotinylated human chromosome paint generated in the laboratory for chromosome 2 as described in section 2.3 and testing all conditions specified in section 3.3.2, results demonstrated that, QDs could be used for FISH experiments. Figure 3.3 illustrates these results.

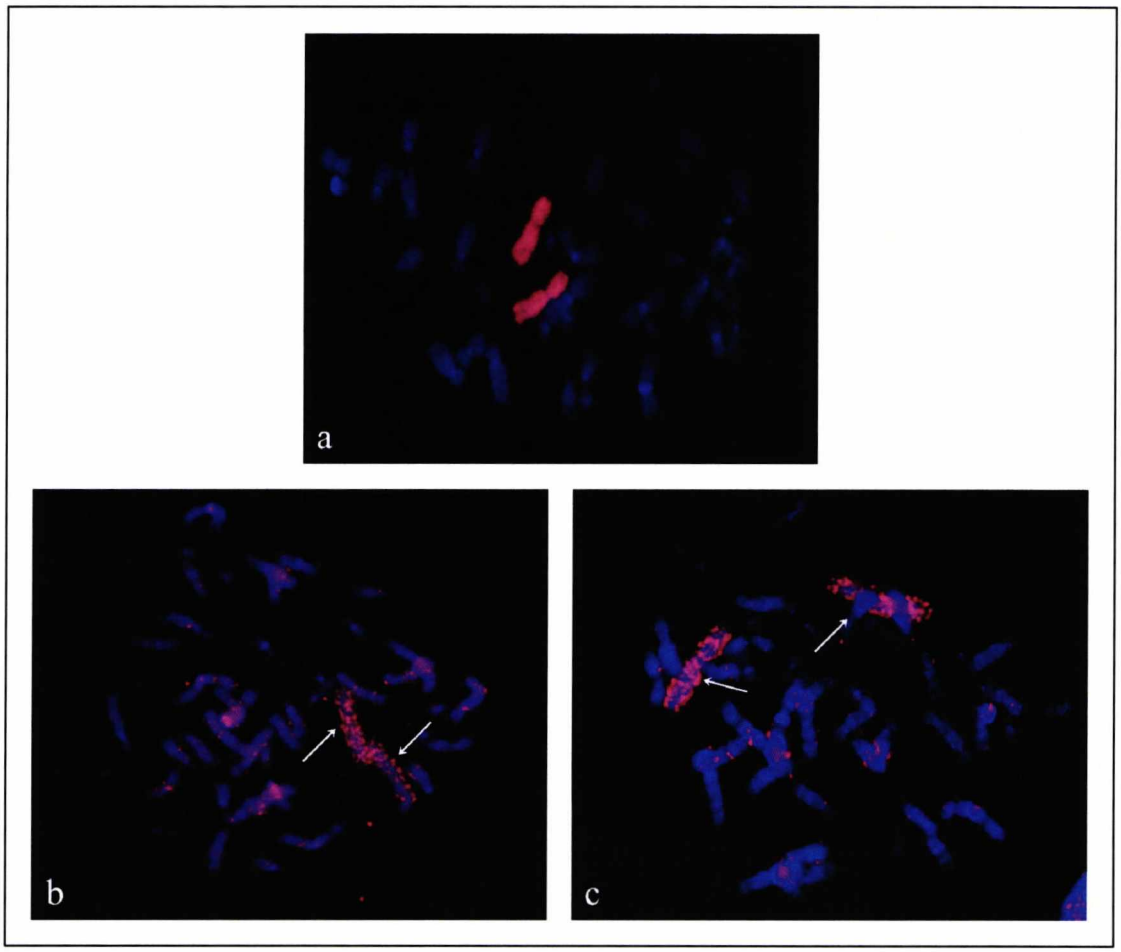

Figure 3.3: Detection of human chromosome 2 paint using Cy3 (a) and QD585 (b and c). QD detection worked under two conditions [pre-detection block, 1hr detection at 37°C (b) or no pre-detection block, 1hr detection at 37°C (c)]. Arrows point at chromosome 2 detected with QD585.

When experiments were successful (incidentally, they were less so, for a chromosome 1 paint) the properties of QDs were apparent. Most notably the signals detection were

significantly brighter (by visual inspection) than the Cy3 and resistant to photobleaching. That is, when Cy3 signals were exposed to UV light, decay occurred after 5 minutes, whereas for QD preparations no appreciable loss of signal was observed even after 1 hour of illumination. On the negative side QD signals were brighter around the periphery of chromosomes (i.e. like a fluorescent sheath-Figure 3.4) and had more non-specific background than Cy3. Another factor was the apparent observation of the lack of reproducibility of the positive results, i.e. under the same conditions; identical experiments would not work even on parallel-processed slides.

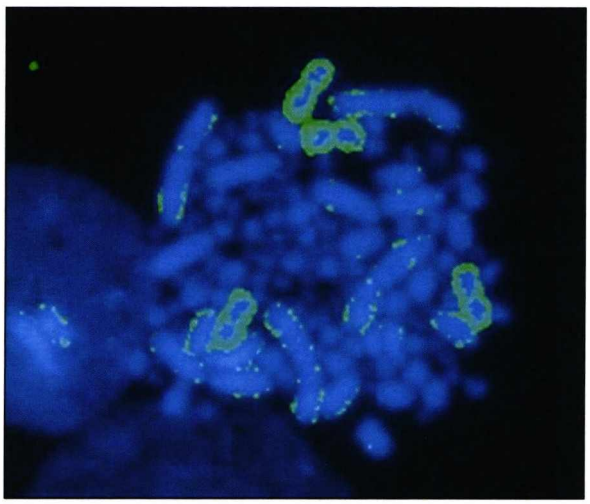

Figure 3.4: Successful human chromosome painting experiment (chromosome 2, tetraploid cell) but with signals predominantly around the periphery of the chromosome (pseudo-coloured green for greater contrast), giving an impression of a fluorescent "sheath."

Thus new strategies were attempted in order to improve the efficacy and reliability of experiments and to remove the "sheath" effect. Since QD molecules were larger than Cy3 (15-30nm vs. 2nm) attempts to reduce the effect of steric hindrance were applied by using a longer carbon atom biotin (biotin-21-dUTP) instead of the normal (biotin-16-dUTP) to provide some extra space for the QD conjugate to bind. The results from this attempt are depicted in Figure 3.5.

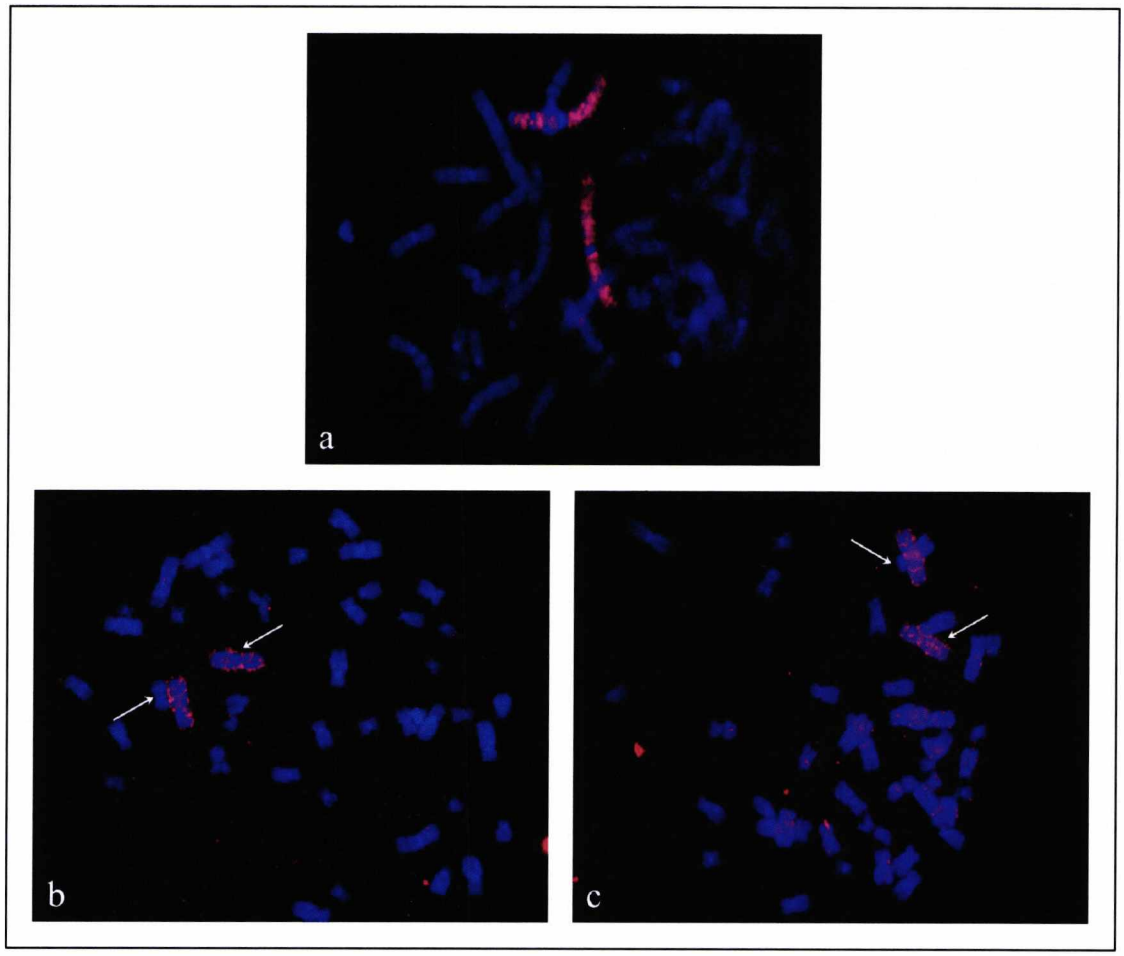

Figure 3.5: Detection of biotinylated (this time with the long carbon biotin) human chromosome paint 2 with a) Cy3 b-c) QD585 (no pre-detection block, 1hr detection 37°C). Arrows point at chromosome 2 detected with QD585.

Although successful under specific conditions (no use of pre-detection block, detection at 37°C for 1 hour), the longer-arm carbon conjugate (biotin-21-dUTP) did not show a noticeable difference in hybridisation efficiency from the normal biotin (16-dUTP). Also lack of reproducibility was evident with this strategy as well.

Another attempt to reduce steric hindrance involved testing different ratios of labelled and unlabelled probes. As with the longer carbon biotin, the rationale was that if the biotin molecules were spread on the length of the chromosome paint then it would allow more efficient binding of QD conjugates thus reducing aggregation of QDs binding the same biotin molecule. Figure 3.6 illustrates the results from the different ratios of labelled and unlabelled probes.

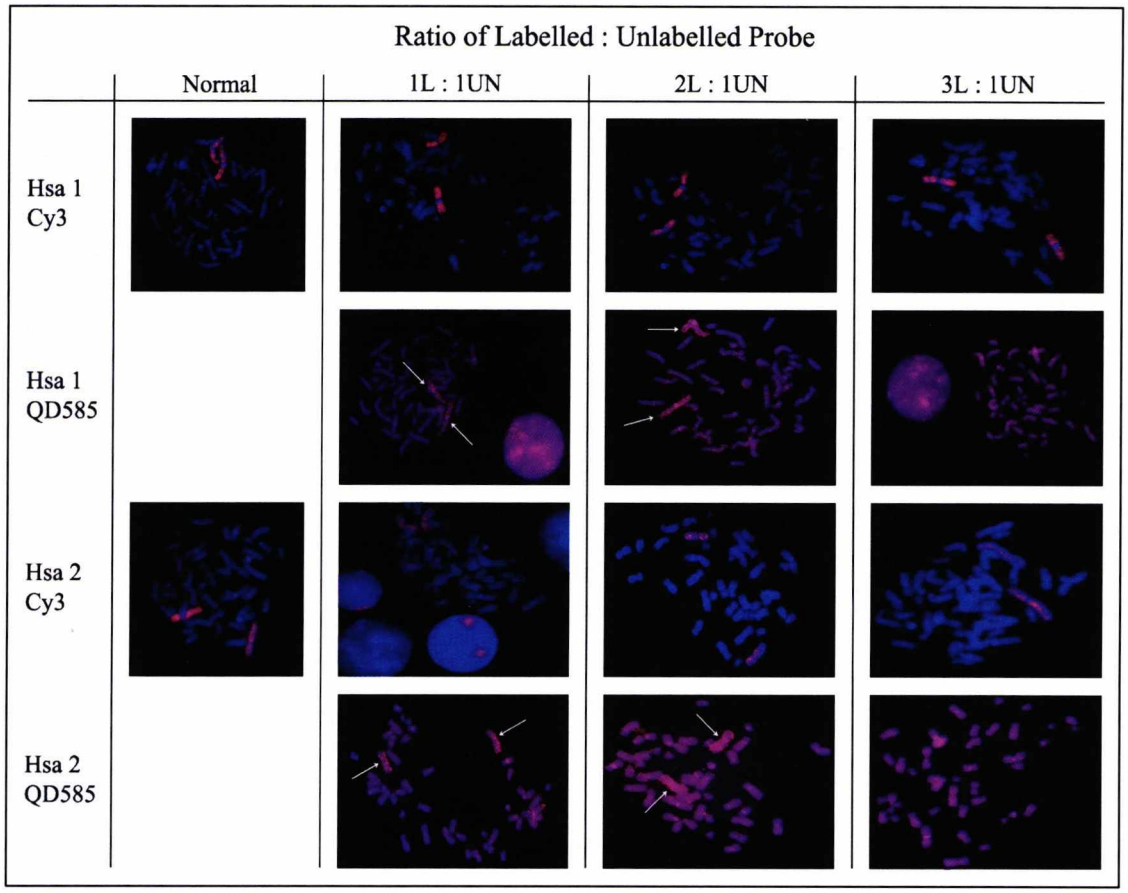

Figure 3.6: Results with increasing ratio of the labelled against unlabelled probe. Hybridisation was successful for Hsa1-QD585 at 1:1 and 2:1 whereas for Hsa2 results were less evident. Positive hybridisation results for Cy3 in all ratios. Arrows point at chromosomes 1 or 2 when detected with QD585. In these particular experiments higher background fluorescence was seen on the chromosomes.

As indicated in Figure 3.6 there was no increase in hybridisation efficiency (although QD detection was seen with specific ratios), as a result of altering the ratios, whereas successful detection was observed for all ratios with Cy3.

A component of the hybridisation buffer was also investigated. Dextran sulphate (DS) is used as a chelating agent to increase the signal intensity of the hybridised probe. In addition there was an indication (in the QD conjugant information sheet) that DS could promote QD aggregation. Thus, controlled experiments were run in the presence or absence of DS. The results are summarised in Figure 3.7.

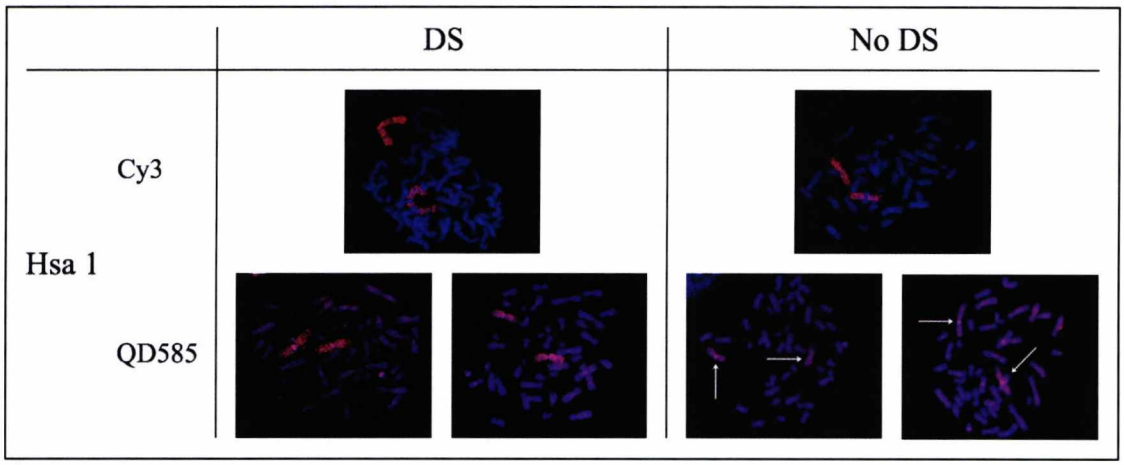

Figure 3.7: Results in the presence (left side) or absence (right side) of Dextran sulphate (DS) in the hybridisation-probe mix. Chromosome paints were detected using Cy3 and QD585. Cy3 worked in either condition, whereas detection with QD585 was brighter and more specific in the presence of DS.

Detection of probes with QDs was improved with a concentration of 7.2% (w/v) DS in the final probe-hybridisation mix. With regard to Cy3, it could detect the biotinylated probe equally well under both conditions.

Other alternative strategies to increase efficacy of QD-FISH included the use of custom made pancentromeric probe (Cambio). In addition the use of a different cell type (sperm) with more densely packed DNA, different chromosome paints (for chromosomes X and Y) and the use of a biotinylated oligonucleotide probe for chromosome 12 (Sigma). The latter probe was pre-labelled with one biotin per binding site again to reduce steric hindrance. Figures 3.8 and 3.9 summarise the results obtained from the use of these probes. In general terms, after several months of experiments, despite the purported advantages of QDs, Cy3 indirect labeled always produced more specific and more reliable results.

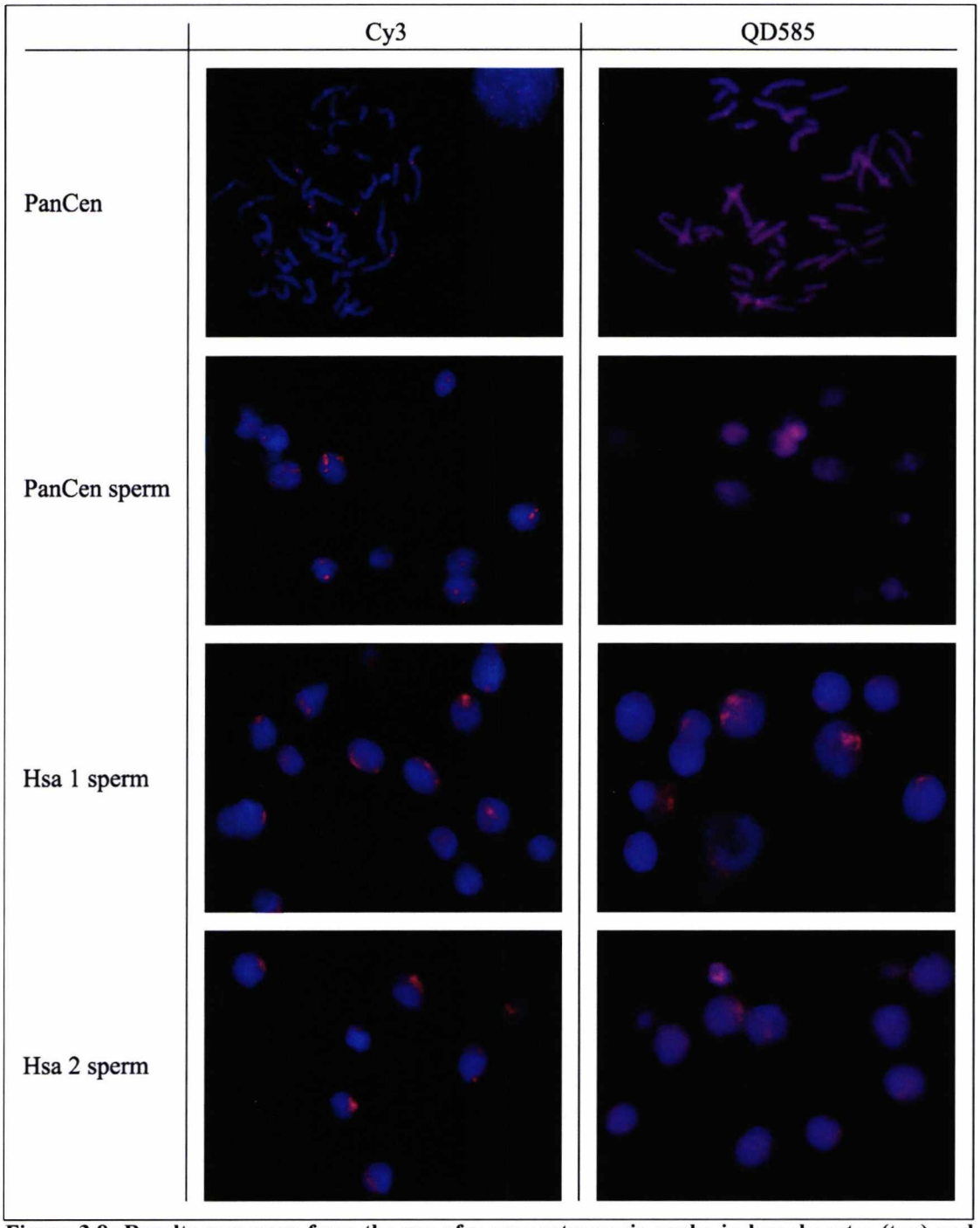

Figure 3.8: Results summary from the use of a pancentromeric probe in lymphocytes (top) and sperm (second from top). In addition paints for chromosomes 1 and 2 were used in sperm (bottom two). Detection with Cy3 is presented on the left whereas detection with QD585 on the right.

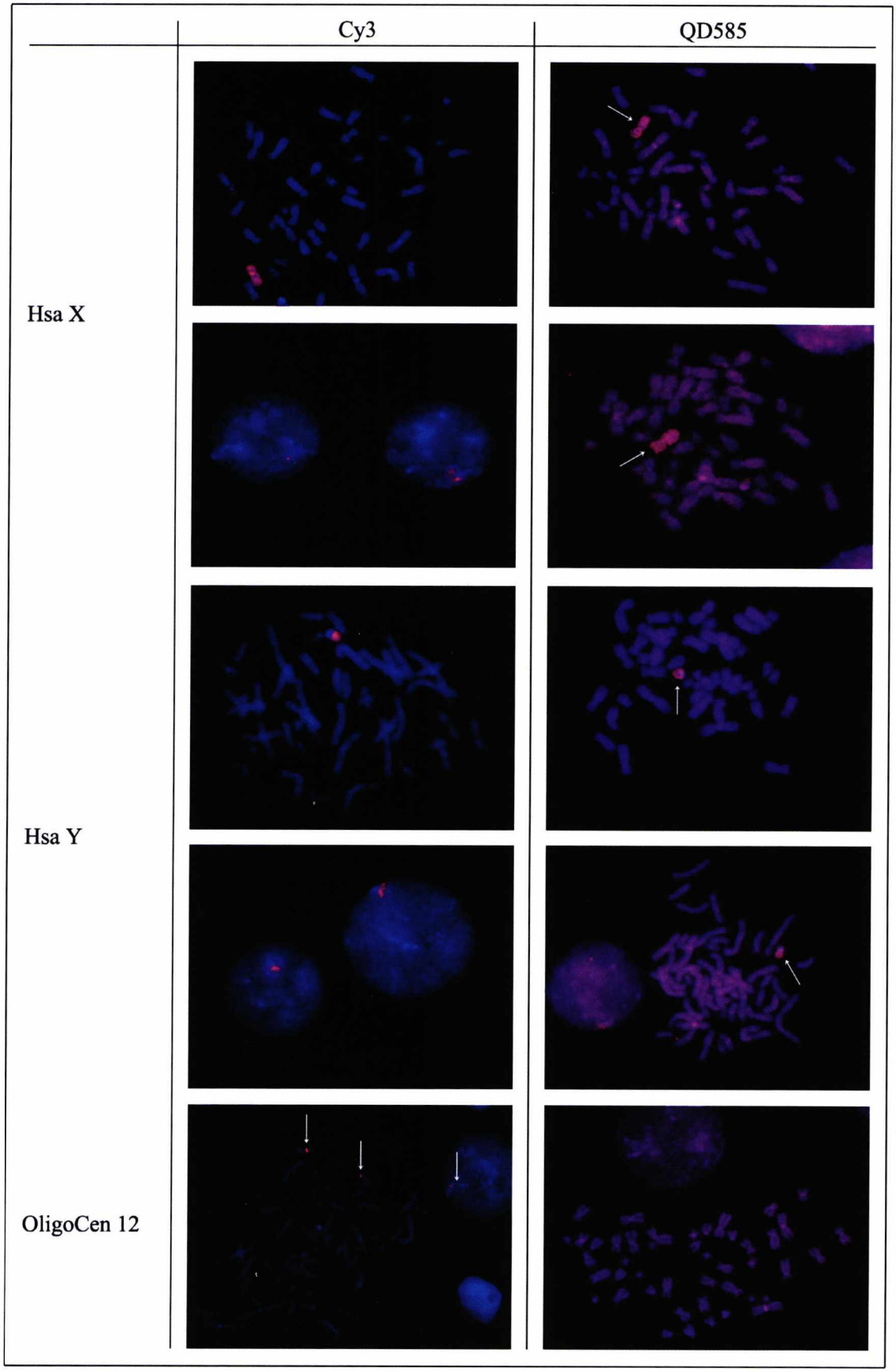

Figure 3.9: Results summary from the use of chromosome paints X, Y and an oligonucleotide probe for centromere 12. Detection using Cy3 is presented on the left whereas detection with QD585 is presented on the right. Arrows point to chromosomes X and Y when detected by QD585 and oligonucleotide probe for centromere 12 when detected with Cy3.

There was no detection of the pancentromeric probe with QD585 both in lymphocytes and sperm. However a signal was observed when QD585 was used to detect human chromosome 1 in sperm. There were successful results from the detection of human chromosome X and Y paints using QD585. With regard to the oligonucleotide probe for chromosome 12 there was not strong evidence of detection with QD585 despite all control experiments working reliably with all probes using Cy3. As with several previous attempts when a signal was observed with QDs this was not later reproduced.

Several more alternative strategies were attempted with no increased efficacy of QD-FISH, this included trying numerous batches of chromosome preparations, labelling probes with digoxigenin (and attempting detection with anti-digoxigenin), methods to increase cell permeability (fixation, pepsin) and use of alternative QD conjugates (QD520, QD605). The only intervention that we did observe that made a degree of success was the use of silicon coated plastic tubes and sonication of the conjugate prior to use. In both conditions we observed an (albeit temporary) improvement in the reliability of the results. Notwithstanding the repeated efforts to increase the robustness the approach, on the whole, outcomes were temperamental or unsuccessful. Figure 3.10 provides examples of some of the inglorious attempts.

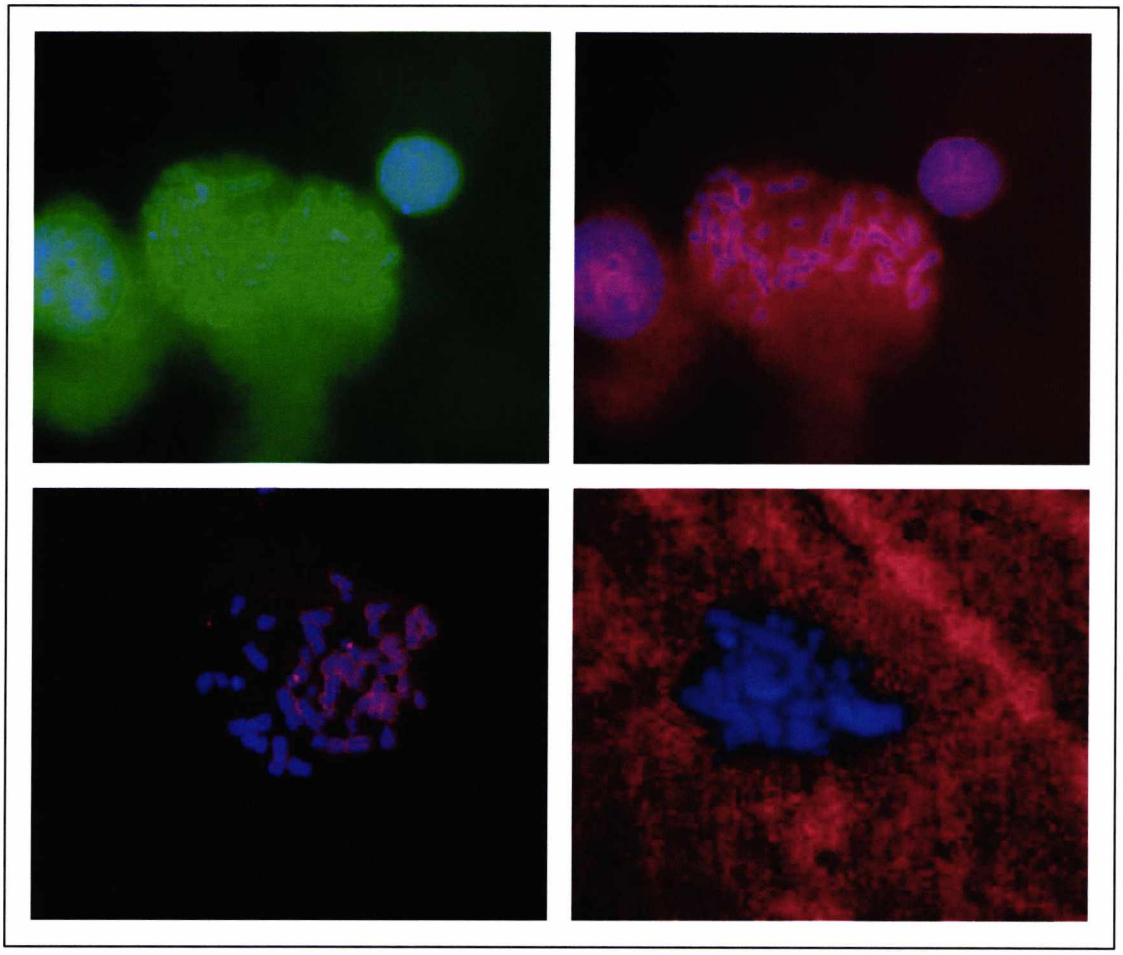

Figure 3.10: Some of the inglorious attempts using QDs. At the top, chromosome painting in human lymphocytes using QD520. No specific signal was seen and the area surrounding the chromosomes has high background (top left) which is bleeding through the red channel (top right). The bottom left image shows an attempt to visualise centromere of human chromosome 12. There is evidence of hybridisation but the preparation has high background. The bottom right image depicts an attempt to detect chromosome paint 2; a bright signal is seen on every part of the slide excluding chromosomes.

It is worth noting that records from all QDs purchased were kept and results were obtained only through the use of Invitrogen samples (Lot 48184A, for QD585). In contrast, there were no results through the use of any of the Evident samples. On the whole, none of the interventions attempted had a significant impact on the indirect FISH approach since the outcomes were temperamental or unsuccessful. In general terms indirect, QD experiments were successful approximately 25-35% of the time compared to Cy3 controls that worked reliably and consistently.

3.3.4. Specific aim 1d: To develop strategies for the direct coupling of quantum dots to biotinylated probes (including oligonucleotides and chromosome paints) for the use in "direct" FISH experiments

As the indirect approach had a limited degree of success, direct conjugation of QDs to FISH probes was attempted. The strategy followed was based on a published method by Bentolila and Weiss (2006). Single biotinylated probes and QDs were incubated at room temperature and allowed to form a construct which was verified through a shift in DNA motility conferred by the conjugation of QDs, as per section 2.8. Following construct confirmation the conjugant was used in direct FISH as previously described in sections 2.7.4 to 2.7.7.

With direct help from the authors we were confident that QD-DNA constructs were generated initially for the oligonucleotide probe for centromere 12 and for chromosome paint 2 (through amplification and labelling as described in section 2.7).

The following figures illustrate motility assays to investigate the formation of QD-DNA construct using oligonucleotide probes (Figure 3.11) and human chromosome 2 paint (Figure 3.12).

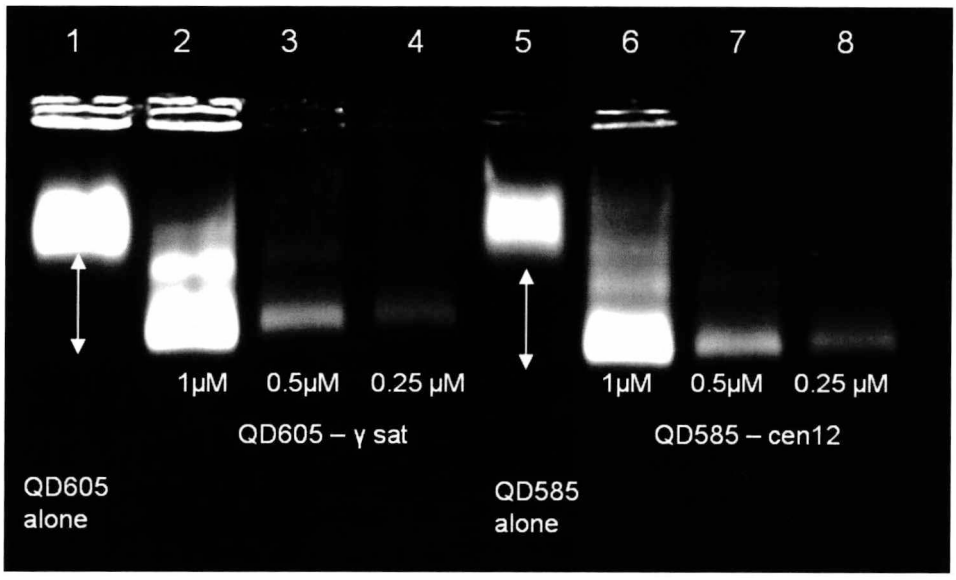

Figure 3.11: The difference in motility between naked QDs (lanes 1 & 5) and QD-DNA complexes at different concentrations of QDs (lanes 2-3-4 & 6-7-8). The shift in motility is evidence of conjugation.

As it can be seen in lanes 2-3-4 and 6-7-8 the QD-DNA travels faster from QD alone (lanes 1 and 5). These constructs were used in a direct FISH experiment, in mouse (QD605-γ sat) and human lymphocytes (QD605-cen12) but there was very little evidence of hybridisation in their respective target cells. Constructs between γ-sat and QD605 were similar to the published study by Bentolila and Weiss and were used as a positive control.

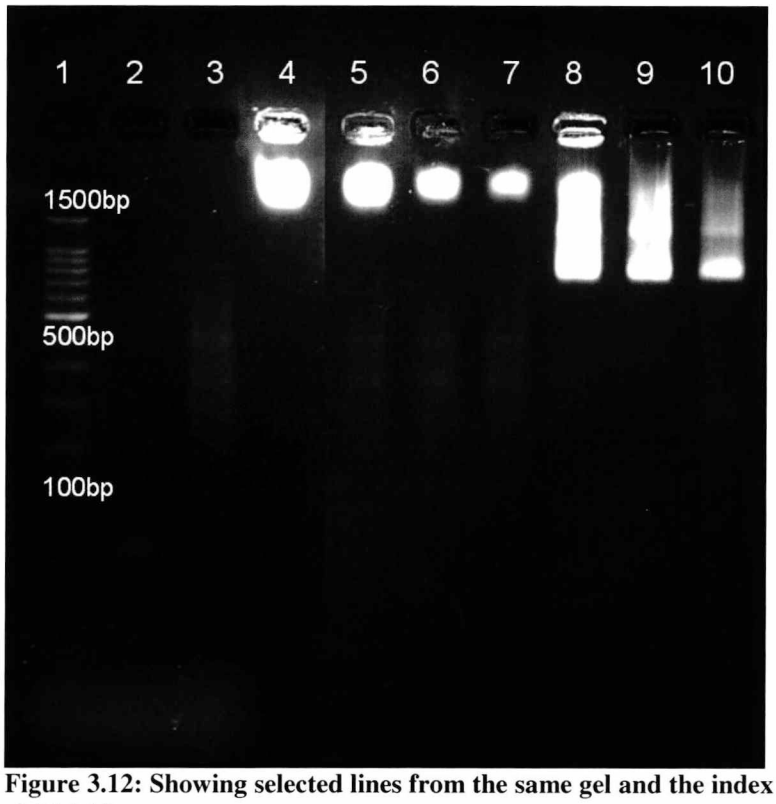

Lane	Sample
1	DNA ladder (100bp)
2	Biotinylated primer alone (50ng/μl)
3	Pooled DNA hsa2 alone (no biotin)
4	QD 585 alone
5	QD + unbiotinylated Hsa2 (**QD1μM**)
6	QD + unbiotinylated Hsa2 (**QD0.5μM**)
7	QD + unbiotinylated Hsa2 (**QD0.25μM**)
8	QD + biotinylated Hsa2 (**QD1μM**)
9	QD + biotinylated Hsa2 (**QD0.5μM**)
10	QD + biotinylated Hsa2 (**QD0.25μM**)

Figure 3.12: Showing selected lines from the same gel and the index for each line of the gel on the right table.

The message from Figure 3.12 was that unbiotinylated DNA (Hsa2-lane 3) runs faster from QD alone (lane 4). The same applies to QD-DNA (lanes 8, 9, 10) compared to QD alone (lane 4) or QD with unbiotinylated DNA (lanes 5, 6, 7). However none of the constructs that were generated either with the oligonucleotide probes or chromosome paint were successfully hybridised in direct FISH experiments. As a control the biotinylated DNA was detected by Cy3 following indirect FISH to prove functionality. Figure 3.13 is an example of results following these attempts.

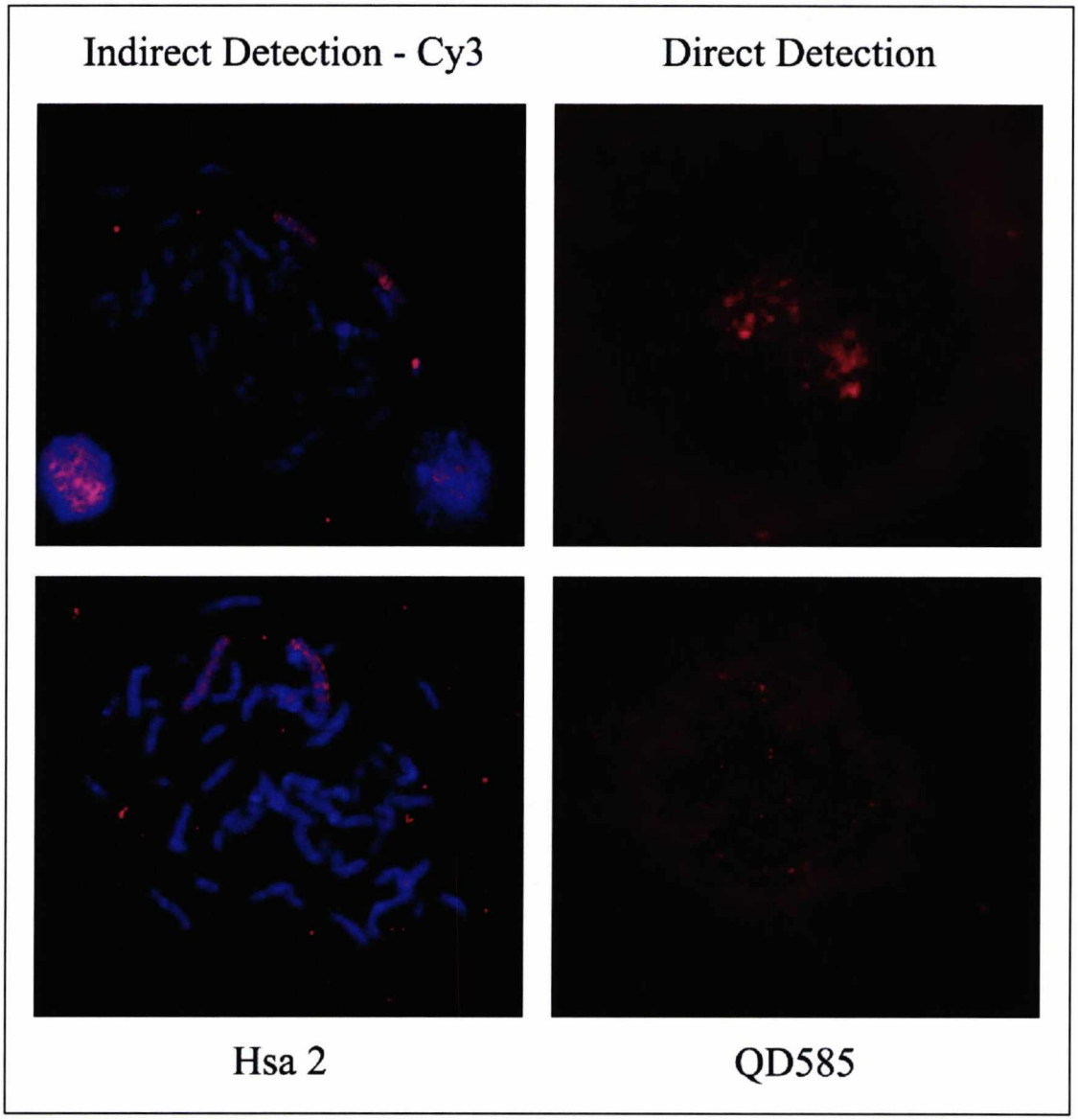

Figure 3.13: The successful detection of human chromosome 2 paint with indirectly Cy3 and the absence of hybridisation when it was used in a construct with QD585.

Despite repeated attempts to generate QD-DNA constructs employing a range of different conditions (stringency, incubation time, different DNA concentrations) without exception they ended in failure to hybridise using QD585.

3.4. Concluding remarks

The "take-home" message of this comprehensive appraisal of the utility of QDs for FISH (either indirect or direct approach) has been that, in their current form, QDs are not suitable materials for FISH applications. In both approaches many alternative strategies were employed to increase efficacy through the use of QDs. By and large

this was not successful. Thus fast hybridising oligonucleotide probes (Chapter 4) were employed as an alternative to be used in the study of nuclear architecture in human sperm and preimplantation embryos.

4. Specific aim 2: To develop a 24 chromosome aneuploidy screening approach applicable to single nuclei and of use for determining nuclear organisation

4.1. Background

As seen from Chapter 3 attempts to make use of novel fluorochromes (QDs) for FISH proved unsuccessful and thus experiments continued using traditional organic fluorochromes. As mentioned in section 1.4.6 for PGS, a 24 chromosome interphase cytogenetics strategy would be desirable but would have to be applicable for a single cell. Also, for sperm cells, to the best of my knowledge no studies have examined all chromosomes concurrently.

As mentioned in the last part of the introduction, section 1.5 onwards, chromosome position in the interphase nucleus is an indicator of nuclear organisation in a variety of cell types and developmental stages (Foster & Bridger 2005). It is widely accepted that chromosomes are organised in discrete positions that appear to be non-random in the nucleus (Cremer *et al.* 2001). Also evidence shows that alterations from those non-random patterns could lead to disease phenotypes (i.e. laminopathies) (Foster & Bridger 2005). As outlined in section 1.6 the principal aim of this thesis was to investigate whether a link exists between aberrant nuclear position and infertility (Chapter 5) or aneuploidy (Chapter 7), by expanding chromosome position assays into the entire human karyotype. Before this could be achieved however, an assay that examined loci from all the chromosomes was necessary.

4.2. Aims

Given the above rationale, the specific aims of this chapter were as follows:

Specific aim 2a: With the help of commercial partners, to design probe sets that target chromosome loci for all chromosomes.

Specific aim 2b: To validate these probe sets and find optimum conditions for their usage, individually and (for when only single nuclei were available) in sequential hybridisation layers.

Specific aim 2c: To evaluate the efficacy of the probe sets on blastomere and sperm cells.

4.3. Results

4.3.1. Specific aim 2a: With the help of commercial partners, to design probe sets that target chromosome loci for all chromosomes

Coupled with the expertise of Kreatech Diagnostics in labelling probes directly with fluorochromes, it was decided, through discussion with all partners, that the best strategy to attempt would involve 4 layers of probes each targeting sequences for 6 chromosomes. Commercial probe sets use the 5 known fluorochromes (Red, Green, Gold, Aqua and Blue) were already in existence; in addition to these a Far Red fluorochrome was employed as well. It was decided that this basic strategy allowed for the fewest number of sequential hybridisations to each layer while avoiding the complications of mixing fluorochromes. Probe sets (6 chromosomes) were divided according to whether centromeric probes were available or not (non centromeric probes requiring longer hybridisation). That is, chromosomes 5, 13, 14, 19, 21, 22 do not have unique centromeric sequences and thus were placed in the same probe mix (that would require longer hybridisation) whereas the others (three sets of 6) formed the centromeric mixes. The probe choice strategy was also to use the brightest probe with the less robust fluorochrome (e.g. Blue and Aqua). Conversely for chromosomes that had small size satellites corresponding to their centromeres (e.g. 2, 3, 4 and 20) they were allocated to strong fluorochromes and distributed in the three centromeric layers.

The following table presents the information regarding the final set of probes and the targeting sequence for each chromosome.

Color	"α" Layer centromeric	"β" Layer centromeric	"γ" Layer centromeric	"ω" Layer unique sequence
DY405 blue	SE **7** (7p11-q11)	SE **11** (11p11-q11)	SE **18** (18p11-q11)	CD37 (**19**q13)
DY415 aqua	SE **1** (1qh)	SE **9** (9qh)	SE **16** (16p11-q11)	EGR1 (**5**q31)
DY495 green	SE **6** (6p11-q11)	SE **20** (20p11-q11)	SE **2** (2p11-q11)	DSCR (**21**q22)
DY547 gold	SE **8** (8p11-q11)	SE **12** (12p11-q11)	SE **X** (Xp11-q11)	BCR (**22**q11)
DY590 red	SE **3** (3p11-q11)	SE **10** (10p11-q11)	SE **Y** (Yq12)	RB (**13**q14)
DY647 far red	SE **4** (4p11-q11)	SE **17** (17p11-q11)	SE **15** (15p11-q11)	IGH (**14**q32)

Table 4.1: Probe names and targets for each of the 4 layers comprising the 24 panel. Each layer is displayed by having the chromosome in the lowest excitation spectrum first. Bold (under each layer) indicates the chromosome number.

Ergo, specific aim 2a was achieved and a probe set for all chromosomal loci was designed. The fact that three layers could hybridise within 30 minutes due to the nature of target provided us with the potential to screen all chromosomes within 24 hours, something that could have implications within a diagnostic setting. For the purposes of this study, probe sets were designated "Alpha" (7, 1, 6, 8, 3, 4), "Beta" (11, 9, 20, 12, 10, 17), "Gamma" (18, 16, 2, X, Y, 15) for the centromeric probes and "Omega" (19, 5, 21, 22, 13, 14) for the unique sequence set. Figure 4.1 shows a sample of experiments performed on lymphocytes for each layer.

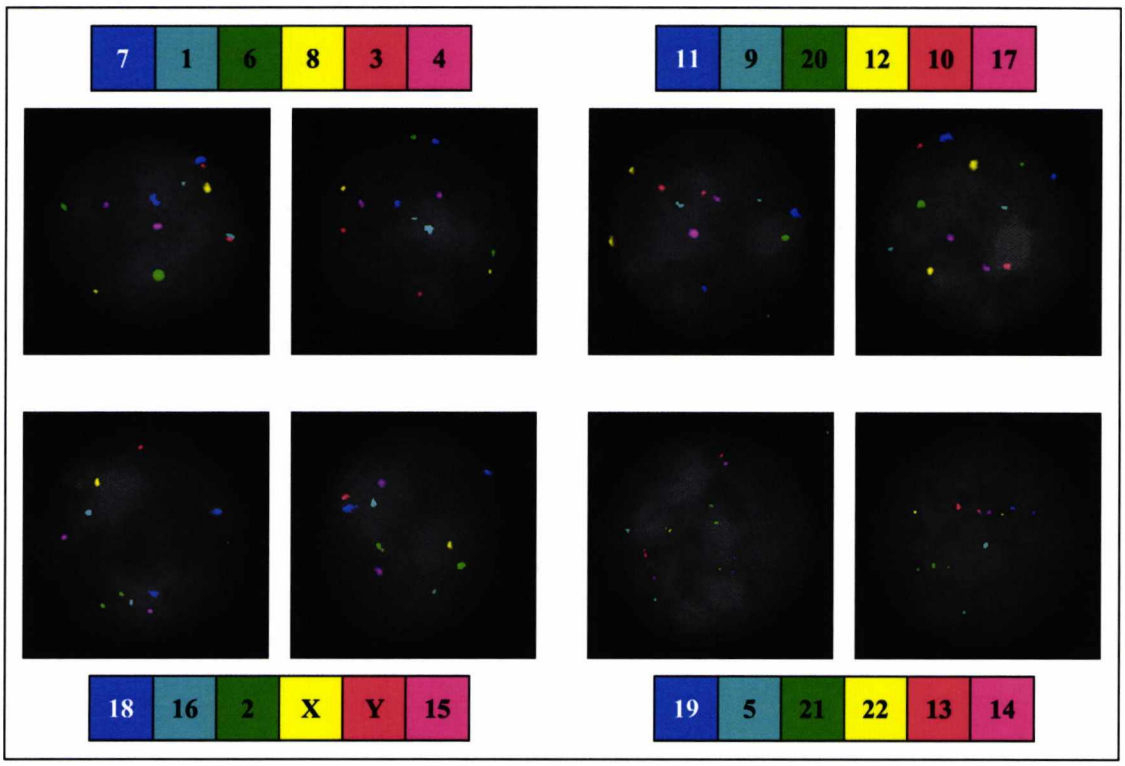

Figure 4.1: A representative sample of lymphocytes from validation experiments with each probe layer to assess probe efficacy.

4.3.2. Specific aim 2b: To validate these probe sets and find optimum conditions for their usage, individually and for (when only single nuclei were available) in sequential hybridisation layers

The full probe set was validated for efficacy against lymphocytes from a karyotypically normal male. Tables 4.2-4.5 display the results of this validation and the % of correct ploidy for all probes per layer.

Chromosome	Two Signals	One Signal	No signal	Success Rate %
7	102	1	0	99
1	97	6	0	94.1
6	100	0	0	100
8	99	4	0	96.1
3	103	0	0	100
4	101	2	0	98
Overall success rate: % of cells with correct ploidy				90.29

Table 4.2: Hybridisation efficiency results for probe set "Alpha" after scoring 103 lymphocytes.

Chromosome	Two Signals	One Signal	No signal	Success Rate %
11	98	5	0	95.14
9	98	5	0	95.14
20	101	2	0	98
12	103	0	0	100
10	102	1	0	99
17	98	5	0	95.14
Overall success rate: % of cells with correct ploidy				82.5

Table 4.3: Hybridisation efficiency results for probe set "Beta" after scoring 103 lymphocytes.

Chromosome	Two Signals	One Signal	No signal	Success Rate %
18	100	3	0	97
16	96	7	0	93.2
2	99	4	0	96.1
X	103	0	0	100
Y	103	0	0	100
15	100	3	0	97.0
Overall success rate: % of cells with correct ploidy				86.4

Table 4.4: Hybridisation efficiency results for probe set "Gamma" after scoring 103 lymphocytes.

Chromosome	Two Signals	One Signal	No signal	Success Rate %
19	100	3	0	97.8
5	99	4	0	96.11
21	102	1	0	99
22	101	2	0	98.05
13	99	4	0	96.11
14	93	8	2	90.29
Overall success rate: % of cells with correct ploidy				76.69

Table 4.5: Hybridisation efficiency results for probe set "Omega" after scoring 103 lymphocytes.

Hybridisation efficiency was above 90% for each chromosome probe, with the Green, Red and Gold fluorochromes having the highest efficiencies per layer. Blue and Aqua had similar efficiencies with Blue being slightly higher. The efficiency of Far Red was satisfactory with the lowest % observed in the unique sequence probe layer ("Omega"). As part of the process of developing a sequential hybridisation strategy certain parameters where investigated for optimisation and are summarised in Table 4.6.

Parameter Investigated	Suggestion from manufacturers	Rationale for Investigation; Importance	Experiment Performed	Outcome
Probe denaturation and hybridisation	Denature probe and target cells at 85°C for 5 minutes. Hybridisation at 37°C for 15 minutes for layers "α-β-γ "& overnight (16 hours) for layer "ω"	Reduce the exposure time of target cells to high temperatures; Crucial for reprobing since target cells would have to be exposed 4 times to high temperature conditions	Compared probe efficacy between two conditions: • Separate denaturation of probe only (73°C for 10 minutes) ensued by a shorter co-denaturation with target cells (90 seconds at 75°C) • Co-denaturation of probes/target (75°C – 3.5 minutes) Hybridisation temperature always 37°C	Higher efficacy with separate denaturation of probe followed by a shorter co-denaturation with target cells.
Actual temperature of short co-denaturation - hybridisation in Thermobrite® (hybridisation chamber)	Display of the machine was 75°C for 90 seconds and 37°C for hybridisation	Investigate any deviation from display readings; Better monitoring of the temperature	Using a temperature-read probe • 10 second interval readings of temperature during the denaturation time • 1 minute interval readings during the hybridisation period Compared with display/adjust if necessary	Actual temperature (denaturation) 2.5°C lower from display, Hybridisation (0.9°C lower from display) When conditions where adjusted to match display – probes did not work. Thus maintained current settings.
Stringency of post-hybridisation wash	0.4 X SSC	Certain fluorochromes had suboptimum performance with current condition (i.e. did not work or bleedthrough); Improve conditions	Compared a high stringent (0.4 X SSC) to a lower stringent condition (0.7 X SSC)	Better performance and less bleedthrough using the lower stringent condition
Counterstain concentration (DAPI)	Antifade (no DAPI)	Presence of DAPI was required for the positional studies to account for the difference in DNA concentration; Use of appropriate concentration so that the blue fluorochrome could be observed	Tested a series of different DAPI concentrations (ranging from 1500, 200, 50, 10, 0,1ng/ml)	Blue fluorochrome was visible with no issues under 0.1ng/ml DAPI

Table 4.6: Summarises of all the technical conditions investigated to increase probe efficacy and performance.

As depicted in Table 4.6, important parameters were investigated to improve probe performance. The most important was the use of a separate denaturation (probe only) condition followed by a short co-denaturation with the target cells. The monitoring of temperature (which showed evidence that the "actual" denaturation temperature was closer to 73°C and thus matched the temperature of probe denaturation), the stringency level of post-hybridisation wash and the concentration of the counterstain were also optimised and the validation results on Tables 4.2-4.5 are by taking into account all the optimised parameters.

Once probe sets were validated with lymphocytes as individual layers, attempts were made to incorporate them in a sequential FISH strategy of four layers. Tables 4.7-4.10 outline how each individual layer performed in three reprobing assays, providing information on signal efficiency and ploidy status. In optimising the strategy, the main decision to make was whether to hybridise "Omega" first or last. As a result of much experimentation involving the alteration of many of the parameters outlined in Table 4.6, it was determined that hybridisation of "Omega" as the first layer led to extensive cell loss and absence of signal, whereas 15 minute hybridisations of "Alpha, Beta, Gamma" kept the nuclei more intact for a final "Omega" layer. An additional reason for having the "Omega" layer last was that this layer occasionally produced "fluorescent blobs" at random. These "blobs" could be superimposed on a cell and thus "stealing" the true signal fluorescence. By having this layer last, this phenomenon was reduced and any blobs were not further transferred to other layers. A further point of consideration was that it was not possible to analyse 100 cells for each layer prior to reprobing as this led to extensive cell loss. Thus in the following experiments, only 10 cells were counted however the identical experiment was repeated on 3 separate occasions (Assays 1-3).

Probe set "Alpha" 7, 1, 6, 8, 3, 4	**Assay 1 (10 cells)**	**Assay 2 (10 cells)**	**Assay 3 (10 cells)**
Cells with signals per layer	9/10 – signals for all 6	10/10 – signals for all 6	10/10 – signals for all 6
Correct ploidy in layer	8/10 – correct ploidy for all 6	10/10 – correct ploidy for all 6	10/10 – correct ploidy for all 6
Details of remaining	1/10 – one signal for 7		
Other details (e.g. damage or cell not found)	1/10 – cell damaged	-	
Correct ploidy % per assay per layer	**80%**	**100%**	**100%**

Table 4.7: Performance of probe set "Alpha" in the reprobing assays. This layer was the first layer in the hybridisation sequence.

Probe set "Beta" 11, 9, 20, 12, 10, 17	**Assay 1 (10 cells)**	**Assay 2 (10 cells)**	**Assay 3 (10 cells)**
Cells with signals per layer	9/10 – signals for all 6	9/10 – signals for all 6	10/10 – signals for all 6
Correct ploidy in layer	8/10 – correct ploidy for all 6	8/10 – correct ploidy for all 6	9/10– correct ploidy for all 6
Details of remaining	1/10 – one signal for 12	1/10 – one signal for 20, 12	1/10 – one signal for 20
Other details (e.g. damage or cell not found)	1/10 – cell damaged	1/10 – cell damaged	
Correct ploidy % per assay per layer	**80%**	**80%**	**90%**

Table 4.8: Performance probe set "Beta" in the reprobing assays. This layer was the second layer in the hybridisation sequence.

Probe set "Gamma" 18, 16, 2, X, Y, 15	**Assay 1 (10 cells)**	**Assay 2 (10 cells)**	**Assay 3 (10 cells)**
Cells with signals per layer	9/10 – signals for all 6	7/10 – signals for all 6	10/10 – signals for all 6
Correct ploidy in layer	8/10 – correct ploidy for all 6	7/10 – correct ploidy for all 6	10/10 – signals for all 6
Details of remaining	1/10 – no clear signal for X	1/10 – no clear signal for Y 1/10 – no clear signal for X	
Other details (e.g. damage or cell not found)	1/10 – cell damaged	1/10 – cell not found	
Correct ploidy % per assay per layer	**80%**	**70%**	**100%**

Table 4.9: Performance of probe set "Gamma" in the reprobing assays. This layer was the third layer in the hybridisation sequence.

Probe set "Omega" 19, 5, 21, 22, 13, 14	**Assay 1 (10 cells)**	**Assay 2 (10 cells)**	**Assay 3 (10 cells)**
Cells with signals per layer	9/10 – signals for all 6	8/10 – signals for all 6	10/10 – signals for all 6
Correct ploidy in layer	8/10 – correct ploidy for all 6	7/10 – correct ploidy for all 6	8/10 – signals for all 6
Details of remaining	1/10 – one signal for 5, 13	1/10 – no clear signal for 14 1/10 – no clear signal for 19	1/10 – one signal for 13 1/10 – one signal for 21
Other details (e.g. damage or cell not found)	1/10 – cell damaged	1/10 – cell not found	
Correct ploidy % per assay per layer	**80%**	**70%**	**80%**

Table 4.10: Performance of probe set "Omega" in the reprobing assays. This layer was the forth layer in the hybridisation sequence.

From the above results the average percentage of correct ploidy for each of the layers throughout the reprobing assays was calculated. For probe set "Alpha" it was 93.3% for probe set "Beta" it was 83.3%, for probe set "Gamma" it was 83.3% and for probe set "Omega" it was 76.67%. Table 4.11 gives an account of the number of cells with correct ploidy for all chromosomes as a result of the 3 assays and Figure 4.2 illustrates a nucleus with correct ploidy for all chromosomes after reprobing.

Chromosomes targeted	**Assay 1 10 cells**	**Assay 2 10 cells**	**Assay 3 10 cells**
46/46	6	5	7
45/46	1	3	2
44/46	1	-	1
42/46	1	1	-
40/46	-	-	-
No result-cell loss or damage	1	1	-
SUM (46/46)	6/10	5/10	7/10

Table 4.11: Correct ploidy efficiency in the experiments testing the reprobing strategy.

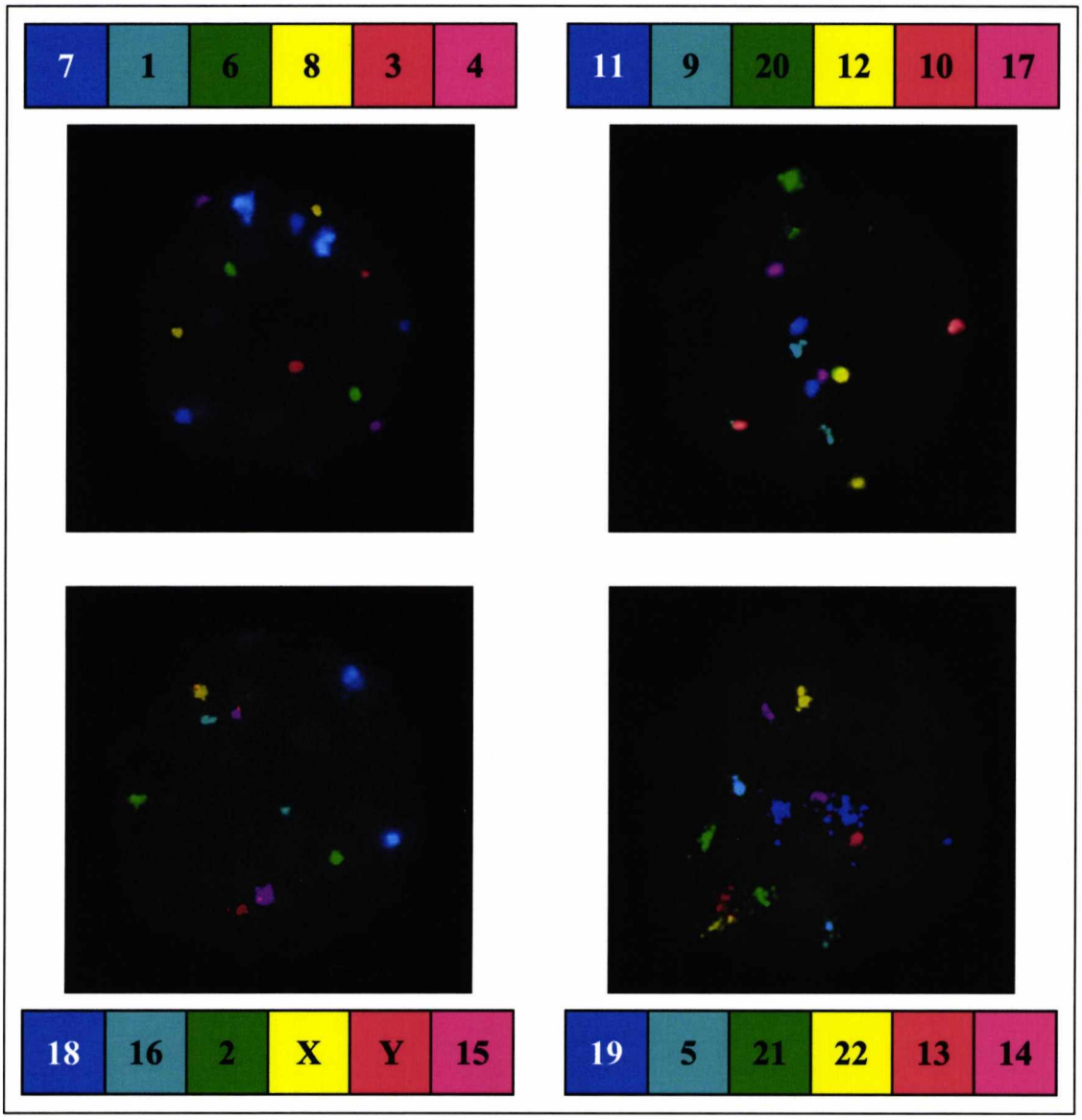

Figure 4.2: Correct ploidy for all chromosomes in a nucleus from control lymphocytes.

The average overall success of the 24 chromosome screening (Table 4.11) in control lymphocytes was 60% or 18/30 cells with correct ploidy status for all chromosomes, 33.3% of cells displaying correct ploidy for less than 46 chromosomes (lowest being 42/46) and 6.67% of cells being subject to damage.

4.3.3. Specific aim 2c: To evaluate the efficacy of the probe sets on blastomere and sperm cells

Blastomeres (especially from whole embryos with good spreading) appeared more tolerant with regard to nuclear integrity after 4 layers of hybridisation. The reprobing strategy worked well as from 360 blastomeres (from 17 whole embryos) 250 blastomeres provided successful hybridisation results in the fourth layer (69.44%).

Unlike with the lymphocytes, assessment was made by visual inspection only, as the chromosome copy number in each of the blastomere nuclei was not known. Figure 4.3 depicts a blastomere after 4 layers of reprobing.

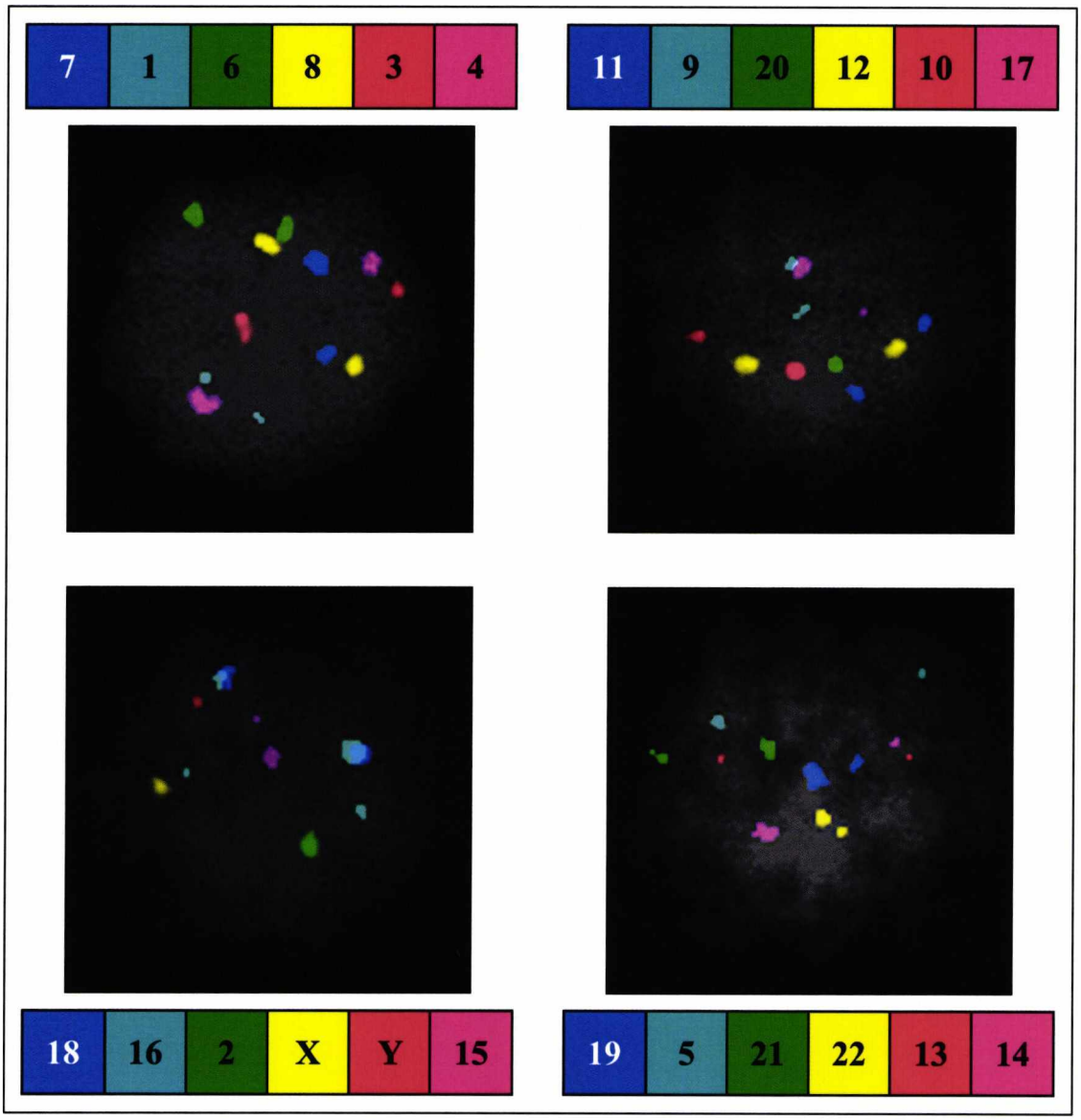

Figure 4.3: A blastomere after 4 layers of hybridisation. This was a normal blastomere for most of the chromosomes. Monosomy for chromosome 2 (one green signal – bottom left) was the only abnormality.

With regard to the sperm heads, each probe set was used in individual FISH experiments (i.e. without reprobing) and a minimum of 100 cells were captured per layer. Table 4.12 provides the overall efficiency per probe layer in both normal and OAT males and Figure 4.4 presents a sperm cell with the 4 different probe layers used.

Probe	Normal (%)	OAT (%)
Alpha	100	100%
Beta	100	99.8
Gamma	100	100
Omega	99.9	99.04

Table 4.12: Overall probe layer efficiencies in normal and OAT males.

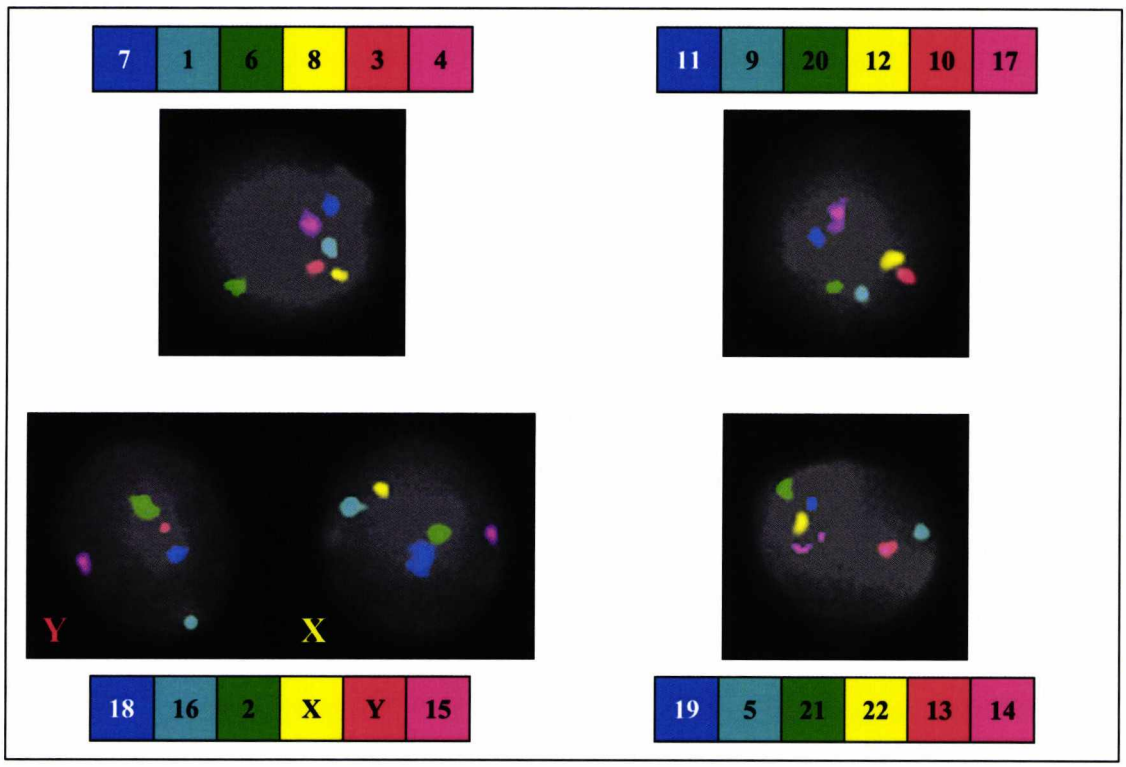

Figure 4.4: A sperm cell under each individual probe layer.

From Table 4.12 it becomes clear that each layer had high efficiency when used as an individual layer in sperm.

4.4. Concluding remarks

Following the lack of success of quantum dots (Chapter 3) as a means of generating multicolour preparations, the approach described here provided the means through which the remaining three chapters (on chromosome copy number and nuclear organisation in sperm and blastomeres) could proceed. The assay to determine efficiency resulted into a complete 24 screening with 60% success (46/46), equivalent to a greater than 95% success rate for each individual probe but nonetheless mindful of the fact that around 40% of the cells would not be completely correctly diagnosed.

5. Specific aim 3: To test the hypothesis that nuclear organisation is altered in men with severely compromised semen parameters by assaying loci for all chromosomes

5.1. Background

As outlined in section 1.3, male factor infertility is a complex phenomenon with multiple causes, many of which are chromosomally related (Shah *et al.* 2003; Tempest & Griffin 2004; Griffin & Finch 2005). To date however, an association between chromosome position in the nucleus (nuclear organisation) and infertility remains under-explored. Nuclear organisation in spermatogenesis has nonetheless been extensively studied in sperm as discussed in section 1.5.7, revealing a defined nuclear architecture with chromosomes adopting a "hairpin" structure with their centromeres pointing towards the interior and the telomeres towards the periphery (reviewed in Zalensky and Zalenskaya (2007)). That is the 23 centromeres cluster into a compact position well inside the nucleus with the sex chromosomes adjacent (Zalensky *et al.* 1993; Zalensky *et al.* 1995; Zalenskaya & Zalensky 2004). It seems reasonable to hypothesise that, since during spermatogenesis a highly ordered set of nuclear organisation events are set in place to prepare sperm for fertilisation, any alterations in the nuclear organisation should be evident in at least a subset of the population with compromised fertility. This link has yet to be established fully, however preliminary results from my laboratory (Finch *et al.* 2008b) for three chromosomes (X, Y and 18) suggested that sex chromosomes adopt a more random position in infertile men compared to controls. The principal aim of this chapter was to study the nuclear address of specific (mostly centromeric) chromosome loci (representing each of the chromosomes) in the sperm heads of men with normal parameters and to test the hypothesis that this position is altered in sperm of men with impaired fertility [i.e. with OligoAsthenoTeratozoospermia (OAT)]. Specifically, the question was asked whether a non-random pattern of distribution could be established in each male and, if so, which part of the nucleus was preferentially occupied. If the primary hypothesis is correct then it could form the basis for a screening test for certain types of infertility.

5.2. Aims and hypotheses

Given the above, the primary purpose of this chapter (Specific aim 3) was to assess the relative nuclear organisation for 24 chromosome loci (18 of which were centromeric, 6 locus specific), in the sperm nuclei of 10 men with normal semen parameters and in 10 men with OAT to test the following hypotheses:

Specific aim 3a: That the nuclear position of all loci tested is non-random in all control males and hence a strict nuclear organisation is apparent in human sperm.

Specific aim 3b: That each locus tested has a defined and consistent nuclear address in each of the control males analysed.

Specific aim 3c: That centromeric and sex chromosomal loci are the most centrally located in the sperm head.

Specific aim 3d: That the nuclear position of the loci is altered in OAT males, either from a non-random, to an apparently random pattern, or to a different, nuclear address. Patients and controls were analysed individually and as two collective groups.

Specific aim 3e: That increased disomy levels in sperm (i.e. the proportion with a greater number of extra chromosomes) are correlated with increased altered nuclear organisation.

As outlined in section 2.12, in order to assess nuclear position a new methodology was applied that utilised a novel plug-in for Image J analysis package (Skinner *et al.* 2009). That is, applications of accepted approaches for 3D extrapolations from 2D data (Federico *et al.* 2008) asked two questions i.e. after analysis of 100+ signals, could a non-random pattern of distribution be detected? (Chi-square test); and if so, which shell (1-5) was predominantly represented in the distribution.

Specific aims 3a-3d are considered together in the following results section.

5.3. Results

5.3.1. Specific aims 3a-3d:

In total, 25,776 signals for all 24 chromosomes were analysed from 10 different men with normal semen parameters. On average for each probe layer (each layer had 6 chromosomal targets) 107 images were analysed. Essentially this translates to 107 data points (signals) recorded and analysed per loci per control (slightly more than 100 sperm heads were captured and analysed in case there was an absence of signal or an ambiguous signal to ensure a minimum of 100 for each). With regard to men with OAT, 25,047 signals for all 24 chromosomes were analysed from 10 different men. On average for each probe layer 104 images (data points) were analysed. Figure 5.1 illustrates an example of the result of a FISH experiment using the 4 probe layers (6 chromosomes each) in sperm, while Figure 5.2 presents the analysis principle once images where captured after FISH.

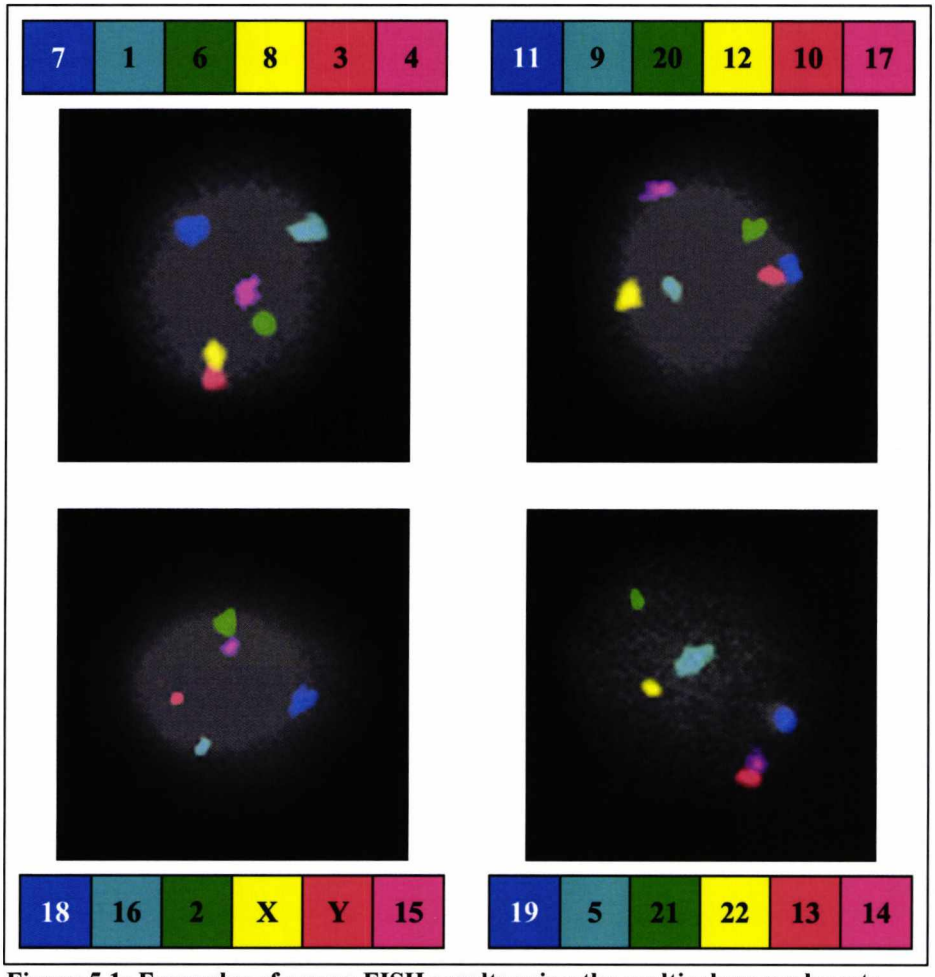

Figure 5.1: Examples of sperm FISH results using the multicolour probe sets.

The following figure displays the principle behind image analysis used for the nuclear address in this thesis.

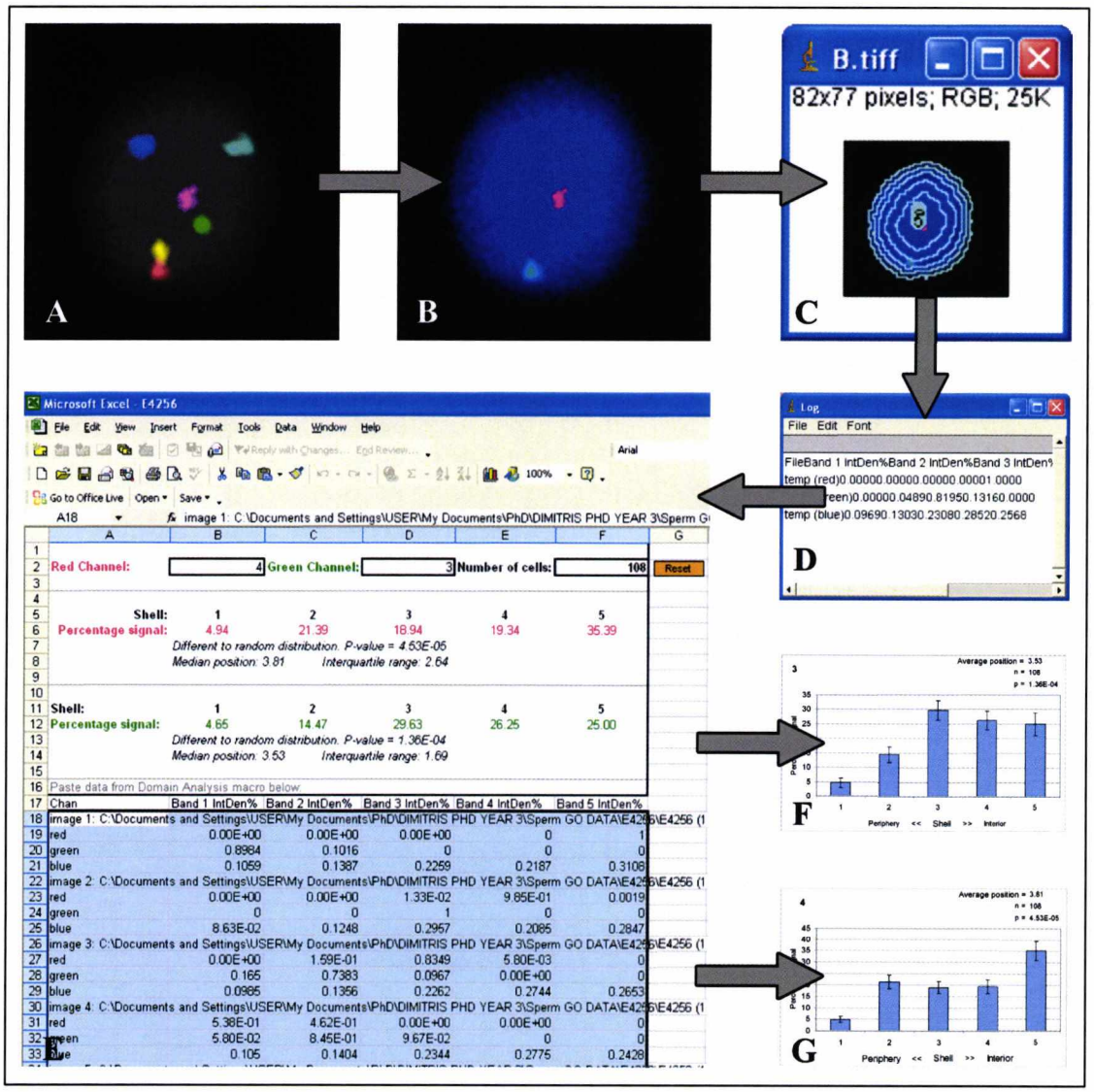

Figure 5.2: The image analysis principle. A hundred images like (A) where acquired. These images were exported in Red–Green–Blue combinations. Red and Green corresponded to signals and Blue to DAPI counterstain (B), then ring analysis was run using the image J plug-in macro (C). A log result for the three channels (red, green, blue) was outputted (D) and the log file was pasted to an excel template (E). Graphs were generated for each chromosome (in this example chromosomes 4 and 3) showing the preferential position of the captured signals (F & G).

As a result of this study 480 graphs were produced (24 chromosomes x 20 men in total because of space constraints and reader empathy they are not all displayed here but are present in their entirety in **Digital appendix A**). The results are however summarised in Tables 5.1 and 5.2 for normal and OAT males respectively. Moreover,

a summary of the pooled results for a) normal controls and b) OAT men is given in Figures 5.7-5.14.

In each individual control male all chromosomal loci positions were non-randomly distributed ($p<0.05$ by chi-squared test). This was also the case for the vast majority of chromosomes in most of the OAT patients. However 4 chromosome loci in 4 different OAT patients showed a distribution that was not statistically distinguishable from random, meaning that either 100 cells were not enough to reach significance or that indeed their position was random. These chromosome loci were the centromeres of chromosomes 4, 6 and 12 plus the locus specific probe on chromosome 13. The chromosome 13 locus displayed a pattern not discernable from random in three OAT patients. The following Figures (5.3-5.6) are representative samples of radial position regarding chromosome loci Y and 13 in each of the 10 normal and OAT males. It should be noted that in all the graphs presented in this chapter (n) indicates the number of nuclei analysed, average position refers to the median value (since our data set is not parametric) and p indicates results of the χ^2 test against a random distribution. All p values were considered statistically significant when $p<0.05$ (4d.f.), otherwise ($p>0.05$) were considered as Not Discernable from a Random Distribution Pattern (NDRDP). Furthermore, in all the graphs presented in this chapter, the following criteria are used in order to classify the signals depending on the shell of preference: Peripheral – Shell 1 or 1/2, Peripheral/Medial – Shell 2 or 1-3, Medial – Shell 3, 2/3, or 3/4, Central/Medial – Shell 4 or 3-5, Central – Shell 5 or 4/5.

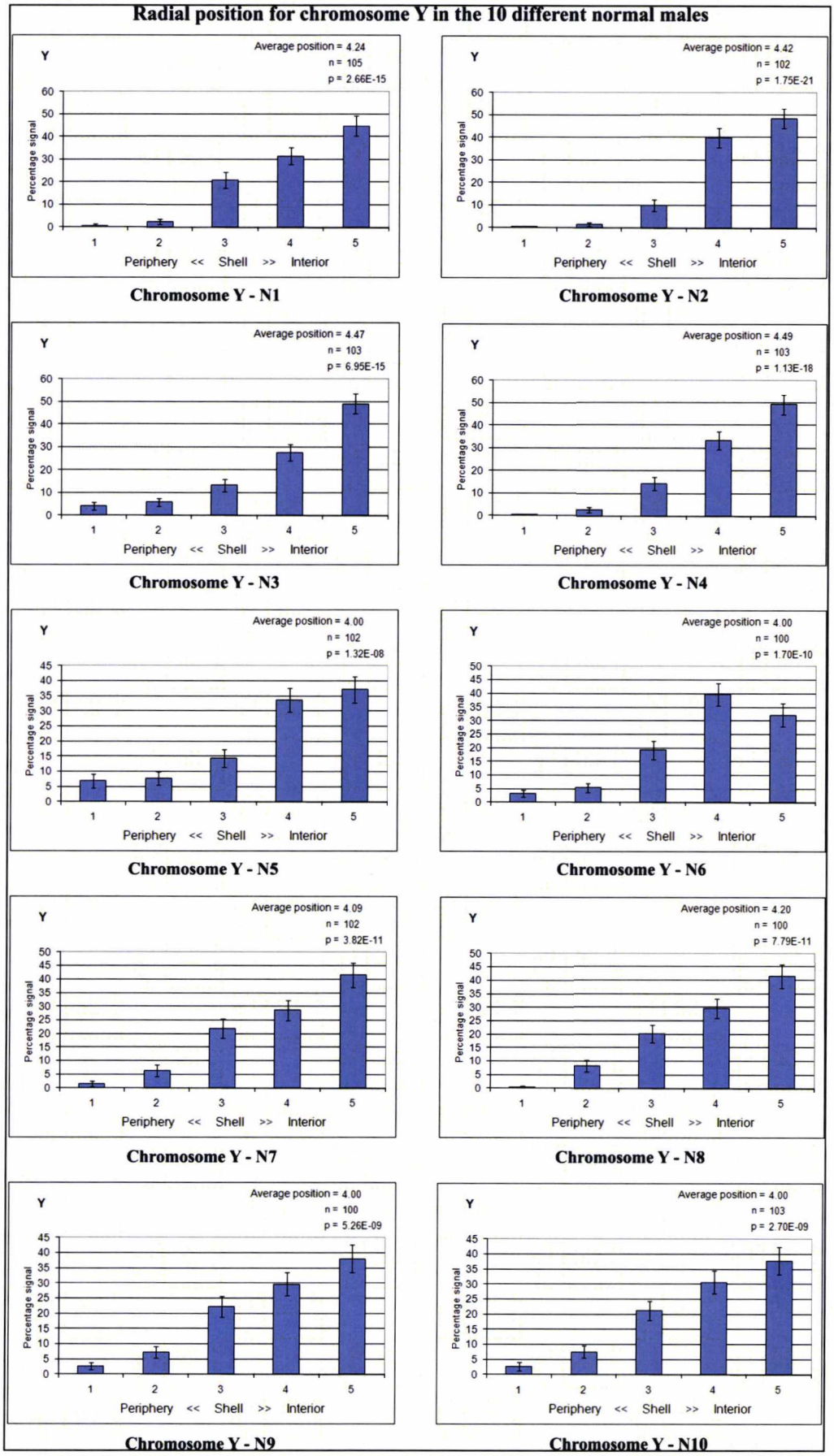

Figure 5.3: Preferential position for the Y centromeric probe in each of the 10 normal males.

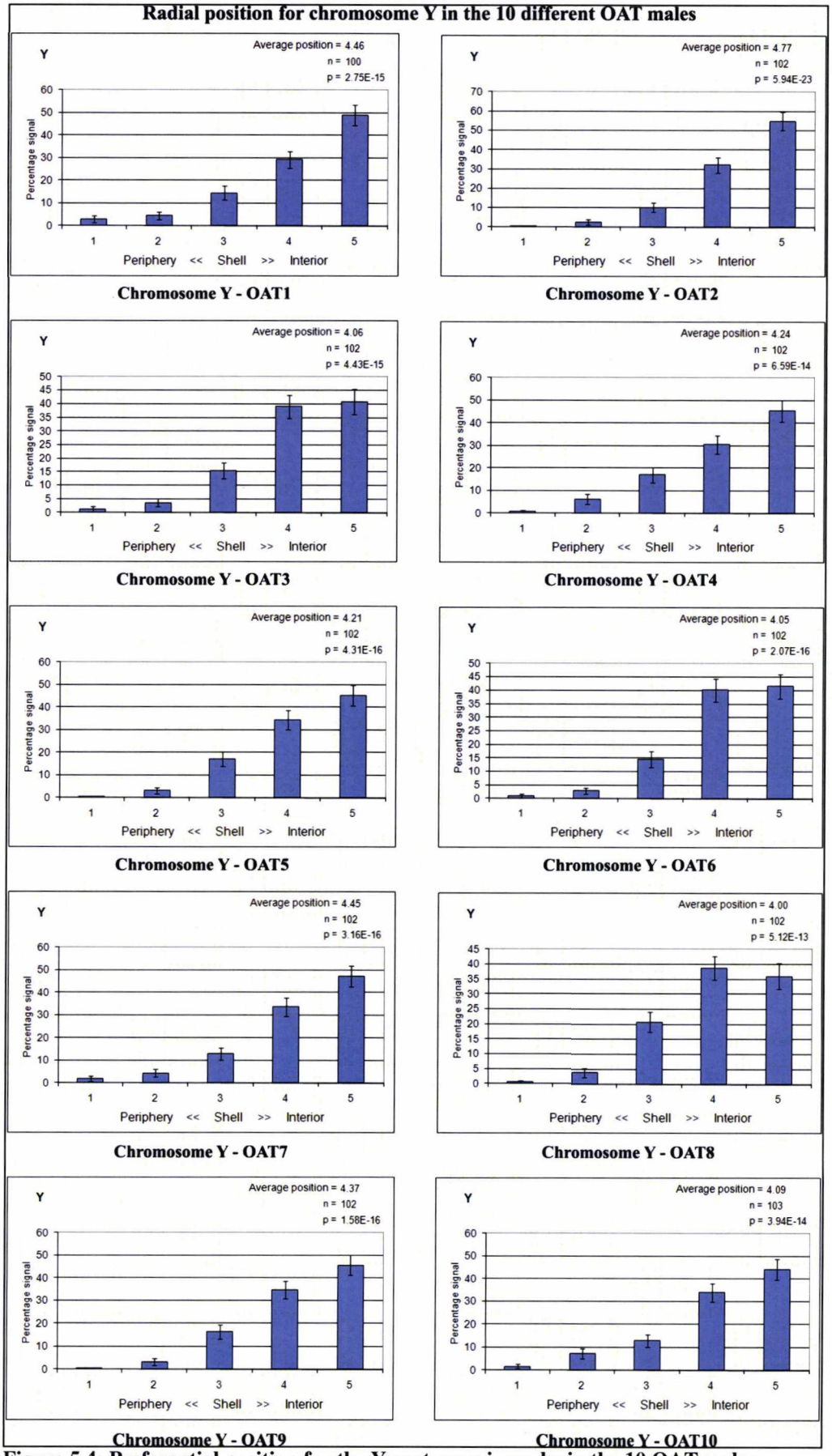

Figure 5.4: Preferential position for the Y centromeric probe in the 10 OAT males.

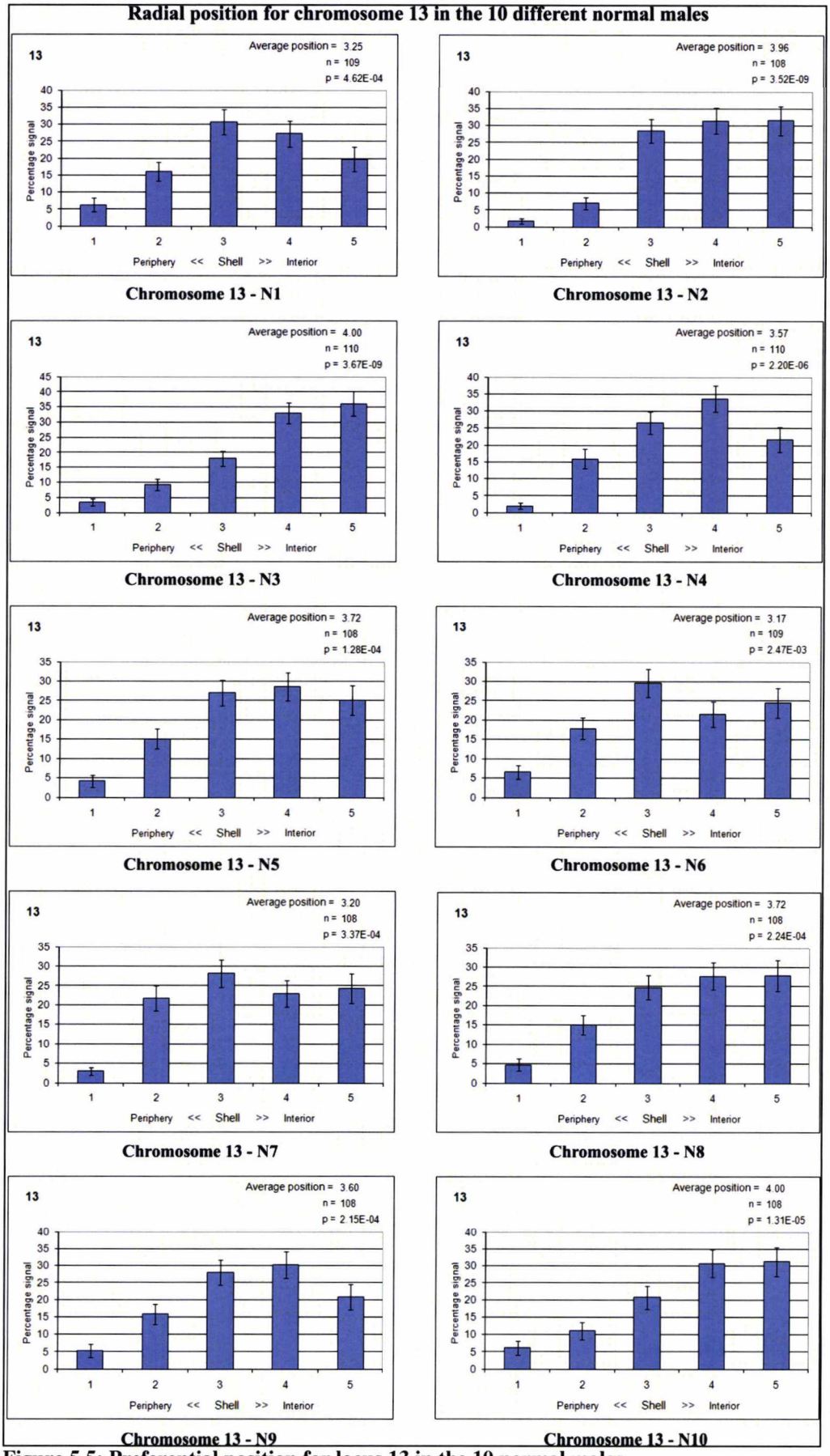

Figure 5.5: Preferential position for locus 13 in the 10 normal males.

Radial position for chromosome 13 in the 10 different OAT males

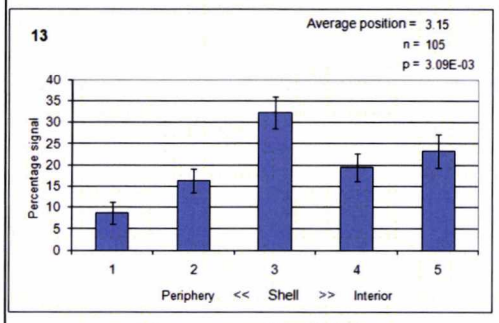

Chromosome 13 - OAT1

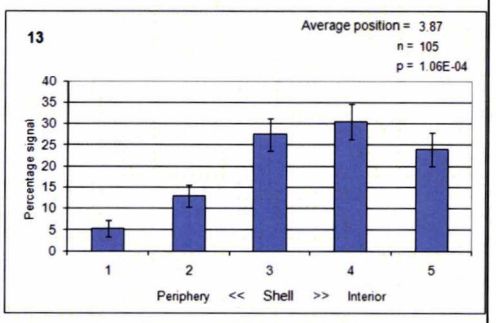

Chromosome 13 - OAT2

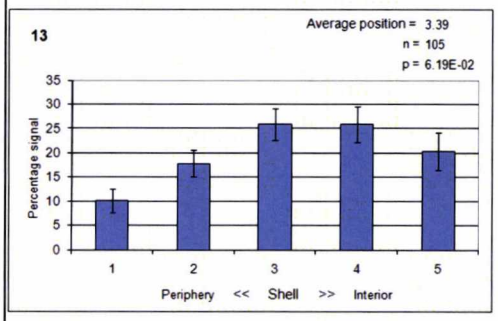

Chromosome 13 - OAT3

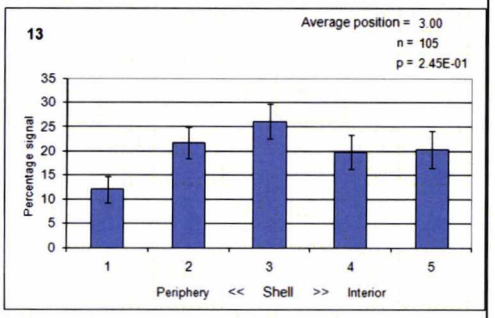

Chromosome 13 - OAT4

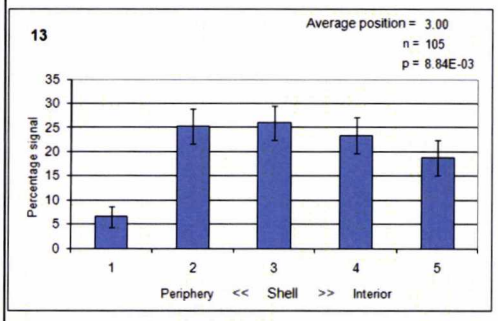

Chromosome 13 - OAT5

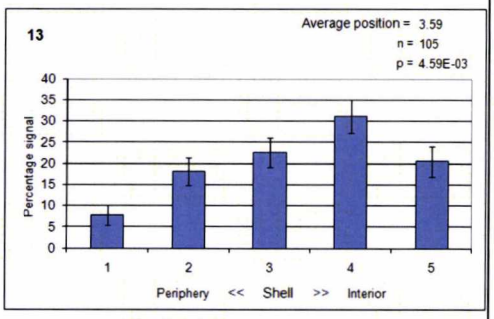

Chromosome 13 - OAT6

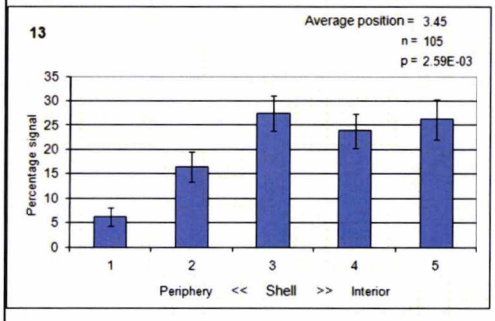

Chromosome 13 - OAT7

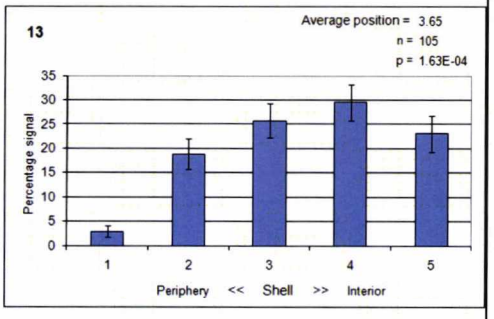

Chromosome 13 - OAT8

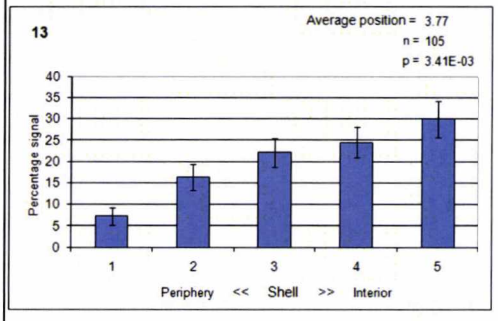

Chromosome 13 - OAT9

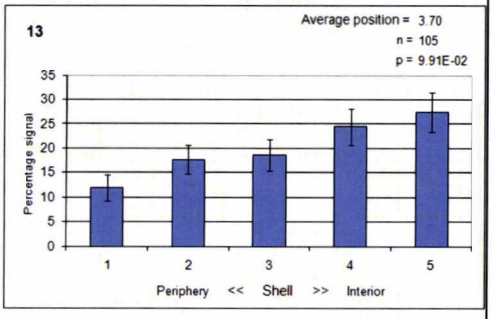

Chromosome 13 - OAT10

Figure 5.6: Preferential position for the locus on chromosome 13 in the 10 OAT males. Position was not discernable to a random distribution pattern for patients 3, 4 and 10.

Assessing radial position for all individual graphs resulted in Tables 5.1 and 5.2 hereafter.

Locus	Shell 3	Shell 3-4	Shell 3-5	Shell 4	Shell 4-5	Shell 5	NDRDP
X	0	0	0	2	3	5	0
Y	0	0	0	1	1	8	0
1	0	0	1	0	4	5	0
2	0	0	2	3	1	4	0
3	0	1	3	1	2	3	0
4	0	0	2	0	3	5	0
6	1	2	2	0	4	1	0
7	0	0	0	0	6	4	0
8	2	0	1	1	5	1	0
9	0	0	0	3	1	6	0
10	0	0	0	2	4	4	0
11	0	0	1	1	1	7	0
12	0	0	1	1	4	4	0
15	0	0	0	0	1	9	0
16	0	0	0	0	3	7	0
17	0	0	0	0	3	7	0
18	0	1	1	1	2	5	0
20	0	0	0	0	3	7	0
5	0	2	2	1	4	1	0
13	1	3	3	1	2	0	0
14	0	0	1	0	4	5	0
19	0	0	0	0	1	9	0
21	0	2	2	0	2	4	0
22	0	0	0	1	5	4	0
Total	4	11	22	19	69	115	0

Table 5.1: The preferential shell position for each locus in each of the control males. Chromosome loci assayed have been divided for presentational reasons, into sex chromosomes first, then the centromeric probes and then the unique sequence (BAC) probes. In each cell of the table, the numbers represent the number of men in which a certain pattern was seen. There were no cases in which a pattern of distribution for a particular locus in a particular male was seen in shells 1 or 2 (the outermost shells) or a not discernable from a random distribution pattern (NDRDP).

Locus	Shell 2-4	Shell 3	Shell 3-4	Shell 3-5	Shell 4	Shell 4-5	Shell 5	NDRDP
X	0	0	0	0	0	1	9	0
Y	0	0	0	0	0	3	7	0
1	0	0	0	0	0	3	7	0
2	0	0	0	2	2	3	3	0
3	0	4	0	3	2	0	1	0
4	1	0	3	2	0	1	1	2
6	0	3	2	2	0	2	0	1
7	0	0	0	2	1	4	3	0
8	0	0	0	3	2	0	5	0
9	0	0	0	1	2	3	4	0
10	0	0	0	0	1	5	4	0
11	0	0	0	2	0	3	5	0
12	0	1	1	2	2	3	0	1
15	0	0	0	0	1	2	7	0
16	0	0	0	0	1	1	8	0
17	0	0	0	0	1	1	8	0
18	0	0	1	2	4	2	1	0
20	0	0	0	0	0	3	7	0
5	0	1	3	1	2	3	0	0
13	1	1	2	1	1	0	1	3
14	0	0	0	0	0	3	7	0
19	0	0	0	0	0	2	8	0
21	0	2	2	3	2	1	0	0
22	0	0	0	0	0	4	6	0
Total	2	12	14	26	24	53	102	7

Table 5.2: The preferential shell position for each locus in each of the OAT males. Chromosome loci assayed have been divided for presentational reasons, into sex chromosomes first, then the centromeric probes and then the unique sequence (BAC) probes. In each cell of the table, the numbers represent the number of men in which a certain pattern was seen. Some differences (shaded) between control and OAT are apparent: The occurrence of not discernable from a random distribution pattern (NDRDP), for certain males (chromosomes 13, 12, 4 and 6), the appearance of a significant number of signals in shell 2 (chromosomes 13 and 4) and, for chromosome 7, less of a tendency to occupy the most central shells in OAT males.

The results suggest evidence for a chromocentre (specific aims 3a, 3b and 3c) for all chromosomal loci assayed in both categories of men. Most centromeric probes appear to be centrally located in both controls and OATs and the sex chromosomes are also centrally located (specific aim 3c). Among the non-centromeric autosomal probes, those where the loci were close to the centromere (chromosomes 14, 19, 21, 22) were consistent, by and large with a chromocentric pattern whereas those at a locus further away from the centromere (5, 13) displayed a more medial position. No probes were seen predominantly in shells 1 or 2 (with the exception of 2 OAT patients where

distributions roughly equally among shells 2-4 were seen). When comparing control vs. OAT males both the tables (above) and the graphs below (Figures 5.7-5.14) were compared. The subsequent graphs indicate the pooled data per chromosome probe for the normal controls (left) and the OAT males (right).

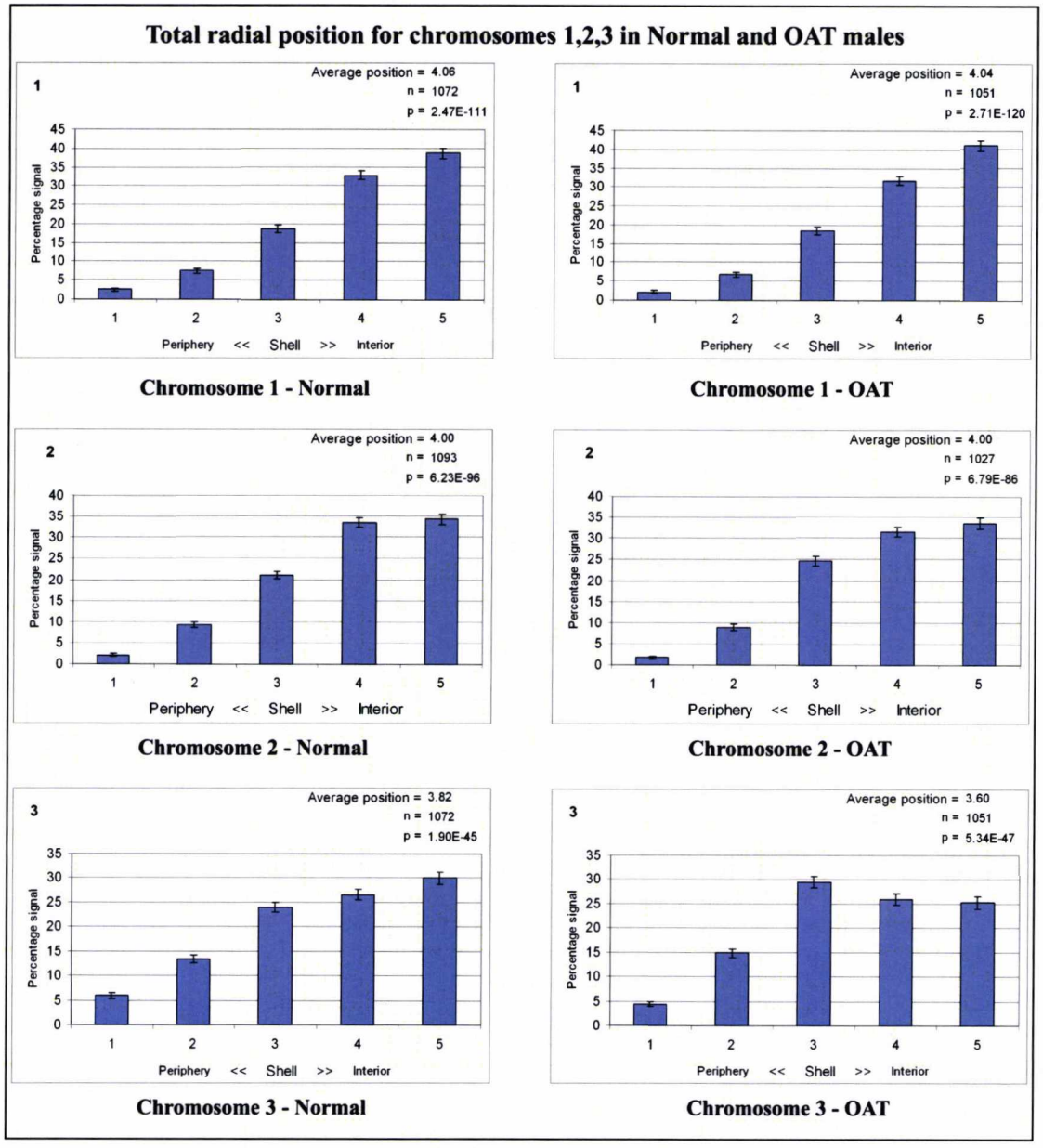

Figure 5.7: Pooled distribution of nuclear position for loci 1, 2, 3 in 10 normal (left) and in 10 OAT (right) males.

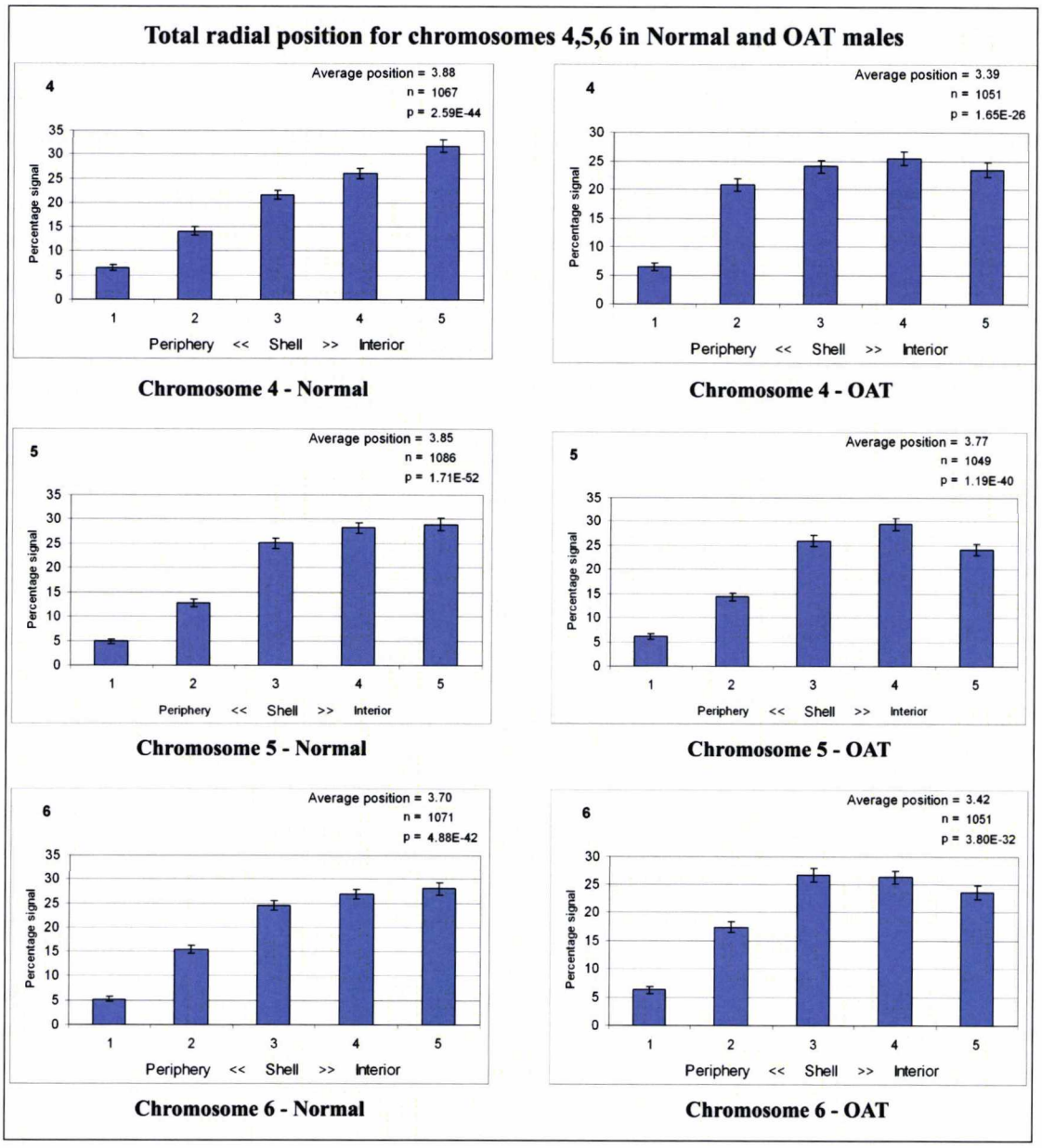

Figure 5.8: Pooled distribution of nuclear position for loci 4, 5, 6 in 10 normal (left) and in 10 OAT (right) males.

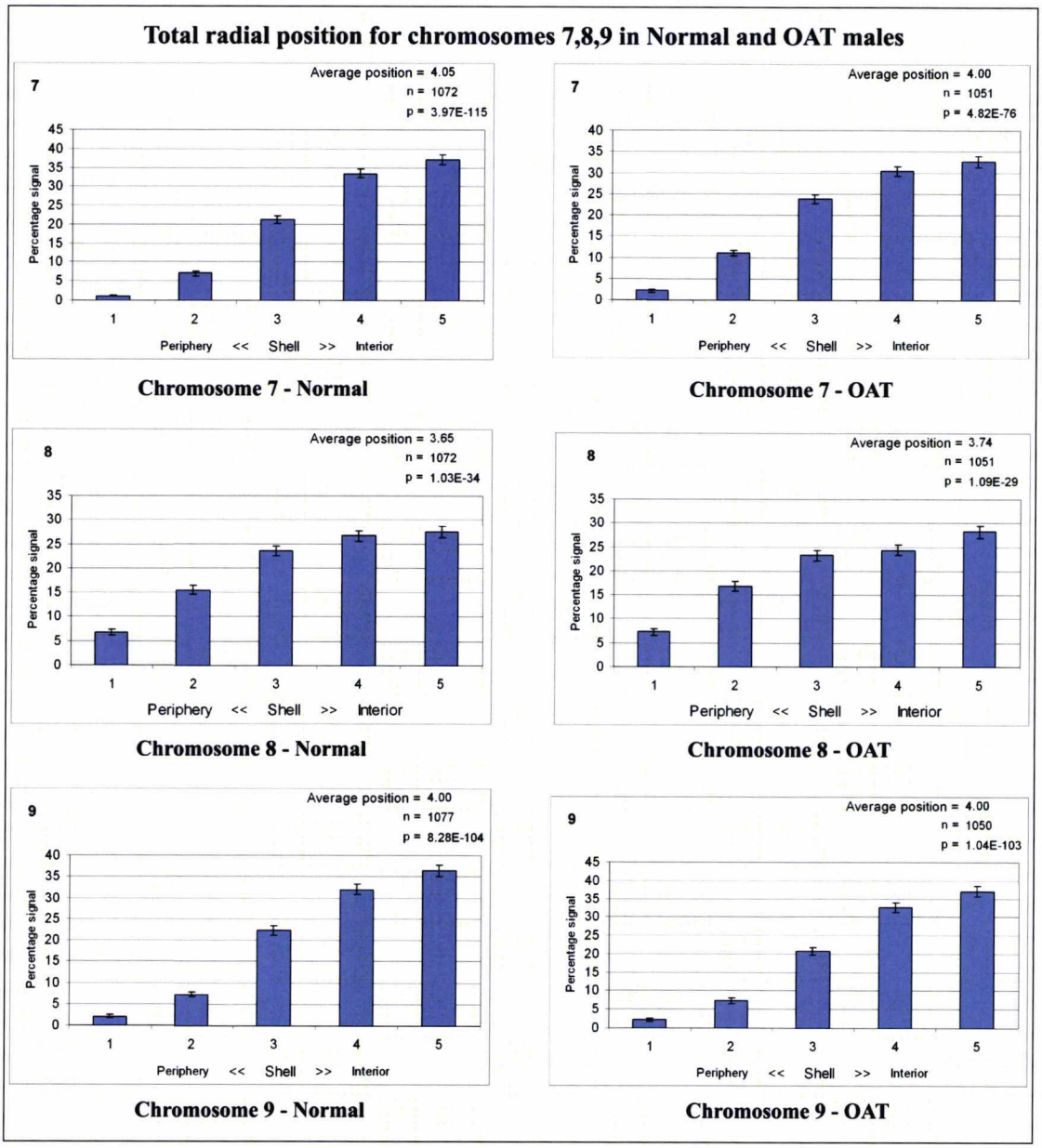

Figure 5.9: Pooled distribution of nuclear position for loci 7, 8, 9 in 10 normal (left) and in 10 OAT (right) males.

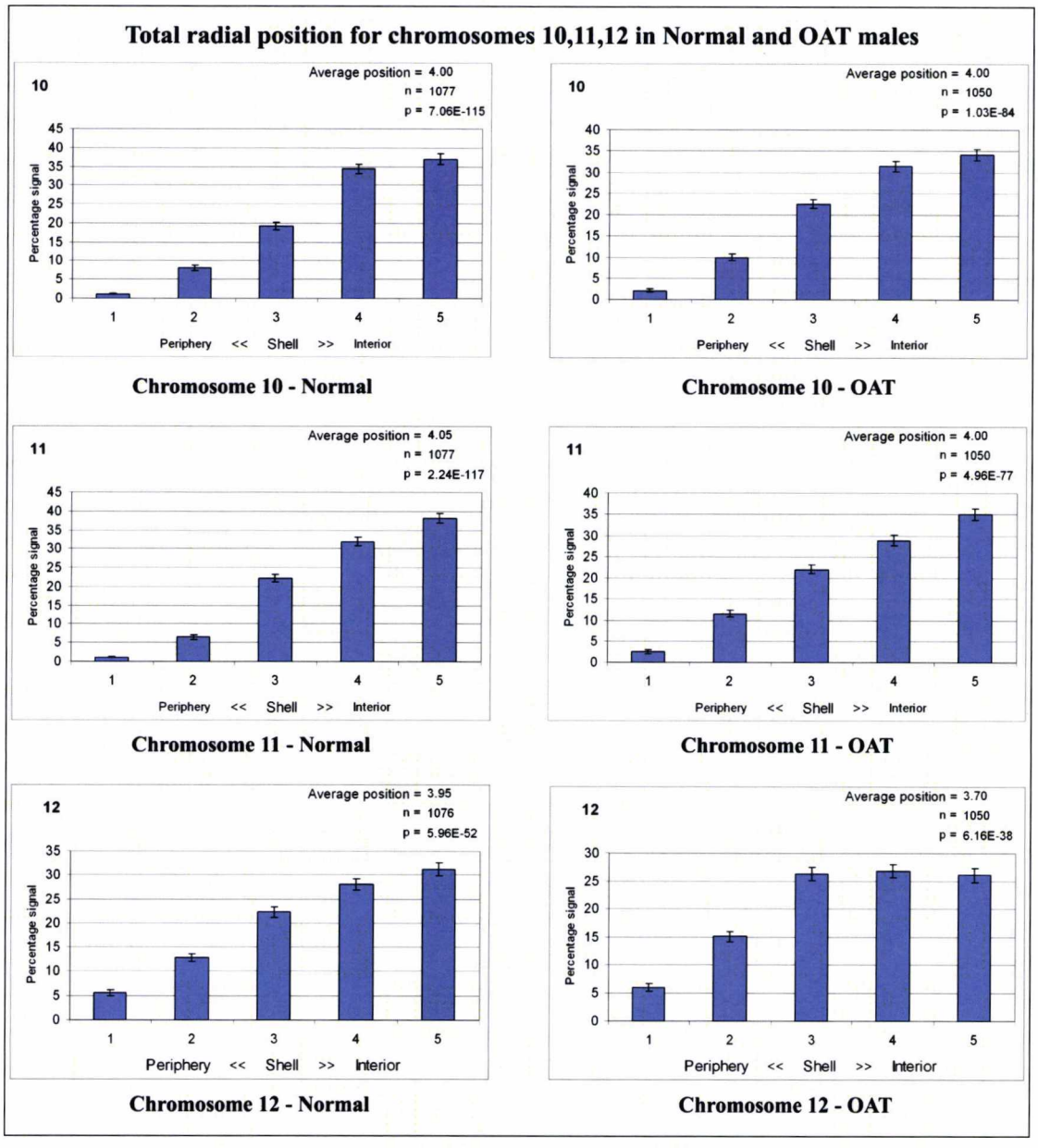

Figure 5.10: Pooled distribution of nuclear position for loci 10, 11, 12 in 10 normal (left) and in 10 OAT (right) males.

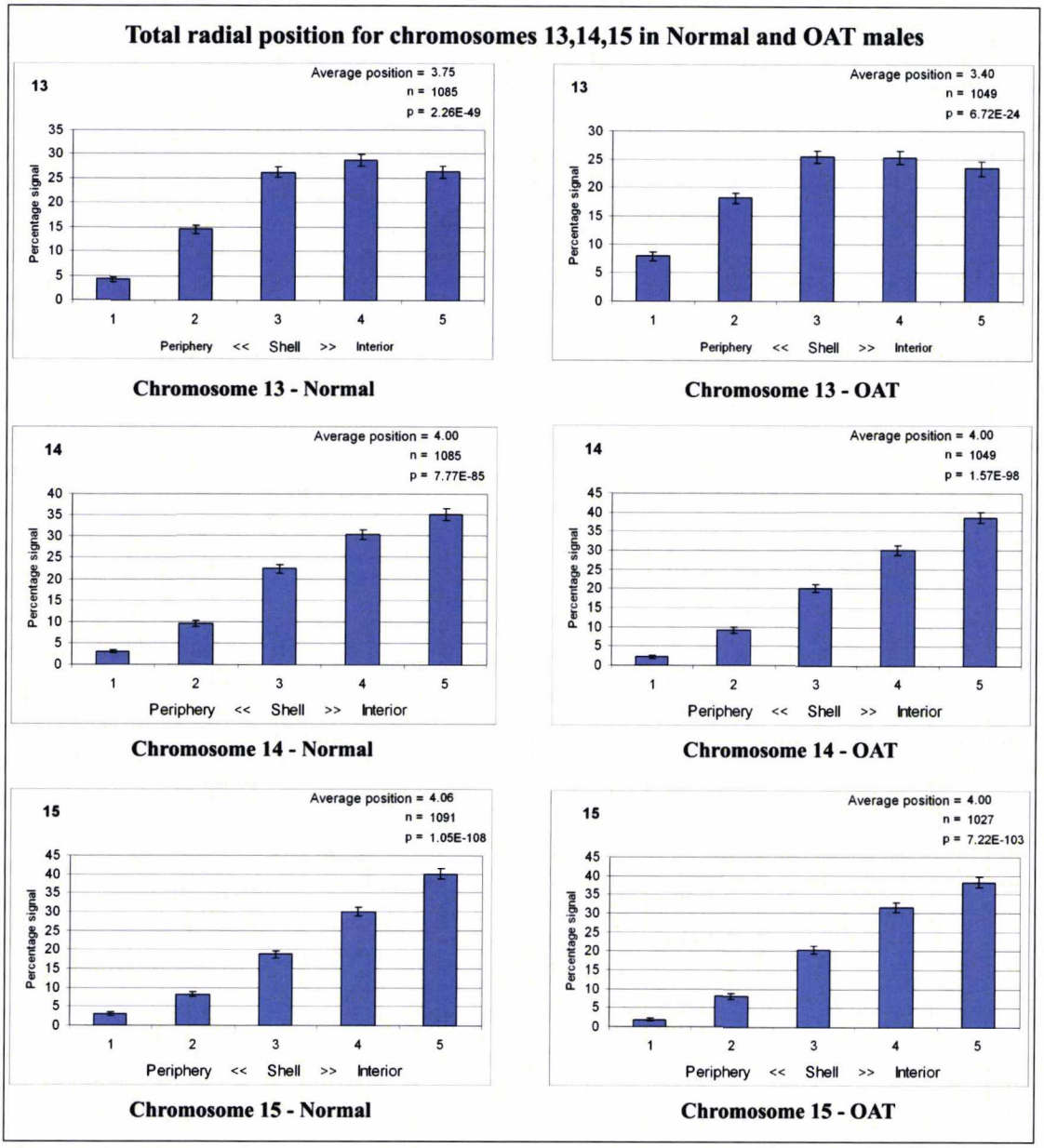

Figure 5.11: Pooled distribution of nuclear position for loci 13, 14, 15 in 10 normal (left) and in 10 OAT (right) males.

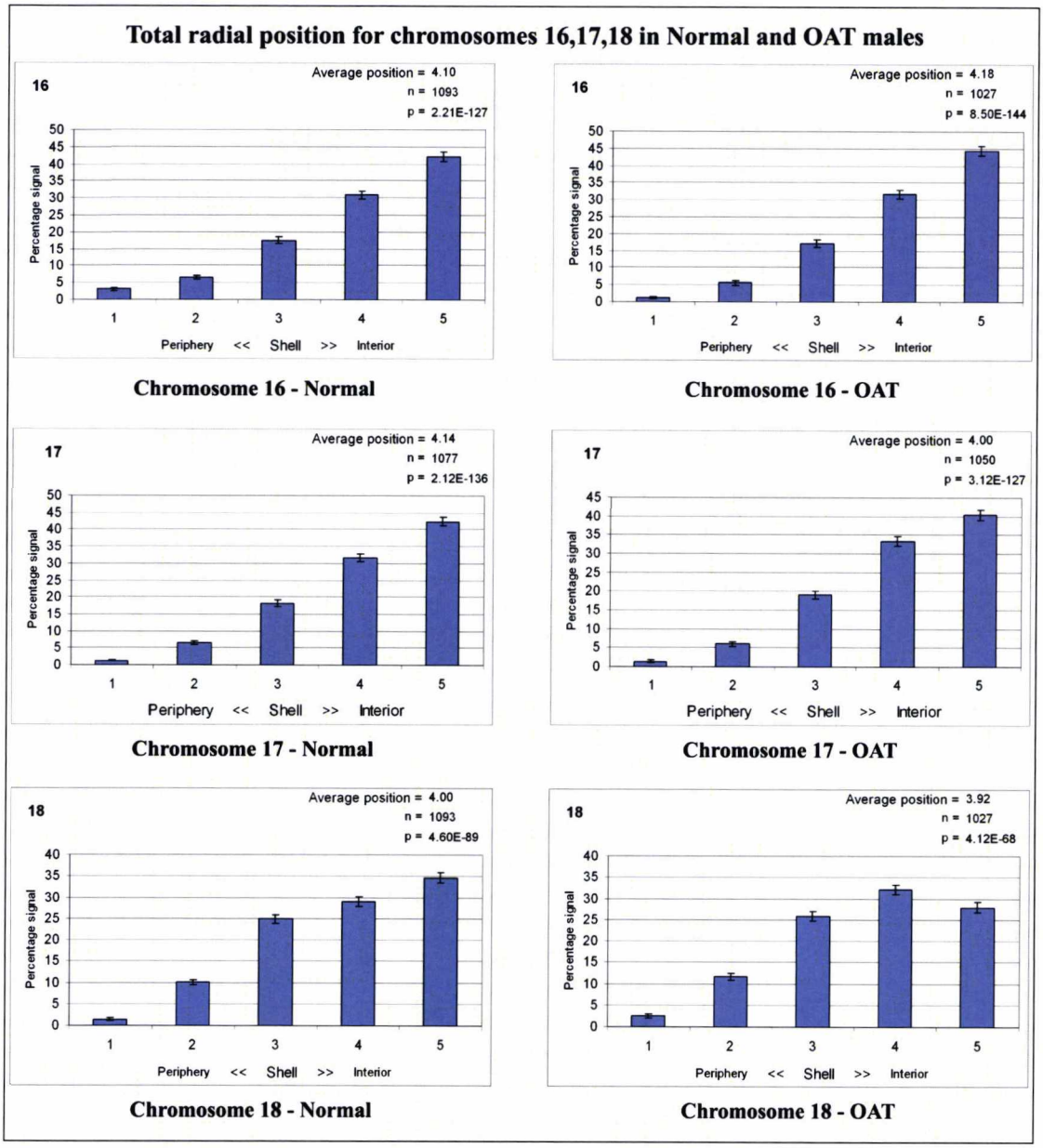

Figure 5.12: Pooled distribution of nuclear position for loci 16, 17, 18 in 10 normal (left) and in 10 OAT (right) males.

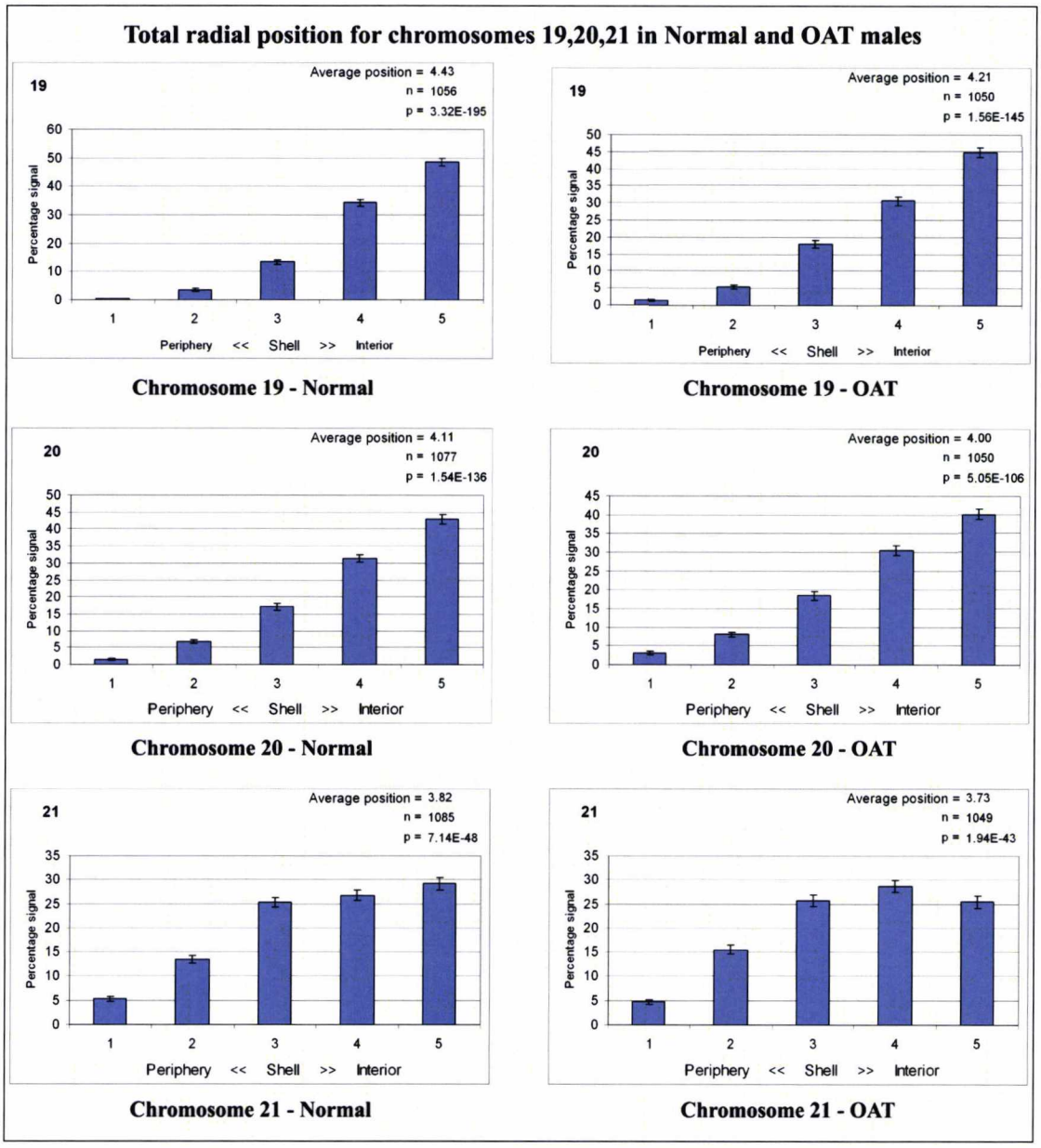

Figure 5.13: Pooled distribution of nuclear position for loci 19, 20, 21 in 10 normal (left) and in 10 OAT (right) males.

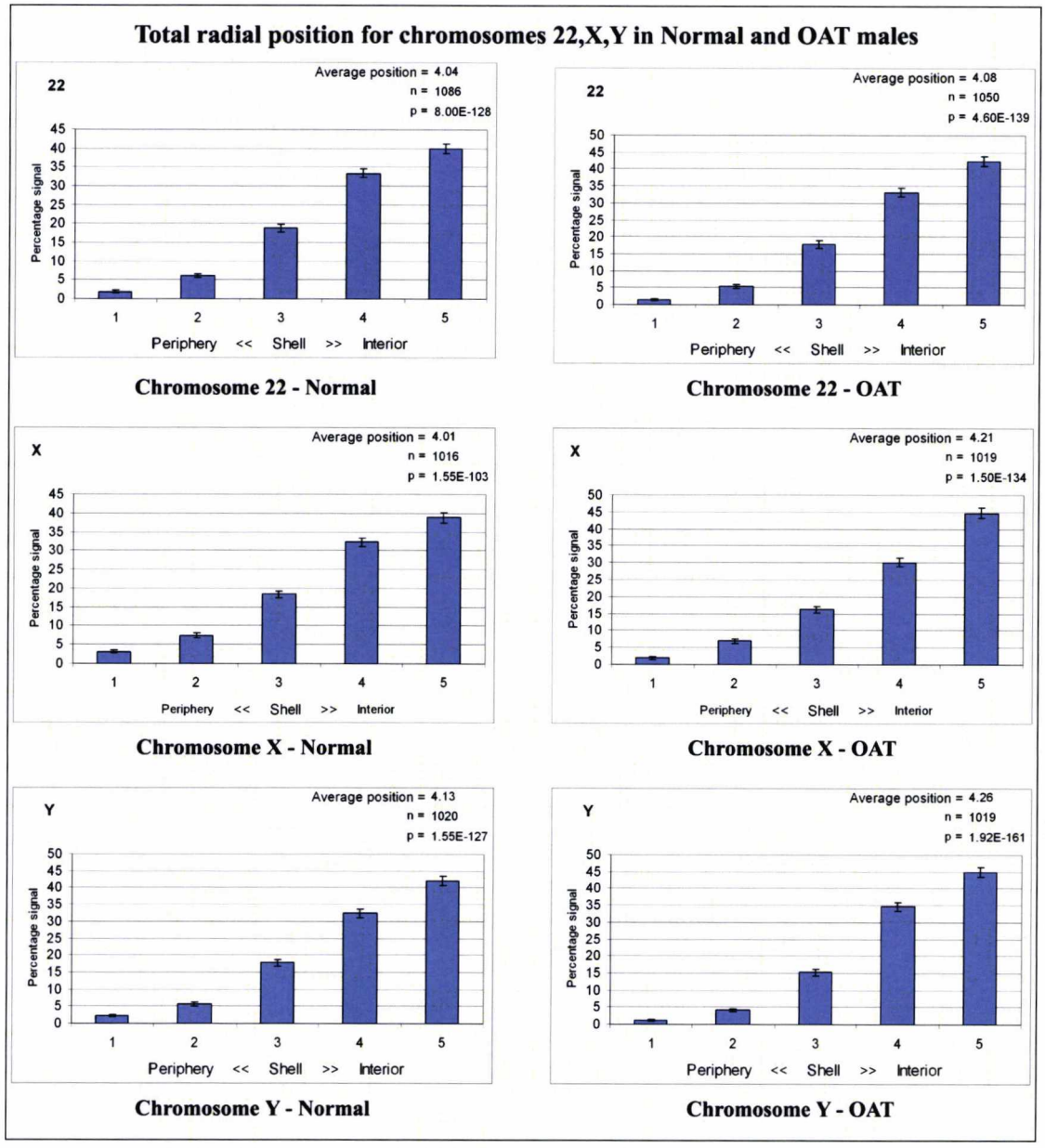

Figure 5.14: Pooled distribution of nuclear position for loci 22, X, Y in 10 normal (left) and in 10 OAT (right) males.

It should be noted for Figures 5.7-5.14 that, when taken as a group, distributions for all chromosomal loci in both normal and OAT were significantly non-random.

By considering the Tables (5.1-5.2) and the graphs (Figures 5.7-5.14), we can make some general inferences about the overall effect of severely compromised semen parameters on nuclear organisation (specific aim 3e). When considered individually, some differences between control and OAT are apparent; these are shaded in the

Table 5.2. The occurrence of apparently patterns not discernable from a random distribution for certain males [chromosomes 13 (OAT 3, 4 &10), 12 (OAT 8), 4 (OAT 8 & 10) and 6 (OAT 10)] suggest that, while not a widespread phenomenon, a tendency to a breakdown in nuclear organisation for certain chromosomes, for certain men may be a factor associated with reduction in fertility. The appearance of a significant number of signals in shell 2 [chromosomes 13 (OAT 5) and 4 (OAT 1)] and, for chromosome 7, less of a tendency to occupy the most central shells in OAT males is further evidence that an effect may be real and measurable but not overt, and not a general rule. Considering the pooled data in the graphs, while all display clearly non-random pattern in the two groups, noticeably, there are several centromeric loci that display, overall, a different nuclear organisation in controls compared to OAT males. Some of the changes are subtle, e.g. chromosome 8 is roughly equally represented in shells 4-5 in normal males whereas in OAT males it predominantly occupies shell 5. In others however the difference is a whole shell (shell 5 in normal males compared to shell 4 in OAT – chromosomes 4, 12 and 18) or more i.e. chromosomes 6 and 3, the latter showing a difference of two shells. Two specific loci that also occupy a central position in normal males (those of chromosomes 5 and 21) predominantly occupied shell 4 in the OAT males. No differences, individually or collectively, were apparent when the sex chromosomes were compared between control and OAT group.

With respect to the hypotheses outlined in specific aims 3a-d therefore the nuclear position of all loci tested was found to be non-random in all control males, thereby providing evidence of a strict nuclear organisation in human sperm heads. Each locus tested had a defined and consistent nuclear address in each of the control males analysed with the centromeric and sex chromosomal loci centrally located. Several of the locus specific probes were also centrally located however those further from the centromeres displayed a more medial organisation. The nuclear position of the loci assayed appeared not to be altered in OAT males as a general rule however, for individual chromosome centromeres there was evidence of a breakdown in the strict organisation of the chromocentre. Moreover, in individual OAT patients, there was evidence of a breakdown in organisation for individual loci and/or evidence of differences in nuclear address.

5.3.2. Specific aim 3e: That increased disomy levels in sperm (i.e. the proportion with a greater number of extra chromosomes) are correlated with increased altered nuclear organisation

In order to address specific aim 3e, the disomy frequencies for a subset of the chromosomes (X, Y, 2, 13, 21, and 22) was determined to derive an overview of the overall disomy rates in the cohort. The disomy rates are summarised in Table 5.3 and, for each patient, a comment on the nuclear organisation is given.

Sample	Sex disomy	Disomy 2	Disomy 13	Disomy 21	Disomy 22	Diploidy	Total disomy (%) for 5 chromosome pairs	Comments on nuclear organisation
N1	6	0	0	0	1	0	0.7	Medial position for 5,6,13
N2	1	0	0	2	1	0	0.4	Most centromeres central
N3	3	0	1	3	0	0	0.7	Most centromeres central
N4	2	0	4	0	0	0	0.6	Medial position for locus 21
N5	1	0	0	3	1	0	0.5	Medial for 3,13,18
N6	1	0	4	3	1	1	0.9	Medial for 6,8,13
N7	1	1	0	2	2	0	0.6	Medial for 8
N8	1	1	5	3	1	0	1.1	Most centromeres central
N9	2	2	0	2	0	0	0.6	Medial for loci 5,13
N10	1	1	3	1	0	0	0.6	Medial for 6,21
OAT1	17	0	3	8	5	2	3.3	Medial for 3,4,5,6,13,18,21
OAT2	8	3	2	6	7	4	2.6	Medial for 4,6,13
OAT3	22	5	5	9	0	4	4.1	Medial for 6,12 and Random for 13
OAT4	8	1	0	6	1	0	1.6	Medial for 3,5,6,21 and Random for 13
OAT5	21	5	4	8	2	0	4.0	Medial for 6,13
OAT6	22	8	1	8	0	4	3.9	Medial for 3,4,12,21
OAT7	8	4	0	4	0	0	1.6	Medial for 4,5
OAT8	4	3	0	3	0	0	1.0	Medial for 13,21 and Random for 4
OAT9	6	7	0	4	0	1	1.7	Medial for centromere 3
OAT10	1	1	0	2	0	1	0.4	Medial for 5 and Random for 4,6,13

Table 5.3: The disomy scoring for each of the chromosomes investigated the total disomy % and a general comment on the nuclear organisation for each patient.

The disomy levels for most control males where of similar value, (4 controls with the same value of 0.6), whereas for OAT patients the values were significantly higher.

With regard to nuclear organisation the results for controls suggest that with increasing disomy levels there is some breakdown into nuclear organisation (from the chromocentre pattern) with certain chromosomes adopting a medial position. Locus specific probes for 13, 5 which are located further away from their centromeres seem to be two common loci adopting a medial position with increasing disomy. Chromosome 6 seems also to be prone in adopting a medial position.

A similar observation can be made for OAT patients. More chromosome loci seem to be prone in adopting medial positions with increasing disomy levels. This seems to be true for centromeres 3, 4, 6 and for the autosomal locus specific probes further apart from their centromeres 13, 21 and 5. There was not an increase in the chromosome numbers adopting a distribution not different to random (for patients) with increasing disomy. Thus a trend of more chromosomes being prone to breakdowns in nuclear organisation seems to be noticeable in patients than in controls.

5.4. Concluding remarks

Nuclear organisation was investigated in 10 control and 10 men with compromised semen parameters. Both categories show evidence of the presence of a chromocentre arrangement.

The occurrence of apparently random patterns for certain OAT males suggest that, while not a widespread phenomenon, a tendency to a breakdown in nuclear organisation for certain chromosomes, for certain men may be a factor associated with reduction in fertility.

In addition a breakdown in genome organisation related with increased disomy levels seems to be more evident in OAT males, with more chromosomes adopting a medial position. The phenomenon seems to be less evident in normal males.

6. Specific aim 4: To apply the 24 chromosome FISH strategy to human blastomeres and assay the level of chromosome abnormalities and assess the efficacy of PGS

6.1. Background

As mentioned in section 1.4.5 the assessment of chromosomal aneuploidy in human embryos by interphase cytogenetics has only been performed using a limited sub-set of chromosomal probes. Chapter 4 however outlined a means by which 24 chromosome FISH could be achieved in a 4-layer, 6-fluorochrome strategy, producing 46/46 signals in known diploid cells in approximately 60% of the cells. As also outlined in section 1.4.6 there is some concern about whether results produced from PGS cases accurately predict the existence of euploidy or aneuploidy in the rest of the remaining embryo.

6.2. Aims and hypotheses

Given the above rationale, the primary purpose of this chapter was to assess chromosome copy number for loci from all 24 chromosomes in human preimplantation embryos with a view to achieving the following specific aims:

Specific aim 4a: To assess chromosome copy number in human cleavage stage embryos on a cell-by-cell basis for all human chromosomes (bearing in mind that, in control cells, 46/46 signals are seen in approximately 60% of control cells).

Specific aim 4b: To test the hypothesis that, as suggested by previous studies, the majority of human embryos are (mosaic) chromosomally abnormal for at least one chromosome.

Specific aim 4c: To test the hypothesis that chromosome loss is more common than chromosome gain and that certain chromosomes are more prone to aneuploidy than others.

Specific aim 4d: To test the hypothesis that PGS diagnosis (for 8 chromosomes) is an accurate predictor of the ploidy status of the rest of the embryo.

6.3. Results

6.3.1. Specific aim 4a: To assess chromosome copy number in human cleavage stage embryos on a cell by cell basis for all human chromosomes

In this study, 25 human embryos (day 5-6, average number of cells per embryo was 18) were assayed and spread on to glass slides with a view to assaying using the 24 chromosome FISH protocol developed in Chapter 4 (as described in section 2.10) Sequential FISH was performed in 20/25 (in 1/25-no cells were found, in 2/25-there was a lot of debris, and in 2/25-the embryos were put to different use – see Table 6.1). Out of the remaining 20 embryos, successful sequential hybridisation results were obtained in 17/20 (in the remaining 3 embryo spreads the sequential experiment had to be terminated due to poor embryo quality and technical difficulties – Table 6.1). The total number of blastomeres that produced successful FISH signals in all 4 layers (same cells probed 4 times) was 250 cells out of a possible 360 (intact cells after the FISH experiment), thus the reprobing efficiency was 69.44%. Table 6.1 summarises the entire whole embryo cultures used, providing information on the initial total number of blastomeres (per embryo-before FISH), commenting on whether reprobing was successful and the efficacy (over 4 layers based on the cells that were intact after FISH). It also comments on the procedure when appropriate. It should be noted that chromosome copy number (and thus nuclear address, see Chapter 7) of chromosome 19 was evaluated in a few number of cells due to a technical fault of the manufacturer resulting in the wrong locus being incorporated in the initial probe mix.

Embryo ID	Starting number of blastomeres	Was reprobing successful (overall)	Intact blastomeres after FISH	Number of reprobed cells	Efficacy (%) of reprobing (based on the intact blastomeres)	Comment
1	9	N/A	N/A	N/A	N/A	Cell under heavy debris- NO FISH
2	25	Yes	12	8	66.66	
3	23	Yes	19	16	84.21	
4	64	Yes	64	63	98.4	
5	0	N/A	N/A	N/A	N/A	No cells found
6	18	Yes	12	9	75	
7	16	Yes*	14	0	0	
8	11	Yes	8	6	75	
9	36	Yes	36	33	91.66	
10	28	Yes**	N/A	N/A	N/A	Experiment stopped after 2nd layer due to cell clumping
11	12	Yes**	N/A	N/A	N/A	
12	11	Yes	11	3	27.27	
13	7	N/A	N/A	N/A	N/A	Experiment stopped after 1st layer due to cells being damaged
14	21	Yes	21	9	42.85	
15	28	Yes	28	16	57.14	
16	13	Yes	13	13	100	
17	28	Yes	28	16	57.14	
18	4	N/A	N/A	N/A	N/A	Cells under heavy debris- NO FISH
19	16	Yes	16	11	68.75	
20	14	Yes	14	11	78.57	
21	11	Yes	11	6	54.54	
22	12	N/A	N/A	N/A	N/A	Embryos used for different research purpose
23	51	N/A	N/A	N/A	N/A	
24	28	Yes	26	11	42.30	
25	29	Yes	27	19	70.3	
Totals	**515**		**360**	**250**	**69.44**	

Table 6.1: Overall representation of the 25 whole embryos, from which 17 (not shaded) were used to assay chromosome copy number (and nuclear address- see Chapter 7). Note: "Yes*" denotes that reprobing worked overall, however there was no same blastomere with FISH results in all 4 layers. "Yes" refers to partial success of the reprobing since the experiment was stopped due to technical difficulties.**

For most of the embryos, reprobing worked effectively however in 4 experiments the reprobing had to be stopped due to cell aggregation or damage. The following figure presents a blastomere from whole embryo culture 4, after being probed four times.

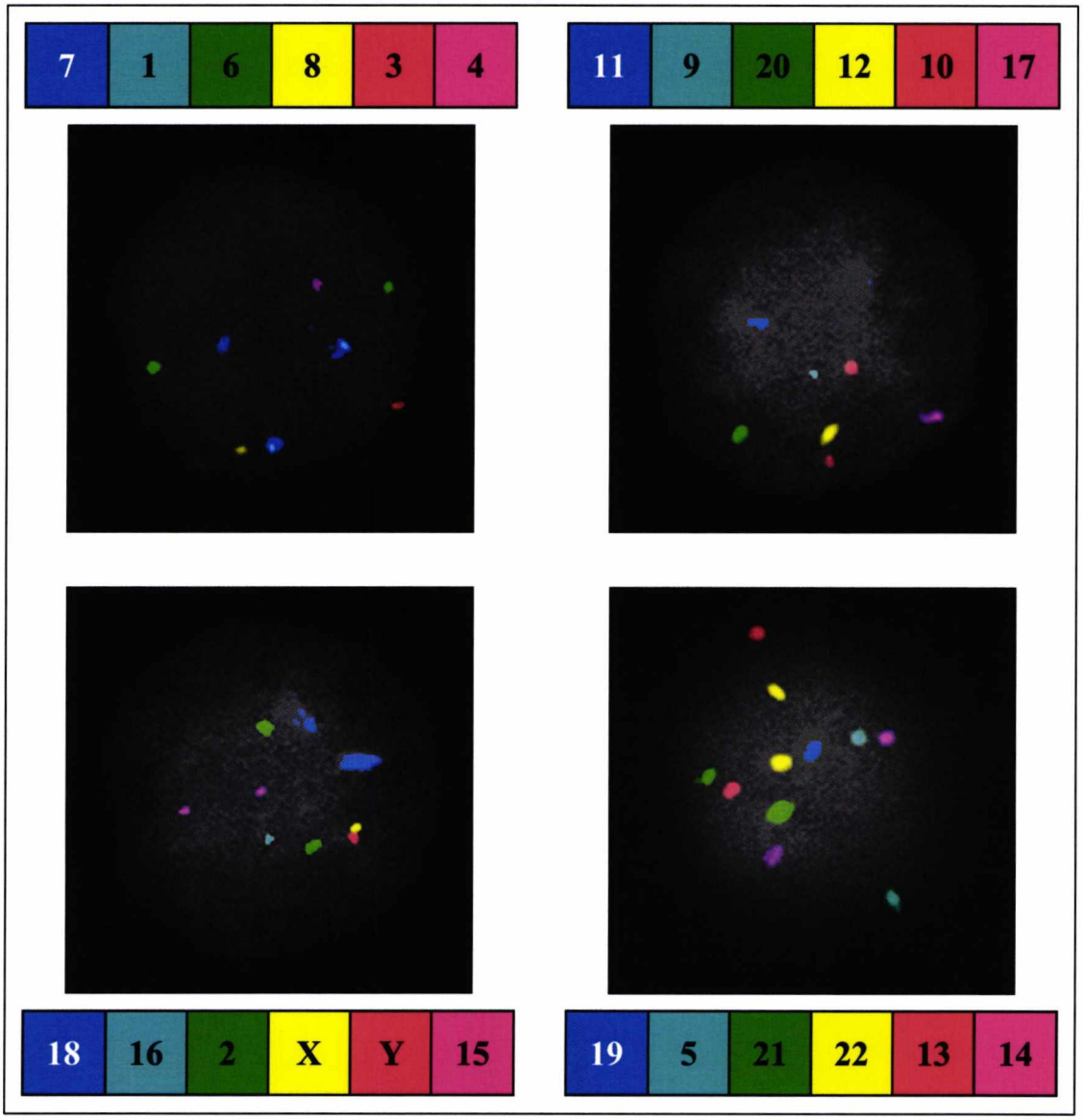

Figure 6.1: A representative blastomere after 4 layers of reprobing.

The following array of Tables (6.2-6.18) illustrates the chromosome copy number results for each blastomere within the 16 whole embryos that gave successful FISH results over the 4 layers. The tables also provide a per-cell comment on the copy number for each blastomere and an overall comment for the whole embryo. For the whole embryos that the wrong chromosome 19 locus probe was used (as mentioned, we were assigned a chromosome 15 probe in error) a (-) has been used in order for it not to be taken into account. Whole embryo 7 is included in the following tables, despite not providing results from reprobing (no same blastomere with results over the four layers – this is denoted with an asterisk in the table for embryo 7), however it was used for the nuclear address experiments (Chapter 7), thus it is presented for completeness.

Embryo	Cell	Comments per-cell	Number of signals per chromosome																							
			1	2	3	4	5	6	7	8	9	10	11	12	13	14	15	16	17	18	19	20	21	22	X	Y
2	1	Gain/loss several chroms. Multiple 21	2	3	3	3	2	3	2	3	0	0	0	1	0	2	1	1	3	2	-	3	6	2	1	1
2	2	Gain/loss several chroms	2	3	4	3	2	2	0	3	2	2	1	3	3	2	2	1	3	2	-	1	3	2	3	3
2	3	Loss of several chroms. Trisomy 7	2	2	0	0	1	0	3	1	2	2	2	2	2	2	1	1	2	0	-	2	1	2	1	1
2	4	Loss of several chroms. Tris 3, Tetras 9	1	2	3	0	1	2	0	2	4	3	2	2	2	2	2	0	2	2	-	2	1	2	1	1
2	5	Loss of several chroms. Trisomy 11,22	1	2	0	0	1	0	2	1	2	2	3	2	2	2	2	1	2	2	-	2	1	3	1	2
2	6	Extensive gain/loss, Tris, Tetras, Pentas	1	4	1	0	3	2	0	2	4	3	0	3	4	3	0	2	3	0	-	4	2	5	2	2
2	7	Loss of several chroms. Trisomy 10,22	0	2	1	0	2	1	0	1	1	3	1	2	2	2	0	2	2	2	-	1	1	3	1	1
2	8	Loss of several chroms. Trisomy 15,22	2	2	1	0	2	1	1	1	1	1	0	2	2	1	3	1	2	0	-	1	1	3	1	2
General comments for embryo 2: Male cell. Independent chromosome loss for 1, 3, 4, 6, 7, 9, 10, 11, 15, 16, 18, 20, 21. Chromosome gain for 2, 4, 9, 17, 20, 21, 22, X and Y. Possible mitotic non-disjunction for chromosomes, 3, 5, 6, 8, 9, 10, 11, 12, 14, 15, 20, 21.																										

Table 6.2: Chromosome copy number results for whole embryo 2.

Embryo	Cell	Comments per-cell	Number of signals per chromosome																							
			1	2	3	4	5	6	7	8	9	10	11	12	13	14	15	16	17	18	19	20	21	22	X	Y
3	1	Extensive chroms. loss	1	2	0	1	1	1	1	1	1	1	2	2	1	1	1	1	1	1	-	2	1	1	1	0
3	2	Extensive chroms. loss	1	1	2	1	1	1	0	1	2	1	1	1	1	1	1	1	1	1	-	1	1	1	1	1
3	3	Extensive chroms. loss, Trisomy 9	1	1	1	1	1	1	1	1	3	2	2	2	1	2	1	0	1	1	-	1	1	1	1	0
3	4	Extensive chroms. loss	1	1	0	1	0	1	1	1	0	1	1	1	1	1	1	0	1	1	-	1	1	1	1	0
3	5	Extensive chroms. loss	1	2	1	1	1	1	1	1	2	1	2	1	1	1	2	2	1	1	-	2	1	1	1	0
3	6	Extensive chroms. loss	1	2	1	1	1	1	1	1	1	1	1	1	1	1	1	1	1	1	-	2	1	1	1	1
3	7	Extensive chroms. loss	1	2	1	1	1	1	1	1	1	1	1	1	1	1	1	2	1	0	-	2	1	1	1	0
3	8	Extensive chroms. loss	1	1	1	1	1	1	1	1	1	1	1	1	1	1	1	2	1	0	-	2	1	1	1	1
3	9	Extensive chroms. loss	1	1	0	1	1	1	1	1	0	1	1	0	1	0	1	0	1	1	-	0	1	1	0	1
3	10	Extensive chroms. loss	1	1	1	1	1	1	1	1	2	1	2	1	1	1	2	2	1	0	-	1	1	1	1	1
3	11	Extensive chroms. loss	1	2	1	1	2	1	1	2	1	2	2	2	2	2	1	2	2	2	-	1	1	2	1	0
3	12	Extensive chroms. loss	2	2	0	1	1	1	1	1	2	1	1	1	2	2	2	0	1	2	-	1	2	2	1	1
3	13	Extensive chroms. loss, Trisomy 22	1	2	0	0	0	0	2	2	1	1	2	1	2	1	1	1	1	0	-	2	1	3	1	0
3	14	Extensive chroms. loss	1	1	0	0	1	1	1	0	1	1	1	1	1	1	1	1	1	1	-	2	1	1	2	0
3	15	Extensive chroms. loss	0	2	0	0	1	0	1	1	1	2	1	1	2	2	1	1	2	0	-	1	2	2	1	1
3	16	Ext. chroms. loss, Tetras 12, 21, 22	0	2	1	1	2	1	2	2	0	2	0	4	2	0	2	0	2	2	-	2	4	4	0	0
General comments for embryo 3: Male cell. General extensive chromosome loss. Gain of chromosome 21? Possible mitotic non-disjunction for chromosomes 9, 22.																										

Table 6.3: Chromosome copy number results for whole embryo 3.

Embryo	Cell	Comments per-cell	Number of signals per chromosome																							
			1	2	3	4	5	6	7	8	9	10	11	12	13	14	15	16	17	18	19	20	21	22	X	Y
4	1	Extensive chroms. loss, Tris. 9,14,15,20	2	2	2	1	2	2	1	2	3	1	1	1	2	3	3	2	2	1	-	3	2	2	1	1
4	2	Extensive chroms. loss, Trisomy 4	2	1	2	3	2	1	1	2	1	2	2	2	2	2	1	2	2	2	-	1	2	2	1	1
4	3	Extensive chroms. loss, Tetrasomy 9	2	2	1	1	2	1	1	2	4	2	2	1	2	2	2	2	1	2	-	1	2	2	1	1
4	4	Extensive chroms. loss, Trisomy 8	2	2	1	1	0	2	1	3	1	2	2	1	2	1	2	1	1	1	-	1	0	1	1	1
4	5	Loss for 3,15,20, Trisomy 8, Tetras 16	2	2	1	2	2	2	2	3	2	2	2	2	2	2	1	4	2	2	-	1	2	2	1	1
4	6	Trisomy 2,5,6,7,17, Tetrasomy 15	2	3	1	2	3	3	3	2	2	2	2	2	2	2	4	1	3	2	-	1	2	2	1	1
4	7	Loss for 3,7,9,20 Trisomy 15,16	2	2	1	2	2	2	1	2	1	2	2	2	2	2	3	3	2	2	-	1	2	2	1	1
4	8	Extensive chroms. loss, Tris 15,16	2	1	2	1	2	1	1	2	1	1	2	1	2	2	3	3	1	2	-	1	1	2	1	1
4	9	Extensive chroms. loss, Tris 4,11	2	1	1	3	2	2	2	2	2	2	3	1	2	2	1	2	2	1	-	2	2	2	1	1
4	10	Extensive chroms. loss, Tris 13, Penta 5	2	1	1	1	5	2	2	2	2	2	2	1	3	2	1	1	1	2	-	2	2	1	1	2
4	11	Extensive chroms. loss, Trisomy 15	2	2	1	1	2	1	1	2	2	1	2	1	2	2	3	2	1	2	-	2	2	1	1	1
4	12	Gain/loss several chroms.	2	2	1	2	3	2	3	2	2	2	1	2	2	3	4	3	2	4	-	2	3	3	1	2
4	13	Extensive chroms. loss	2	1	2	2	2	2	2	2	2	1	2	2	2	2	2	2	2	1	-	1	1	2	1	1
4	14	Extensive chroms. loss, Trisomy 2	1	3	1	1	2	1	2	2	1	1	2	1	2	2	1	2	1	1	-	1	2	2	1	1
4	15	Extensive chroms. loss	2	2	2	2	2	1	1	2	2	2	2	1	2	2	1	2	1	2	-	1	2	2	2	1
4	16	Extensive chroms. loss, Trisomy 8	2	2	2	1	2	2	1	3	2	1	2	2	2	1	2	2	1	1	-	1	1	2	1	2
4	17	Loss for 4,7,10,17 Trisomy 2,9	2	3	2	1	2	2	1	2	3	1	2	2	2	2	2	2	1	2	-	2	2	2	1	1
4	18	Extensive chroms. loss	0	2	1	1	1	1	1	2	2	1	2	2	1	1	1	2	1	1	-	1	2	2	2	1
4	19	Extensive chroms. loss, Trisomy 2,11	2	3	2	1	2	2	2	2	2	1	3	1	2	1	2	2	1	2	-	2	2	2	1	1
4	20	Ext. chroms. loss, Tris 2,6,8,11, Tetra 5	1	3	1	2	4	3	1	3	1	1	3	1	2	2	2	2	1	2	-	1	2	2	1	1
4	21	Extensive chroms. loss, Tris 7,9	2	2	1	2	2	1	3	1	3	2	1	2	2	2	2	2	2	2	-	1	2	2	1	1
4	22	Extensive chroms. loss, Tris 11,18,Y	2	2	1	1	1	2	1	2	2	1	3	1	2	1	2	2	2	3	-	1	2	2	2	3
4	23	Gain/loss several chroms.	2	2	2	1	2	4	1	2	1	2	3	2	2	3	2	2	2	4	-	1	3	3	1	2
4	24	Extensive chroms. loss, Tris 16	1	1	2	1	2	1	2	1	1	2	1	2	2	2	2	3	2	2	-	1	2	2	1	1
4	25	Extensive chroms. loss, Tris 1,16	3	2	1	1	2	2	2	2	1	2	1	1	2	2	2	3	1	2	-	1	2	2	1	1
4	26	Extensive chroms. loss, Tris 9,11,12	1	2	2	2	2	2	1	1	3	1	3	3	2	2	1	2	2	2	-	1	2	2	1	1
4	27	Extensive chroms. loss	2	2	1	1	2	2	1	1	1	2	2	2	2	2	2	1	1	2	-	1	2	2	1	1
4	28	Gain/loss several chroms, Multiple 18	2	2	1	1	4	2	3	1	2	2	2	1	5	2	2	3	2	6	-	1	2	4	1	1
4	29	Extensive chroms. loss, Tris 10,11,12	1	2	2	1	2	1	2	2	2	3	3	3	2	1	1	1	2	2	-	1	1	1	1	1
4	30	Loss for 15,18,20, Gain for 9,12,17	2	2	2	2	2	2	2	2	3	2	0	3	2	2	1	0	3	1	-	1	2	2	1	1
4	31	Gain/loss several chroms.	1	4	1	2	3	2	2	3	1	1	1	1	2	4	3	3	2	3	-	1	4	3	2	2
4	32	Gain/loss several chroms	1	3	1	2	3	2	1	2	1	1	2	2	3	4	2	3	1	3	-	1	3	5	1	1
4	33	Extensive chroms. loss, Trisomy 11	2	2	1	1	2	1	1	1	1	2	3	2	2	2	2	2	2	2	-	1	2	2	1	1
4	34	Extensive chroms. loss, Trisomy 9,11	2	2	1	1	2	1	2	1	3	1	3	1	2	2	2	2	1	2	-	2	1	2	1	1

4	35	Extensive chroms. loss, Trisomy 2,12	1	3	1	1	2	2	2	1	1	1	2	3	2	2	1	2	1	2	-	1	2	2	1	1
4	36	Extensive chroms. loss, Tetrasomy 2	2	4	1	2	2	2	2	2	2	1	2	1	2	1	2	0	1	2	-	1	2	1	1	1
4	37	Extensive chroms. loss	2	1	1	2	2	2	1	1	2	1	2	1	2	2	2	2	1	2	-	1	1	2	1	1
4	38	Extensive chroms. loss	1	1	1	1	2	1	0	2	2	1	2	1	2	2	2	2	2	2	-	2	2	2	2	0
4	39	Extensive chroms.loss, Trisomy 15	2	2	1	1	2	2	2	1	1	2	1	2	2	2	3	2	1	2	-	1	2	2	1	1
4	40	Loss for 4,7,12, Trisomy 1	3	2	2	1	2	2	1	2	2	2	2	1	2	2	2	2	2	2	-	2	2	2	1	1
4	41	Extensive chroms. loss	1	2	1	1	2	2	2	2	2	2	0	2	2	2	1	2	2	2	-	1	2	2	1	1
4	42	Extensive chroms. loss, Tetrasomy 16	2	1	1	1	2	2	1	2	2	2	2	2	2	2	1	4	2	1	-	1	2	2	1	1
4	43	Extensive chroms. loss, Trisomy 11	2	1	2	2	2	1	1	2	1	2	3	2	2	1	0	1	2	1	-	1	2	2	1	1
4	44	Loss for 3,7,12, Gain for 4,15	2	2	1	3	2	2	1	2	2	2	2	1	2	2	3	2	2	2	-	2	2	2	1	1
4	45	Extensive chroms. loss	2	2	2	1	2	2	1	2	1	2	1	2	2	2	1	2	2	2	-	1	2	2	1	1
4	46	Extensive chroms. loss	2	1	1	1	2	2	1	1	2	2	2	1	2	2	2	2	1	1	-	0	1	2	1	1
4	47	Extensive chroms. loss, Tris 2,15,18	1	3	1	1	1	2	2	2	1	2	1	2	1	2	3	2	2	3	-	1	1	2	1	1
4	48	Extensive chroms. loss	1	1	1	2	2	2	2	2	2	2	2	2	2	2	1	1	1	2	-	1	2	2	1	1
4	49	Extensive chroms. loss, Tris 1,16	3	1	1	1	2	1	1	1	2	2	1	1	2	2	1	3	2	1	-	1	2	2	1	1
4	50	Extensive chroms. loss, Tris 8	2	1	1	2	2	1	1	3	1	2	1	0	2	2	2	1	1	2	-	2	2	2	1	1
4	51	Extensive chroms. loss, Tris 11	1	2	1	2	2	1	0	1	2	1	3	1	2	1	1	1	2	2	-	1	2	2	1	1
4	52	Extensive chroms. loss	2	2	1	2	2	2	1	2	2	1	2	1	2	2	2	1	1	2	-	1	2	2	1	1
4	53	Extensive chroms. loss	2	2	1	1	2	2	1	2	2	2	2	2	2	2	1	0	1	0	-	1	2	2	1	1
4	54	Extensive chroms. loss, Tris 15,21	2	2	2	1	2	2	1	2	1	2	2	2	2	1	3	2	1	1	-	1	3	1	2	1
4	55	Extensive chroms. loss	2	2	1	1	2	2	1	2	1	1	1	1	2	2	2	2	1	1	-	1	2	2	1	1
4	56	Extensive chroms. loss	2	2	1	2	2	2	1	2	1	1	2	2	2	2	2	2	1	2	-	1	2	2	1	1
4	57	Extensive chroms. loss, Trisomy 2	1	3	1	1	2	2	1	1	1	2	1	2	2	2	2	1	2	2	-	1	2	2	1	1
4	58	Extensive chroms. loss	2	2	1	2	2	2	1	2	2	2	2	1	2	2	1	1	2	1	-	1	2	2	1	1
4	59	Extensive chroms. loss	2	1	1	1	2	2	2	1	1	2	2	2	2	2	2	2	1	1	-	2	2	2	1	1
4	60	Gain/loss several chroms.	1	4	1	1	4	3	2	2	1	1	3	2	2	4	3	1	3	2	-	2	4	4	1	1
4	61	Gain/loss several chroms.	1	2	2	2	4	3	1	1	2	2	3	2	3	4	4	2	2	4	-	1	4	4	1	1
4	62	Gain/loss several chroms.	1	3	3	1	2	2	1	2	1	4	3	3	2	4	1	1	1	2	-	1	2	4	1	2
4	63	Gain/loss several chroms.	2	3	2	2	4	1	2	3	1	2	3	2	3	4	1	1	1	1	-	1	3	4	2	1
General comments for embryo 4: Male cell. Independent chromosome loss for 3, 4, 7, 9, 12, 17, 20. Chromosome gain for 11, 14, 15. Possible mitotic non-disjunction for chromosomes 2, 6, 8, 9, 11, 15, 16.																										

Table 6.4: Chromosome copy number results for whole embryo 4.

Embryo	Cell	Comments per-cell	Number of signals per chromosome																							
			1	2	3	4	5	6	7	8	9	10	11	12	13	14	15	16	17	18	19	20	21	22	X	Y
6	1	Loss for 14,15,17,20, Trisomy 3,	2	2	3	2	2	2	2	2	2	2	2	2	2	1	1	2	1	2	-	1	2	2	1	1
6	2	Loss for 10,15,16,17, Trisomy 9	2	2	2	2	2	2	2	2	3	1	2	2	2	2	1	1	1	2	-	2	2	2	1	1
6	3	Extensive chroms. loss, Tetras 9	2	1	1	1	2	1	2	2	4	2	2	2	2	1	2	0	2	2	-	2	1	2	1	1
6	4	Extensive chroms. loss	2	2	1	1	1	2	1	2	2	2	2	1	2	2	2	2	2	2	-	1	1	2	1	1
6	5	Extensive chroms. loss	2	1	2	1	1	2	2	2	1	2	2	1	1	2	1	0	2	2	-	1	1	1	1	2
6	6	Extensive chroms. loss	2	1	1	1	2	1	1	2	2	2	2	2	1	2	2	2	2	2	-	1	2	2	2	1
6	7	Ext. chroms. loss, Tris 15, Tetra X	2	2	2	1	0	2	1	2	2	2	2	2	1	1	3	1	2	2	-	1	2	2	4	1
6	8	Extensive chroms. loss, Tetra 9	2	2	2	2	1	2	1	2	4	2	1	2	1	0	1	2	2	2	-	1	2	2	2	0
6	9	Loss for 20, Tetrasomy 15	2	2	2	2	0	3	2	2	2	2	2	2	2	2	4	2	2	2	-	1	2	2	1	1
General comments for embryo 6: Male cell. Independent chromosome loss for 2, 3, 4, 5, 6, 7, 13, 14, 15, 16, 20. Chromosome gain for 9, X. Possible mitotic non-disjunction for chromosomes 3, 6, 9, 15.																										

Table 6.5: Chromosome copy number results for whole embryo 6.

Embryo	Cell	Comments per-cell	Number of signals per chromosome																							
			1	2	3	4	5	6	7	8	9	10	11	12	13	14	15	16	17	18	19	20	21	22	X	Y
7	1	Loss for 7,20	2	*	2	0	*	2	1	2	2	2	2	2	*	*	*	*	2	*	-	1	*	*	*	*
7	2	Loss for 6,8,20	2	*	2	2	*	1	2	1	2	2	2	2	*	*	*	*	2	*	-	1	*	*	*	*
7	3	Loss for 4,20	2	*	2	1	*	2	2	2	2	2	2	2	*	*	*	*	2	*	-	1	*	*	*	*
7	4	Extensive chroms. loss	1	*	2	2	1	2	1	2	2	1	2	2	1	1	*	*	2	*	-	1	1	2	*	*
7	5	Extensive chroms. loss	1	*	1	1	2	2	1	1	2	2	2	2	2	2	*	*	2	*	-	1	2	2	*	*
7	6	Loss for 9,20	2	*	2	2	*	2	2	2	1	2	2	2	*	*	*	*	2	*	-	1	*	*	*	*
7	7	Loss for 8,20	2	*	2	2	*	2	2	1	2	2	2	2	*	*	*	*	2	*	-	1	*	*	*	*
7	8	Loss for 3,4,6,15	2	2	1	1	*	1	2	2	2	2	2	2	*	*	1	0	2	2	-	2	*	*	1	1
7	9	Loss for 2,4,6,16	2	1	2	1	*	1	2	2	2	2	2	2	*	*	2	1	2	2	-	2	*	*	1	1
7	10	Loss for 7	2	2	2	2	*	2	1	2	2	2	2	2	*	*	2	2	2	2	-	2	*	*	1	1
7	11	Loss for 2,4,7,15	2	1	2	1	*	2	1	2	2	2	2	2	*	*	1	0	2	2	-	2	*	*	1	1
7	12	Loss for 1,2,4,8	1	1	2	1	*	2	2	1	2	2	2	2	*	*	2	2	2	2	-	2	*	*	1	1
7	13	Loss for 4,11, Trisomy 3	2	2	3	1	*	2	2	2	2	2	1	2	*	*	2	2	2	2	-	2	*	*	1	1
7	14	Loss for 8	2	2	2	2	*	2	2	1	2	2	2	2	*	*	2	2	2	2	-	2	*	*	1	1
General comments for embryo 7: Male cell. Independent chromosome loss for 2, 4, 20.																										

Table 6.6: Chromosome copy number results for whole embryo 7. The (*) refers to non obtainable results for that particular chromosome/layer through reprobing.

Embryo	Cell	Comments per-cell	Number of signals per chromosome																							
			1	2	3	4	5	6	7	8	9	10	11	12	13	14	15	16	17	18	19	20	21	22	X	Y
8	1	Loss for 2,9,13,17,22	2	1	2	2	2	2	2	2	1	2	2	2	1	2	2	2	1	2	-	2	2	1	2	0
8	2	Loss for 5,13,14,21, Pentasomy 9	2	2	2	2	1	2	2	2	5	2	2	2	1	1	2	2	2	2	-	2	1	2	1	1
8	3	Extensive chroms.gain	4	2	4	1	4	4	4	5	4	3	6	2	3	3	0	0	3	0	-	2	6	4	3	1
8	4	Extensive chroms. loss	1	2	1	1	2	1	1	2	2	2	2	1	2	1	2	0	2	0	-	1	1	1	1	1
8	5	Loss for 1,3,6,14, Trisomy 4,9,11,	1	2	1	3	2	1	0	2	3	2	3	2	2	1	2	0	2	0	-	2	2	2	1	0
8	6	Extensive chroms. loss, Trisomy 9	1	1	1	2	2	1	1	2	3	2	2	1	2	1	2	1	2	1	-	1	2	2	2	0
General comments for embryo 8: Unclear gender. Independent chromosome loss for 2, 3, 4, 5, 6, 7, 13, 14, 16, 20. Chromosome gain for 9, X. Possible mitotic non-disjunction for chromosomes 3, 6, 9.																										

Table 6.7: Chromosome copy number results for whole embryo 8.

Table 6.8: (below & overleaf) Chromosome copy number results for whole embryo 9.

Embryo	Cell	Comments per-cell	Number of signals per chromosome																							
			1	2	3	4	5	6	7	8	9	10	11	12	13	14	15	16	17	18	19	20	21	22	X	Y
9	1	Extensive chroms. loss	2	2	2	2	2	2	1	1	1	2	2	1	2	2	1	2	2	1	-	2	1	1	1	1
9	2	Extensive chroms. loss, Trisomy 2	2	3	1	2	2	2	2	2	1	2	1	2	1	1	2	2	2	2	-	2	2	1	2	1
9	3	Extensive chroms. loss, Trisomy 2	2	3	2	1	2	1	1	1	1	2	2	1	2	2	2	2	2	1	-	1	1	1	1	1
9	4	Extensive chroms. loss	1	2	2	2	2	1	1	1	1	1	1	2	2	2	1	2	1	1	-	1	2	1	1	0
9	5	Loss for 3,4,13,18, Trisomy 16	2	2	1	1	2	2	2	2	2	2	2	2	1	2	2	3	2	1	-	2	2	2	1	1
9	6	Extensive chroms. loss	1	1	0	1	2	2	1	1	2	0	1	2	1	1	1	1	0	1	-	1	2	2	1	1
9	7	Extensive chroms. loss	1	1	1	1	2	2	1	2	2	1	1	2	1	1	1	1	1	1	-	0	2	1	1	1
9	8	Extensive chroms. loss, Trisomy 12	1	2	1	1	2	2	0	1	1	1	1	3	1	1	1	2	1	2	-	1	1	1	1	1
9	9	Extensive chroms. loss	2	2	1	2	2	2	2	2	1	2	1	1	2	1	2	2	1	2	-	1	2	1	2	2
9	10	Extensive chroms. loss	1	2	2	2	1	1	2	1	1	1	1	0	1	1	2	2	1	2	-	1	1	1	1	0
9	11	Extensive chroms. loss	1	1	2	1	1	1	1	1	1	1	1	1	1	1	1	1	1	2	-	2	1	1	2	1
9	12	Extensive chroms. loss	1	1	1	1	2	2	1	2	1	1	1	2	1	1	2	1	1	1	-	0	2	1	2	0
9	13	Extensive chroms. loss	1	1	1	2	1	2	1	1	1	1	2	1	1	1	1	2	1	1	-	2	1	1	1	1
9	14	Extensive chroms. loss	1	1	1	2	1	2	1	1	2	2	2	2	1	1	1	1	1	1	-	2	1	1	1	1
9	15	Extensive chroms. loss, Trisomy 15	1	2	1	1	2	2	2	1	1	1	1	2	2	2	3	1	2	1	-	1	2	2	2	0
9	16	Extensive chroms. loss, Trisomy 1,13	3	1	1	1	2	2	1	2	2	2	2	2	3	2	1	2	1	2	-	1	2	2	1	1
9	17	Extensive chroms. loss	2	2	1	1	2	1	2	2	1	2	1	2	2	2	1	1	1	2	-	1	2	2	2	0

9	18	Loss for 3,4,15,18,20	2	2	1	1	2	2	2	2	2	2	2	2	2	2	1	2	2	1	-	1	2	2	1	1
9	19	Loss for 8,9, Trisomy 20	2	2	2	2	2	2	2	1	1	2	2	2	2	2	2	2	2	2	-	3	2	2	1	1
9	20	Extensive chroms. loss, Trisomy 5,	1	2	1	2	3	2	1	1	1	2	1	1	1	1	1	2	1	2	-	1	2	1	0	1
9	21	Loss for 8,9, Trisomy 20	2	2	2	2	2	2	2	1	1	2	2	2	2	2	2	0	2	2	-	3	2	2	1	1
9	22	Loss for 6,9,20, Trisomy 15	2	2	2	2	2	1	2	2	1	2	2	2	2	2	3	2	2	2	-	1	2	2	2	0
9	23	Extensive chroms. loss	2	1	1	2	1	2	2	2	2	1	1	2	2	2	2	2	2	2	-	1	2	2	1	1
9	24	Extensive chroms. loss	2	2	1	1	2	2	2	1	2	1	1	2	2	2	1	2	2	2	-	2	2	2	2	0
9	25	Loss for 6,9,14,15,18, Tris 3,14, Pent 20	0	2	3	2	2	1	2	2	1	2	2	2	2	3	1	1	2	1	-	5	2	2	2	0
9	26	Extensive chroms. loss, Trisomy 14,15	2	2	1	1	2	1	1	2	1	1	2	1	2	3	3	1	2	2	-	1	2	1	1	1
9	27	Loss for 3,8,9,10,20, Trisomy 14	2	2	1	2	2	2	2	1	1	1	2	2	2	3	2	2	2	2	-	1	2	2	1	1
9	28	Extensive chroms. loss, Trisomy 14	1	2	1	1	1	2	1	2	1	2	2	1	2	3	1	1	2	1	-	2	2	2	2	1
9	29	Extensive chroms. loss, Trisomy 15	1	2	1	2	2	2	1	1	1	2	1	2	2	2	3	2	2	2	-	1	2	2	2	0
9	30	Extensive chroms. loss, Trisomy 1,14	3	1	1	1	2	1	2	1	1	1	1	2	2	3	2	2	1	1	-	1	2	2	1	1
9	31	Extensive chroms. loss	2	2	1	2	2	2	1	1	1	2	1	1	2	2	1	1	2	2	-	2	2	2	1	1
9	33	Extensive chroms. loss, Trisomy 14,15	2	2	2	1	2	1	1	1	2	2	2	1	2	3	3	1	2	2	-	1	2	2	1	0
9	33	Extensive chroms. loss, Trisomy 15	2	1	1	1	2	2	2	2	1	1	1	2	2	2	3	1	2	2	-	1	2	2	2	0
General comments for embryo 3: Male cell. Independent chromosome loss for 3, 4, 8, 9, 11, 15, 20. Chromosome gain for 14, 15. Possible mitotic non-disjunction for chromosomes 14, 15.																										

Embryo	Cell	Comments per-cell	Number of signals per chromosome																							
			1	2	3	4	5	6	7	8	9	10	11	12	13	14	15	16	17	18	19	20	21	22	X	Y
12	1	Extensive chroms. loss	2	1	1	1	2	1	2	2	1	1	2	1	2	1	1	1	1	2	-	1	1	2	1	1
12	2	Extensive chroms. loss, Trisomy 15	2	1	1	1	2	1	1	1	2	2	2	1	2	2	3	1	1	2	-	1	2	2	1	1
12	3	Loss for 10,12,15,17,20	2	2	2	2	2	2	2	2	2	1	2	1	2	2	1	2	1	2	-	1	2	2	1	1
General comments for embryo 12: Male cell. Independent chromosome loss for 2, 3, 4, 6, 10, 12, 15, 16, 17, 20. Chromosome gain for 15. Possible mitotic non-disjunction for chromosome 15.																										

Table 6.9: Chromosome copy number results for whole embryo 12.

Embryo	Cell	Comments per-cell	Number of signals per chromosome																							
			1	2	3	4	5	6	7	8	9	10	11	12	13	14	15	16	17	18	19	20	21	22	X	Y
14	1	Gain/loss several chroms	3	2	1	1	0	3	3	3	2	1	3	3	3	2	4	1	1	2	-	1	3	6	0	2
14	2	Loss for 3,14,20,22, Trisomy 21	2	2	1	2	2	2	2	2	2	2	2	2	2	1	2	2	2	2	-	1	3	1	1	1
14	3	Extensive chroms. loss	1	2	1	2	2	1	2	2	1	2	1	2	1	1	2	2	2	2	-	2	2	1	2	1
14	4	Extensive chroms. loss, Tetrasomy 22	2	1	2	2	2	2	1	1	2	1	2	1	2	2	2	1	2	2	-	1	2	4	1	1
14	5	Gain/loss several chroms	1	1	2	2	2	3	1	4	2	2	2	3	1	0	2	1	3	4	-	2	1	2	0	2
14	6	Gain/loss several chroms	1	1	3	3	3	1	0	3	2	3	2	2	1	1	2	2	3	4	-	2	2	4	1	1
14	7	Gain/loss several chroms	1	3	3	1	1	1	3	3	4	3	3	3	3	1	3	4	3	4	-	2	2	2	2	1
14	8	Extensive chroms. loss, Tris 22, Tetra 7	1	1	1	2	2	2	4	1	1	1	2	2	2	2	1	1	2	2	-	1	1	3	1	1
14	9	Extensive chroms. loss, Tris 22	2	1	1	1	2	2	0	1	1	1	2	1	2	2	1	1	1	2	-	1	1	3	1	1
General comments for embryo 14: Male cell. Independent chromosome loss for 1, 2, 3, 10, 16, 20. Chromosome gain for 7, 8, 12, 17, 18, 22. Possible mitotic non-disjunction for chromosomes 3, 6, 7, 8, 10, 12, 13, 17, 21, 22.																										

Table 6.10: Chromosome copy number results for whole embryo 14.

Embryo	Cell	Comments per-cell	Number of signals per chromosome																							
			1	2	3	4	5	6	7	8	9	10	11	12	13	14	15	16	17	18	19	20	21	22	X	Y
15	1	Extensive chroms. loss, Trisomy 9,11	2	1	1	1	2	1	2	1	3	2	3	2	2	2	2	2	2	2	-	2	1	2	2	2
15	2	Extensive chroms. loss, Trisomy 11,18,	1	2	0	2	2	2	1	2	1	1	3	2	1	2	1	1	2	3	-	2	1	1	1	2
15	3	Loss for 13,15,17,20,21, Trisomy 5,11	2	2	0	2	3	2	2	2	2	2	3	2	1	2	1	2	1	2	-	1	1	2	1	2
15	4	Extensive chroms. loss	2	2	0	1	2	1	1	1	1	2	2	2	2	2	0	1	2	1	-	1	1	1	1	1
15	5	Extensive chroms. loss	2	2	2	1	2	1	2	1	2	2	2	2	2	2	2	0	1	2	-	1	1	2	2	2
15	6	Loss for 11	2	2	0	2	2	2	2	2	2	2	1	2	2	2	2	2	2	2	-	2	1	1	1	1
15	7	Loss for 10,11,14,16,20, Trisomy 15	2	2	0	2	2	2	2	2	0	1	1	2	2	1	3	1	2	2	-	1	2	2	1	1
15	8	Extensive chroms. loss, Trisomy 11	1	2	1	1	2	2	2	2	1	2	3	2	2	2	1	1	2	2	-	1	1	2	1	1
15	9	Loss for 7	2	2	0	2	2	2	1	2	2	2	2	2	2	2	2	2	2	2	-	2	2	2	1	2
15	10	Extensive chroms. loss, Trisomy 2,16	2	3	1	1	2	2	0	2	1	2	1	2	2	1	1	3	1	1	-	2	1	2	1	2
15	11	Extensive chroms. loss	2	2	0	1	2	2	2	2	2	1	2	1	2	2	1	2	2	2	-	1	1	2	1	1
15	12	Extensive chroms. loss	2	2	0	1	2	2	1	2	1	0	0	1	2	2	1	1	2	2	-	0	1	2	1	1
15	13	Extensive chroms. loss	2	2	0	1	2	2	2	2	1	1	1	1	2	2	1	1	2	2	-	1	1	2	1	1
15	14	Extensive chroms. loss	2	1	1	1	1	2	2	2	2	1	1	2	2	2	1	2	2	2	-	0	1	2	1	1
15	15	Loss for 4,10,15,20,21	2	2	0	1	2	2	2	2	2	1	2	2	2	2	1	2	2	2	-	1	1	2	1	1
15	16	Extensive chroms. loss	2	2	0	2	2	1	0	1	2	2	2	1	2	2	2	1	2	2	-	1	1	2	1	1

General comments for embryo 15: Male cell. Independent chromosome loss for 3,4, 15, 16, 20, 21. Chromosome gain for 11. Possible mitotic non-disjunction for chromosome 11.

Table 6.11: Chromosome copy number results for whole embryo 15.

Embryo	Cell	Comments per-cell	Number of signals per chromosome																							
			1	2	3	4	5	6	7	8	9	10	11	12	13	14	15	16	17	18	19	20	21	22	X	Y
16	1	Loss for 1,2,22	1	1	2	2	2	2	2	2	2	2	2	2	2	2	2	2	2	2	-	2	2	1	1	1
16	2	Loss for 2,11,20,21	2	1	2	2	2	2	2	2	2	2	1	2	2	2	2	2	2	2	-	1	2	1	1	1
16	3	Extensive chroms. loss	2	1	2	2	2	2	2	2	1	2	1	2	2	2	2	2	2	2	-	1	1	1	1	1
16	4	Extensive chroms. loss, Trisomy 18	1	1	2	2	2	2	1	1	2	2	2	2	2	2	1	2	1	3	-	1	2	1	1	1
16	5	Extensive chroms. loss	2	1	2	2	2	2	1	2	2	2	2	2	1	1	2	1	2	2	-	1	1	1	1	1
16	6	Extensive chroms. loss, Trisomy 11	2	1	2	2	1	2	2	2	1	2	3	2	2	2	2	1	2	2	-	1	1	1	1	1
16	7	Extensive chroms. loss, Trisomy 9	2	1	2	2	2	1	2	1	3	1	2	2	2	2	2	1	2	2	-	1	1	1	1	1
16	8	Loss for 2,4,21,22	2	1	2	1	2	2	2	2	2	2	2	2	2	2	2	2	2	2	-	2	1	1	1	1
16	9	Loss for 2,14,18,20,22	2	1	2	2	2	2	2	2	2	2	2	2	2	1	2	0	2	1	-	1	2	1	1	1
16	10	Loss for 2,20	2	1	2	2	2	2	2	2	2	2	2	2	2	2	2	2	2	2	-	1	2	2	1	1
16	11	Loss for 2,11,14,21,22	2	1	2	2	2	2	2	2	2	2	1	2	2	1	2	2	2	2	-	2	1	1	1	1
16	12	Extensive chroms. loss	2	1	2	2	2	1	2	2	2	2	2	2	2	1	2	1	1	1	-	1	2	1	1	1
16	13	Extensive chroms. loss	1	2	2	2	2	2	2	1	2	2	2	2	2	2	1	2	1	1	-	1	1	1	1	1
General comments for embryo 16: Male cell. Independent chromosome loss for 2, 20, 21, 22.																										

Table 6.12: Chromosome copy number results for whole embryo 16.

Embryo	Cell	Comments per-cell	Number of signals per chromosome																							
			1	2	3	4	5	6	7	8	9	10	11	12	13	14	15	16	17	18	19	20	21	22	X	Y
17	1	Extensive chroms. loss	2	1	0	2	2	2	1	1	1	0	2	2	2	1	1	0	2	0	-	2	0	0	1	0
17	2	Loss for 8,11,12,14, Trisomy 7	2	2	2	2	2	2	3	1	2	2	1	1	2	1	0	0	2	2	-	0	2	2	1	1
17	3	Extensive chroms. loss	1	2	2	2	2	2	0	1	2	2	2	1	1	2	2	2	1	1	-	0	2	2	2	0
17	4	Extensive chroms. loss, Trisomy 2,4	2	3	2	3	2	2	2	1	1	1	2	2	2	2	2	1	2	1	-	0	1	1	2	0
17	5	Gain/loss several chroms	2	3	2	2	2	4	1	2	2	4	1	4	2	1	3	1	1	0	-	0	2	2	2	0
17	6	Gain/loss several chroms	2	2	4	4	1	3	2	1	3	4	1	3	3	1	4	2	1	1	-	0	2	2	2	0
17	7	Extensive chroms. loss, Trisomy 2,9	2	3	2	1	2	1	2	1	3	2	2	2	1	0	2	1	2	1	-	2	2	2	2	2
17	8	Extensive chroms. loss, Trisomy 4	2	2	2	3	1	2	2	1	1	2	1	2	1	0	0	0	1	0	-	2	1	1	2	0
17	9	Extensive chroms. loss	2	1	1	2	1	2	2	1	1	2	2	2	1	1	2	1	2	0	-	0	2	1	2	0
17	10	Loss for 8,16,17,18, Tris 22, Tetras 21	2	2	2	2	2	2	2	1	2	2	2	2	2	0	2	1	1	1	-	2	4	3	2	0
17	11	Gain/loss several chroms	2	2	3	2	2	3	2	1	3	2	2	4	3	1	3	2	2	1	-	1	2	1	2	0

17	12	Extensive chroms. loss, Trisomy 5,10,	2	1	1	2	3	1	2	1	2	3	2	2	0	1	2	1	2	1	-	1	2	1	1	0
17	13	Extensive chroms. loss,	2	2	2	2	1	2	2	1	1	2	2	2	0	0	2	1	2	1	-	1	2	2	2	0
17	14	Gain/loss several chroms	3	4	2	3	2	2	2	2	2	2	3	3	0	3	3	1	2	1	-	2	1	3	2	0
17	15	Extensive chroms. loss, Trisomy 21	2	1	2	2	1	1	2	1	1	1	1	2	0	1	1	1	1	2	-	1	3	2	2	0
17	16	Gain/loss several chroms	4	3	5	4	1	4	2	2	2	2	4	3	0	1	3	1	1	1	-	2	2	2	1	0
General comments for embryo 17: Female cell. Independent chromosome loss for 8, 14, 16, 18, 22. Chromosome gain for 2, 4, 12, 15. Possible mitotic non-disjunction for chromosome 2, 9.																									

Table 6.13: Chromosome copy number results for whole embryo 17.

Embryo	Cell	Comments per-cell	Number of signals per chromosome																							
			1	2	3	4	5	6	7	8	9	10	11	12	13	14	15	16	17	18	19	20	21	22	X	Y
19	1	Extensive chroms. loss, Tris 6, Tetras 8	2	1	2	2	1	3	2	4	1	1	0	2	0	1	2	0	2	0	-	0	1	2	1	1
19	2	Extensive chroms. loss	1	1	1	1	2	1	2	2	1	2	1	2	0	1	1	1	2	1	-	0	2	1	1	1
19	3	Extensive chroms. loss, Trisomy 18	2	1	1	1	0	1	1	2	0	2	0	1	1	0	1	1	1	3	-	0	1	1	1	1
19	4	Extensive chroms. loss, Tris 7,8,12	2	2	1	1	2	1	3	3	1	1	0	3	2	1	1	2	1	0	-	0	2	2	1	2
19	5	Extensive chroms. loss	1	2	0	1	2	1	1	1	0	1	0	2	2	1	1	0	2	1	-	1	1	2	1	1
19	6	Extensive chroms. loss, Trisomy 22	0	1	1	0	2	1	2	1	2	1	0	1	1	0	1	1	2	1	-	0	2	3	1	1
19	7	Extensive chroms. loss, Tetrasomy 10	2	1	1	2	2	2	2	3	2	4	2	1	1	0	1	1	2	2	-	0	1	1	1	1
19	8	Gain/loss several chroms	2	2	2	2	2	2	3	4	2	3	0	4	2	1	1	1	0	4	-	0	1	2	1	1
19	9	Gain/loss several chroms	4	4	1	2	3	3	3	3	2	2	0	4	0	3	2	0	2	3	-	0	2	3	0	1
19	10	Extensive chroms. loss, Tris 2,17,18,21	1	3	1	2	2	1	1	1	2	2	0	2	2	2	2	2	3	3	-	0	3	2	2	1
19	11	Ext.chroms. loss, Tris 10,11, Tetra 9	1	2	1	2	2	2	2	2	4	3	3	2	1	2	2	2	1	2	-	0	1	2	1	1
General comments for embryo 19: Male cell. Independent chromosome loss for 2, 3, 6, 10, 13, 14, 15, 16, 21. Chromosome gain for 8, 18. Possible mitotic non-disjunction for chromosomes 7, 8, 18.																										

Table 6.14: Chromosome copy number results for whole embryo 19.

Embryo	Cell	Comments per-cell	Number of signals per chromosome																							
			1	2	3	4	5	6	7	8	9	10	11	12	13	14	15	16	17	18	19	20	21	22	X	Y
20	1	Extensive chroms. loss	2	2	1	2	0	2	2	2	1	1	1	1	0	1	1	2	2	2	2	1	1	1	2	0
20	2	Extensive chroms. loss	2	2	2	1	2	2	1	2	2	2	1	1	1	1	2	2	1	2	2	2	2	1	2	0
20	3	Extensive chroms. loss, Trisomy 8	1	1	2	2	1	2	2	3	2	1	1	1	1	1	2	2	1	2	0	1	1	1	2	0
20	4	Extensive chroms. loss, Trisomy 21	2	1	2	1	1	1	2	2	2	1	1	1	0	0	1	2	1	2	0	1	3	1	2	0
20	5	Extensive chroms. loss	2	1	2	1	1	1	1	2	2	1	1	1	1	1	1	1	2	2	0	2	2	1	2	0
20	6	Extensive chroms. loss	2	1	2	1	2	1	2	2	1	1	0	1	0	1	2	1	1	1	2	1	2	1	2	0
20	7	Extensive chroms. loss	1	2	1	2	1	2	1	1	1	2	0	1	1	1	1	0	2	2	1	1	1	1	2	0

20	8	Extensive chroms. loss, Trisomy 8	1	2	2	2	2	2	2	3	1	1	0	2	1	1	1	1	2	2	2	2	2	1	2	0
20	9	Extensive chroms. loss	2	2	2	2	2	1	1	2	2	2	1	2	1	1	1	1	1	2	2	2	2	1	2	0
20	10	Extensive chroms. loss	1	1	0	1	2	1	1	2	1	1	1	1	1	1	1	1	1	1	2	1	2	1	1	1
20	11	Extensive chroms. loss	1	2	1	2	1	1	1	2	2	2	0	2	1	1	1	1	1	1	0	1	0	1	1	1
General comments for embryo 20: Female cell. Independent chromosome loss for 5, 6, 7, 10, 11, 12, 13, 14, 15, 16, 17, 19, 20, 22.																									

Table 6.15: Chromosome copy number results for whole embryo 20.

Embryo	Cell	Comments per-cell	Number of signals per chromosome																						
			1	2	3	4	5	6	7	8	9	10	11	12	13	14	15	16	17	18	19	20	21	22	X	Y
21	1	Extensive chroms. loss	2	2	1	1	2	1	1	2	1	2	0	1	1	1	2	2	2	2	0	1	2	1	2	0
21	2	Extensive chroms. loss	1	2	2	2	2	2	1	1	1	2	2	1	1	2	2	2	2	2	1	0	1	2	2	0
21	3	Extensive chroms. Loss, Trisomy 5	2	2	2	1	3	2	1	2	2	2	2	2	1	1	2	2	2	1	1	1	1	2	2	0
21	4	Extensive chroms. loss	1	2	2	1	2	2	1	2	2	1	0	2	1	2	1	2	2	2	0	0	1	2	2	0
21	5	Extensive chroms. Loss, Trisomy 22	2	2	2	1	2	2	1	2	2	2	1	2	2	2	2	1	2	2	1	1	1	3	1	0
21	6	Extensive chroms. Loss, Trisomy 22	2	2	1	2	2	2	1	2	2	2	1	2	1	2	2	1	2	1	0	1	1	3	2	0
General comments for embryo 21: Female cell. Independent chromosome loss 4, 7, 13, 20, 21. Chromosome gain for 22. Possible mitotic non-disjunction for chromosome 22.																									

Table 6.16: Chromosome copy number results for whole embryo 21.

Embryo	Cell	Comments per-cell	Number of signals per chromosome																						
			1	2	3	4	5	6	7	8	9	10	11	12	13	14	15	16	17	18	19	20	21	22	X	Y
24	1	Extensive chroms. loss	1	2	2	0	2	0	2	1	1	1	1	0	2	2	2	0	1	1	2	1	2	2	1	1
24	2	Extensive chroms. loss	1	2	1	0	0	1	1	1	1	2	2	0	0	2	1	0	0	0	0	1	0	1	1	1
24	3	Extensive chroms. loss	2	2	1	0	0	0	1	1	1	1	0	1	0	0	1	0	0	1	0	0	0	1	1	0
24	4	Extensive chroms. loss	1	1	0	0	1	0	1	1	1	1	0	1	1	1	2	1	1	2	0	1	0	1	1	1
24	5	Extensive chroms. loss	1	2	2	0	2	0	1	2	2	1	0	1	0	1	2	0	1	2	0	1	1	2	1	1
24	6	Extensive chroms. loss	0	2	1	0	0	1	2	2	2	1	1	0	0	0	0	0	1	1	0	0	2	2	1	0
24	7	Extensive chroms. loss	0	2	2	0	2	1	1	1	2	1	0	0	1	0	2	0	1	1	1	1	2	2	1	2
24	8	Extensive chroms. loss	1	2	1	0	0	1	0	2	2	1	1	0	0	2	2	1	1	2	0	1	2	2	1	1
24	9	Extensive chroms. loss	1	1	1	0	0	1	0	2	1	1	0	0	0	1	2	1	1	1	0	1	2	2	1	1
24	10	Extensive chroms. loss	2	1	1	0	0	2	0	2	1	2	2	0	2	2	1	0	1	1	2	0	0	2	1	1
24	11	Extensive chroms. Loss, Trisomy 1,2,3	3	3	3	0	1	2	0	2	0	1	1	0	0	1	2	0	1	2	1	1	1	2	2	1
General comments for embryo 24: Male cell. Independent chromosome loss for 2, 3, 4, 5, 6, 7, 9, 10, 11, 12, 13, 14, 16, 17, 18, 19, 20, 21.																									

Table 6.17: Chromosome copy number results for whole embryo 24.

Embryo	Cell	Comments per-cell	Number of signals per chromosome																							
			1	2	3	4	5	6	7	8	9	10	11	12	13	14	15	16	17	18	19	20	21	22	X	Y
25	1	Extensive chroms. Loss, Tetrasomy 2	2	4	1	0	2	2	1	2	2	1	1	0	1	1	2	2	2	2	1	1	2	2	2	0
25	2	Extensive chroms. loss	1	2	2	1	0	1	1	2	2	2	2	1	1	1	2	0	1	2	0	1	2	2	1	0
25	3	Extensive chroms. loss	1	2	1	1	2	1	2	2	1	2	1	2	2	2	2	2	1	2	0	1	2	1	2	0
25	4	Extensive chroms. loss	1	2	1	2	1	1	2	2	2	2	1	1	1	2	2	1	2	1	2	1	1	1	2	0
25	5	Extensive chroms. loss	1	2	2	0	2	0	1	2	1	2	0	1	0	1	1	0	1	1	0	1	1	2	2	0
25	6	Extensive chroms. loss	2	2	1	1	0	0	1	2	2	1	0	0	0	2	2	2	0	2	0	1	2	2	2	0
25	7	Extensive chroms. loss	0	2	1	0	0	0	2	2	1	2	0	1	0	1	2	1	0	1	0	1	2	2	2	0
25	8	Extensive chroms. loss	2	2	1	0	0	0	2	2	2	2	0	1	0	0	2	0	0	2	0	1	1	2	2	0
25	9	Extensive chroms. loss	0	2	2	0	0	0	1	2	2	2	0	2	0	0	2	0	2	2	0	1	0	2	2	0
25	10	Extensive chroms. loss	2	2	0	0	0	0	1	1	2	2	0	2	0	0	2	1	1	1	0	0	0	2	1	0
25	11	Extensive chroms. loss	2	2	2	0	0	0	2	1	1	2	0	1	0	0	1	1	0	1	0	1	0	2	2	0
25	12	Extensive chroms. loss	1	2	1	0	0	1	0	2	2	2	1	1	0	0	2	2	2	2	0	1	0	2	2	0
25	13	Extensive chroms. loss	2	2	1	1	0	1	1	2	2	1	0	1	0	0	1	1	1	2	0	1	2	2	2	0
25	14	Extensive chroms. Loss, Trisomy 8	2	2	1	0	2	1	1	3	2	2	0	1	0	0	1	2	2	2	0	1	0	1	2	0
25	15	Gain/loss several chroms	3	3	1	0	0	1	2	2	2	4	2	3	0	0	4	1	2	3	0	2	0	3	4	0
25	16	Extensive chroms. loss	0	2	1	0	1	1	2	2	1	2	0	1	0	2	2	0	1	2	0	1	2	2	2	0
25	17	Extensive chroms. loss	2	2	1	0	1	1	1	2	2	2	2	2	1	1	1	1	2	2	0	1	2	2	2	0
25	18	Extensive chroms. loss	0	2	2	1	2	0	1	2	2	2	1	2	0	1	2	1	2	2	0	2	2	2	2	0
25	19	Extensive chroms. gain	4	3	4	0	2	3	4	3	2	3	0	2	2	1	4	2	3	3	2	2	2	2	3	0
General comments for embryo 25: Female cell. Independent chromosome loss for 3, 4, 5, 6, 7, 11, 12, 13, 14, 16, 17, 19, 20. Chromosome gain for 2. Possible mitotic non-disjunction for chromosome 2, 3, 7.																										

Table 6.18: Chromosome copy number results for whole embryo 25.

An immediate conclusion from the above tables is that aneuploidy was present in every whole embryo (and indeed possibly every blastomere) that was examined through the reprobing assay. In the following section I examine the nature of the abnormalities and the chromosomes that were more prone to aneuploidy from the above data set.

6.3.2. Specific aim 4b: To test the hypothesis that, as suggested by previous studies, the majority of human embryos are (mosaic) chromosomally abnormal for at least one chromosome

As seen from Table 6.1, in section 6.3.1 once the chromosome copy number was assayed in the 17 whole embryos, there was strong evidence suggesting that, at least this subset of embryos were all chromosomally abnormal. Indeed, no single nucleus showed 46/46 signals and consistent patterns (other than widespread chromosome loss).

6.3.3. Specific aim 4c: To test the hypothesis that chromosome loss is more common than chromosome gain and that certain chromosomes are more prone to aneuploidy than others

Table 6.19 summarises the data from Tables 6.2-6.18 and under each ploidy status refers the number of cells (out of 250) that this occurred.

Chrom	Normal	Monosomy	Trisomy	>3	No signal	Blastomeres analysed (n)
1	143	82	8	6	11	250
2	143	75	24	8	0	250
3	84	126	9	5	26	250
4	95	109	10	2	34	250
5	160	48	11	7	24	250
6	127	90	13	4	16	250
7	104	113	11	3	19	250
8	139	87	19	4	1	250
9	116	102	15	9	8	250
10	139	91	11	5	4	250
11	109	76	26	2	37	250
12	126	90	16	5	13	250
13	142	63	11	2	32	250
14	121	87	13	6	23	250
15	113	96	25	8	8	250
16	105	94	11	3	37	250
17	125	106	12	0	7	250
18	138	74	11	8	19	250
19	10	7	0	0	30	47
20	64	152	4	2	28	250
21	134	85	11	7	13	250
22	144	77	16	12	1	250
XY	133	3	14	9	0	159*
XX	52	20	12	2	0	86
Total signals/ status	2766	1953	313	119	391	TOTAL
%	49.86%	35.21%	5.64%	2.15%	7.05%	99.91*

Table 6.19: Overview of the ploidy status of the 250 blastomeres (from 16 whole embryos) that provided successful hybridisation results over the 4 layers of reprobing. The category of >3 refers to the blastomeres with polyploidy (more than 3 copies) for the specific chromosome. Note: *Five blastomeres with signals that cannot be classified to any of the above categories for XY are not included in the above table. They account for 0.09% of all chromosomes per cell analysed (5/5,547).

Thus, from the 5,547 chromosomes per cell analysed monosomy was present in 35.21% (1,953 signals), trisomy was present in 5.64% (313 signals), whereas no signal was present at 7.05% (391). Polyploidy was present in 2.15% of cells. Hence, even when the expected number of single signals was taken into account (by extrapolation of control lymphocyte data, chromosomal loss (monosomy) occurred at a frequency several times greater than chromosome gain (trisomy) in this population of embryos (specific aim 4c). It should also be noted however that 74% of cells (185/250) had correct status for the sex chromosomes, whereas monosomy (XO, YO)

or trisomy (XXY, XYY, XXX) occurred at a similar frequency (9.2 and 10.4% respectively).

From Table 6.19 certain conclusions can be drawn with regard to which chromosomes are more prone to aneuploidy (specific aim 4c) and Tables 6.20-6.21 depict the least and most aneuploid chromosomes for trisomy and monosomy (as shown in Table 6.19). The % of the frequency (out of 250 cells) is shown as well for each category.

Trisomy	%
19	0.00
20	1.60
1	3.20
3	3.60
4	4.00
5	4.40
7	4.40
10	4.40
13	4.40
16	4.40
18	4.40
21	4.40
17	4.80
6	5.20
14	5.20
9	6.00
12	6.40
22	6.40
8	7.60
2	9.60
15	10.00
11	10.40

Table 6.20: % trisomy by chromosome. Chromosome 19 is shaded due to the small number of cells assessed.

Monosomy	%
19	2.80
5	19.20
13	25.20
18	29.60
2	30.00
11	30.40
22	30.80
1	32.80
21	34.00
8	34.80
14	34.80
6	36.00
12	36.00
10	36.40
16	37.60
15	38.40
9	40.80
17	42.40
4	43.60
7	45.20
3	50.40
20	60.80

Table 6.21: % monosomy by chromosome. Chromosome 19 is shaded due to the small number of cells assessed.

Chromosome 11 was the most prone to trisomy (10.4%) followed by 15 and 2 (10 and 9.6% respectively). Trisomy 21 was observed in only 4.4% of the cells analysed (Table 6.20). By contrast, the chromosome with the highest frequency of chromosome loss was 20 (60.8%) followed by chromosomes 3, 7, 4, 17 and 9 (all above 40%), (Table 6.21). Two chromosomes labelled with weak fluorochromes (Aqua and Blue) for 16, 11 where the chromosomes for which no signal (nullisomy or hybridisation failure) could be seen.

6.3.4. Specific aim 4d: To test the hypothesis that PGS diagnosis (for 8 chromosomes) is an accurate predictor of the ploidy status of the rest of the embryo

As stated in section 2.1.4 the whole embryo preparations used in this thesis originated from clinical PGS cases. These embryos were not used for transfer due to the diagnosis of abnormality from biopsy on day 3. Normally a follow up diagnosis using the same set of probes (as in the single cell level) would provide a confirmation (or not) of the initial diagnosis. The opportunity to do this as well as provide evidence for other potential abnormalities (that the current test would not detect) was however

explored here. The following table presents the PGS results from a single blastomere, compared to the results on the whole embryo (24 chromosome screening) and illustrates any additional abnormalities found (in bold). Additional abnormalities are reported only when the percentage exceeds 50% of the amount of cells that the diagnosis was made.

Embryo	PGS Diagnosis	24 chromosome diagnosis (in bold)	Confirmation of PGS
4	No result (poor embryos)	**Monosomy 3,4,7,20**	N/A
10	Trisomy 15	No result (poor fixed embryos)	N/A
11	Monosomy 21	No result (poor fixed embryos)	N/A
12	Trisomy 15 Monosomy 16, XY	Monosomy 15 Normal 16 XY **Monosomy 3,4,6,10,12,17,20**	No for 15,16 Yes for XY gender
13	Trisomy 13 No result XY	No result (poor fixed embryos)	N/A
14	Trisomy 22 Monosomy 18 No result XY	Trisomy & Tetrasomy 22 Normal 18 XY **Monosomy 2,14**	Partial for 22 No for 18
15	Monosomy 21, XY	Monosomy 21, XY **Monosomy 4,15**	Yes
16	Monosomy 21,22, XY	Monosomy 21,22, XY **Monosomy 2,20**	Yes
17	Monosomy 18 XXX	Monosomy 18 XX **Monosomy 8,14,16**	Yes for 18 No for X
18	Trisomy 22 Monosomy 21	No result (embryos under heavy debris)	N/A
19	Nucleus not found	**Monosomy 3,6,14,15,21**	N/A
20	Monosomy 13,15,16,22 XX	Monosomy 13,15,16,22 XX **Monosomy 9,11,12,14,20**	Yes
21	Trisomy 22 Monosomy 13,16 Nullisomy 21 No result X,Y	Normal 16,22 Monosomy 13, Monosomy 21 XX **Monosomy 7,20**	No 16,21,22 Yes for 13
24*	No result	Monosomy 1,3,4,6,7,8,10,17	N/A
25*	Nullisomy 7	Monosomy 7 **Monosomy 3,20**	Yes

Table 6.22: Comparison of results from PGS diagnosis (single cells) and 24 chromosome screening. The initial PGS diagnostic test used for 24 & 25 was polar body array CGH.

In terms of whether the single cell was a representative of the whole embryo, at least in the data set presented on Table 6.22 (and for the chromosomes investigated on the single cell level), in 7 of the embryos a correlation could not be made due to an

unclear result either in the PGS, or in the follow-up. In seven of the remaining embryos the diagnosis was confirmed (if only partially) and, in one case (embryo 12) a trisomy 15 in the biopsied blastomere but monosomy 15 in the follow up embryo might suggest a mitotic non-disjunction error.

6.4. Concluding remarks

The results herewith presented demonstrate a proof of principle for the use of a 24 chromosome FISH based aneuploidy screening for use on to whole embryos of single blastomeres for PGS. Most or all embryos and individual blastomeres appeared to be chromosomally abnormal with apparent chromosome losses more frequent rather than gain. In addition the original diagnosis made on some of the single blastomeres (day 3 - from which the whole embryos developed) allowed us to compare the efficacy of single cell diagnosis and our 24 chromosome approach, confirming the PGS in some but not all cases.

7. Specific aim 5: To apply the 24 chromosome FISH strategy to investigate nuclear organisation in human blastomeres

7.1. Background

Previous results from my own laboratory (Finch *et al.* 2008a) have demonstrated that FISH experiments can also be used to assess the spatial and temporal localisation of chromatin (nuclear address) in the interphase nucleus of blastomeres (as outlined in section 1.5.9) and correlated with whether the cell (or indeed the embryo) is chromosomally normal or abnormal. Again however, such experiments have been limited to a small subset of chromosomes, indeed, as outlined in section 1.4.8 very few studies have investigated nuclear architecture through means of chromosome position assays in the interphase nucleus of preimplantation embryos. Unlike in sperm cells where there is a plethora of available cells to study, blastomeres are of limited availability. A further drawback of previous work (McKenzie *et al.* 2004); (Finch *et al.* 2008a) is that "home-made" assays were used to measure mean chromosome position. As outlined in this thesis (section 2.12) a novel methodology to analyse radial position has been used and thus more accurate assessments of relative nuclear positions in blastomeres is now possible. If chromosome position is a reliable marker of nuclear health, then it can be assumed that significant alterations from "normal" levels in human preimplantation embryos could be suggestive of aberrant or arrested development and related to the mechanisms leading to numerical chromosome abnormalities (Finch *et al.* 2008a). Finch *et al.* (2008a) restricted analysis to individual cells, again using a subset of chromosomes, and suggested that cells that were apparently chromosomally normal were more prone to random patterns of nuclear organisation whereas those that were aneuploid had defined chromosome positions. With a 24 chromosome assay (Chapter 4) and a sufficient number of cells per embryo the association between aneuploidy and nuclear organisation in early human development may be assessed more fully, not only on a cell-by-cell basis, but also on an embryo by embryo basis.

7.2. Aims and hypotheses

Given the above rationale, the primary purpose of this chapter was to assess relative nuclear organisation for loci from all 24 chromosomes in human preimplantation embryos with a view to achieving the following specific aims:

Specific aim 5a: To assess the relative nuclear position of 24 chromosomal loci in individual blastomeres and ask whether those that are chromosomally abnormal display different patterns of nuclear organisation compared their more "normal" counterparts.

Specific aim 5b: To assess the relative nuclear position of 24 chromosomal loci and ask whether in whole embryos there is a relationship between increased chromosome abnormality and altered nuclear organisation.

Specific aim 5c: To test the hypothesis that the radial position of the chromosomal loci differs between different types of cells (specifically lymphocytes, sperm, and blastomeres).

Specific aim 5d: To test the hypothesis that human embryos adopt a "chromocentre pattern" of nuclear organisation similar to human sperm and mouse preimplantation embryos.

7.3. Results

7.3.1. Specific aim 5a: To assess the relative nuclear position of 24 chromosome loci in individual blastomeres and ask whether those that are chromosomally abnormal display different patterns of nuclear organisation compared their more "normal" counterparts

In all the previous studies examining nuclear organisation in human preimplantation embryos, blastomeres were classified as normal based on ploidy from either 5 chromosomes (13, 18, 21, X, Y) (McKenzie *et al.* 2004), 7 chromosomes (13, 16, 18, 21, 22, X, Y) (Diblik *et al.* 2007) or 8 chromosomes (13, 15, 16, 18, 21, 22, X, Y) (Finch *et al.* 2008a). In essence this is what happens at the clinical level with PGS.

The results presented in this thesis expanded upon the above, with all loci from all chromosomes examined both for ploidy and nuclear address. Nonetheless, in this study, as no single blastomere had 46/46 correct signals, the cells were divided on their "relative" levels of abnormality. In these studies therefore, 50 blastomeres were placed in the "normal" group by virtue of the fact that they had no more than 40% of the signals with apparent monosomy. Fifty is consistent with the minimum standard number used on most nuclear organisation studies; all remaining blastomeres comprised the "abnormal" group. The following graphs present the results from the analysis of nuclear organisation for each locus in the "normal" group (on the left) and the "abnormal" group (on the right). It should be noted that for every graph (n) indicates the number of nuclei analysed, average position refers to the median value (since our data set is not parametric) of the assigned shell (1-5) and p indicates results of the χ^2 test against a random distribution. All p values were considered statistically significant when $p<0.05$ (4d.f.), otherwise those $p>0.05$ were considered as Not Discernable from a Random Distribution Pattern and thus assigned the status "NDRDP." The same rules of classification of signals (depending on the shell of preference) as in Chapter 5 have been applied for all graphs presented here. Thus Peripheral – Shell 1 or 1/2, Peripheral/Medial – Shell 2 or 1-3, Medial – Shell 3, 2/3, or 3/4, Central/Medial – Shell 4 or 3-5, Central – Shell 5 or 4/5.

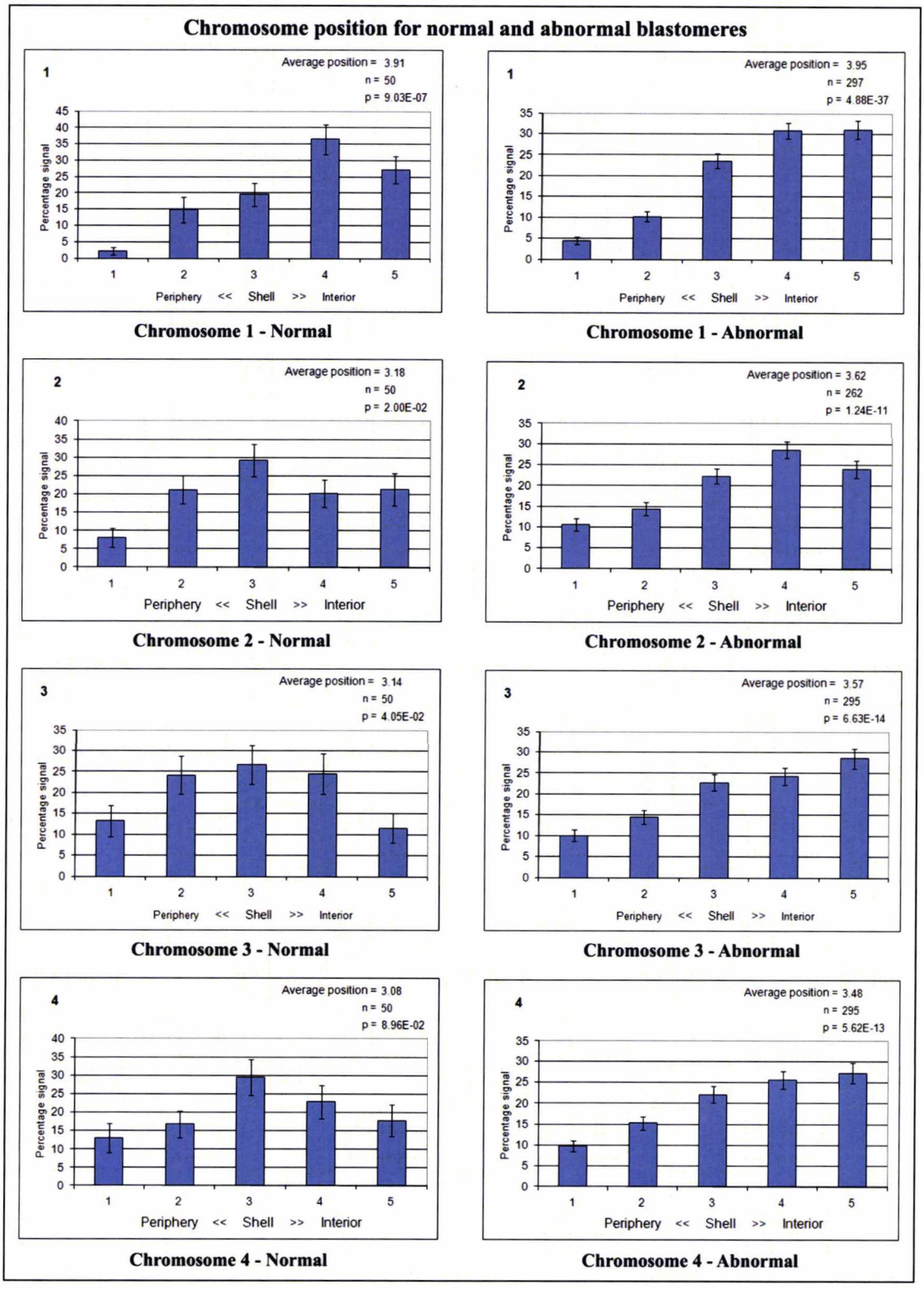

Figure 7.1: Chromosome position for loci 1, 2, 3 and 4 when analysed on a cell-by-cell basis. On the left is the "normal" blastomere group, whereas on the right is the "abnormal" group.

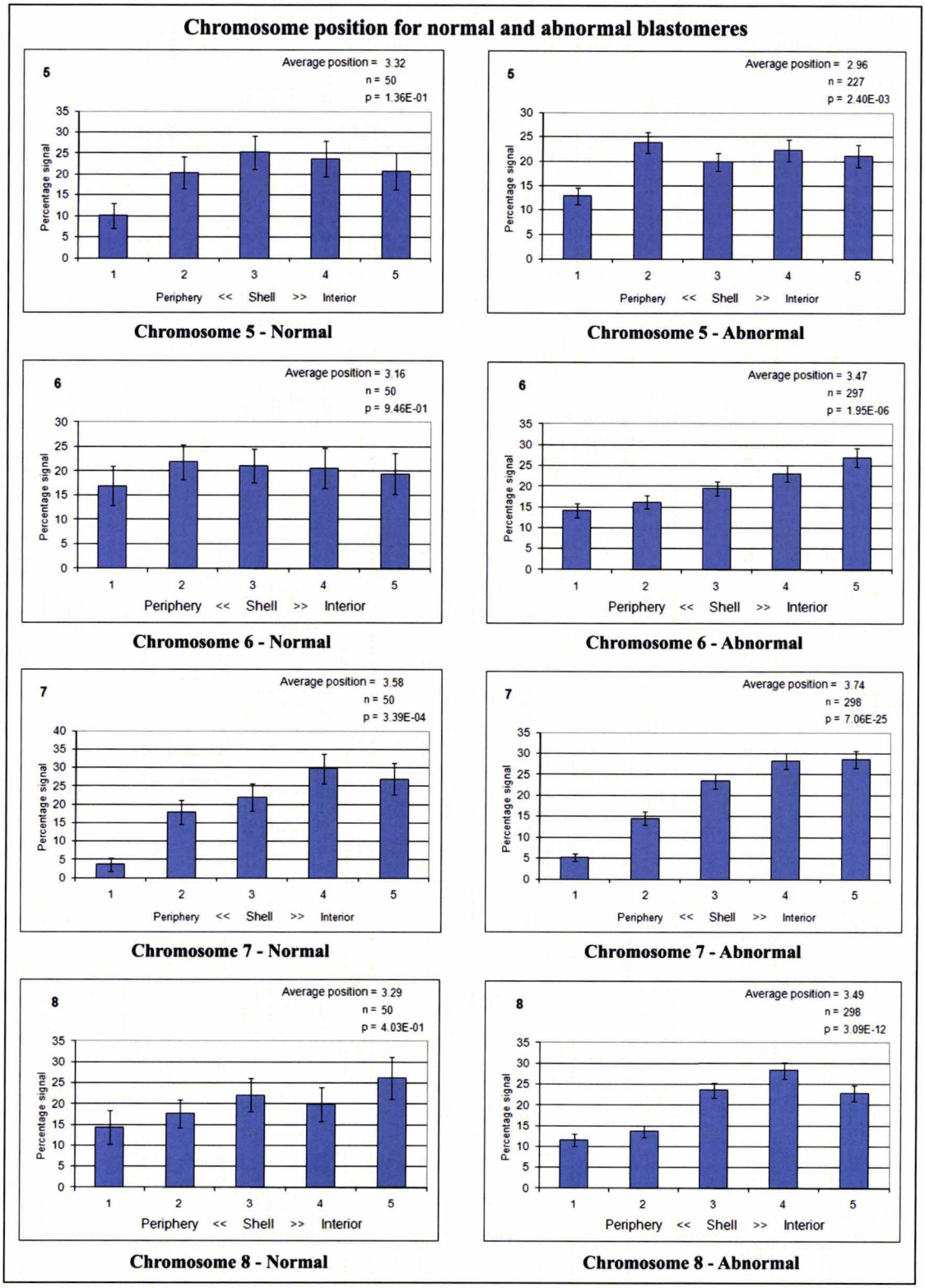

Figure 7.2: Chromosome position for loci 5, 6, 7 and 8 when analysed on a cell-by-cell basis. On the left is the "normal" blastomere group, whereas on the right is the "abnormal" group.

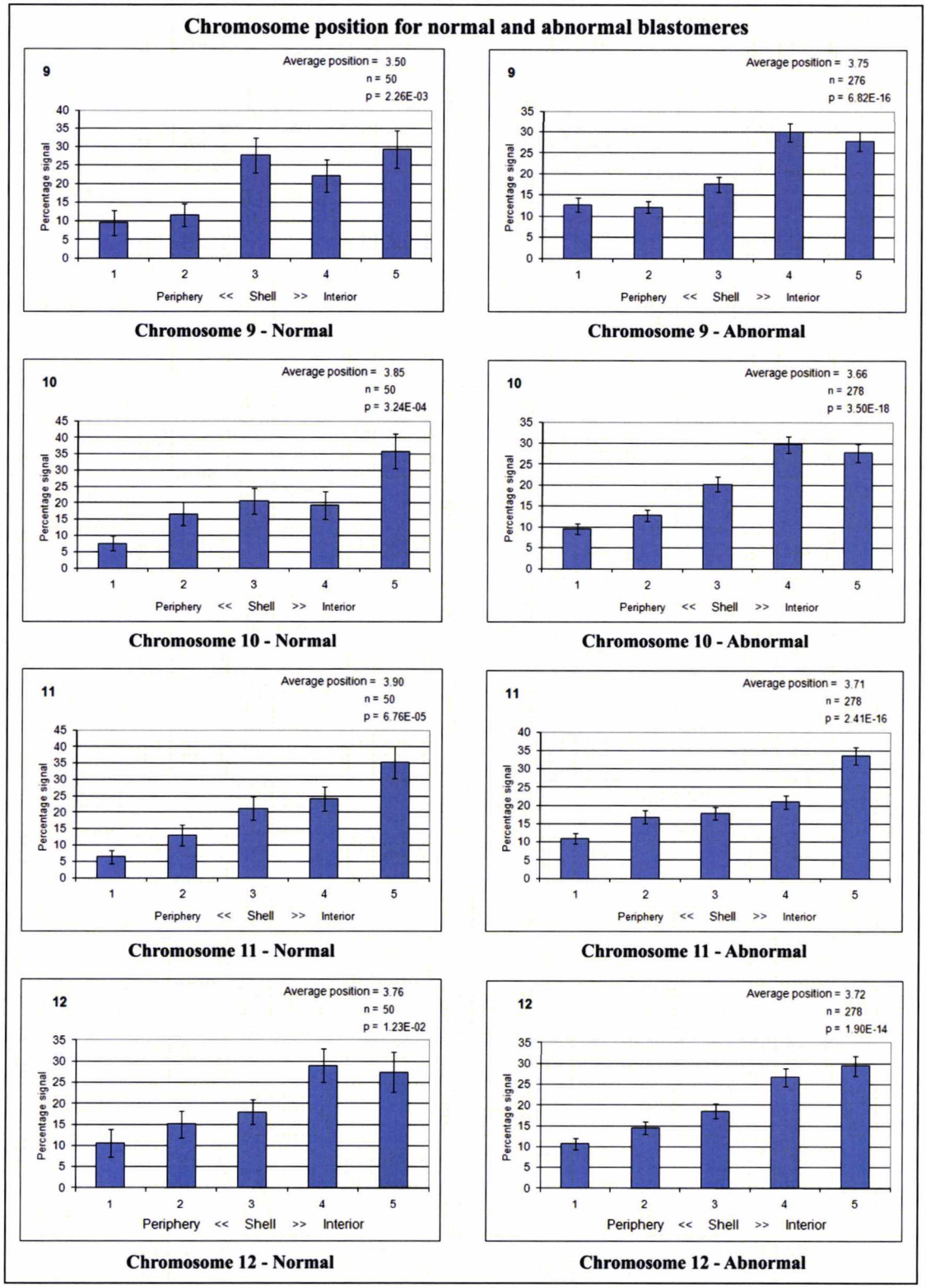

Figure 7.3: Chromosome position for loci 9, 10, 11 and 12 when analysed on a cell-by-cell basis. On the left is the "normal" blastomere group, whereas on the right is the "abnormal" group.

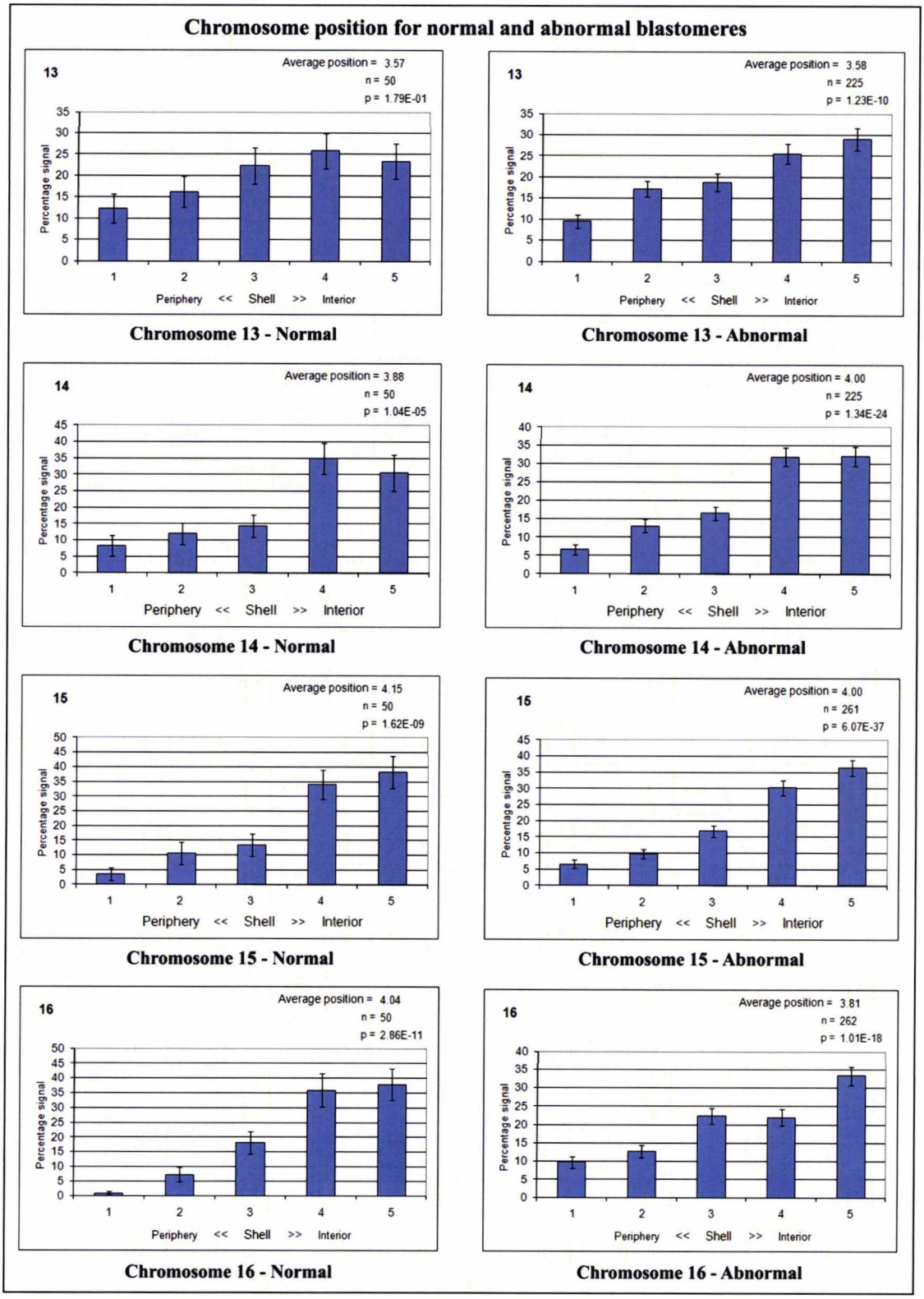

Figure 7.4: Chromosome position for loci 13, 14, 15 and 16 when analysed on a cell-by-cell basis. On the left is the "normal" blastomere group, whereas on the right is the "abnormal" group.

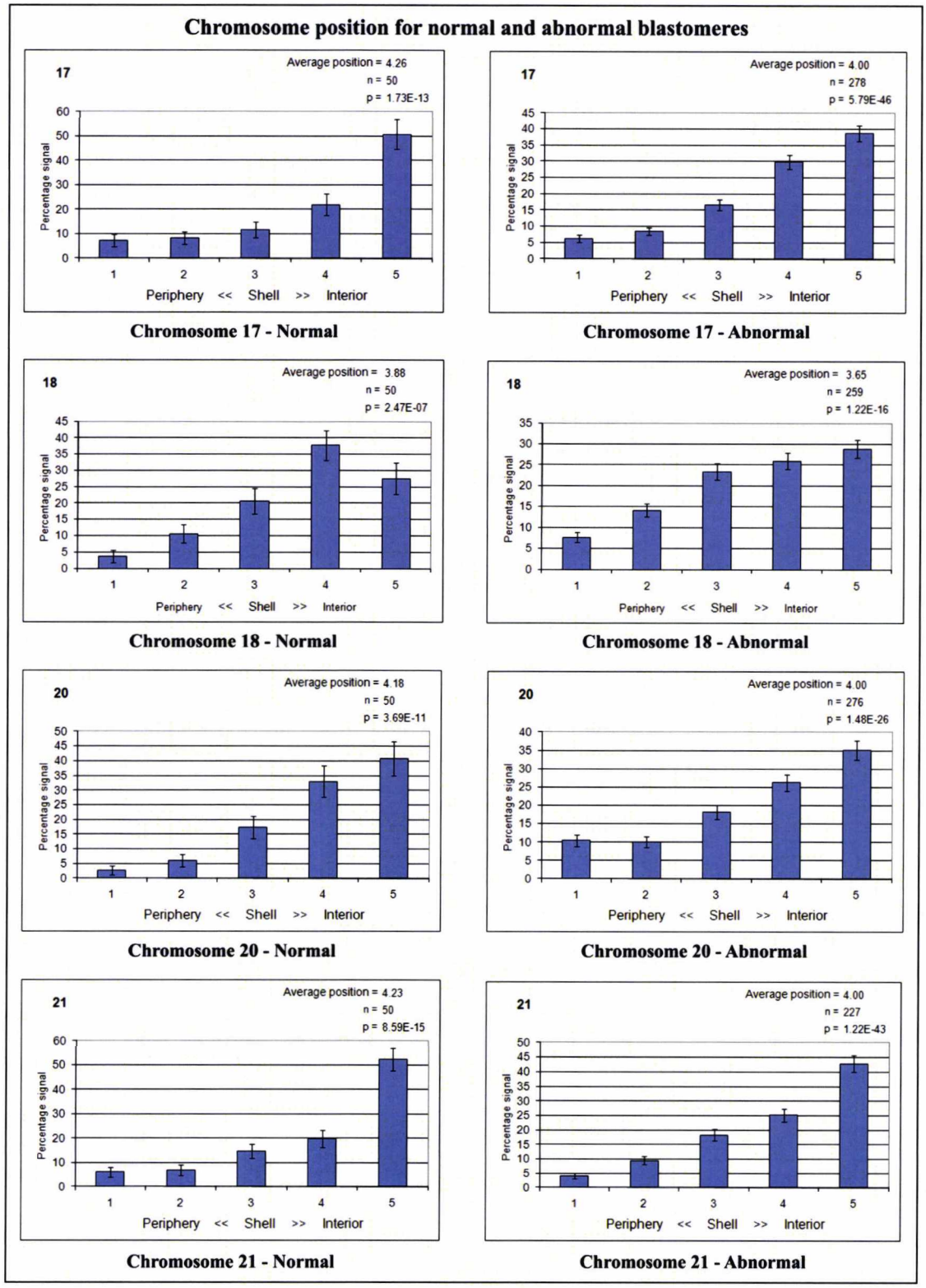

Figure 7.5: Chromosome position for loci 17, 18, 20 and 21 when analysed on a cell-by-cell basis. On the left is the "normal" blastomere group, whereas on the right is the "abnormal" group. Locus 19 has been removed from this analysis due to a small number of cells.

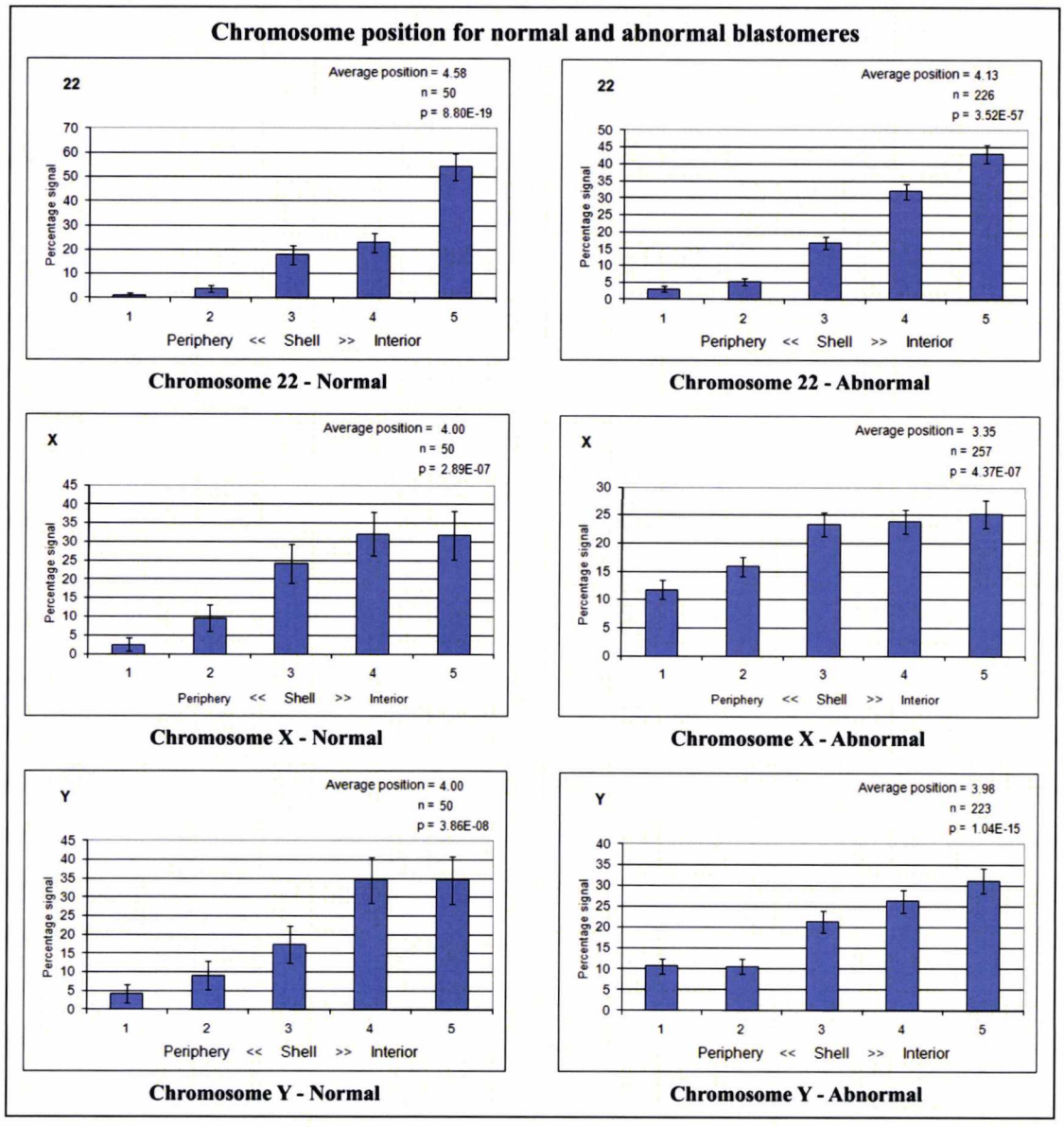

Figure 7.6: Chromosome position for loci 22, X, and Y when analysed on a cell-by-cell basis. On the left is the "normal" blastomere group, whereas on the right is the "abnormal" group.

The following table summarises the results from the cell-by-cell analysis done on blastomeres from the 17 whole embryos.

Classification of locus	Chromosome	"Normal"	Abnormal
Sex chromosome	X	Central	Central/Medial
	Y	Central	Central
Centromeric	1	Central/Medial	Central
	2	Medial	Central
	3	Medial	Central
	4	NDRDP	Central
	6	NDRDP	Central
	7	Central	Central
	8	NDRDP	Central/Medial
	9	Central/Medial	Central
	10	Central	Central
	11	Central	Central
	12	Central	Central
	15	Central	Central
	16	Central	Central
	17	Central	Central
	18	Central/Medial	Central
	20	Central	Central
Non-centromeric	22	Central	Central
	21	Central	Central
	19	NDRDP*	NDRDP*
	14	Central	Central
	5	NDRDP	Peripheral/Medial
	13	NDRDP	Central

Table 7.1: Comparison of the radial position for all loci (except 19) based on the cell-by-cell classification of blastomeres to "normal" and abnormal. Note: NDRDP: not discernable from a random distribution pattern. *Too few cells were analysed for chromosome 19 to reach statistical significance.

One conclusion from this data is that the "NDRDP" designation occurred more commonly in the "normal" group (i.e. for the probes for chromosomes 4, 5, 6, 8 and 13) whereas this was not seen for any locus in the abnormal group. Moreover there was clear evidence of a deviation from the mostly central positions occupied by the probes in the "abnormal" group with the loci occupying more medial positions for chromosomes 1, 2, 3, 9 and 18. This would suggest that the nuclear organisation is more "relaxed" in nuclei that are relatively chromosomally normal.

7.3.2. Specific aim 5b: To assess the relative position of 24 chromosome loci and ask in whole embryos whether there is a relationship between increased chromosome abnormality and altered nuclear organisation

As seen in section 6.3.2 all of the embryos assessed appeared to be chromosomally abnormal and mosaic. In order to classify them into roughly equally sized groups of relatively "normal" and "abnormal" embryos (i.e. with similar numbers of blastomeres), for the purposes of this thesis, the proportion of chromosome pairs with the normal diploid number was expressed as a proportion of the total. That is, "100%" would indicate that all cells had 24/24 chromosome pairs with the normal diploid number in all cells; "0%" would indicate no cells with a normal chromosome number for any chromosome. By this classification the embryos were grouped in to those with >50% (the "normal" group) and those with <50% (the "abnormal" group) (Table 7.2). The relative position was investigated for the 17 embryos (Table 7.2) and graphs for all the chromosomes (per classification category) are presented in Figures 7.7 to 7.12.

Embryo ID	Proportion of chromosome pairs normal diploid	Designation
2	39.89	Abnormal
3	21.43	Abnormal
4	55.33	"Normal"
6	66.67	"Normal"
7	76.21	"Normal"
8	51.59	"Normal"
9	52.38	"Normal"
12	53.97	"Normal"
14	42.86	Abnormal
15	60.41	"Normal"
16	70.69	"Normal"
17	47.62	Abnormal
19	35.49	Abnormal
20**	39.67	Abnormal
21**	56.06	"Normal"
24**	26.85	Abnormal
25**	40.67	Abnormal

Table 7.2: Classification of whole embryos according to aforementioned criteria ("normal" and abnormal). Note: Chromosome 19 was included (in determining "normal" and abnormal embryos) for embryos 20, 21, 24, 25 (**), since there were sufficient cells with results.

Using the above criteria, nine whole embryos were classified in the normal category and eight in the abnormal. It should be noted that during each hybridisation layer every effort was made to diagnose all cells, however this was not always possible, due

to embryo fixation problems (e.g. debris) or microscopy issues (e.g. fluorescent debris).

The following Figures (7.7-7.12) present the results for each chromosome in the "normal" (>50%) and abnormal (<50%) category for whole embryos. As stated previously, in every graph (n) indicates the number of nuclei analysed, average position refers to the median value (since our data set is not parametric) and p indicates results of the χ^2 test against a random distribution. All p values were considered statistically significant when $p<0.05$ (4d.f.), otherwise ($p>0.05$) were considered as Not Discernable from a Random Distribution Pattern (NDRDP).

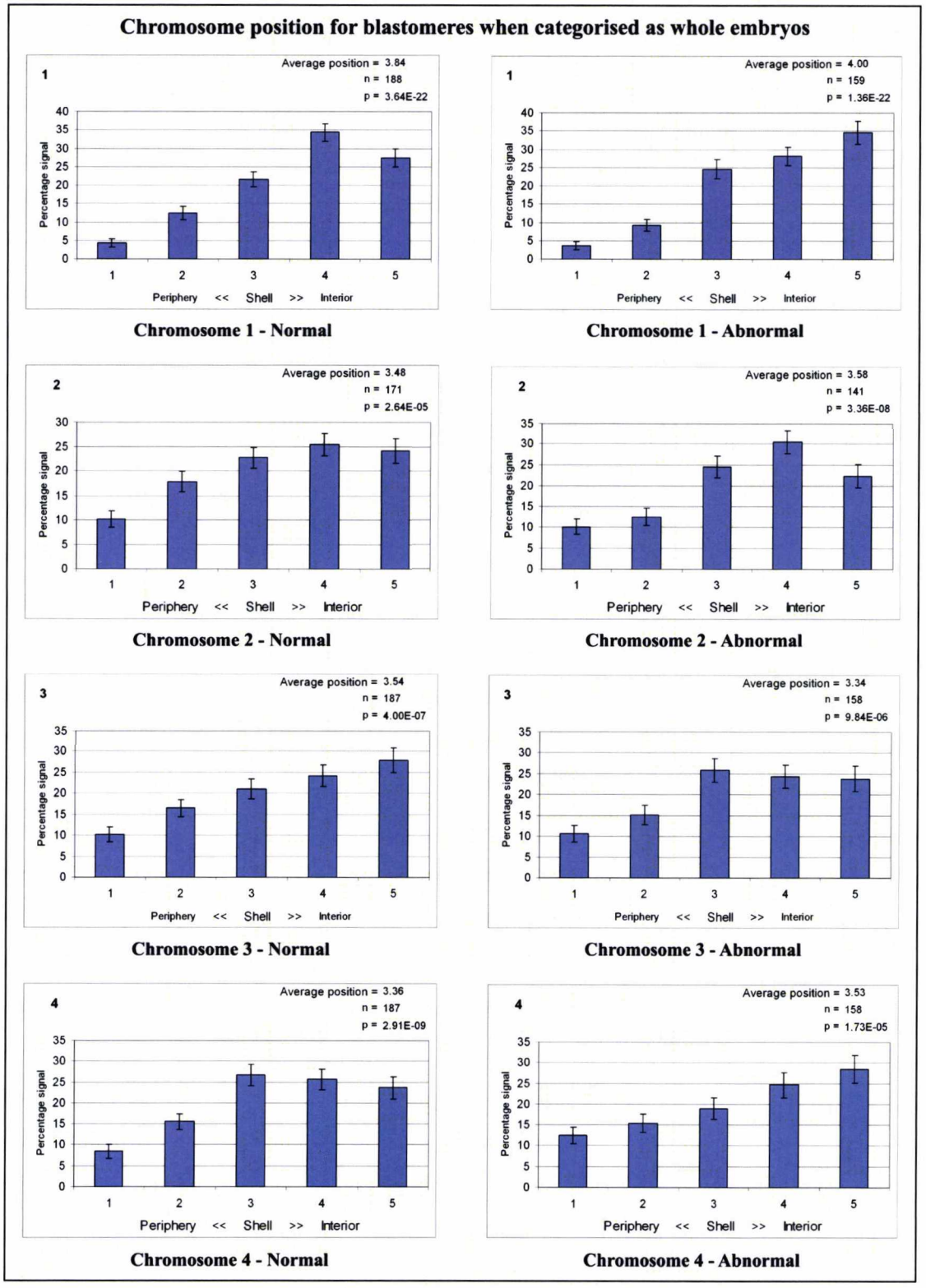

Figure 7.7: Chromosome position for loci 1, 2, 3 and 4 when analysed on a whole embryo basis. On the left are the "normal" (>50%) whole embryos, whereas on the right are the "abnormal" (<50%) whole embryos.

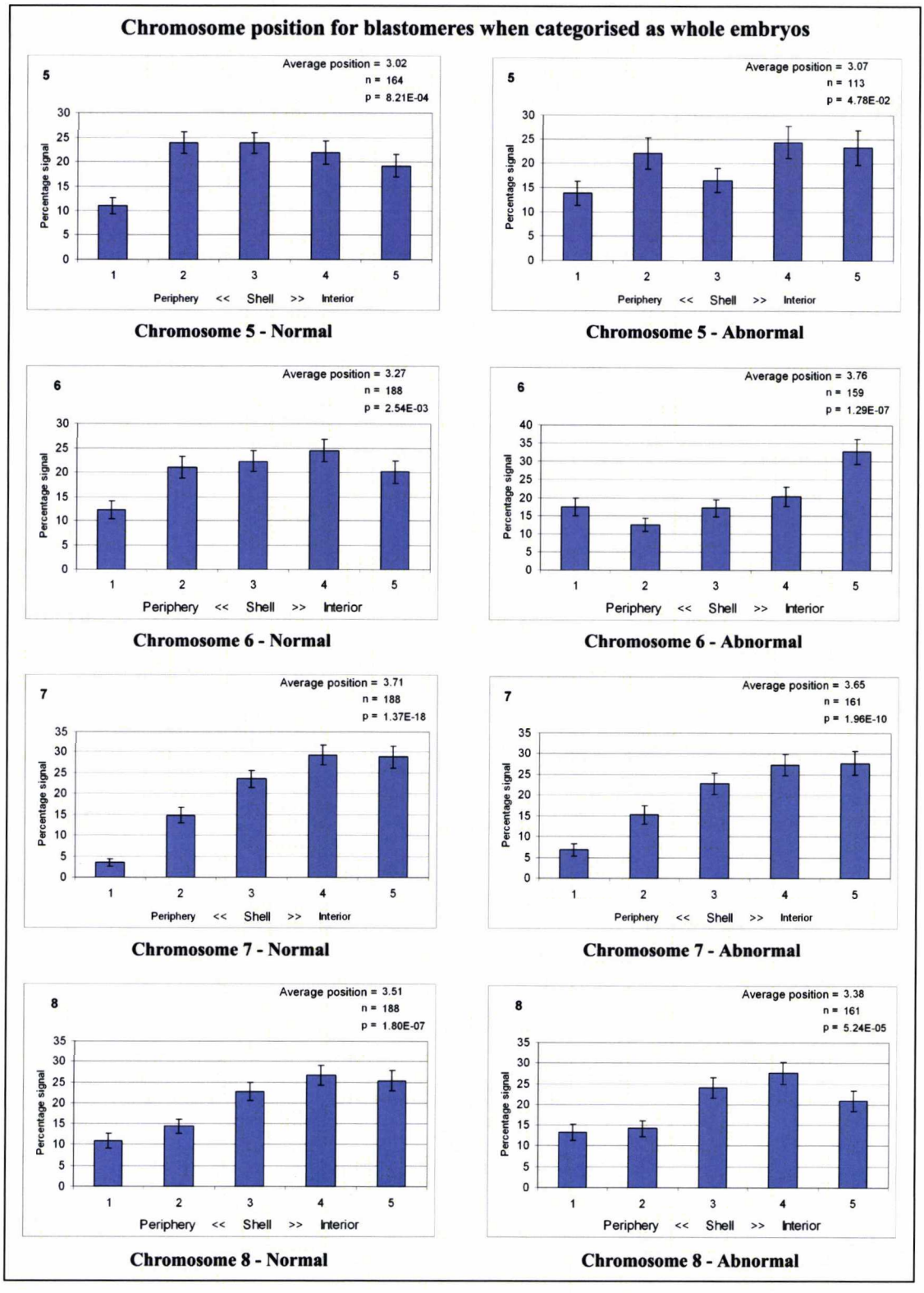

Figure 7.8: Chromosome position for loci 5, 6, 7 and 8 when analysed on a whole embryo basis. On the left are the "normal" (>50%) whole embryos, whereas on the right are the "abnormal" (<50%) whole embryos.

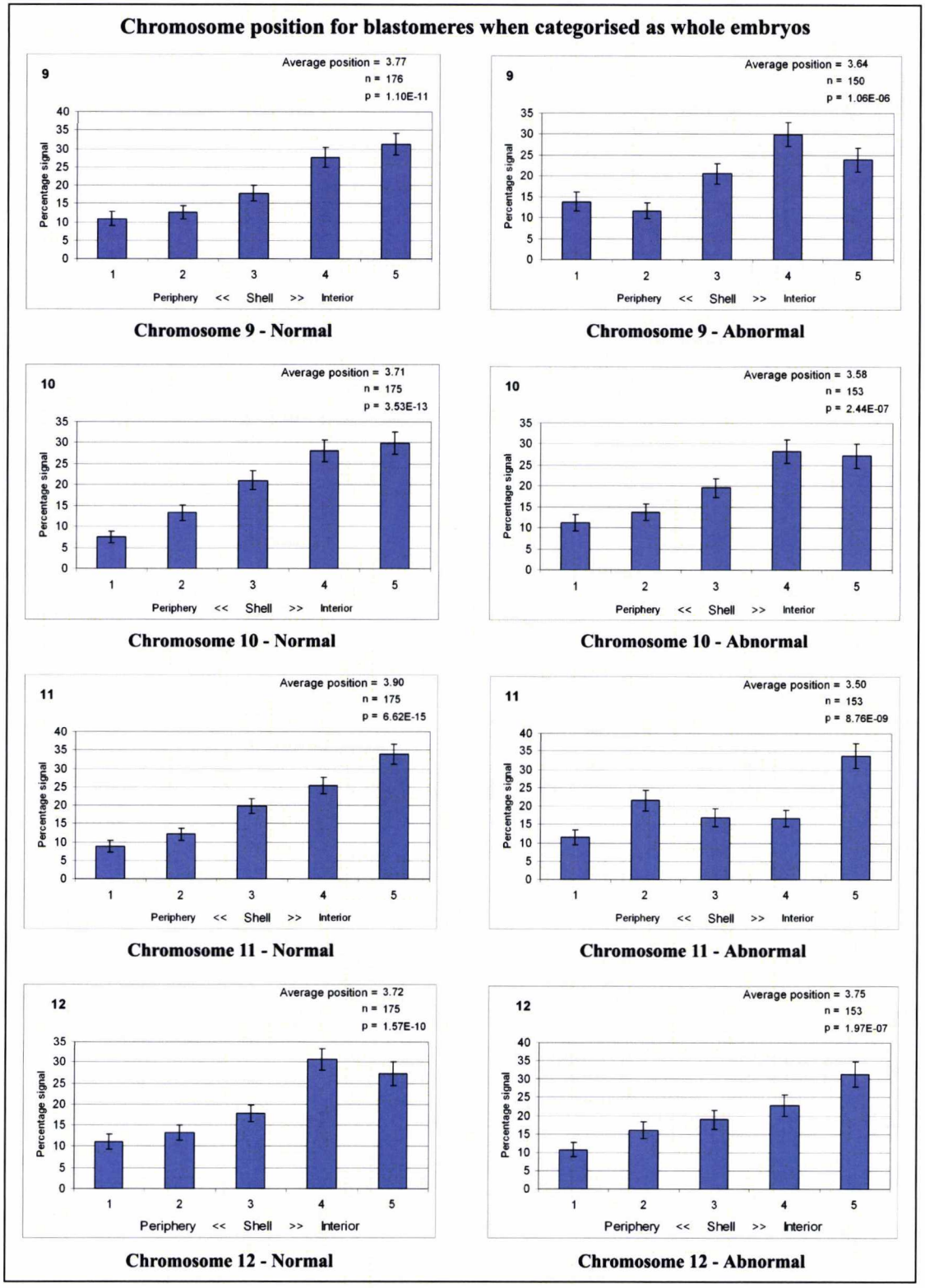

Figure 7.9: Chromosome position for loci 9, 10, 11 and 12 when analysed on a whole embryo basis. On the left are the "normal" (>50%) whole embryos, whereas on the right are the "abnormal" (<50%) whole embryos.

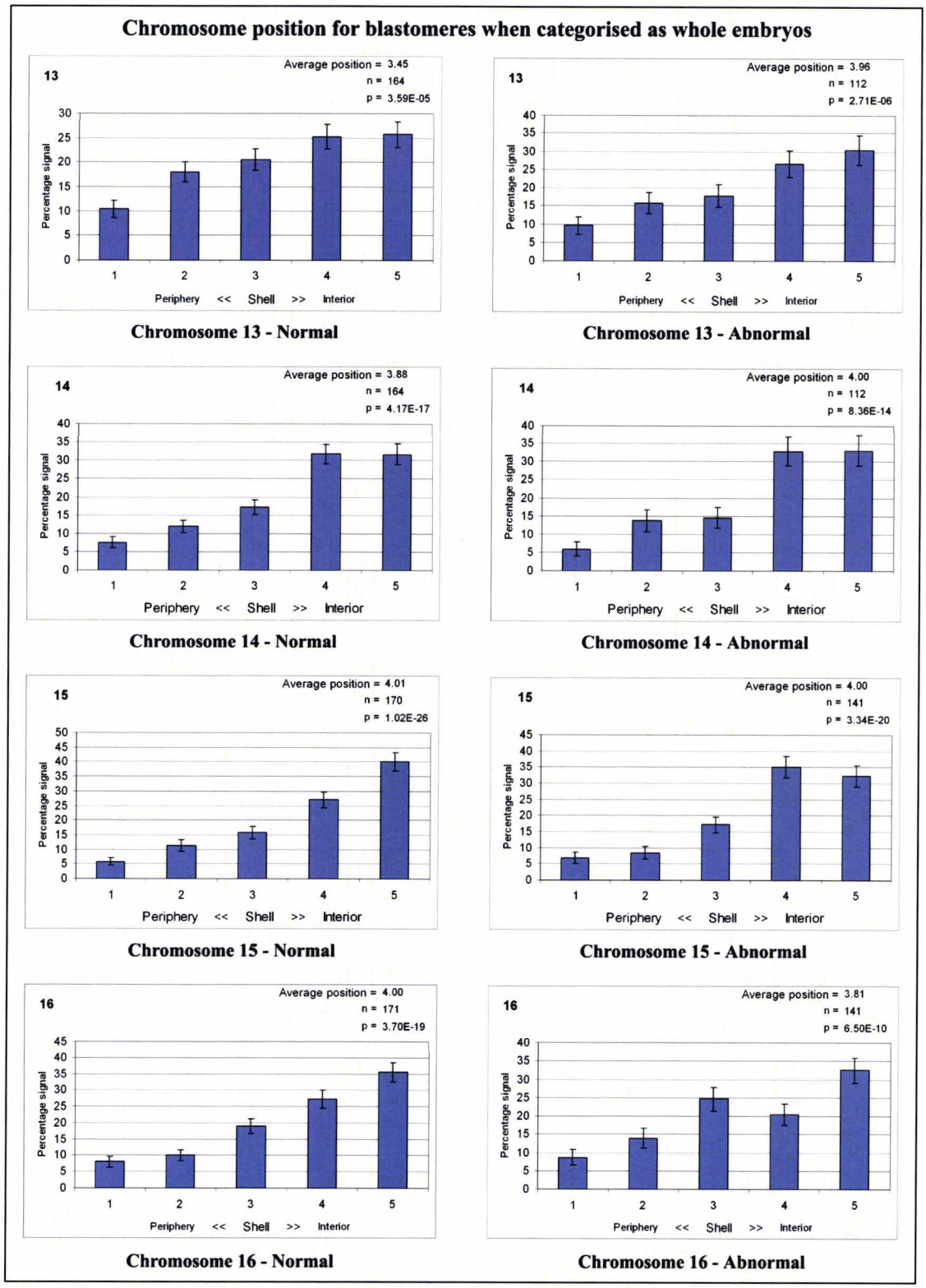

Figure 7.10: Chromosome position for loci 13, 14, 15 and 16 when analysed on a whole embryo basis. On the left are the "normal" (>50%) whole embryos, whereas on the right are the "abnormal" (<50%) whole embryos.

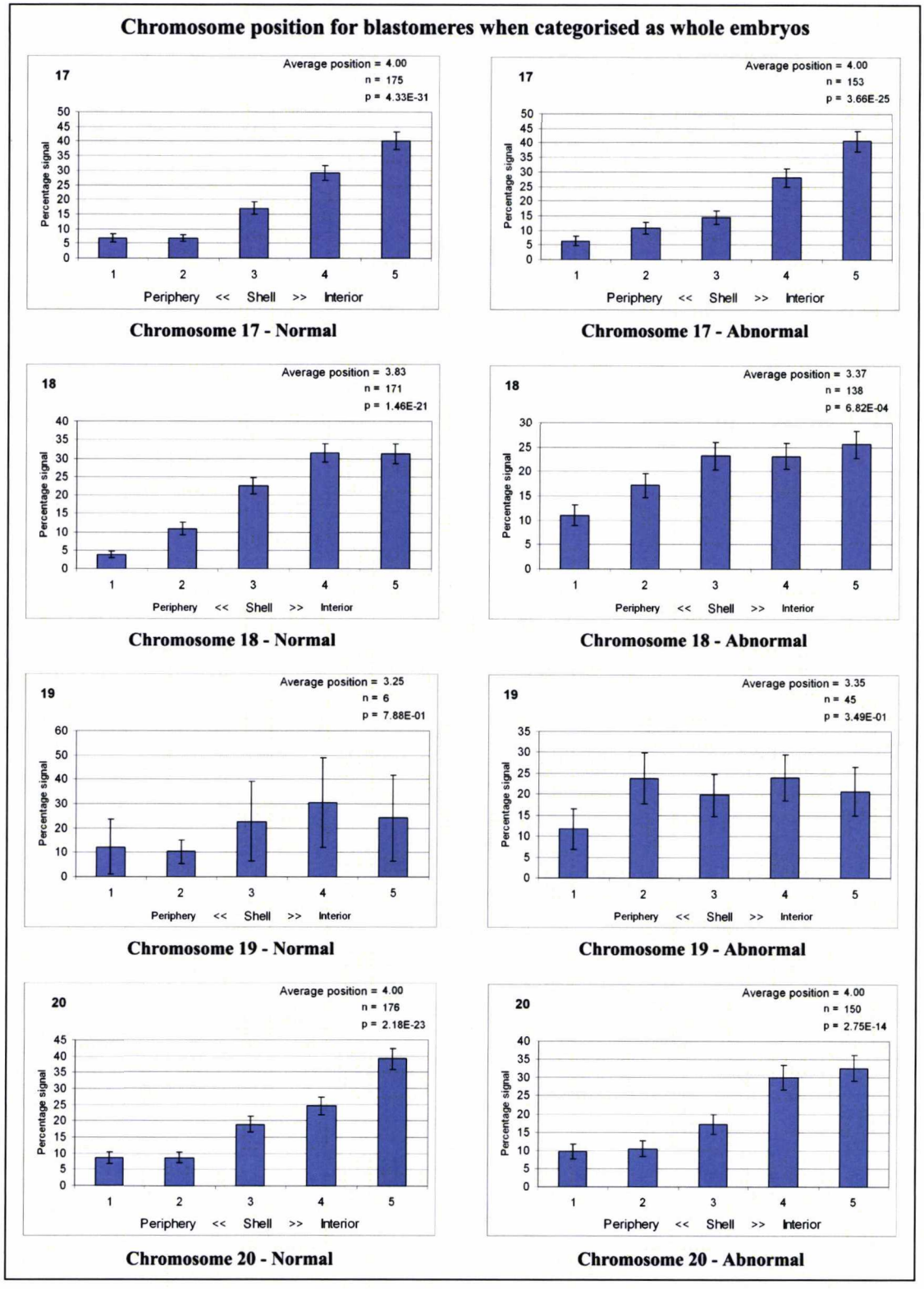

Figure 7.11: Chromosome position for loci 17, 18, 19 and 20 when analysed on a whole embryo basis. On the left are the "normal" (>50%) whole embryos, whereas on the right are the "abnormal" (<50%) whole embryos.

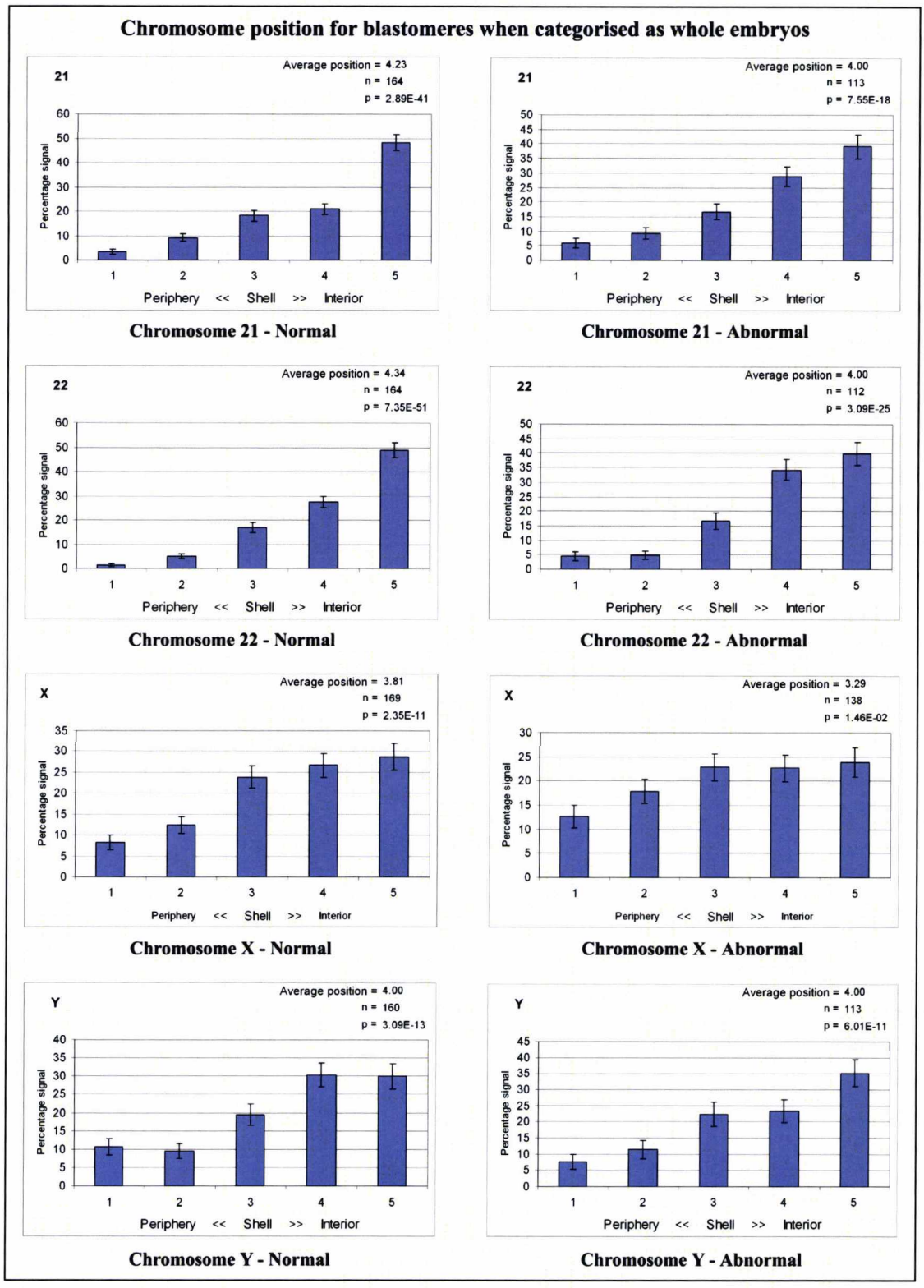

Figure 7.12: Chromosome position for loci 21, 22, X and Y when analysed on a whole embryo basis. On the left are the "normal" (>50%) whole embryos, whereas on the right are the "abnormal" (<50%) whole embryos.

When results are summarised from Figures 7.7-7.12, then the radial position for each locus is as presented in Table 7.3.

Classification of locus	Chromosome	"Normal" embryos	Abnormal embryos
Sex chromosome	X	Central/Medial	Central/Medial
	Y	Central	Central
Centromeric	1	Central/Medial	Central
	2	Central/Medial	Central/Medial
	3	Central	Central/Medial
	4	Central/Medial	Central
	6	Peripheral/Medial	Central
	7	Central	Central/Medial
	8	Central/Medial	Medial
	9	Central	Central/Medial
	10	Central	Central/Medial
	11	Central	Central
	12	Central	Central
	15	Central	Central
	16	Central	Central
	17	Central	Central
	18	Central	Central/Medial
	20	Central	Central/Medial
Non-centromeric	22	Central	Central
	21	Central	Central
	19	NDRDP	NDRDP
	14	Central	Central
	5	Peripheral/Medial	Bimodal
	13	Central	Central

Table 7.3: Comparison of the radial position for all loci based on whole embryo classification. Note: NDRDP refers to not discernable from random distribution pattern.

The results suggest that, in both categories of embryos, loci occupy distinct positions within the nucleus (with the exception of the chromosome 19 locus for which there were too few cells). Differences between the groups are however subtle, with a central/medial position in the "normal" group but a central one on the "abnormal" group (chromosomes 1 and 4) or *vice versa* (chromosomes 3, 7, 9, 10, 18, 20). Other, slightly more marked differences include chromosomes 5, 6, and 8.

7.3.3. Specific aim 5c: To test the hypothesis that the radial position of the chromosomal loci differs between different types of cells (specifically lymphocytes, sperm, and blastomeres)

In the current study, nuclear organisation was investigated primarily in lymphocytes, in sperm from normal and patients with OAT (Chapter 5), and human preimplantation embryos (this chapter). In the control lymphocytes (from a karyotypically normal male) the position of the loci was recorded by capturing 103 cells per chromosome. In addition position for the sex chromosomes was recorded from a karyotypically normal female. Table 7.4 summarises the radial position results from the different cell types.

Loci	Lymphocytes	Sperm (normal males)	Sperm (OAT males)	Blastomeres (pooled)
X	NDRDP	Central	Central	Central/Medial
Y	NDRDP	Central	Central	Central
1	NDRDP	Central	Central	Central
2	Central	Central	Central	Central/Medial
3	NDRDP	Central	Central/Medial	Central/Medial
4	NDRDP	Central	Central/Medial	Central/Medial
6	NDRDP	Central/Medial	Central/Medial	Central
7	NDRDP	Central	Central	Central
8	Peripheral	Central/Medial	Central	Central/Medial
9	Central	Central	Central	Central
10	Peripheral	Central	Central	Central
11	45% central vs. 25% peripheral	Central	Central	Central
12	NDRDP	Central	Central/Medial	Central
15	Central	Central	Central	Central
16	Central	Central	Central	Central
17	Central	Central	Central	Central
18	NDRDP	Central	Central	Central
20	Central	Central	Central	Central
22	Central	Central	Central	Central
21	Central	Central/Medial	Central/Medial	Central
19	Central	Central	Central	NDRDP
14	Central	Central	Central	Central
5	NDRDP	Central/Medial	Medial	Peripheral/Medial
13	Central/Medial	Central/Medial	Central/Medial	Central

Table 7.4: Comparison of radial positions in all different cell types. The position results for X is the sum of positions for X from XY and XX lymphocytes, whereas the position results for Y are only from the XY cells. It should be noted that graphs with total radial position for the different cell types are presented in the Digital Appendix B.

Comparing the position between the different cell types observations suggest that sperm and blastomeres (or whole embryos) seem to have a clear pattern of nuclear

organisation, as depicted by the fact that all loci occupy distinct positions that are, by and large, central. This is in contrast with the more random pattern seen in lymphocytes.

7.3.4. Specific aim 5d: To test the hypothesis that human embryos adopt a "chromocentre pattern" of nuclear organisation similar to human sperm and mouse preimplantation embryos

Furthermore most centromeric loci adopt a central position in human blastomeres (pooled results). With regard to the autosomal locus specific probes, one of the furthest away from the centromere (locus 5) adopts a medial position in blastomeres (remaining loci are central) suggesting the presence of a chromocentre in human embryos similar to mouse embryos.

7.4. Concluding remarks

In this chapter, the nuclear address for loci from all chromosomes was assessed by classifying whole embryos, and on a cell-by-cell basis. It seems that the nuclear organisation in blastomeres is more akin to that of sperm than lymphocytes and that differences in nuclear address are more apparent when blastomeres are compared on a cell-by-cell, rather than an embryo-by-embryo basis.

8. Discussion

Overall, this thesis was successful in the fulfilment of proposed aims, by providing insight into the use of novel inorganic fluorochromes for FISH applications, developing a FISH based 24 chromosome screen with multiple uses both research and potentially clinical and, for the first time, expanding into the entire karyotype nuclear organisation studies in sperm and human preimplantation embryos. More specifically:

- A thorough investigation into the use of quantum dots for FISH applications revealed, by exploiting many different strategies (both indirect and direct labelling), that QDs are not in their current state at an optimum for use in FISH.

- As a result of the appraisal of QDs, novel strategies were developed using fast hybridising oligonucleotide probes labelled with *organic* fluorochromes. A 24 chromosome interphase cytogenetics assay was developed in a four layer sequential experiment. This assay was designed for general use but, for the purposes of this thesis, in determining chromosome copy number and nuclear address in the interphase nuclei of human sperm and embryos.

- Nuclear organisation for every human chromosome was investigated in the nuclei of sperm from men with normal semen parameters and compared with nuclei from men with impaired semen parameters (OAT). Results suggest that, while not a widespread phenomenon, there is a tendency to alteration in nuclear organisation for certain chromosomes, in certain infertile men. By contrast, the nuclear organisation was consistent and ordered in control males suggesting that, for certain men, altered nuclear organisation may be a factor associated with reduction in fertility.

- The level of aneuploidy was assessed in whole embryos not required for transfer following PGS. Results suggested very high levels of abnormality mostly associated with mosaicism, further calling into question the efficacy of FISH for PGS.

- Nuclear organisation of each human chromosome in the interphase nuclei of human preimplantation embryos was investigated with regard to its relationship with increased aneuploidy. Differences between two groups, one with multiple abnormalities, the other with relatively fewer abnormalities, were revealed. This study provides some of the first evidence regarding the nuclear organisation of individual blastomeres as well as whole embryos.

8.1. Specific aim 1: To investigate whether inorganic nanomaterials (quantum dots – QDs) can be used in place of organic fluorochromes with a view to multiplex experiments

8.1.1. Optical properties of QDs; from theory to practise

During the course of the experiments, certain properties of QDs were immediately apparent. When experiments were successful, signals were brighter (by visual inspection) than the Cy3 counterparts and resistant to photo-decay as was seen by exposing the signals to UV light. However a perplexing issue was that the emission spectra of the QDs appeared to be not as narrow as the manufacturers claimed, since "bleed-through" between channels was observed, despite making use of narrow band-pass filters. Apparently this phenomenon is not as uncommon as the literature might suggest (Bentolila, L *pers. comm.*) and could be a batch variable. Controlling the size of the core during synthesis (that will tune the colour that the QD will emit) requires high technical skills and sometimes nanoparticles are larger than expected. Addressing the QD size control is important in particular for multicolour detection or imaging and could hold the key to the success of multicolour experiments in QD-FISH. Moreover abnormalities in their shape (failure of quality control) could result in the same effect (Bentolila, L *pers. comm.*). An additional possible explanation for this emission bleed-through to other channels was that QDs were not monodisperse (or the batches used were not), in other words different sized-QDs existed in the same solution mix. Simple "spotting" experiments confirmed this. Figure 8.1 shows a QD605-conjugate dissolved in hybridisation mix where different QD populations could be observed under the different band pass filters.

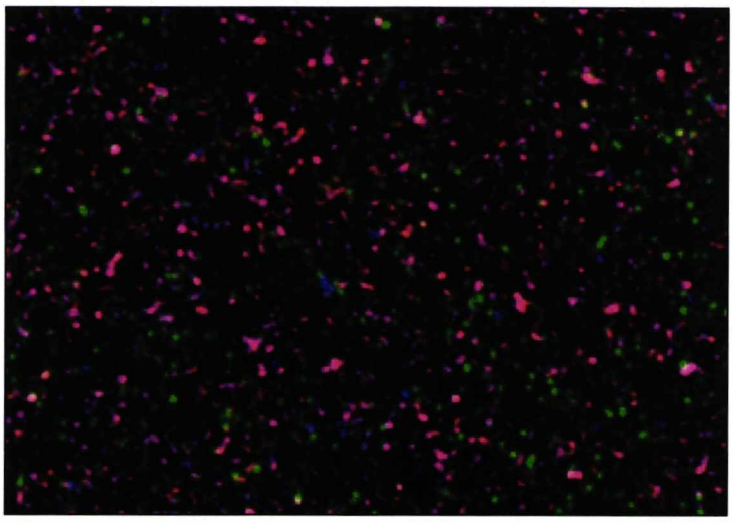

Figure 8.1: QD605 dissolved in hybridisation mix and viewed directly under the microscope using four barrier filters: 525 nm (blue), 565 nm (green), 585 nm (red) and 605 nm (far red but pseudo-coloured purple for the purposes of this figure). The image represents a merge of all four filters. The QDs are predominantly purple (as would be expected), but a smaller number of green, blue and red QDs are seen. The discrete appearance of QDs of one or other of the colours indicates there is a mixed population of QDs. Adapted from (Ioannou *et al.* 2009).

The different colours seen in the figure above represent different size QDs that emit at longer (towards the red – large QDs) or shorter (towards the blue – small QDs) wavelengths. These findings are consistent with those of Bawendi and colleagues who have tried to address monodispersity of QD preparations (Murray *et al.* 2000). All these technical features that were attributed to the chemical synthesis of the QDs maybe require more experimental attention in order to improve QD synthesis. Of course we cannot rule out the possibility that bleed-through and monodispersity are batch-specific problems, we did not, after all, test more than 3 or 4 batches for each QD. However I saw no evidence of batch-specific variance; future similar experiments similar to these on a larger number of batches would address this issue.

A further QD feature that I observed was "blinking"; a phenomenon unknown in conventional FISH where the QD alternates between an emitting (on) and non-emitting (off) state (Michler *et al.* 2000; Pinaud *et al.* 2006). Blinking has been explained according to an Auger ionisation model (Efros & Rosen 1997) and affects single molecule detection applications by saturation of the signal. It may however be suppressed by using thiol groups to passivate the QD surface (Hohng & Ha 2004; Bentolila & Weiss 2006). A second phenomenon, photobrightening, where the fluorescence intensity increases rapidly at the first stage of illumination and then

stabilises, can impose a limit on quantitative studies (Gerion *et al.* 2001). Both of these properties are associated with mobile charges on the surface of the QDs (Fu *et al.* 2005). It is also noteworthy that, although preparations often displayed blinking, they could go to an irreversible photo-darkened state without easy explanation. The latter statement was mostly observed in the direct conjugation attempts of QDs with DNA.

8.1.2. The message for QD-FISH

The message from the comprehensive appraisal of the utility of QDs for FISH has been that, in their current form, QDs are not suitable material for FISH applications. Further evidence can be found in the fact that traditional fluorochromes have not, for any application, been replaced by QDs, despite the great potential of the latter. The number of peer-reviewed studies pertaining to QD-FISH remains few and I am unaware of any company marketing QD labelled FISH probes. Based on the experience gained from the use of QDs (in both indirect and direct experiments) and following discussions with colleagues from other interested groups, lack of reproducibility appears to be a distinguishing feature of QD-FISH in contrast to the more robust applications with organic fluorophores-streptavidin conjugates. Although I would not claim that every possible avenue with respect to QD-FISH has been explored; parallel QD based experiments (mostly in avian and human cells) paints a general picture of a non-reproducible approach when QDs are used in place of organic fluorochromes.

The unreliable nature of QDs (at least for FISH) is perhaps not totally unexpected as other colleagues have had similar experiences to my own (Bruchez 2007; Muller *et al.* 2009). There is clearly a challenging set of conditions with regard to intracellular delivery of QDs and, since there are no reliable FISH protocols for this, individual adaptations need empirical establishment (Resch-Genger *et al.* 2008). If this were achieved then the reliability may well improve and the benefits of QDs observed in this and other studies (e.g. increased brightness, resistance to photo-bleaching) may be properly realised.

Taking all the above into account it is possible to speculate about reasons for the lack of reproducibility of QD-FISH results. Clues about QD size and chemistry during

synthesis may be a starting point: QDs vary in size (this is the basis of the fluorescent colour that they emit) from 2 to 10 nm. A Cy3 molecule on the other hand is <2 nm in size (Bailey *et al.* 2004). This may explain in part why my successful FISH experiments gave the impression of larger fluorescent particles and why there was a greater degree of background for most experiments. It might also explain an observed fluorescent 'sheath' effect seen on some metaphases (Ioannou *et al.* 2009) and why certain preparations gave bright signals in decondensed interphase nuclei, but not in highly coiled metaphase chromosomes. That is, steric hindrance may have led to signals being brighter in areas where the chromatin is less compact (e.g. at the edge of the chromosomes and/or in the interphase nucleus), indeed steric hindrance has been an issue reported in many studies (Bentolila & Weiss 2006; Muller *et al.* 2006; Ma *et al.* 2008; Choi *et al.* 2009). If this were true, I might have expected to see an improvement when the ratio of labelled to unlabelled dUTPs was used and/or when I made use of a "longer arm" biotin dUTP. This was not the case. Again however a general background of intermittent success may have masked any appreciable difference seen in any given experiment. Furthermore as QD-streptavidin conjugates were used throughout these experiments it is worth pointing out that it is not entirely clear how streptavidin binds on the actual polymer site of the QD. For this reason the number of free streptavidin sites varies per individual QD (10 to 15). Incidentally, these sites can break off from the nanoparticle (for no reported reason) rendering the probe unstable or even detached, with immediate effect on the hybridisation signal (Bentolila, L *pers. comm.*). I am also informed that QD streptavidin conjugates can easily degrade (a batch-specific attribute) and this can be due to barely discernable temperature changes during storage. Additionally I am given to understand that QDs are prone to adhere to tubes sides and tips (Chan, P *pers. comm.*). My attempts to reduce this problem using siliconised tubes and regular sonication met with a degree of success however did not eliminate the technical issues completely.

8.1.3. Success of other labs using QDs and the future

A possible reason to explain the positive results arising from groups that have published in this area (Xiao & Barker 2004a; Bentolila & Weiss 2006; Ma *et al.* 2008) is that their labs were equipped with the ability to synthesise and batch-test their own conjugates (a luxury not afforded to most groups) and were not dependent on commercial suppliers. Ma *et al.* (2008) suggested that the QDs that they used were

significantly smaller than those available commercially and may thus have reduced steric hindrance and increased hybridisation ability. Several laboratories (Xiao & Barker 2004a; Bentolila & Weiss 2006; Ma *et al.* 2008) have however generated QD-oligonucleotides conjugates and report that, during the time of annealing, steric hindrance has little effect but it may limit the QDs access to the target at the time of detection (Bentolila & Weiss 2006; Ma *et al.* 2008). This may provide a possible explanation for my lack of success in generating usable conjugates. Furthermore negative hybridisation was potentially caused by unbound QD left over after the incubation between QD and DNA (to generate a conjugant) that prevented the complex to enter cells and hybridise (acted as a competitor). Excess cytoplasm around the chromosomes cannot solely be blamed as pepsin treatments were introduced to reduce it.

Taking all of the above into consideration, the future of QD-FISH requires further research and interaction within the interested groups. Advances in nanomaterial synthesis (regarding uniformity and size control) and solubility will assist conjugation to biomolecules. Yao *et al.* (2006) described a new generation of nanocrystals called "FloDots". These are dye-doped silica nanoparticles that possess all QD optical properties but, due to the silica matrix that encompassed the dots, it is easier to make them water soluble and, according to the authors, the silica surface could be modified to contain functional groups for bio-conjugation. In addition, a study by Choi *et al.* (2007) introduces a novel class of nanocrystals, "C-dots" that could be 2-3 times brighter than QDs, less toxic and an ideal material for *in vivo* applications and cancer studies. Time will tell whether these or novel nanocrystals will be used robustly in FISH applications.

8.2. Specific aim 2: To develop a 24 chromosome aneuploidy screening approach applicable to single nuclei and of use for determining nuclear organisation

8.2.1. The need for alternative strategies to QDs

As outlined in section 8.1 it became clear that, despite the comprehensive appraisal for the use of QDs in FISH applications, these novel fluorochromes were not, in their

current state, suitable. An alternative strategy therefore was developed in the form of a multicolour protocol that would target all chromosomes. With help from Kreatech Diagnostics, four multicolour probe combinations containing target loci for six chromosomes in each mix were designed and tested. The rationale for having four layers (probe mixes) rather than any other combination was to reduce the effect that the cycling of denaturation/hybridisation would have into the target cells as eventually the probe mixes would be incorporated in a single FISH experiment to be able to assess nuclear address in preimplantation embryos (Chapter 7).

The presence of highly repetitive sequences (α satellite) makes the centromere an attractive target for the generation of probes for this application as it allows rapid chromosome specific detection for most chromosomes and gives bright signals (due to the repetitive nature of the target). The use of centromeric probes is commonly seen in FISH studies (Egozcue *et al.* 1997; O'Keefe *et al.* 1997; Sbracia *et al.* 2002; Finch *et al.* 2008b; Olszewska *et al.* 2008) and most companies market centromeric probes either for individual chromosomes or as part of a multiprobe mix (e.g. Kreatech http://www.kreatech.com/Default.aspx?tabid=134, Abbott Molecular (ex Vysis) http://www.abbottmolecular.com/ChromosomeEnumerationProbes_5112.aspx, and Cytocell www.genycell.com/images/productos/brochures/lpe__.pdf). Centromeric targets were used for 18 out of 24 probes, however chromosomes 5/19, 13/21 and 14/22 share similarities into their repetitive sequences and thus cannot be discriminated using centromeric targets. As a result of this, all these chromosomes were incorporated into one layer, using unique sequence specific probes (the so-called "omega" layer) which required overnight hybridisation.

The most important feature that made a significant impact into the efficacy of probe hybridisation was the choice of a longer separate denaturation step (probe only, 73°C for 10 minutes) followed by a much shorter codenaturation (probe and target cells-75°C for 90 seconds) before hybridisation was performed. This was possible because the probes were not pre-denatured when manufactured, which allows also their storage at 4°C and reduces the effect from thawing/freezing, since other commonly used (e.g. Abbott) are recommended for storage at -20°C. Probes had higher efficiency with the separate denaturation; correct ploidy for all 6 chromosomes was 82.5%-90.29% for the centromeric probe combinations compared to 53%-62% when

co-denaturation of probe and target was used. Individually, each chromosome probe hybridised at high efficiency rates with some at 100% success rate (X, Y, 3, 6, 12 – Tables 4.2, 4.3, 4.4 – Chapter 4) and the remaining having efficiencies above 90%. When results are looked at collectively (% of overall correct ploidy per probe set) the centromeric probe combinations ("alpha", "beta" and "gamma") respectively had 90.29% (1, 3, 4, 6, 7, 8), 82.5% (9, 10, 11, 12, 17, 20) 86.4% (2, 15, 16, 18, X, Y) overall correct ploidy, while the combination containing BAC probes ("omega") had a 76.69% efficiency. The overall efficacy in the "omega" combination seems to be reduced because of chromosome 14, that in 8/103 cells, had only one clear signal. However as it was demonstrated when these probes were used individually to assess the radial position in the sperm of control and OAT males (Chapter 5) they had high efficiencies (99.9% in controls and 99.71% in OAT males; Table 4.12, Chapter 4).

With regard to the four layer reprobing strategy, the strategy that was adopted was to use first the centromeric probe combinations ("alpha", "beta" and "gamma") and subject the target cells (lymphocytes or blastomeres) to short periods of hybridisation, followed by an overnight hybridisation with the "omega" layer. The validity of this decision was confirmed when the signal efficiency was compared when the "omega" layer was used first, followed by a centromeric probe layer (data not shown). An additional reason for having the "omega" layer last was that this layer produced greater fluorescent background than the others resulting in background "blobs" on the nucleus.

An important parameter that was observed during evaluation of reprobing was the spreading of the target cells that is the evaluation assays used a small (controlled) number of cells that were distantly apart. Lymphocytes were less tolerant than blastomeres into the denaturing/hybridisation cycles that caused some cells to swell and lose their integrity. Under the controlled assays, in three separate experiments 6/10 cells showed correct ploidy for all 46 chromosomes, while for cells without correct ploidy for all chromosomes it was mostly failure of the probe to hybridise to both chromosomes (apparent monosomy, presumably due to overlapping signals) rather than complete absence of hybridisation. On the whole, the reprobing assay in blastomeres produced brighter signals that were easier to analyse, confirming the tolerant nature of these nuclei to the repeated hybridisation compared to lymphocytes.

8.2.2. Applications and limitations of the 24-FISH based interphase cytogenetics screening

As discussed in the introduction, section 1.4.5, there is considerable controversy over the current use of FISH for PGS as data from the RCTs suggests that it does not increase pregnancy rates (Mastenbroek *et al.* 2007; Twisk *et al.* 2008; Schoolcraft *et al.* 2009b). High resolution techniques such as array CGH and SNP genotyping seem to be the future of diagnostics but are still at a validation point and are expensive (Harper & Harton 2010). Despite this, an interesting paradox is forming as there are papers that support the use of FISH through the screening of more chromosomes in more layers (DeUgarte *et al.* 2008; Colls *et al.* 2009; Mir *et al.* 2010b; Munne *et al.* 2010) that could help identify more abnormalities in a PGS setting. Thus it can be postulated that there may be still a room for 24 chromosome FISH aneuploidy screening [until the high resolution SNP techniques become accessible to all or concurrently with other techniques (e.g. array CGH)]. The 24 chromosome FISH aneuploidy screen developed here would allow screening within the clinical window required for transfer of embryos on day 5.

Furthermore there are other advantages of the use of a 24 chromosome interphase cytogenetics aneuploidy screening other than PGS of a single cell. That is, screening of whole embryos for follow up of non-transferred embryos can provide insight into whether the single cell is a representative of the whole embryo and highlight other abnormalities. In addition it can be used in conjunction with other techniques (array-based) as a means of comparison and provide concordance rates for each technique. Recently a study by Munne *et al.* (2010) showed using a 10-12 chromosome FISH test kit allowed the detection of up to 91% of abnormalities in blastocysts, that compares well to the theoretical 100% potential of the array based techniques. In this year's ESHRE meeting (Rome 2010) a paper was presented with high concordance rates of FISH and array CGH in abnormal blastomeres analysed from day 3 (with FISH) and compared with array CGH results on day 4 (using blastomeres from the embryo cultures that were diagnosed abnormal using FISH on day 3) (Mir *et al.* 2010a). These rates reached 92.3% providing additional evidence that a robust comparison of techniques needs to be performed.

A potential drawback from the current 24 chromosome screening described in Chapter 4 of this thesis, comes from the incorporation of the Far Red fluorochrome, which is not visible by eye. This could be a problem in the clinical setting if operators are unused to scoring signals that they cannot see. Finally this type of screening could find applications in the study of genome organisation for instance with its association with cancer since there is evidence in literature for perturbed genome organisation in certain tumours (Foster & Bridger 2005). Another application is for the determination of nuclear address in sperm and embryos and asking whether it is related to aneuploidy in blastomeres. This formed the basis of the investigations in specific aims 3 and 5 (Chapters 5 and 7).

8.3. Specific aim 3: To test the hypothesis that nuclear organisation is altered in men with severely compromised semen parameters by assaying loci for all chromosomes

As described in the introduction, section 1.5.7 of this thesis, nuclear organisation in sperm has been extensively studied and well defined (Haaf & Ward 1995; Zalensky *et al.* 1995; Hazzouri *et al.* 2000; Tilgen *et al.* 2001; Mudrak *et al.* 2005). The position of the chromosomes is non-random with the centromeres clustering at the nuclear centre to form the chromocentre (well inside the nucleus) and the telomeres located towards the periphery where they interact to form dimers (Zalensky *et al.* 1993; Zalensky *et al.* 1995; Luetjens *et al.* 1999; Solov'eva *et al.* 2004; Zalenskaya & Zalensky 2004). Furthermore, nuclear organisation has been associated with disease when altered patterns have been observed as per section 1.5.6. A highly ordered set of nuclear organisation events take place in spermatogenesis (through chromatin remodelling) to prepare it for fertilisation. Thus any perturbations could affect this process and be evident in a subset of a population with compromised fertility (Luetjens *et al.* 1999; Zalensky & Zalenskaya 2007) such as those with OAT. This possible link is yet to be fully established through alterations of the radial position of chromosomes in men with compromised semen parameters. Thus far, preliminary evidence for altered radial position of the sex chromosomes in men with OAT has been reported by my own laboratory (Finch *et al.* 2008b). One aim of this thesis was

to focus specifically on men in the OAT category, since there is well-established evidence of high aneuploidy levels in their sperm as per section 1.2.2.2 which contributes to their compromised fertility status. In addition it seemed logical to expand the observations on radial position for all chromosome loci. The results suggest that specific loci occupy a different radial position in some OAT males from the strict organisation seen in controls as follows:

8.3.1. Nuclear address of all chromosome loci in the sperm of men with normal semen parameters

The general conclusion from assessing radial position for all the loci in normal control males is that they consistently adopt specific addresses, thus providing evidence of a highly ordered level of nuclear organisation. Furthermore, all centromeric loci adopt central positions confirming strong evidence of the presence of a chromocentre in sperm (Zalensky *et al.* 1995; Zalenskaya & Zalensky 2004). Further evidence of this model is provided by the non-centromeric autosomal probes that are located close to their centromeres (loci 14, 19, 21, 22) that also occupy central positions, whereas the loci located further away from their centromeres (5, 13) adopt more medial positions. This pattern of organisation is consistent by and large, when results are analysed on a per-patient basis. Exceptions to this include the centromeric loci for chromosomes 6 and 8 that do not occupy quite such a central position in certain control males. Further evidence for this model would be provided by the examination of telomeric probes and such work is ongoing in the laboratory at present.

8.3.2. Positioning of all chromosome loci in the sperm of men with OAT

The results from the OAT males, when examined collectively, suggest that certain loci occupy different positions compared to controls. These changes are subtle for some loci (e.g. the centromere of chromosome 8 – half a shell difference, 5 vs. 4/5), intermediate [e.g. the loci on chromosomes for 4, 12, 18, 5, 21 – are in predominantly different positions to the order of one shell (4 vs. 5)], or more overt [e.g. the centromeres for 3 and 6 that occupy different positions to the order of two shells (3 vs. 5)]. The general message therefore was that certain loci tended to occupy a less central position in OAT males. Thus this could be evidence of a breakdown in the chromocentre arrangement associated with OAT. A similar kind of observation, with alterations in the occupied area of the chromocentre in infertile men has been

observed in a study assaying the longitudinal position of 4 chromosomes compared to normal controls (Olszewska *et al.* 2008). It would also be interesting to investigate whether these differences could be manifested through sperm DNA damage assays; e.g. comet assay (Tarozzi *et al.* 2007).

When results are examined on a per-patient basis, there is evidence of some patterns that are not discernable from a random distribution for 3 centromeric loci (4, 6 and 12) and for a non-centromeric locus (13q14) in specific OAT males. Indeed the non-centromeric locus for chromosome 13 showed a pattern not discernable from a random distribution in 3 OAT patients (3, 4 and 10). By contrast, all the control males displayed clear evidence of non-random pattern. It is worth pointing out that patient 10 had three loci (4, 6, 13) displaying this apparently "random" pattern. When the details (age/semen parameters) of this patient are looked into more detail, he was the third oldest (48 years, oldest was 52), second lowest in terms of sperm count (1.5ml x 10^6, lowest was 1.0ml x 10^6) and motility (2%, lowest was 1%). However a statistically significant correlation between the observations of patterns not discernable from a random distribution and semen parameters (or age) could not be established. Thus it can be concluded that in both categories of men, a strictly ordered level of nuclear organisation (chromocentre) is evident in the sperm heads overall however individual loci in OAT males appear to be somewhat different. The presence of loci with positions not discernable from a random distribution in certain OAT males suggests that the phenomenon of breaking from the strict organisation may be patient-specific.

8.3.3. Comparison of results with the previous study

The only available study of which I am aware that has assessed radial position of chromosome loci in normal and men with impaired semen parameters is by my own laboratory (Finch *et al.* 2008b). The two studies have some methodological differences that are highlighted in the following table.

Study	Finch *et al.*(2008b)	Current
Target Sample	Many categories of infertile men (including OATs)	OATs only
Sample Size	9 Controls – 2 OATs (plus different types of infertile men)	10 Controls – 10 OATs
Chromosomes assessed	X,Y,18	All 24
Assay type	Manual – [see Methods of Finch *et al.*(2008b)	Automatic – (Section 2.12)
Probes	Centromeric for 18,X,Y	Centromeric for all but 5, 13, 14, 19, 21, 22 and Y

Table 8.1: Comparison for the two studies assessing radial position of chromosomes in normal and infertile men.

There are three main inferences that can be drawn by comparison of the two studies. Overall results from both suggest that, in control males, chromosome loci occupy distinct positions that appear to be central. The same can be said for the OAT patients (although the overall number of patients in the previous study (Finch *et al.* 2008b) was lower from this one) where all commonly investigated loci have non-random positions. Inter-patient differences exist however with two of the normal males demonstrating apparently "random" patterns for X and Y in previous study (Finch *et al.* 2008b) and similarly for one OAT patient for the centromere of the X chromosome. No apparently random pattern was seen for any of these loci in this study in either normal or OAT males. However an important message from the previous study (Finch *et al.* 2008b) was that overall the sex chromosomes were prone in displaying patterns not discernable from random, in certain infertile men, a feature not apparent for the centromere of chromosome 18. This was not observed in this study (although only one category of infertile men was examined) and explanations could lie within the methodological approach used. However it would be important to extend these complete assays to other types of infertile men.

8.3.4. Sperm disomy and nuclear address

There is now over ten years of evidence from the literature (Bernardini *et al.* 1997; Storeng *et al.* 1998; Pang *et al.* 1999; Pfeffer *et al.* 1999; Ushijima *et al.* 2000; Gole *et al.* 2001; Tempest & Griffin 2004; Zhang & Lu 2004; Durakbasi-Dursun *et al.* 2008) confirming that OAT males have significantly higher levels of aneuploidy in their sperm compared to normal controls. All the above studies have suggested that there might be a risk for these males when undergoing ICSI. My results from assaying disomy levels for 5 chromosomes (2, 13, 21, 22, X and Y) were that OAT males had significantly higher rates of disomy (and diploidy) than normal males. When disomy frequencies were investigated in combination with the radial position of chromosome loci, a trend for some loci to break from the strict organisation of the chromocentre as disomy increased in both controls and OAT man can be implied. However more chromosomes were involved in this altering of position in the OAT patients compared to controls (chromosome loci 3, 4, 5, 6, 13, 21 vs. 5 and 13). There was not an increase in the not discernable from random distribution patterns when disomy levels increased in either group.

8.3.5. Technical notes criticism and future prospects

This study has expanded in many ways upon the initial radial assessment previously performed (Finch *et al.* 2008b); that is by looking at all the chromosomes and focusing on a specific cohort of men with impaired fertility (OAT). The methodology presented in this thesis, to assess the radial position is more robust since the creation of the computer programme that divides the sperm head into 5 areas of equal area (from which signal position is assessed) is not based on a "home-made" template manually overlaid on the nucleus: rather it is a direct representation of the nucleus shape and size through the "pixel translation" of the DAPI counterstain into the borders of the nucleus. Thus any surface perturbation in the shape of the nucleus (e.g. corners, "pointy bits") can be better captured (the same applies to the scoring of the signals, as they are measured through the intensity of the pixels and a better representation of the signal output in its respective rings can be generated).

In addition the sample size has been more controlled since 10 patients have been looked at in each category and the number of images captured was nearly identical (n=107 in controls vs. n=103 in OATs). By capturing similar number of cells, an

important parameter (cell number) is kept at a constant, which becomes important with regard to the statistical significance of the results (since similar numbers are compared). Furthermore, since the results presented here are extrapolations of 3D objects from 2D images, by having a higher number of cells the 2D effect is somewhat reduced. Evidence that 2D data extrapolation provides a good correspondence of the 3D image comes from recent studies (Federico *et al.* 2008). Also the DAPI normalisations of all the results to account for the difference in DNA content are a better fit for each nucleus since they are based on the pixel intensity (of the blue counterstain) found under each of the 5 rings. Hence they are nucleus-specific rather than average standardised values from assessing a number of cells. Another important difference is that every individual cell analysed has been captured (>8,000 images). Although labour intensive, due to DNA compactness in sperm, signals can be found on different focal planes, which becomes difficult to visualise if more than one cells are in the same focal/capture plane. By capturing each cell this is eliminated and offers a better representation of the signals (plus single cell capturing is compatible with our analysis software, whereas multi-cells on a capture plane are not analysable).

To the best of my knowledge this is the first study that looks into the radial position of all chromosome loci in normal and men with impaired fertility (specifically OAT). The differences in topology for certain chromosomes in certain OAT men could be due to the breaking down of the strict organisation in chromosome migration, present in meiosis (Olszewska *et al.* 2008). The disturbance in this strict organisation could be due to the presence of aneuploidy (e.g. disomic) chromosomes that have as a consequence the topological changes observed for certain loci in OAT. Turner *et al.* (2006) described a mechanism for the silencing of unsynapsed chromatin (MSUC) as a control measure to prevent the gamete from excessive aneuploidy, it could be that in infertile men this controlling mechanism is not operating efficiently enough. Furthermore, if chromosome topology is the result of arrangement on the basis of transcriptional activity (Olszewska *et al.* 2008) then if this activity is altered in infertile men resulting in different topology, then this becomes the causative mechanism of incorrect chromosome segregation in male meiosis. Zalensky and Zalenskaya (2007) propose that, apart from the nuclear malformations or chromosome/chromatin defects, a new class of sperm chromosome abnormality

related to atypical packing of territories and/or aberrant nuclear position could have an impact on fertilisation and early development. This underlines the necessity for more studies with regard to nuclear address in sperm.

A study that looked into 30 sperm from a fertile donor using a 3D technique was recently published showing proof of principle (Manvelyan *et al.* 2008) for this approach. It remains to be seen whether this will find widespread applicability. A great advancement for the radial assessment of chromosome position would be from automating the capturing process which is the most time consuming and demanding due to the nature of the sperm cell. The concept of automated scoring is under explored (Perry *et al.* 2007) and difficulties arise from the need to "train" the software to capture in similar manner to the operator. This "training" could be facilitated by the use of a library of images. Currently I have a significant number of images captured from this study and the prospects of using them for developing automated capturing software for sperm cells are explored. Automated sperm screening would offer great insight into nuclear address concurrently with the assessment of chromosome copy number in sperm which has been adopted by some clinics especially for men with high risk due to impaired semen parameters (e.g. OAT). Finally based on my results screening for the position of loci 4, 6, 12 and 13 in infertile men could be indicative of whether chromosome position can constitute another semen parameter for investigation or ultimately a diagnostic test for infertility.

8.4. Specific aim 4: To apply the 24 chromosome FISH strategy to human blastomeres and assay the level of chromosome abnormalities and assess the efficacy of PGS

As mentioned in the introduction, section 1.4.8 the assessment of chromosome aneuploidy in human embryos has previously been attempted using a limited subset of probes (Munne *et al.* 1995; Delhanty *et al.* 1997; Munne *et al.* 2004).

Here, the aim was to expand such studies using the methodology from Chapter 4, and evaluate the levels of aneuploidy, for all chromosomes, from whole embryos spread on average on day 5 or 6 post fertilisation. It should be noted that, for most of the

embryos, a single cell had previously been biopsied on day 3 (post fertilisation) and used for aneuploidy screening using probes for 8 chromosomes (i.e. PGS). Thus comparison of the single cell result with the result from the remaining embryo has been made; further insight into the accuracy of PGS on the single cell level is also provided.

8.4.1. Assessment of chromosome copy number in whole embryos

Chromosome copy number was assessed in 250 blastomeres from 17 whole embryos. The most striking finding was that there was no blastomere with correct ploidy for all chromosomes. There are certain reasons that could explain this lack of 46/46 correct ploidy. From a methodological point of view, results from Chapter 4 in control lymphocytes suggest a 60% of cells with correct ploidy (46/46) after reprobing. Furthermore, the whole embryos were spread using HCl:Tween and there is evidence in the literature that this method is not as good as methanol:acetic acid in terms of producing nuclei with large diameter and thus better signals with less overlapping (Velilla *et al.* 2002). Thus failure of hybridisation (i.e. apparent chromosome loss) could be a side effect of the spreading method. From a biological perspective human embryos generated via IVF protocols have a high degree of abnormalities (>50% in cleavage stage) (Delhanty 2005) and in addition all whole embryos used in this study were not applicable for transfer after PGS and thus might be expected to have high levels of abnormalities. This fact supports the statement that if an embryo has abnormal chromosome complement on day 3 it has a high probability for a similar status on day 5 (Daphnis *et al.* 2008). It would be interesting to have follow up analysis from non-transferred embryos with correct chromosome complement (e.g. in cases where 3 or more embryos with correct status were available), but this is extremely difficult in an IVF setting as these embryos would be frozen and used on subsequent cycles pending the result of PGS. Moreover, some of the whole embryos could have been arrested due to chromosome abnormalities (Munne *et al.* 1994a). Thus a combination of the aforementioned reasons could account for the lack of 46/46 ploidy status. This was the reason that I could not apply the mosaic classification criteria (Delhanty *et al.* 1997) and an alternative set of criteria was selected to classify whole embryos for the purposes of nuclear address. This study also highlights the difficulties (methodological, biological) for the use of this FISH-based approach in a PGS setting.

8.4.2. Mosaicism and types of aneuploidy in whole embryos

Despite not using the previously described mosaic classification criteria for describing the mosaic status (e.g. normal, minor mosaic, major mosaic, chaotic) of whole embryos, the patterns seen in the individual blastomeres from most point towards the diploid/aneuploid mosaicism being the most common type of mosaicism seen in preimplantation embryos (Munne *et al.* 1994b; Delhanty *et al.* 1997; Daphnis *et al.* 2005). According to Munne *et al.* (1994b) this form of mosaicism originates in the first few cleavage divisions and it persists due to failure of cell cycle checkpoints during the cleavage stage (e.g. checkpoint that allows mitosis to proceed after successful chromosome segregation) (Delhanty & Handyside 1995). This type of mosaicism is also observed in the blastocyst stage (Bielanska *et al.* 2005). According to Daphnis *et al.* (2005) this type of mosaicism arises due to mitotic non-disjunction which confers reciprocal chromosome loss or gain in the daughter cells, with chromosome duplication and anaphase lag being also postulated as possible mechanisms.

The ability to evaluate copy number for all chromosomes in individual cells allows preliminary investigations into asking whether there are chromosome-specific mechanisms of error, (i.e. is there a greater likelihood of certain chromosomes to be involved in mal-segregation event). Chromosome loss was seen primarily in the current data set for most chromosomes in all embryos, with gains being observed at a much lower frequency. The fact that more monosomies were observed (35.21%) compared to trisomies (5.64%) seems to be in accordance with previous data (Munne *et al.* 2004) and also suggests it as the predominant mechanism (chromosome loss) leading to this type of mosaicism. However the presence of certain nuclei (within embryos) that contained monosomies and trisomies for the same chromosome seems to confirm that mitotic non-disjunction is another mechanism involved in the generation of these mosaic embryos.

With regard to trisomy, chromosomes 11 and 15 were the most prone to trisomy (10.4% and 10%), whereas chromosome 21 was one of the least involved (4.4%). When looking at monosomies, chromosome 20 dominated with 60.8% frequency and

was followed by chromosomes 3, 7, 4, 17 and 9 (all above 40%). More studies are needed to evaluate and confirm these results, but they provide proof of principle for comparisons with chromosomal error in embryos (foetuses) at later stages of development. Hassold and Hunt (2001) reported that different aneuploidies are represented among spontaneous abortions including trisomies for nearly all chromosomes, but trisomies 16, 21 and 22 contribute to 50% of all the observed trisomies.

The high level of monosomy for chromosomes 15, 16, 21, 22 (all above 30%) seems to be in agreement with previous data (Munne *et al.* 2004). Furthermore, the fact that most of the cells had correct ploidy status for the sex chromosomes is also in concordance with previous data (Munne *et al.* 1995; Marquez *et al.* 2000; Munne *et al.* 2004). Thus, in summary, the results presented here argue that the dominant mechanism for the presence of mosaicism was chromosome loss (occurring post-zygotically), followed by chromosome gain, and some individual examples for chromosomes with mitotic non-disjunction.

8.4.3. The efficacy of PGS

The accuracy of single cell diagnosis from a PGS setting was evaluated for a subset of embryos in this study. Out of the 15 cases, results from both day 3 and whole embryo were available in 8 (53.3%). In the remaining 7, either results were not obtained on day 3 (3/7) or not with the 24 screen due to poor fixed embryos (4/7). A full PGS confirmation (for the chromosomes looked at on the single cell level) was seen in 4/8 cases. In the remaining 4 there was either a partial or no confirmation. On the whole however, based on the full results from the 24 chromosome screen, no single cell would qualify to be transferred and thus, from this perspective, day 3 diagnosis was correct. In a study by DeUgarte *et al.* (2008), day 3 diagnosis was compared with whole embryos a positive correlation was identified for 83% of the cells, whereas 17% was misdiagnosed as abnormal on day 3. This is another piece of evidence that confirms the high level of mosaicism on cleavage stage and highlights the importance of the comparison between single cell and whole embryo diagnosis. Potentially all clinics that offer PGS for aneuploidy could encourage their patients in having follow up diagnosis by highlighting the benefits in terms of providing a more complete diagnosis and future advice. However one should take into account that this would

add to the cost of the treatment and sometimes is subjected to personal ethical constraints.

The second clear conclusion was that additional abnormalities could be diagnosed with the 24 chromosome screen in all the cases where the single cell result was compared to diagnosis from the whole embryo. This provides further weight to the suggestion that additional chromosome screening is required, in order to improve the diagnostic potential of PGS until the high resolution techniques (SNP arrays) become widely available (Colls *et al.* 2009; Munne *et al.* 2010). Even if PGS does turn to high resolution techniques, follow up analysis of non-transferred embryos by FISH (or a combination of techniques) can be an added research and clinical tool into the evaluation of the whole embryo on a cell by cell basis, something prohibitively expensive by array-based approaches.

8.5. Specific aim 5: To apply the 24 chromosome FISH strategy to investigate nuclear organisation in human blastomeres

Using the methodology developed in Chapter 4, as well as assessing chromosome copy number in blastomeres, I also investigated the radial position for all chromosome loci, taking into account patterns both for individual cells, and for whole embryos. These investigations expanded on previous studies assessing the radial position of loci in blastomeres comparing also relative nuclear patterns between abnormally classified blastomeres/whole embryos and those with relatively few abnormalities (McKenzie *et al.* 2004; Diblik *et al.* 2007; Finch *et al.* 2008a).

8.5.1. Assessment of nuclear address in individual blastomeres: How do results compare to previous studies?

In the previous studies investigating nuclear address in blastomeres, classification of cells as "normal" or "abnormal" was relatively easy since they all were based on the diagnosis from 5-8 chromosomes (McKenzie *et al.* 2004; Diblik *et al.* 2007; Finch *et al.* 2008a). Since, in this study, all chromosome loci where investigated and no individual blastomere showed correct ploidy for all chromosomes different classification criteria were used to differentiate the two groups. Here, blastomeres were classified according to the "relative" levels of abnormality. Thus in the "normal"

category, single blastomeres (that had successful hybridisation over the 4 layers), with less than 40% of the total signals as monosomies were placed. This translated to correct ploidy for at least 15 pairs of chromosomes including the sex chromosomes Also the total number of such cells was 50, i.e. that of previous studies designed to assess nuclear address as a "minimum number" (Foster *et al.* 2005) [NB, n=33 in the (McKenzie *et al.* 2004) study, n=49 in the (Diblik *et al.* 2007) study]. The remaining blastomeres made up the abnormal category. When results are compared in both groups, only the relatively "normal" blastomeres showed evidence for some loci adopting patterns not discernable from a random distribution (loci 4, 6, 8, 13 and 5) whereas all loci in the abnormal category adopt defined positions that were mostly central (22/24 loci). Furthermore, certain loci in the "normal" group of blastomeres adopt more medial positions (loci 1, 2, 3, 9 and 18) than their abnormal counterparts implying a more "relaxed" nuclear organisation in the relative "normal" blastomeres and consistent, in broad terms, with previous results from my own laboratory (Finch *et al.* 2008a).

Thus far, the total number of studies (including this one) that have assessed radial position for certain loci is four. The current study and that of Finch *et al.* (2008a) study are more comparable in some aspects of the methodology (they are, after all, from the same laboratory) since they both take into account the difference in chromatin distribution within a nucleus and thus results are normalised (through different means). The remaining two studies (McKenzie *et al.* 2004; Diblik *et al.* 2007) do not take into account this chromatin difference. In addition, in all 3 previous studies (McKenzie *et al.* 2004; Diblik *et al.* 2007; Finch *et al.* 2008a), there are subtly different means to analyse the relative position of signals in nuclei, with (McKenzie *et al.* 2004) using a 5-concentric ring with increasing diameter sizes (thus shells of different areas), (Diblik *et al.* 2007) used a 9-concentric ring model, whereas (Finch *et al.* 2008a) used a concentric ring of 5 shells of equal area. All the above models had to "best-fit" the ring template on top of the nucleus, whereas, in this study, a concentric 5 shell ring was still used but it was designed to "retro-fit" on the nucleus, thereby better taking into account any shape alterations. Moreover the chromatin normalisation values for each ring (shell) took into account the actual amount of chromatin in each nucleus (from counterstain pixel intensity) rather than standardised values obtained from a number of cells (Finch *et al.* 2008a). Another difference of this

study compared to the previous 3 is that the blastomeres used in this study were biopsied from embryos on day 5-6 post fertilisation, compared to blastomeres from day 3-4 in the previous studies.

The following table summarises all the relative radial position with regard to the common loci investigated in the four different studies.

Study	**McKenzie *et al.* (2004)**		**Diblik *et al.* (2007)**		**Finch *et al.* (2008a)**		**Current study**	
Locus	Normal	Abnormal	Normal	Abnormal	Normal	Abnormal	Normal	Abnormal
13	Central	Peripheral	Random	Random	Random	Peripheral	Random	Central
15	N/A	N/A	N/A	N/A	Random	Central	Central	Central
16	Peripheral	Peripheral	Random	Random	Random	Central	Central /Medial	Central
18	Central	Peripheral	Central	Random	Random	Peripheral /Medial	Central	Central
21	Central	Peripheral	Random	Random	Random	Central	Central	Central
22	Peripheral	Peripheral	Random	Random	Random	Central	Central	Central
X	Central	Peripheral	Random	Random	Random	Random	Central	Central /Medial
Y	Peripheral	Peripheral	Random	Random	Random	Random	Central	Central

Table 8.2: Comparison of the radial position in four different studies for 8 loci. Note: The grey shaded boxes denote concordance data between different studies for the Normal blastomeres. The red shaded boxes denote concordance for two studies, although there is also a different concordance for the remaining two studies (e.g. 21, X). The green shaded boxes denote concordance of data between different studies for the Abnormal blastomeres.

Thus the current study with regard to the abnormal blastomeres resembles more the results from the Finch *et al.* (2008a) study (loci 15, 16, 21 and 22). With reference to the "normal" blastomeres, my results for locus 13 agree with both the others (Diblik *et al.* 2007; Finch *et al.* 2008a), whereas results for loci 18, 21 and X agree with the other study (McKenzie *et al.* 2004). Nevertheless, it appears that the "relaxed" nuclear organisation proposed by the previous work of my lab (Finch *et al.* 2008a) seems to be apparent (although less obvious when all chromosomes are looked at) in the relatively "normal" blastomeres of this study, while all loci in the abnormal blastomeres group occupy distinct positions without any evidence of "random" distribution of the sex chromosomes as suggested previously (Finch *et al.* 2008a).

Aside from the methodological differences between the current and the Finch *et al.* (2008a) study (normalisation, cell number) that could partially explain the differences in the results, the different levels of mosaicism observed in each category of

blastomeres could be also responsible. That is, different population of cells could account for not reaching significant levels due to different locations of the loci investigated.

8.5.2. Assessment of nuclear address in whole embryos

The results discussed in the previous section analysed individual blastomeres nuclei, partly to report on all chromosome loci and also to further expand on the previous studies. However nuclear organisation (for all loci) is something that, to the best of my knowledge, had not yet been measured between whole embryos.

Since all the whole embryos assessed were abnormal and mosaic, in order to classify them into roughly equal sized groups I classified them according to their relative normal diploid number when expressed as a proportion of the total. Using this manner of analysis, two categories were generated (i.e. >50% of chromosome pairs diploid in the first group; and <50% of chromosome pairs diploid in the abnormal group). This constituted 9 and 8 whole embryos in each group respectively.

The results suggest that, in both categories, all loci (excluding chromosome 19 due to too few cells being analysed) occupy distinct nuclear addresses. There are subtle differences between the two groups with loci for chromosome 1 and 4 occupying a central/medial position in the "normal" group but a more defined central position in the abnormal group. The reverse was observed for loci 3, 7, 9, 10, 18 and 20. In addition loci 5, 6 and 8 are also involved in different positioning between the two groups.

Thus nuclear address differences were, nonetheless, more evident when blastomeres were analysed on a per cell basis, rather than a whole embryos basis. A biological explanation for this could be the dramatic changes that occur in nuclear architecture and chromatin structure at the beginning of development (Martin *et al.* 2006a), and could be manifested as non defined positions in the nucleus; however as these rearrangements are completed by the blastocyst stage, it could be that by then the positions become more defined, resembling the strict positions observed in the "normal" and abnormal whole embryos. Study of more embryos would be required to

make confident claims about any differences and associations between aneuploidy and nuclear address.

8.5.3. Assessment of nuclear address in whole embryos: Is there evidence of a chromocentre formation?

Further analysis of the total data set suggests that the presence of a chromocentre in human preimplantation embryos is analogous to that seen in sperm as all centromeric loci adopt mostly central positions and the same can be said for most of the autosomal loci, with locus on chromosome 5 (distally located from the centromere) occupying a peripheral/medial position. Although a chromocentre has not been demonstrated on day 1 or 2 human embryos, its presence has been shown in mouse day 1-2 cells (pro-chromocentre), that becomes a mature chromocentre by the blastocyst stage due to the changes in pericentric chromatin, activation of replication and chromatin structure (Martin *et al.* 2006a). This "mature" chromocentre establishment appears to occur concurrently with the onset of zygote transcription thus conferring a functional significance for the regulation of gene expression (Martin *et al.* 2006a). Thus, for the first time, I report the presence of a chromocentre formation in day 5-6 human embryos and it would be interesting to further explore its potential functional significance for gene expression in the newly developing zygote. Two of the previous studies (McKenzie *et al.* 2004; Diblik *et al.* 2007) showed no evidence of a chromocentre, whereas in the other (Finch *et al.* 2008a) there is some evidence for a chromocentre in the abnormal blastomeres from the central position that loci for chromosomes 15 and 16 occupied.

8.5.4. Nuclear address in different cell types (all chromosome loci)

As part of this thesis, nuclear organisation was compared in different cell types, including lymphocytes, sperm (controls and OATs) and whole embryos. The results suggest that sperm and whole embryos have a similar nuclear organisation compared to lymphocyte nuclei. That is, all chromosomal loci occupy distinct positions in sperm and blastomeres, whereas in lymphocytes there is evidence for pattern not discernable from a random distribution. More specifically, the sex chromosome loci appear to be "random" in lymphocytes compared to the central positions in sperm and embryos. Most of the remaining centromeric loci, have central or central/medial positions in sperm and embryos whereas loci for 1, 3, 4, 6, 7, 12 and 18 adopt a distribution not

discernable from a random position pattern in lymphocytes. Finally the non-centromeric autosomal loci (those close to their centromeres) have a central or central/medial position in all types of cells. Nevertheless the locus on chromosome 5 occupies a defined (mostly medial) position in sperm and embryos but an apparently "random" one in lymphocytes, whereas the most distally (from the centromere) located locus of chromosome 13 has a central/medial position in lymphocytes and sperm, but a more defined central position in blastomeres.

When the results in lymphocytes are compared to previous studies that have assessed the nuclear organisation of whole chromosome territories in proliferating lymphoblasts and fibroblasts (Croft *et al.* 1999; Boyle *et al.* 2001; Cremer *et al.* 2003; Meaburn *et al.* 2005) there are some similarities (i.e. the interior position of loci 15, 19 and 22), and discrepancies (with whole territories for 13, 18, X ,Y being peripherally located compared to a pattern not discernable from random in the lymphocytes of this study). This difference could be due to the different probes used in this study or that more cells were required in order for the "random" pattern of these chromosome loci to be shifted into a more distinct position.

In this study, human embryos most resemble the sperm cells (both in terms of chromocentre formation and distinct position) rather than the other somatic cells. An obvious explanation for this resides with the classification of blastomeres to their relative normal and abnormal groups as the number of chromosomes investigated increases. A blastomere normal for 8 pairs of chromosomes does not necessarily mean that it will be normal for all 23 and *vice versa*. Furthermore the level of mixed population of cells (i.e. mosaic) is different when single cells from day 3 are evaluated compared to blastomeres/whole embryos from days 5 or 6.

8.5.5. Technical notes, criticism and future prospects

In this study, embryo spreading was performed using HCl:Tween method. A clear observation was that, when embryo cells were not well separated, they tended to swell after the 1st or 2nd hybridisation round leading to no discernable borders between them (e.g. embryos 10, 11 and 13 - Table 6.1) and low hybridisation efficiencies. However, when spreading was optimum, all cells reprobed without a problem (e.g. embryo 16, Table 6.1). Whether the sub optimal conditions of embryo spreading are associated

with the method, the operator or the day (post fertilisation) of spreading is not clear. One piece of evidence from the literature with regard to the spreading method, suggests that methanol/acetic acid, although technically demanding, gives the best results in terms of nuclei with a large diameter, which in turn results into better signals and less overlapping (thus FISH errors) (Velilla *et al.* 2002). Studies directly comparing the approach adopted in this thesis with the methanol acetic acid approach are yet to be performed.

The use of different types of probes (e.g. telomeric) will provide a better understanding on the position of whole chromosome territories and also confirm abnormalities seen by using a different reference point. Potentially reprobing protocols can include more layers if blastomeres are tolerant enough. My personal experience has shown that blastomeres can be used in 5 layer FISH experiments (data not shown) pending good spreading. Obviously more time dedicated to protocols like this can improve (together with the testing of embryo spreading techniques) their efficacy and reproducibility.

8.6. Concluding Remarks

This thesis has attempted to use interphase cytogenetics to provide further insight primarily into the chromosome copy number and nuclear organisation of sperm and embryos in order to assess whether altered nuclear organisation is associated with infertility (in sperm) or aneuploidy (in human embryos). It has expanded on previous interphase cytogenetic studies by, for the first time, investigating all chromosomes in the karyotype. The future of nuclear organisation and infertility seems promising if methodologies like the one described here become fully automated to provide the basis for determining levels of aneuploidy in sperm (concurrently with radial position). However the biggest promise comes from the novel high resolution techniques (SNP arrays) that will take over, as DNA from men with elevated sperm aneuploidy could be used in genome association studies to identify candidate SNPs or CNVs that could be associated with infertility. Furthermore using a strategy such as Karyomapping (Handyside *et al.* 2009) can provide insight into the origin of sperm aneuploidy (e.g. reduced recombination, or altered recombination patterns in infertile men) and the nature of abnormalities (numerical or structural). The hope is to be able

to understand better the different types of infertility and provide better diagnoses to men undergoing ICSI.

With regard to aneuploidy the use of the new diagnostic techniques (array or SNP based), together with alternative biopsy techniques (polar body or blastocysts), advancement in freezing of embryos (i.e. vitrification) coupled with well-designed trials can help provide better, complete diagnosis which will help to increase implantation but more importantly the take-home baby rates. Also important research questions into the origin and type of aneuploidy can be addressed at the same time.

FISH has put interphase cytogenetics and preimplantation diagnosis onto the map of the research world by addressing important insights into the early spermatogenesis and embryogenesis; however the new techniques that FISH is giving way to promise to fill the empty parts of this map and navigate towards treatment of infertility and more complete diagnostics.

9. References

Aitken R.J. & De Iuliis G.N. (2007) Origins and consequences of DNA damage in male germ cells. *Reprod Biomed Online* **14**, 727-33.

Aitken R.J. & De Iuliis G.N. (2009) On the possible origins of DNA damage in human spermatozoa. *Mol Hum Reprod.*

Akerman M.E., Chan W.C., Laakkonen P., Bhatia S.N. & Ruoslahti E. (2002) Nanocrystal targeting in vivo. *Proc Natl Acad Sci U S A* **99**, 12617-21.

Alberts B., Bray D., Lewis J., Raff M., Roberts K. & Watson J.D. (1994) *Molecular biology of the cell.* Garland Publishing, New York and London.

Alivisatos (1996) Nanocrystals:building blocks for modern materials design. *Endeavour* **21**, 56-0.

Alivisatos A.P., Gu W. & Larabell C. (2005) Quantum dots as cellular probes. *Annu Rev Biomed Eng* **7**, 55-76.

Ambartsumyan G. & Clark A.T. (2008) Aneuploidy and early human embryo development. *Hum Mol Genet* **17**, R10-5.

Arnold N., Wienberg J., Ermert K. & Zachau H.G. (1995) Comparative mapping of DNA probes derived from the V kappa immunoglobulin gene regions on human and great ape chromosomes by fluorescence in situ hybridization. *Genomics* **26**, 147-50.

Arya H., Kaul Z., Wadhwa R., Taira K., Hirano T. & Kaul S.C. (2005) Quantum dots in bio-imaging: Revolution by the small. *Biochem Biophys Res Commun* **329**, 1173-7.

Baart E.B., van den Berg I., Martini E., Eussen H.J., Fauser B.C. & Van Opstal D. (2007) FISH analysis of 15 chromosomes in human day 4 and 5 preimplantation embryos: the added value of extended aneuploidy detection. *Prenat Diagn* **27**, 55-63.

Bailey R.E., Smith A.M. & Nie S. (2004) Quantum dots in biology and medicine. *Physica E* **25**, 1-12.

Ballou B., Ernst L.A., Andreko S., Fitzpatrick J.A., Lagerholm B.C., Waggoner A.S. & Bruchez M.P. (2009) Imaging vasculature and lymphatic flow in mice using quantum dots. *Methods Mol Biol* **574**, 63-74.

Barbash-Hazan S., Frumkin T., Malcov M., Yaron Y., Cohen T., Azem F., Amit A. & Ben-Yosef D. (2008) Preimplantation aneuploid embryos undergo self-correction in correlation with their developmental potential. *Fertil Steril.*

Barratt C.L., Aitken R.J., Bjorndahl L., Carrell D.T., de Boer P., Kvist U., Lewis S.E., Perreault S.D., Perry M.J., Ramos L., Robaire B., Ward S. & Zini A. (2010) Sperm DNA: organization, protection and vulnerability: from basic science to clinical applications--a position report. *Hum Reprod.*

Bentolila L.A. & Weiss S. (2006) Single-step multicolor fluorescence in situ hybridization using semiconductor quantum dot-DNA conjugates. *Cell Biochem Biophys* **45**, 59-70.

Bernardini L., Martini E., Geraedts J.P., Hopman A.H., Lanteri S., Conte N. & Capitanio G.L. (1997) Comparison of gonosomal aneuploidy in spermatozoa of normal fertile men and those with severe male factor detected by in-situ hybridization. *Mol Hum Reprod* **3**, 431-8.

Beyer C.E., Osianlis T., Boekel K., Osborne E., Rombauts L., Catt J., Kralevski V., Aali B.S. & Gras L. (2009) Preimplantation genetic screening outcomes are associated with culture conditions. *Hum Reprod.*

Bielanska M., Jin S., Bernier M., Tan S.L. & Ao A. (2005) Diploid-aneuploid mosaicism in human embryos cultured to the blastocyst stage. *Fertil Steril* **84**, 336-42.

Bjorndahl L. & Kvist U. (2009) Human Sperm Chromatin Stabilization - a Proposed Model Including Zinc Bridges. *Mol Hum Reprod.*

Bolzer A., Kreth G., Solovei I., Koehler D., Saracoglu K., Fauth C., Muller S., Eils R., Cremer C., Speicher M.R. & Cremer T. (2005) Three-dimensional maps of all chromosomes in human male fibroblast nuclei and prometaphase rosettes. *PLoS Biol* **3**, e157.

Boyle S., Gilchrist S., Bridger J.M., Mahy N.L., Ellis J.A. & Bickmore W.A. (2001) The spatial organization of human chromosomes within the nuclei of normal and emerin-mutant cells. *Hum Mol Genet* **10**, 211-9.

Branco M.R. & Pombo A. (2006) Intermingling of chromosome territories in interphase suggests role in translocations and transcription-dependent associations. *PLoS Biol* **4**, e138.

Branco M.R. & Pombo A. (2007) Chromosome organization: new facts, new models. *Trends Cell Biol* **17**, 127-34.

Braude P. (2006) Preimplantation diagnosis for genetic susceptibility. *N Engl J Med* **355**, 541-3.

Bridger J.M., Boyle S., Kill I.R. & Bickmore W.A. (2000) Re-modelling of nuclear architecture in quiescent and senescent human fibroblasts. *Curr Biol* **10**, 149-52.

Bruchez M. (2007) Quantum dots for ultra-sensitive multicolor detection of proteins and genes. In: *16th International Chromosome Conference (16th ICC) Amsterdam*, pp. 1-108. Springer Netherlands.

Bruchez M., Jr., Moronne M., Gin P., Weiss S. & Alivisatos A.P. (1998) Semiconductor nanocrystals as fluorescent biological labels. *Science* **281**, 2013-6.

Calogero A., Polosa R., Perdichizzi A., Guarino F., La Vignera S., Scarfia A., Fratantonio E., Condorelli R., Bonano O., Barone N., Burello N., D'Agata R. & Vicari E. (2009) Cigarette smoke extract immobilizes human spermatozoa and induces sperm apoptosis. *RBM Online* **19**, 564-71.

Carrell D.T. & Hammoud S.S. (2009) The Human Sperm Epigenome and its Potential Role in Embryonic Development. *Mol Hum Reprod.*

Caspersson T., Farber S., Foley G.E., Kudynowski J., Modest E.J., Simonsson E., Wagh U. & Zech L. (1968) Chemical differentiation along metaphase chromosomes. *Exp Cell Res* **49**, 219-22.

Cavalli G. (2007) Chromosome kissing. *Curr Opin Genet Dev* **17**, 443-50.

Chan P., Yuen T., Ruf F., Gonzalez-Maeso J. & Sealfon S.C. (2005) Method for multiplex cellular detection of mRNAs using quantum dot fluorescent in situ hybridization. *Nucleic Acids Res* **33**, 1-8.

Chan W.C. (2006) Bionanotechnology progress and advances. *Biol Blood Marrow Transplant* **12**, 87-91.

Chan W.C., Maxwell D.J., Gao X., Bailey R.E., Han M. & Nie S. (2002) Luminescent quantum dots for multiplexed biological detection and imaging. *Curr Opin Biotechnol* **13**, 40-6.

Chan W.C. & Nie S. (1998) Quantum dot bioconjugates for ultrasensitive nonisotopic detection. *Science* **281**, 2016-8.

Checa M.A., Alonso-Coello P., Sola I., Robles A., Carreras R. & Balasch J. (2009) IVF/ICSI with or without preimplantation genetic screening for aneuploidy in

couples without genetic disorders: a systematic review and meta-analysis. *J Assist Reprod Genet.*

Cheng E.Y., Hunt P.A., Naluai-Cecchini T.A., Fligner C.L., Fujimoto V.Y., Pasternack T.L., Schwartz J.M., Steinauer J.E., Woodruff T.J., Cherry S.M., Hansen T.A., Vallente R.U., Broman K.W. & Hassold T.J. (2009) Meiotic recombination in human oocytes. *PLoS Genet* **5**, e1000661.

Chiamchanya C., Visutakul P., Gumnarai N. & Su-angkawatin W. (2008) Preimplantation genetic screening (PGS) in infertile female age > or = 35 years by fluorescence in situ hybridization of chromosome 13, 18, 21, X and Y. *J Med Assoc Thai* **91**, 1644-50.

Choi J., Burns A.A., Williams R.M., Zhou Z., Flesken-Nikitin A., Zipfel W.R., Wiesner U. & Nikitin A.Y. (2007) Core-shell silica nanoparticles as fluorescent labels for nanomedicine. *J Biomed Opt* **12**, 064007.

Choi Y., Kim H.P., Hong S.M., Ryu J.Y., Han S.J. & Song R. (2009) In situ visualization of gene expression using polymer-coated quantum-dot-DNA conjugates. *Small* **5**, 2085-91.

Ciarlo M., Russo P., Cesario A., Ramella S., Baio G., Neumaier C.E. & Paleari L. (2009) Use of the semiconductor nanotechnologies "quantum dots" for in vivo cancer imaging. *Recent Pat Anticancer Drug Discov* **4**, 207-15.

Cohen J. & Grifo J.A. (2007) Multicentre trial of preimplantation genetic screening reported in the New England Journal of Medicine: an in-depth look at the findings. *Reprod Biomed Online* **15**, 365-6.

Cohen J., Wells D., Howles C.M. & Munne S. (2009) The role of preimplantation genetic diagnosis in diagnosing embryo aneuploidy. *Curr Opin Obstet Gynecol.*

Colls P., Goodall N., Zheng X. & Munne S. (2009) Increased efficiency of preimplantation genetic diagnosis for aneuploidy by testing 12 chromosomes. *RBM Online* **19**, 532-8.

Corrales J.J., Burgo R.M., Miralles J.M. & Villar E. (2000) Abnormalities in sperm acid glycosidases from infertile men with idiopathic oligoasthenoteratozoospermia. *Fertil Steril* **73**, 470-8.

Cremer M., Kupper K., Wagler B., Wizelman L., von Hase J., Weiland Y., Kreja L., Diebold J., Speicher M.R. & Cremer T. (2003) Inheritance of gene density-related higher order chromatin arrangements in normal and tumor cell nuclei. *J Cell Biol* **162**, 809-20.

Cremer M., von Hase J., Volm T., Brero A., Kreth G., Walter J., Fischer C., Solovei I., Cremer C. & Cremer T. (2001) Non-random radial higher-order chromatin arrangements in nuclei of diploid human cells. *Chromosome Res* **9**, 541-67.

Cremer T. & Cremer C. (2001) Chromosome territories, nuclear architecture and gene regulation in mammalian cells. *Nat Rev Genet* **2**, 292-301.

Cremer T. & Cremer C. (2006a) Rise, fall and resurrection of chromosome territories: a historical perspective. Part I. The rise of chromosome territories. *Eur J Histochem* **50**, 161-76.

Cremer T. & Cremer C. (2006b) Rise, fall and resurrection of chromosome territories: a historical perspective. Part II. Fall and resurrection of chromosome territories during the 1950s to 1980s. Part III. Chromosome territories and the functional nuclear architecture: experiments and models from the 1990s to the present. *Eur J Histochem* **50**, 223-72.

Cremer T. & Cremer M. (2010) Chromosome territories. *Cold Spring Harb Perspect Biol* **2**, a003889.

Cremer T., Cremer M., Dietzel S., Muller S., Solovei I. & Fakan S. (2006) Chromosome territories--a functional nuclear landscape. *Curr Opin Cell Biol* **18**, 307-16.

Cremer T., Landegent J., Bruckner A., Scholl H.P., Schardin M., Hager H.D., Devilee P., Pearson P. & van der Ploeg M. (1986) Detection of chromosome aberrations in the human interphase nucleus by visualization of specific target DNAs with radioactive and non-radioactive in situ hybridization techniques: diagnosis of trisomy 18 with probe L1.84. *Hum Genet* **74**, 346-52.

Croft J.A., Bridger J.M., Boyle S., Perry P., Teague P. & Bickmore W.A. (1999) Differences in the localization and morphology of chromosomes in the human nucleus. *J Cell Biol* **145**, 1119-31.

Dabbousi B.O., Rodriguez-Viejo J., Mikulec F.V., Heine J.R., Mattoussi H., Ober R., Jensen K.F. & Bawendi M.G. (1997) (CdSe)ZnS Core-Shell Quantum Dots: Synthesis and Characterization of a Size Series of Highly Luminescent Nanocrystallites *J. Phys. Chem. B,* **101**, 9463 -75.

Dahan M., Levi S., Luccardini C., Rostaing P., Riveau B. & Triller A. (2003) Diffusion dynamics of glycine receptors revealed by single-quantum dot tracking. *Science* **302**, 442-5.

Daphnis D.D., Delhanty J.D., Jerkovic S., Geyer J., Craft I. & Harper J.C. (2005) Detailed FISH analysis of day 5 human embryos reveals the mechanisms leading to mosaic aneuploidy. *Hum Reprod* **20**, 129-37.

Daphnis D.D., Fragouli E., Economou K., Jerkovic S., Craft I.L., Delhanty J.D. & Harper J.C. (2008) Analysis of the evolution of chromosome abnormalities in human embryos from Day 3 to 5 using CGH and FISH. *Mol Hum Reprod* **14**, 117-25.

Dauwerse H.G., Smit E.M., Giles R.H., Slater R., Breuning M.H., Hagemeijer A. & van der Reijden B.A. (1999) Two-colour FISH detection of the inv(16) in interphase nuclei of patients with acute myeloid leukaemia. *Br J Haematol* **106**, 111-4.

de Ravel T.J., Devriendt K., Fryns J.P. & Vermeesch J.R. (2007) What's new in karyotyping? The move towards array comparative genomic hybridisation (CGH). *Eur J Pediatr* **166**, 637-43.

Debrock S., Melotte C., Spiessens C., Peeraer K., Vanneste E., Meeuwis L., Meuleman C., Frijns J.P., Vermeesch J.R. & D'Hooghe T.M. (2009) Preimplantation genetic screening for aneuploidy of embryos after in vitro fertilization in women aged at least 35 years: a prospective randomized trial. *Fertil Steril.*

Delbes G., Hales B.F. & Robaire B. (2009) Toxicants and human sperm chromatin integrity. *Mol Hum Reprod.*

Delhanty J.D. (2005) Mechanisms of aneuploidy induction in human oogenesis and early embryogenesis. *Cytogenet Genome Res* **111**, 237-44.

Delhanty J.D. & Handyside A.H. (1995) The origin of genetic defects in the human and their detection in the preimplantation embryo. *Hum Reprod Update* **1**, 201-15.

Delhanty J.D., Harper J.C., Ao A., Handyside A.H. & Winston R.M. (1997) Multicolour FISH detects frequent chromosomal mosaicism and chaotic division in normal preimplantation embryos from fertile patients. *Hum Genet* **99**, 755-60.

Desmyttere S., Bonduelle M., Nekkebroeck J., Roelants M., Liebaers I. & De Schepper J. (2009) Growth and health outcome of 102 2-year-old children

conceived after preimplantation genetic diagnosis or screening. *Early Hum Dev*.

DeUgarte C.M., Li M., Surrey M., Danzer H., Hill D. & DeCherney A.H. (2008) Accuracy of FISH analysis in predicting chromosomal status in patients undergoing preimplantation genetic diagnosis. *Fertil Steril* **90**, 1049-54.

Dey S.K. (2010) How we are born. *J Clin Invest* **120**, 952-5.

Diblik J., Macek M., Sr., Magli M.C., Krejci R. & Gianaroli L. (2007) Chromosome topology in normal and aneuploid blastomeres from human embryos. *Prenat Diagn* **27**, 1091-9.

Donoso P., Staessen C., Fauser B.C. & Devroey P. (2007) Current value of preimplantation genetic aneuploidy screening in IVF. *Hum Reprod Update* **13**, 15-25.

Dubertret B., Skourides P., Norris D.J., Noireaux V., Brivanlou A.H. & Libchaber A. (2002) In vivo imaging of quantum dots encapsulated in phospholipid micelles. *Science* **298**, 1759-62.

Durakbasi-Dursun H.G., Zamani A.G., Kutlu R., Gorkemli H., Bahce M. & Acar A. (2008) A new approach to chromosomal abnormalities in sperm from patients with oligoasthenoteratozoospermia: detection of double aneuploidy in addition to single aneuploidy and diploidy by five-color fluorescence in situ hybridization using one probe set. *Fertil Steril* **89**, 1709-17.

Efros A.L. & Rosen M. (1997) Random telegraph signal in the photolyminescence intensity of a single quantum dot. *Physical Rev Lett* **78**, 1110-3.

Egozcue J. (1993) Sex selection: why not? *Hum Reprod* **8**, 1777.

Egozcue J., Blanco J. & Vidal F. (1997) Chromosome studies in human sperm nuclei using fluorescence in-situ hybridization (FISH). *Hum Reprod Update* **3**, 441-52.

Egozcue S., Blanco J., Vendrell J.M., Garcia F., Veiga A., Aran B., Barri P.N., Vidal F. & Egozcue J. (2000) Human male infertility: chromosome anomalies, meiotic disorders, abnormal spermatozoa and recurrent abortion. *Hum Reprod Update* **6**, 93-105.

Ekong R. & Wolfe j. (1998) Advances in fluorescence in situ hybridization. *Curr Opin Biotech* **9**, 19-24.

Elcock L.S. & Bridger J.M. (2010) Exploring the relationship between interphase gene positioning, transcriptional regulation and the nuclear matrix. *Biochem Soc Trans* **38**, 263-7.

Ellis P.J. & Affara N.A. (2006) Spermatogenesis and sex chromosome gene content: an evolutionary perspective. *Hum Fertil (Camb)* **9**, 1-7.

Farfalli V.I., Magli M.C., Ferraretti A.P. & Gianaroli L. (2007) Role of aneuploidy on embryo implantation. *Gynecol Obstet Invest* **64**, 161-5.

Fauser B.C. (2008) Preimplantation genetic screening: the end of an affair? *Hum Reprod* **23**, 2622-5.

Federico C., Cantarella C.D., Di Mare P., Tosi S. & Saccone S. (2008) The radial arrangement of the human chromosome 7 in the lymphocyte cell nucleus is associated with chromosomal band gene density. *Chromosoma* **117**, 399-410.

Fedorova E. & Zink D. (2009) Nuclear genome organization: common themes and individual patterns. *Curr Opin Genet Dev* **19**, 166-71.

Ferguson-Smith M.A. (2008) Cytogenetics and the evolution of medical genetics. *Genet Med* **10**, 553-9.

Ferlin A., Raicu F., Gatta V., Zuccarello D., Palka G. & Foresta C. (2007) Male infertility: role of genetic background. *Reprod Biomed Online* **14**, 734-45.

Ferrara D.E., Weiss D., Carnell P.H., Vito R.P., Vega D., Gao X., Nie S. & Taylor W.R. (2006) Quantitative 3D fluorescence technique for the analysis of en face preparations of arterial walls using quantum dot nanocrystals and two-photon excitation laser scanning microscopy. *Am J Physiol Regul Integr Comp Physiol* **290**, R114-23.

Finch K.A., Fonseka G., Ioannou D., Hickson N., Barclay Z., Chatzimeletiou K., Mantzouratou A., Handyside A., Delhanty J. & Griffin D.K. (2008a) Nuclear organisation in totipotent human nuclei and its relationship to chromosomal abnormality. *J Cell Sci* **121**, 655-63.

Finch K.A., Fonseka K.G., Abogrein A., Ioannou D., Handyside A.H., Thornhill A.R., Hickson N. & Griffin D.K. (2008b) Nuclear organization in human sperm: preliminary evidence for altered sex chromosome centromere position in infertile males. *Hum Reprod* **23**, 1263-70.

Foster H.A., Abeydeera L.R., Griffin D.K. & Bridger J.M. (2005) Non-random chromosome positioning in mammalian sperm nuclei, with migration of the sex chromosomes during late spermatogenesis. *J Cell Sci* **118**, 1811-20.

Foster H.A. & Bridger J.M. (2005) The genome and the nucleus: a marriage made by evolution. Genome organisation and nuclear architecture. *Chromosoma* **114**, 212-29.

Fragouli E., Alfarawati S., Katz-Jaffe M., Stevens J., Colls P., Goodall N.N., Tormasi S., Gutierrez-Mateo C., Prates R., Schoolcraft W.B., Munne S. & Wells D. (2009) Comprehensive chromosome screening of polar bodies and blastocysts from couples experiencing repeated implantation failure. *Fertil Steril.*

Francastel C., Schubeler D., Martin I.K.D. & Groudine M. (2000) Nuclear compartmentalization and gene activity. *Nature Reviews.Molecular Cell Biology* **1**, 137-43.

Freeman S.B., Allen E.G., Oxford-Wright C.L., Tinker S.W., Druschel C., Hobbs C.A., O'Leary L.A., Romitti P.A., Royle M.H., Torfs C.P. & Sherman S.L. (2007) The National Down Syndrome Project: design and implementation. *Public Health Rep* **122**, 62-72.

Fritz M.A. (2008) Perspectives on the efficacy and indications for preimplantation genetic screening: where are we now? *Hum Reprod* **23**, 2617-21.

Fu A., Alivisatos A.P., Gu W. & Larabell C. (2005) Semiconductor nanocrystals for biological imaging. *Curr Opin Neurobiol* **15**, 568-75.

Gao X., Chan W.C. & Nie S. (2002) Quantum-dot nanocrystals for ultrasensitive biological labeling and multicolor optical encoding. *J Biomed Opt* **7**, 532-7.

Gao X., Cui Y., Levenson R.M., Chung L.W. & Nie S. (2004) In vivo cancer targeting and imaging with semiconductor quantum dots. *Nat Biotechnol* **22**, 969-76.

Gao X., Yang L., Petros J.A., Marshall F.F., Simons J.W. & Nie S. (2005) In vivo molecular and cellular imaging with quantum dots. *Curr Opin Biotechnol* **16**, 63-72.

Garrisi J.G., Colls P., Ferry K.M., Zheng X., Garrisi M.G. & Munne S. (2009) Effect of infertility, maternal age, and number of previous miscarriages on the outcome of preimplantation genetic diagnosis for idiopathic recurrent pregnancy loss. *Fertil Steril* **92**, 288-95.

Geraedts J., Collins J., Gianaroli L., Goossens V., Handyside A., Harper J., Montag M., Repping S. & Schmutzler A. (2009) What next for preimplantation genetic screening? A polar body approach! *Hum Reprod.*

Geraedts J.P. & De Wert G.M. (2009) Preimplantation genetic diagnosis. *Clin Genet* **76**, 315-25.

Gerion D., Parak W.J., Williams S.C., Zanchet D., Micheel C.M. & Alivisatos A.P. (2002) Sorting fluorescent nanocrystals with DNA. *J Am Chem Soc* **124**, 7070-4.

Gerion D., Pinaud F., Williams S.C., Parak W.J., Zanchet D., Weiss S. & Alivisatos A.P. (2001) Synthesis and properties of biocompatible water-soluble silica-coated CdSe/ZnS semiconductor quantum dots. *J. Phys Chem B* **105**, 8861-71.

Gianaroli L., Plachot M., van Kooij R., Al-Hasani S., Dawson K., DeVos A., Magli M.C., Mandelbaum J., Selva J. & van Inzen W. (2000) ESHRE guidelines for good practice in IVF laboratories. Committee of the Special Interest Group on Embryology of the European Society of Human Reproduction and Embryology. *Hum Reprod* **15**, 2241-6.

Goldman E.R., Balighian E.D., Kuno M.K., Labrenz S., Tran P.T., Anderson G.P., Mauro J.M. & Mattoussi H. (2002a) Luminescent quantum dot-adaptor protein-antibody conjugates for use in fluoroimmunoassays. *Phys. Stat. Sol. B* **229**, 407-14.

Goldman E.R., Balighian E.D., Mattoussi H., Kuno M.K., Mauro J.M., Tran P.T. & Anderson G.P. (2002b) Avidin: A Natural Bridge for Quantum Dot-Antibody Conjugates. *J.Am.Chem Soc* **124**, 6378 - 82.

Gole L.A., Wong P.F., Ng P.L., Wang X.Q., Ng S.C. & Bongso A. (2001) Does sperm morphology play a significant role in increased sex chromosomal disomy? A comparison between patients with teratozoospermia and OAT by FISH. *J Androl* **22**, 759-63.

Goossens V., Harton G., Moutou C., Traeger-Synodinos J., Van Rij M. & Harper J.C. (2009) ESHRE PGD Consortium data collection IX: cycles from January to December 2006 with pregnancy follow-up to October 2007. *Hum Reprod* **24**, 1786-810.

Greaves I.K., Rens W., Ferguson-Smith M.A., Griffin D. & Marshall Graves J.A. (2003) Conservation of chromosome arrangement and position of the X in mammalian sperm suggests functional significance. *Chromosome Res* **11**, 503-12.

Green M. (2004) Semiconductor quantum dots as biological imaging agents. *Angew Chem Int Ed Engl* **43**, 4129-31.

Griffin D.K. (1994) Fluorescent in situ hybridization for the diagnosis of genetic disease at postnatal, prenatal, and preimplantation stages. *Int Rev Cytol* **153**, 1-40.

Griffin D.K. (1996) The incidence, origin, and etiology of aneuploidy. *Int Rev Cytol* **167**, 263-96.

Griffin D.K. & Finch K.A. (2005) The genetic and cytogenetic basis of male infertility. *Hum Fertil (Camb)* **8**, 19-26.

Griffin D.K., Handyside A.H., Penketh R.J., Winston R.M. & Delhanty J.D. (1991) Fluorescent in-situ hybridization to interphase nuclei of human preimplantation embryos with X and Y chromosome specific probes. *Hum Reprod* **6**, 101-5.

Griffin D.K., Wilton L.J., Handyside A.H., Atkinson G.H., Winston R.M. & Delhanty J.D. (1993) Diagnosis of sex in preimplantation embryos by fluorescent in situ hybridisation. *Bmj* **306**, 1382.

Guelen L., Pagie L., Brasset E., Meuleman W., Faza M.B., Talhout W., Eussen B.H., de Klein A., Wessels L., de Laat W. & van Steensel B. (2008) Domain

organization of human chromosomes revealed by mapping of nuclear lamina interactions. *Nature* **453**, 948-51.

Haaf T. & Ward D.C. (1995) Higher order nuclear structure in mammalian sperm revealed by in situ hybridization and extended chromatin fibers. *Exp Cell Res* **219**, 604-11.

Habermann F.A., Cremer M., Walter J., Kreth G., von Hase J., Bauer K., Wienberg J., Cremer C., Cremer T. & Solovei I. (2001) Arrangements of macro- and microchromosomes in chicken cells. *Chromosome Res* **9**, 569-84.

Handel M.A. & Schimenti J.C. (2010) Genetics of mammalian meiosis: regulation, dynamics and impact on fertility. *Nat Rev Genet* **11**, 124-36.

Handyside A. & Thornhill A. (2007) In vitro fertilisation with preimplantation genetic screening. *N Engl J Med* **357**, 1770.

Handyside A.H. & Delhanty J.D. (1997) Preimplantation genetic diagnosis: strategies and surprises. *Trends Genet* **13**, 270-5.

Handyside A.H., Harton G.L., Mariani B., Thornhill A.R., Affara N.A., Shaw M.A. & Griffin D.K. (2009) Karyomapping: a Universal Method for Genome Wide Analysis of Genetic Disease based on Mapping Crossovers between Parental Haplotypes. *J Med Genet.*

Handyside A.H., Kontogianni E.H., Hardy K. & Winston R.M. (1990) Pregnancies from biopsied human preimplantation embryos sexed by Y-specific DNA amplification. *Nature* **344**, 768-70.

Hardarson T., Hanson C., Lundin K., Hillensjo T., Nilsson L., Stevic J., Reismer E., Borg K., Wikland M. & Bergh C. (2008) Preimplantation genetic screening in women of advanced maternal age caused a decrease in clinical pregnancy rate: a randomized controlled trial. *Hum Reprod* **23**, 2806-12.

Harper J., Coonen E., De Rycke M., Fiorentino F., Geraedts J., Goossens V., Harton G., Moutou C., Pehlivan Budak T., Renwick P., Sengupta S., Traeger-Synodinos J. & Vesela K. (2010a) What next for preimplantation genetic screening (PGS)? A position statement from the ESHRE PGD Consortium steering committee. *Hum Reprod.*

Harper J., Goossens V. & Harton G. (2010b) Data from the ESHRE PDG consortium. In: *ESHRE* pp. i17-i8. Oxford University Press, Rome.

Harper J., Sermon K., Geraedts J., Vesela K., Harton G., Thornhill A., Pehlivan T., Fiorentino F., SenGupta S., de Die-Smulders C., Magli C., Moutou C. & Wilton L. (2008) What next for preimplantation genetic screening? *Hum Reprod* **23**, 478-80.

Harper J.C. & Harton G. (2010) The use of arrays in preimplantation genetic diagnosis and screening. *Fertil Steril.*

Hassold T., Abruzzo M., Adkins K., Griffin D., Merrill M., Millie E., Saker D., Shen J. & Zaragoza M. (1996) Human aneuploidy: incidence, origin, and etiology. *Environ Mol Mutagen* **28**, 167-75.

Hassold T., Hall H. & Hunt P. (2007) The origin of human aneuploidy: where we have been, where we are going. *Hum Mol Genet* **16 Spec No 2**, R203-8.

Hassold T. & Hunt P. (2001) To err (meiotically) is human: the genesis of human aneuploidy. *Nat Rev Genet* **2**, 280-91.

Hassold T. & Hunt P. (2009) Maternal age and chromosomally abnormal pregnancies: what we know and what we wish we knew. *Curr Opin Pediatr* **21**, 703-8.

Hassold T.J., Sherman S.L., Pettay D., Page D.C. & Jacobs P.A. (1991) XY chromosome nondisjunction in man is associated with diminished recombination in the pseudoautosomal region. *Am J Hum Genet* **49**, 253-60.

Hazzouri M., Rousseaux S., Mongelard F., Usson Y., Pelletier R., Faure A.K., Vourc'h C. & Sele B. (2000) Genome organization in the human sperm nucleus studied by FISH and confocal microscopy. *Mol Reprod Dev* **55**, 307-15.

Heard E. & Bickmore W. (2007) The ins and outs of gene regulation and chromosome territory organisation. *Curr Opin Cell Biol* **19**, 311-6.

Hernandez E.R. (2009) What next for preimplantation genetic screening? Beyond aneuploidy. *Hum Reprod*.

Hohng S. & Ha T. (2004) Near-complete suppression of quantum dot blinking in ambient conditions. *J Am Chem Soc* **126**, 1324-5.

Hulten M.A., Patel S.D., Tankimanova M., Westgren M., Papadogiannakis N., Jonsson A.M. & Iwarsson E. (2008) On the origin of trisomy 21 Down syndrome. *Mol Cytogenet* **1**, 21.

Hunt P.A. (1998) The control of mammalian female meiosis: factors that influence chromosome segregation. *J Assist Reprod Genet* **15**, 246-52.

Hunt P.A. (2006) Meiosis in mammals: recombination, non-disjunction and the environment. *Biochem Soc Trans* **34**, 574-7.

Hunt P.A. & Hassold T.J. (2008) Human female meiosis: what makes a good egg go bad? *Trends Genet* **24**, 86-93.

Invitrogen (2006) Qdot Nanocrystal Technology. URL http://probes.invitrogen.com/products/qdot/overview.html.

Ioannou D. & Griffin D.K. (2010a) Male Fertility, Chromosome Abnormalities, and Nuclear Organization. *Cytogenet Genome Res*.

Ioannou D. & Griffin D.K. (2010b) Nanotechnology and molecular cytogenetics: the future has not yet arrived. In: *Nano Reviews*.

Ioannou D., Tempest H.G., Skinner B.M., Thornhill A.R., Ellis M. & Griffin D.K. (2009) Quantum dots as new-generation fluorochromes for FISH: an appraisal. *Chromosome Res* **17**, 519-30.

Jaiswal J.K., Mattoussi H., Mauro J.M. & Simon S.M. (2003) Long-term multiple color imaging of live cells using quantum dot bioconjugates. *Nat Biotechnol* **21**, 47-51.

Jaiswal J.K. & Simon S.M. (2004) Potentials and pitfalls of fluorescent quantum dots for biological imaging. *Trends Cell Biol* **14**, 497-504.

Jansen R.P., Bowman M.C., de Boer K.A., Leigh D.A., Lieberman D.B. & McArthur S.J. (2008) What next for preimplantation genetic screening (PGS)? Experience with blastocyst biopsy and testing for aneuploidy. *Hum Reprod* **23**, 1476-8.

Julien C., Bazin A., Guyot B., Forestier F. & Daffos F. (1986) Rapid prenatal diagnosis of Down's syndrome with in-situ hybridisation of fluorescent DNA probes. *Lancet* **2**, 863-4.

Kalmarova M., Smirnov E., Kovacik L., Popov A. & Raska I. (2008) Positioning of the NOR-bearing chromosomes in relation to nucleoli in daughter cells after mitosis. *Physiol Res* **57**, 421-5.

Kalmarova M., Smirnov E., Masata M., Koberna K., Ligasova A., Popov A. & Raska I. (2007) Positioning of NORs and NOR-bearing chromosomes in relation to nucleoli. *J Struct Biol*.

Kanavakis E. & Traeger-Synodinos J. (2002) Preimplantation genetic diagnosis in clinical practise. *Journal of Medical Genetics* **39**, 6-11.

Kang W.J., Chae J.R., Cho Y.L., Lee J.D. & Kim S. (2009) Multiplex imaging of single tumor cells using quantum-dot-conjugated aptamers. *Small* **5**, 2519-22.

Khalil A., Grant J.L., Caddle L.B., Atzema E., Mills K.D. & Arneodo A. (2007) Chromosome territories have a highly nonspherical morphology and nonrandom positioning. *Chromosome Res* **15**, 899-916.

Kim S. & Bawendi M.G. (2003) Oligomeric ligands for luminescent and stable nanocrystal quantum dots. *J Am Chem Soc* **125**, 14652-3.

Kim S., Lim Y.T., Soltesz E.G., De Grand A.M., Lee J., Nakayama A., Parker J.A., Mihaljevic T., Laurence R.G., Dor D.M., Cohn L.H., Bawendi M.G. & Frangioni J.V. (2004) Near-infrared fluorescent type II quantum dots for sentinel lymph node mapping. *Nat Biotechnol* **22**, 93-7.

Koehler D., Zakhartchenko V., Froenicke L., Stone G., Stanyon R., Wolf E., Cremer T. & Brero A. (2009) Changes of higher order chromatin arrangements during major genome activation in bovine preimplantation embryos. *Exp Cell Res* **315**, 2053-63.

Krieg S.A., Lathi R.B., Behr B. & Westphal L.M. (2009) Normal pregnancy after tetraploid karyotype on trophectoderm biopsy. *Fertil Steril.*

Kuroda M., Tanabe H., Yoshida K., Oikawa K., Saito A., Kiyuna T., Mizusawa H. & Mukai K. (2004) Alteration of chromosome positioning during adipocyte differentiation. *J Cell Sci* **117**, 5897-903.

Langer P.R., Waldrop A.A. & Ward D.C. (1981) Enzymatic synthesis of biotin-labeled polynucleotides: novel nucleic acid affinity probes. *Proc Natl Acad Sci U S A* **78**, 6633-7.

Larson D.R., Zipfel W.R., Williams R.M., Clark S.W., Bruchez M.P., Wise F.W. & Webb W.W. (2003) Water-soluble quantum dots for multiphoton fluorescence imaging in vivo. *Science* **300**, 1434-6.

Lee S.F. & Osborne M.A. (2009) Brightening, blinking, bluing and bleaching in the life of a quantum dot: friend or foe? *Chemphyschem* **10**, 2174-91.

Li C., Shi Z., Zhang L., Huang Y., Liu A., Jin Y., Yu Y., Bai J., Chen D., Gendron C., Liu X. & Fu S. (2009) Dynamic changes of territories 17 and 18 during EBV-infection of human lymphocytes. *Mol Biol Rep.*

Li Z., Haines C.J. & Han Y. (2008) "Micro-deletions" of the human Y chromosome and their relationship with male infertility. *J Genet Genomics* **35**, 193-9.

Lichter J.B., Difilippantonio M.J., Pakstis A.J., Goodfellow P.J., Ward D.C. & Kidd K.K. (1993) Physical and genetic maps for chromosome 10. *Genomics* **16**, 320-4.

Lidke D.S., Nagy P., Heintzmann R., Arndt-Jovin D.J., Post J.N., Grecco H.E., Jares-Erijman E.A. & Jovin T.M. (2004) Quantum dot ligands provide new insights into erbB/HER receptor-mediated signal transduction. *Nat Biotechnol* **22**, 198-203.

Liebaers I., Desmyttere S., Verpoest W., De Rycke M., Staessen C., Sermon K., Devroey P., Haentjens P. & Bonduelle M. (2009) Report on a consecutive series of 581 children born after blastomere biopsy for preimplantation genetic diagnosis. *Hum Reprod.*

Lieberman-Aiden E., van Berkum N.L., Williams L., Imakaev M., Ragoczy T., Telling A., Amit I., Lajoie B.R., Sabo P.J., Dorschner M.O., Sandstrom R., Bernstein B., Bender M.A., Groudine M., Gnirke A., Stamatoyannopoulos J., Mirny L.A., Lander E.S. & Dekker J. (2009) Comprehensive mapping of long-range interactions reveals folding principles of the human genome. *Science* **326**, 289-93.

Lipovskii A., Kolobkova E., Petrikov V., Kang I., Olkhovets A., Krauss T., Thomas M., Silcox J. & Wise F. (1997) Synthesis and characterization of PbSe quantum dots in phosphate glass. *Appl Phys Lett* **71**, 3406-8.

Liu C.H., Tsao H.M., Cheng T.C., Wu H.M., Huang C.C., Chen C.I., Lin D.P. & Lee M.S. (2004) DNA fragmentation, mitochondrial dysfunction and chromosomal aneuploidy in the spermatozoa of oligoasthenoteratozoospermic males. *J Assist Reprod Genet* **21**, 119-26.

Lorda-Sanchez I., Binkert F., Maechler M., Robinson W.P. & Schinzel A.A. (1992) Reduced recombination and paternal age effect in Klinefelter syndrome. *Hum Genet* **89**, 524-30.

Los F.J., Van Opstal D. & van den Berg C. (2004) The development of cytogenetically normal, abnormal and mosaic embryos: a theoretical model. *Hum Reprod Update* **10**, 79-94.

Lounis B., Bechtel H.A., Gerion D., Alivisatos P.A. & Moerner W.E. (2000) Photon antibunching in single CdSe/ZnS quantum dot fluorescence. *Chem Phys Lett* **329**, 399 - 404.

Loutradi K.E., Kolibianakis E.M., Venetis C.A., Papanikolaou E.G., Pados G., Bontis I. & Tarlatzis B.C. (2008) Cryopreservation of human embryos by vitrification or slow freezing: a systematic review and meta-analysis. *Fertil Steril* **90**, 186-93.

Luetjens C.M., Payne C. & Schatten G. (1999) Non-random chromosome positioning in human sperm and sex chromosome anomalies following intracytoplasmic sperm injection. *Lancet* **353**, 1240.

Lukasova E., Kozubek S., Kozubek M., Falk M. & Amrichova J. (2002) The 3D structure of human chromosomes in cell nuclei. *Chromosome Res* **10**, 535-48.

Ma L., Wu S.M., Huang J., Ding Y., Pang D.W. & Li L. (2008) Fluorescence in situ hybridization (FISH) on maize metaphase chromosomes with quantum dot-labeled DNA conjugates. *Chromosoma* **117**, 181-7.

Magli M.C., Van den Abbeel E., Lundin K., Royere D., Van der Elst J. & Gianaroli L. (2008) Revised guidelines for good practice in IVF laboratories. *Hum Reprod* **23**, 1253-62.

Mahmoud W., Sukhanova A., Oleinikov V., Rakovich Y.P., Donegan J.F., Pluot M., Cohen J.H., Volkov Y. & Nabiev I. (2009) Emerging applications of fluorescent nanocrystals quantum dots for micrometastases detection. *Proteomics*.

Mansson A., Sundberg M., Balaz M., Bunk R., Nicholls I.A., Omling P., Tagerud S. & Montelius L. (2004) In vitro sliding of actin filaments labelled with single quantum dots. *Biochem Biophys Res Commun* **314**, 529-34.

Manuelidis L. (1990) A view of interphase chromosomes. *Science* **250**, 1533-40.

Manvelyan M., Hunstig F., Bhatt S., Mrasek K., Pellestor F., Weise A., Simonyan I., Aroutiounian R. & Liehr T. (2008) Chromosome distribution in human sperm - a 3D multicolor banding-study. *Mol Cytogenet* **1**, 25.

Marella N.V., Bhattacharya S., Mukherjee L., Xu J. & Berezney R. (2009a) Cell type specific chromosome territory organization in the interphase nucleus of normal and cancer cells. *J Cell Physiol* **221**, 130-8.

Marella N.V., Seifert B., Nagarajan P., Sinha S. & Berezney R. (2009b) Chromosomal rearrangements during human epidermal keratinocyte differentiation. *J Cell Physiol* **221**, 139-46.

Marquez C., Sandalinas M., Bahce M., Alikani M. & Munne S. (2000) Chromosome abnormalities in 1255 cleavage-stage human embryos. *Reprod Biomed Online* **1**, 17-26.

Marshall W.F. (2002) Order and disorder in the nucleus. *Curr Biol* **12**, R185-92.

Martin C., Beaujean N., Brochard V., Audouard C., Zink D. & Debey P. (2006a) Genome restructuring in mouse embryos during reprogramming and early development. *Dev Biol* **292**, 317-32.

Martin C., Brochard V., Migne C., Zink D., Debey P. & Beaujean N. (2006b) Architectural reorganization of the nuclei upon transfer into oocytes accompanies genome reprogramming. *Mol Reprod Dev* **73**, 1102-11.

Martin R.H. (2003) Chromosome abnormalities in human sperm. *Adv Exp Med Biol* **518**, 181-8.

Martin R.H. (2005) Mechanisms of nondisjunction in human spermatogenesis. *Cytogenet Genome Res* **111**, 245-9.

Martin R.H. (2006) Meiotic chromosome abnormalities in human spermatogenesis. *Reprod Toxicol* **22**, 142-7.

Martin R.H. (2008) Meiotic errors in human oogenesis and spermatogenesis. *Reprod Biomed Online* **16**, 523-31.

Martin R.H., Ko E. & Rademaker A. (1991) Distribution of aneuploidy in human gametes: comparison between human sperm and oocytes. *Am J Med Genet* **39**, 321-31.

Mason J.N., Tomlinson I.D., Rosenthal S.J. & Blakely R.D. (2005) Labeling cell-surface proteins via antibody quantum dot streptavidin conjugates. *Methods Mol Biol* **303**, 35-50.

Mastenbroek S., Twisk M., van Echten-Arends J., Sikkema-Raddatz B., Korevaar J.C., Verhoeve H.R., Vogel N.E., Arts E.G., de Vries J.W., Bossuyt P.M., Buys C.H., Heineman M.J., Repping S. & van der Veen F. (2007) In vitro fertilization with preimplantation genetic screening. *N Engl J Med* **357**, 9-17.

Mattheakis L.C., Dias J.M., Choi Y.J., Gong J., Bruchez M.P., Liu J. & Wang E. (2004) Optical coding of mammalian cells using semiconductor quantum dots. *Anal Biochem* **327**, 200-8.

McKenzie L.J., Carson S.A., Marcelli S., Rooney E., Cisneros P., Torskey S., Buster J., Simpson J.L. & Bischoff F.Z. (2004) Nuclear chromosomal localization in human preimplantation embryos: correlation with aneuploidy and embryo morphology. *Hum Reprod* **19**, 2231-7.

Meaburn K.J., Levy N., Toniolo D. & Bridger J.M. (2005) Chromosome positioning is largely unaffected in lymphoblastoid cell lines containing emerin or A-type lamin mutations. *Biochem Soc Trans* **33**, 1438-40.

Meaburn K.J. & Misteli T. (2007) Cell biology: chromosome territories. *Nature* **445**, 379-781.

Meaburn K.J., Newbold R.F. & Bridger J.M. (2008) Positioning of human chromosomes in murine cell hybrids according to synteny. *Chromosoma*.

Meistrich M.L., Mohapatra B., Shirley C.R. & Zhao M. (2003) Roles of transition nuclear proteins in spermiogenesis. *Chromosoma* **111**, 483-8.

Mersereau J.E., Pergament E., Zhang X. & Milad M.P. (2008) Preimplantation genetic screening to improve in vitro fertilization pregnancy rates: a prospective randomized controlled trial. *Fertil Steril* **90**, 1287-9.

Meyer-Ficca M., Muller-Navia J. & Scherthan H. (1998) Clustering of pericentromeres initiates in step 9 of spermiogenesis of the rat (Rattus

norvegicus) and contributes to a well defined genome architecture in the sperm nucleus. *J Cell Sci* **111 (Pt 10)**, 1363-70.

Michalet X., Pinaud F., Thilo D.L., Dahan M., Bruchez M.P., Alivisatos A.P. & Weiss S. (2001) Properties of Fluorescent Semiconductor Nanocrystals and their Application to Biological Labeling. *Single Molecules* **2**, 261-76.

Michalet X., Pinaud F.F., Bentolila L.A., Tsay J.M., Doose S., Li J.J., Sundaresan G., Wu A.M., Gambhir S.S. & Weiss S. (2005) Quantum dots for live cells, in vivo imaging, and diagnostics. *Science* **307**, 538-44.

Michler P., Imamoglu A., Mason M.D., Carson P.J., Strouse G.F. & Buratto S.K. (2000) Quantum correlation among photons from a single quantum dot at room temperature. *Nature* **406**, 968-70.

Middelburg K.J., Jan Heineman M., Haadsma M.L., Bos A.F., Kok J.H. & Hadders-Algra M. (2010) Neurological condition of infants born after in vitro fertilization with preimplantation genetic screening. *Pediatr Res.*

Miller D., Brinkworth M. & Iles D. (2010) Paternal DNA packaging in spermatozoa: more than the sum of its parts? DNA, histones, protamines and epigenetics. *Reproduction* **139**, 287-301.

Miller D.A.B., Chemla D.S. & Schmittrink S. (1986) Absorption Saturation of Semiconductor Quantum Dots. *J.Opt. Soc. Am. B* **3**, 42 Part 2.

Mir P., Rodrigo L., Cervero A., Mercader A., Delgado A., Buendia P., Pellicer A., Rubio C. & Martin J. (2010a) Validation of aeeayCGH on day-4 single blastomeres from day-3 embryos diagnoses as abnormal by FISH. In: *ESHRE* pp. i61-i3. Oxford University Press, Rome.

Mir P., Rodrigo L., Mateu E., Peinado V., Milan M., Mercader A., Buendia P., Delgado A., Pellicer A., Remohi J. & Rubio C. (2010b) Improving FISH diagnosis for preimplantation genetic aneuploidy screening. *Hum Reprod.*

Misteli T. (2005) Concepts in nuclear architecture. *Bioessays* **27**, 477-87.

Moosani N., Pattinson H.A., Carter M.D., Cox D.M., Rademaker A.W. & Martin R.H. (1995) Chromosomal analysis of sperm from men with idiopathic infertility using sperm karyotyping and fluorescence in situ hybridization. *Fertil Steril* **64**, 811-7.

Mora L., Sanchez I., Garcia M. & Ponsa M. (2006) Chromosome territory positioning of conserved homologous chromosomes in different primate species. *Chromosoma* **115**, 367-75.

Mudrak O., Chandra R., Jones E., Godfrey E. & Zalensky A. (2009) Reorganisation of human sperm nuclear architecture during formation of pronuclei in a model system. *Reprod Fertil Dev* **21**, 665-71.

Mudrak O., Tomilin N. & Zalensky A. (2005) Chromosome architecture in the decondensing human sperm nucleus. *J Cell Sci* **118**, 4541-50.

Muller F., Houben A., Barker P.E., Xiao Y., Kas J.A. & Melzer M. (2006) Quantum dots - a versatile tool in plant science? *J Nanobiotechnology* **4**, 5.

Muller S., Cremer M., Neusser M., Grasser F. & Cremer T. (2009) A Technical Note on Quantum Dots for Multi-Color Fluorescence in situ Hybridization. *Cytogenetic Genome Research* **124**, 351-9.

Munne S. (2003) Preimplantation genetic diagnosis and human implantation--a review. *Placenta* **24 Suppl B**, S70-6.

Munne S., Alikani M., Tomkin G., Grifo J. & Cohen J. (1995) Embryo morphology, developmental rates, and maternal age are correlated with chromosome abnormalities. *Fertil Steril* **64**, 382-91.

Munne S., Bahce M., Sandalinas M., Escudero T., Marquez C., Velilla E., Colls P., Oter M., Alikani M. & Cohen J. (2004) Differences in chromosome susceptibility to aneuploidy and survival to first trimester. *Reprod Biomed Online* **8**, 81-90.

Munne S., Chen S., Colls P., Garrisi J., Zheng X., Cekleniak N., Lenzi M., Hughes P., Fischer J., Garrisi M., Tomkin G. & Cohen J. (2007a) Maternal age, morphology, development and chromosome abnormalities in over 6000 cleavage-stage embryos. *Reprod Biomed Online* **14**, 628-34.

Munne S., Cohen J. & Simpson J.L. (2007b) In vitro fertilization with preimplantation genetic screening. *N Engl J Med* **357**, 1769-70.

Munne S., Fragouli E., Colls P., Katz-Jaffe M.G., W.B. S. & Wells D. (2010) Improved detection of aneuploid blastocysts using a new 12-chromosome FISH test. *Reproductive Biomedicine Online* **20**.

Munne S., Gianaroli L., Tur-Kaspa I., Magli C., Sandalinas M., Grifo J., Cram D., Kahraman S., Verlinsky Y. & Simpson J.L. (2007c) Substandard application of preimplantation genetic screening may interfere with its clinical success. *Fertil Steril* **88**, 781-4.

Munne S., Grifo J., Cohen J. & Weier H.U. (1994a) Chromosome abnormalities in human arrested preimplantation embryos: a multiple-probe FISH study. *Am J Hum Genet* **55**, 150-9.

Munne S., Weier H.U., Grifo J. & Cohen J. (1994b) Chromosome mosaicism in human embryos. *Biol Reprod* **51**, 373-9.

Murray C.B., Kagan C.R. & Bawendi M. (2000) Synthesis and characterization of monodisperse nanocrystals and close-packed nanocrystal assemblies. *Annual Review of Materials Science* **30**, 545-610.

Murray C.B., Norris D.J. & Bawendi M.G. (1993) Synthesis and characterization of nearly monodisperse CdE (E = S, Se, Te) semiconductor nanocrystallites. *J. Am. Chem. Soc.* **115**, 8706-15.

O'Flynn O' Brien K.L., Varghese A.C. & Agarwal A. (2010) The genetic causes of male factor infertility: A review. *Fertility and Sterility* **93**, 1-12.

O'Keefe C.L., Griffin D.K., Bean C.J., Matera A.G. & Hassold T.J. (1997) Alphoid variant-specific FISH probes can distinguish autosomal meiosis I from meiosis II non-disjunction in human sperm. *Hum Genet* **101**, 61-6.

Oliver B. & Misteli T. (2005) A non-random walk through the genome. *Genome Biol* **6**, 214.

Olszewska M., Wiland E. & Kurpisz M. (2008) Positioning of chromosome 15, 18, X and Y centromeres in sperm cells of fertile individuals and infertile patients with increased level of aneuploidy. *Chromosome Res* **16**, 875-90.

Osaki F., Kanamori T., Sando S., Sera T. & Aoyama Y. (2004) A quantum dot conjugated sugar ball and its cellular uptake. On the size effects of endocytosis in the subviral region. *J Am Chem Soc* **126**, 6520-1.

Palermo G., Joris H., Devroey P. & Van Steirteghem A.C. (1992) Pregnancies after intracytoplasmic injection of single spermatozoon into an oocyte. *Lancet* **340**, 17-8.

Palermo G.D., Colombero L.T. & Rosenwaks Z. (1997) The human sperm centrosome is responsible for normal syngamy and early embryonic development. *Rev Reprod* **2**, 19-27.

Pang M.G., Hoegerman S.F., Cuticchia A.J., Moon S.Y., Doncel G.F., Acosta A.A. & Kearns W.G. (1999) Detection of aneuploidy for chromosomes 4, 6, 7, 8, 9, 10, 11, 12, 13, 17, 18, 21, X and Y by fluorescence in-situ hybridization in

spermatozoa from nine patients with oligoasthenoteratozoospermia undergoing intracytoplasmic sperm injection. *Hum Reprod* **14**, 1266-73.

Parada L. & Misteli T. (2002) Chromosome positioning in the interphase nucleus. *Trends Cell Biol* **12**, 425-32.

Parada L.A., McQueen P.G. & Misteli T. (2004) Tissue-specific spatial organization of genomes. *Genome Biol* **5**, R44.

Parak W.J., Boudreau R., Le Gros M.A., Gerion D., Zanchet D., Micheel C.M., Williams S.C., A.P. A. & Larabell C.A. (2002) Cell motility and metastatic potential studies based on quantum dot imaging of phagokinetic tracks. *Adv Mater* **14**, 882-5.

Parak W.J., Gerion D., Pellegrino T., Zanchet D., Micheel C., Williams S.C., Boudreau R., Le Gros M.A., Larabell C.A. & Alivisatos P.A. (2003) Biological applications of colloidal nanocrystals. *Nanotechnology* **14**, R15–R27.

Parak W.J., Pellegrino T. & Plank C. (2005) Labelling of cells with quantum dots. *Nanotechnology* **16**, R9–R25.

Pardue M.L. & Gall J.G. (1969) Molecular hybridization of radioactive DNA to the DNA of cytological preparations. *Proc Natl Acad Sci U S A* **64**, 600-4.

Pathak S., Choi S.K., Arnheim N. & Thompson M.E. (2001) Hydroxylated quantum dots as luminescent probes for in situ hybridization. *J Am Chem Soc* **123**, 4103-4.

Pellegrino T., Manna L., Kudera S., Liedl T., Koktysh D., Rogach A.L., Keller S., Radler J., Natile G. & Parak W.J. (2004) Hydrophobic nanocrystals coated with an amphiphilic polymer shell: A general route to water soluble nanocrystals. *Nano Lett* **4**, 703-7.

Pellestor F., Andreo B., Arnal F., Humeau C. & Demaille J. (2002) Mechanisms of non-disjunction in human female meiosis: the co-existence of two modes of malsegregation evidenced by the karyotyping of 1397 in-vitro unfertilized oocytes. *Hum Reprod* **17**, 2134-45.

Perry M.J., Chen X. & Lu X. (2007) Automated scoring of multiprobe FISH in human spermatozoa. *Cytometry A* **71**, 968-72.

Petit F.M., Frydman N., Benkhalifa M., Le Du A., Aboura A., Fanchin R., Frydman R. & Tachdjian G. (2005) Could sperm aneuploidy rate determination be used as a predictive test before intracytoplasmic sperm injection? *J Androl* **26**, 235-41.

Petrova N.V., Yakutenko, II, Alexeevski A.V., Verbovoy V.A., Razin S.V. & Iarovaia O.V. (2007) Changes in chromosome positioning may contribute to the development of diseases related to X-chromosome aneuploidy. *J Cell Physiol.*

Pfeffer J., Pang M.G., Hoegerman S.F., Osgood C.J., Stacey M.W., Mayer J., Oehninger S. & Kearns W.G. (1999) Aneuploidy frequencies in semen fractions from ten oligoasthenoteratozoospermic patients donating sperm for intracytoplasmic sperm injection. *Fertil Steril* **72**, 472-8.

Pinaud F., King D., Moore H.P. & Weiss S. (2004) Bioactivation and cell targeting of semiconductor CdSe/ZnS nanocrystals with phytochelatin-related peptides. *J Am Chem Soc* **126**, 6115-23.

Pinaud F., Michalet X., Bentolila L.A., Tsay J.M., Doose S., Li J.J., Iyer G. & Weiss S. (2006) Advances in fluorescence imaging with quantum dot bio-probes. *Biomaterials* **27**, 1679-87.

Pinkel D., Straume T. & Gray J.W. (1986) Cytogenetic analysis using quantitative, high-sensitivity, fluorescence hybridization. *Proc Natl Acad Sci U S A* **83**, 2934-8.

Plastira K., Msaouel P., Angelopoulou R., Zanioti K., Plastiras A., Pothos A., Bolaris S., Paparisteidis N. & Mantas D. (2007) The effects of age on DNA fragmentation, chromatin packaging and conventional semen parameters in spermatozoa of oligoasthenoteratozoospermic patients. *J Assist Reprod Genet* **24**, 437-43.

QuantumDotCorporation (2006) Qdot Nanocrystals. URL http://www.qdots.com/live/render/content.asp?id=71.

Ravel C., Chantot-Bastaraud S., El Houate B., Rouba H., Legendre M., Lorenco D., Mandelbaum J., Siffroi J.P. & McElreavey K. (2009) Y-chromosome AZFc structural architecture and relationship to male fertility. *Fertil Steril* **92**, 1924-33.

Reddy K.L., Zullo J.M., Bertolino E. & Singh H. (2008) Transcriptional repression mediated by repositioning of genes to the nuclear lamina. *Nature* **452**, 243-7.

Reed M.A., Bate R.T., Bradshaw W.M., Duncan W.R., Frensley J.W.L. & Shih H.D. (1986) Spatial quantization in GaAs-AlGaAs multiple quantum dots. *J. Vac. Sci. Technol. B* **4**, 358-60.

Resch-Genger U., Grabolle M., Cavaliere-Jaricot S., Nitschke R. & Nann T. (2008) Quantum dots versus organic dyes as fluorescent labels. *Nat Methods* **5**, 763-75.

Rezazadeh Valojerdi M., Eftekhari-Yazdi P., Karimian L., Hassani F. & Movaghar B. (2009) Vitrification versus slow freezing gives excellent survival, post warming embryo morphology and pregnancy outcomes for human cleaved embryos. *J Assist Reprod Genet.*

Rieger S., Kulkarni R.P., Darcy D., Fraser S.E. & Koster R.W. (2005) Quantum dots are powerful multipurpose vital labeling agents in zebrafish embryos. *Dev Dyn* **234**, 670-81.

Rodrigo L., Peinado V., Mateu E., Remohi J., Pellicer A., Simon C., Gil-Salom M. & Rubio C. (2009) Impact of different patterns of sperm chromosomal abnormalities on the chromosomal constitution of preimplantation embryos. *Fertil Steril.*

Sanchez-Castro M., Jimenez-Macedo A.R., Sandalinas M. & Blanco J. (2009) Prognostic value of sperm fluorescence in situ hybridization analysis over PGD. *Hum Reprod.*

Sbracia M., Baldi M., Cao D., Sandrelli A., Chiandetti A., Poverini R. & Aragona C. (2002) Preferential location of sex chromosomes, their aneuploidy in human sperm, and their role in determining sex chromosome aneuploidy in embryos after ICSI. *Hum Reprod* **17**, 320-4.

Schneider R. & Grosschedl R. (2007) Dynamics and interplay of nuclear architecture, genome organization, and gene expression. *Genes Dev* **21**, 3027-43.

Schoolcraft W.B., Fragouli E., Stevens J., Munne S., Katz-Jaffe M.G. & Wells D. (2009a) Clinical application of comprehensive chromosomal screening at the blastocyst stage. *Fertil Steril.*

Schoolcraft W.B., Katz-Jaffe M.G., Stevens J., Rawlins M. & Munne S. (2009b) Preimplantation aneuploidy testing for infertile patients of advanced maternal age: a randomized prospective trial. *Fertil Steril* **92**, 157-62.

Seli E. & Sakkas D. (2005) Spermatozoal nuclear determinants of reproductive outcome: implications for ART. *Hum Reprod Update* **11**, 337-49.

Sermondade N. & Mandelbaum J. (2009) [Mastenbroek controversy or how much ink is spilled on preimplantation genetic screening subject.]. *Gynecol Obstet Fertil.*

Shah K., Sivapalan G., Gibbons N., Tempest H. & Griffin D.K. (2003) The genetic basis of infertility. *Reproduction* **126**, 13-25.

Shi Q. & Martin R.H. (2000) Aneuploidy in human sperm: a review of the frequency and distribution of aneuploidy, effects of donor age and lifestyle factors. *Cytogenet Cell Genet* **90**, 219-26.

Shi Q., Spriggs E., Field L.L., Ko E., Barclay L. & Martin R.H. (2001) Single sperm typing demonstrates that reduced recombination is associated with the production of aneuploid 24,XY human sperm. *Am J Med Genet* **99**, 34-8.

Simpson J.L. (2008) What next for preimplantation genetic screening? Randomized clinical trial in assessing PGS: necessary but not sufficient. *Hum Reprod* **23**, 2179-81.

Singhal S., Nie S. & Wang M.D. (2010) Nanotechnology applications in surgical oncology. *Annu Rev Med* **61**, 359-73.

Skinner B.M. (2009) Comparative cytogenomics between chicken and duck: wider insights into genome evolution and organisation. In: *Biosciences*, p. 210. University of Kent, Canterbury.

Skinner B.M., Volker M., Ellis M. & Griffin D.K. (2009) An Appraisal of Nuclear Organisation in Interphase Embryonic Fibroblasts of Chicken, Turkey and Duck. *Cytogenet Genome Res* **126**, 156-64.

Solov'eva L., Svetlova M., Bodinski D. & Zalensky A.O. (2004) Nature of telomere dimers and chromosome looping in human spermatozoa. *Chromosome Res* **12**, 817-23.

Solovei I., Kreysing M., Lanctot C., Kosem S., Peichl L., Cremer T., Guck J. & Joffe B. (2009) Nuclear architecture of rod photoreceptor cells adapts to vision in mammalian evolution. *Cell* **137**, 356-68.

Stack S.M., Brown D.B. & Dewey W.C. (1977) Visualization of interphase chromosomes. *J Cell Sci* **26**, 281-99.

Staessen C., Platteau P., Van Assche E., Michiels A., Tournaye H., Camus M., Devroey P., Liebaers I. & Van Steirteghem A. (2004) Comparison of blastocyst transfer with or without preimplantation genetic diagnosis for aneuploidy screening in couples with advanced maternal age: a prospective randomized controlled trial. *Hum Reprod* **19**, 2849-58.

Staessen C., Verpoest W., Donoso P., Haentjens P., Van der Elst J., Liebaers I. & Devroey P. (2008) Preimplantation genetic screening does not improve delivery rate in women under the age of 36 following single-embryo transfer. *Hum Reprod* **23**, 2818-25.

Steptoe P.C. & Edwards R.G. (1978) Birth after the reimplantation of a human embryo. *Lancet* **2**, 366.

Storeng R.T., Plachot M., Theophile D., Mandelbaum J., Belaisch-Allart J. & Vekemans M. (1998) Incidence of sex chromosome abnormalities in spermatozoa from patients entering an IVF or ICSI protocol. *Acta Obstet Gynecol Scand* **77**, 191-7.

Sullivan K.F. (2001) A solid foundation: functional specialization of centromeric chromatin. *Curr Opin Genet Dev* **11**, 182-8.

Sumner A.T., Evans H.J. & Buckland R.A. (1971) New technique for distinguishing between human chromosomes. *Nat New Biol* **232**, 31-2.

Sun F., Mikhaail-Philips M., Oliver-Bonet M., Ko E., Rademaker A., Turek P. & Martin R.H. (2008) The relationship between meiotic recombination in human spermatocytes and aneuploidy in sperm. *Hum Reprod* **23**, 1691-7.

Sun F., Trpkov K., Rademaker A., Ko E. & Martin R.H. (2005) Variation in meiotic recombination frequencies among human males. *Hum Genet* **116**, 172-8.

Sun H.B., Shen J. & Yokota H. (2000) Size-dependent positioning of human chromosomes in interphase nuclei. *Biophys J* **79**, 184-90.

Sutcliffe A.G. (2000) Intracytoplasmic sperm injection and other aspects of new reproductive technologies. *Arch Dis Child* **83**, 98-101.

Szczerbal I., Foster H.A. & Bridger J.M. (2009) The spatial repositioning of adipogenesis genes is correlated with their expression status in a porcine mesenchymal stem cell adipogenesis model system. *Chromosoma* **118**, 647-63.

Takeda M., Tada H., Higuchi H., Kobayashi Y., Kobayashi M., Sakurai Y., Ishida T. & Ohuchi N. (2008) In vivo single molecular imaging and sentinel node navigation by nanotechnology for molecular targeting drug-delivery systems and tailor-made medicine. *Breast Cancer* **15**, 145-52.

Takizawa T., Meaburn K.J. & Misteli T. (2008) The meaning of gene positioning. *Cell* **135**, 9-13.

Tanabe H., Kupper K., Ishida T., Neusser M. & Mizusawa H. (2005) Inter- and intra-specific gene-density-correlated radial chromosome territory arrangements are conserved in Old World monkeys. *Cytogenet Genome Res* **108**, 255-61.

Tanabe H., Muller S., Neusser M., von Hase J., Calcagno E., Cremer M., Solovei I., Cremer C. & Cremer T. (2002) Evolutionary conservation of chromosome territory arrangements in cell nuclei from higher primates. *Proc Natl Acad Sci U S A* **99**, 4424-9.

Tarozzi N., Bizzaro D., Flamigni C. & Borini A. (2007) Clinical relevance of sperm DNA damage in assisted reproduction. *Reprod Biomed Online* **14**, 746-57.

Tempest H.G. & Griffin D.K. (2004) The relationship between male infertility and increased levels of sperm disomy. *Cytogenet Genome Res* **107**, 83-94.

Thornhill A.R., deDie-Smulders C.E., Geraedts J.P., Harper J.C., Harton G.L., Lavery S.A., Moutou C., Robinson M.D., Schmutzler A.G., Scriven P.N., Sermon K.D. & Wilton L. (2005) ESHRE PGD Consortium 'Best practice guidelines for clinical preimplantation genetic diagnosis (PGD) and preimplantation genetic screening (PGS)'. *Hum Reprod* **20**, 35-48.

Tilgen N., Guttenbach M. & Schmid M. (2001) Heterochromatin is not an adequate explanation for close proximity of interphase chromosomes 1--Y, 9--Y, and 16--Y in human spermatozoa. *Exp Cell Res* **265**, 283-7.

Trask B.J. (2002) Human cytogenetics: 46 chromosomes, 46 years and counting. *Nat Rev Genet* **3**, 769-78.

Turner J.M., Mahadevaiah S.K., Ellis P.J., Mitchell M.J. & Burgoyne P.S. (2006) Pachytene asynapsis drives meiotic sex chromosome inactivation and leads to substantial postmeiotic repression in spermatids. *Dev Cell* **10**, 521-9.

Twisk M., Mastenbroek S., Hoek A., Heineman M.J., van der Veen F., Bossuyt P.M., Repping S. & Korevaar J.C. (2008) No beneficial effect of preimplantation genetic screening in women of advanced maternal age with a high risk for embryonic aneuploidy. *Hum Reprod* **23**, 2813-7.

Uher P., Baborova P., Kralickova M., Zech M.H., Verlinsky Y. & Zech N.H. (2009) Non-informative results and monosomies in PGD: the importance of a third round of re-hybridization. *RBM Online* **19**, 539-46.

Ushijima C., Kumasako Y., Kihaile P.E., Hirotsuru K. & Utsunomiya T. (2000) Analysis of chromosomal abnormalities in human spermatozoa using multi-colour fluorescence in-situ hybridization. *Hum Reprod* **15**, 1107-11.

Varghese A.C., du Plessis S.S. & Agarwal A. (2008) Male gamete survival at stake: causes and solutions. *Reprod Biomed Online* **17**, 866-80.

Velilla E., Escudero T. & Munne S. (2002) Blastomere fixation techniques and risk of misdiagnosis for preimplantation genetic diagnosis of aneuploidy. *Reprod Biomed Online* **4**, 210-7.

Verschure P.J. (2004) Positioning the genome within the nucleus. *Biol Cell* **96**, 569-77.

Wang Y.A., Li J.J., Chen H. & Peng X. (2002) Stabilization of inorganic nanocrystals by organic dendrons. *J Am Chem Soc* **124**, 2293-8.

Ward W.S. (2009) Function of Sperm Chromatin Structural Elements in Fertilization and Development. *Mol Hum Reprod.*

Ward W.S. & Coffey D.S. (1991) DNA packaging and organization in mammalian spermatozoa: comparison with somatic cells. *Biol Reprod* **44**, 569-74.

Ward W.S., Kimura Y. & Yanagimachi R. (1999) An intact sperm nuclear matrix may be necessary for the mouse paternal genome to participate in embryonic development. *Biol Reprod* **60**, 702-6.

Wells D. & Delhanty J.D. (2001) Preimplantation genetic diagnosis: applications for molecular medicine. *Trends Mol Med* **7**, 23-30.

Wiland E., Zegalo M. & Kurpisz M. (2008) Interindividual differences and alterations in the topology of chromosomes in human sperm nuclei of fertile donors and carriers of reciprocal translocations. *Chromosome Res* **16**, 291-305.

Wilton L., Thornhill A., Traeger-Synodinos J., Sermon K.D. & Harper J.C. (2009) The causes of misdiagnosis and adverse outcomes in PGD. *Hum Reprod.*

Wilton L.J. (2007) In vitro fertilization with preimplantation genetic screening. *N Engl J Med* **357**, 1770; author reply -1.

Wu S.M., Zhao X., Zhang Z.L., Xie H.Y., Tian Z.Q., Peng J., Lu Z.X., Pang D.W. & Xie Z.X. (2006) Quantum-dot-labeled DNA probes for fluorescence in situ hybridization (FISH) in the microorganism Escherichia coli. *Chem Phys Chem* **7**, 1062-7.

Wu X., Liu H., Liu J., Haley K.N., Treadway J.A., Larson J.P., Ge N., Peale F. & Bruchez M.P. (2003) Immunofluorescent labeling of cancer marker Her2 and other cellular targets with semiconductor quantum dots. *Nat Biotechnol* **21**, 41-6.

Wykes S.M. & Krawetz S.A. (2003) The structural organization of sperm chromatin. *J Biol Chem* **278**, 29471-7.

Xiao Y. & Barker P.E. (2004a) Semiconductor nanocrystal probes for human chromosomes and DNA. *Minerva Biotec* **16**, 281-8.

Xiao Y. & Barker P.E. (2004b) Semiconductor nanocrystal probes for human metaphase chromosomes. *Nucleic Acids Res* **32**, e28.

Xiao Y., Telford W.G., Ball J.C., Locascio L.E. & Barker P.E. (2005) Semiconductor nanocrystal conjugates, FISH and pH. *Nat Methods* **2**, 723.

Yao G., Wang L., Wu Y., Smith J., Xu J., Zhao W., Lee E. & Tan W. (2006) FloDots: luminescent nanoparticles. *Anal Bioanal Chem* **385**, 518-24.

Yu W.W., Chang E., Drezek R. & Colvin V.L. (2006) Water-soluble quantum dots for biomedical applications. *Biochem Biophys Res Commun* **348**, 781-6.

Zalenskaya I.A. & Zalensky A.O. (2004) Non-random positioning of chromosomes in human sperm nuclei. *Chromosome Res* **12**, 163-73.

Zalensky A. & Zalenskaya I. (2007) Organization of chromosomes in spermatozoa: an additional layer of epigenetic information? *Biochem Soc Trans* **35**, 609-11.

Zalensky A.O., Allen M.J., Kobayashi A., Zalenskaya I.A., Balhorn R. & Bradbury E.M. (1995) Well-defined genome architecture in the human sperm nucleus. *Chromosoma* **103**, 577-90.

Zalensky A.O., Breneman J.W., Zalenskaya I.A., Brinkley B.R. & Bradbury E.M. (1993) Organization of centromeres in the decondensed nuclei of mature human sperm. *Chromosoma* **102**, 509-18.

Zhang Q.F. & Lu G.X. (2004) Investigation of the frequency of chromosomal aneuploidy using triple fluorescence in situ hybridization in 12 Chinese infertile men. *Chin Med J (Engl)* **117**, 503-6.

Zhang X., Trokoudes K.M. & Pavlides C. (2009) Vitrification of biopsied embryos at cleavage, morula and blastocyst stage. *Reprod Biomed Online* **19**, 526-31.

Zheng J., Ghazani A.A., Song Q., Mardyani S., Chan W.C. & Wang C. (2006) Cellular imaging and surface marker labeling of hematopoietic cells using quantum dot bioconjugates. *Lab Hematol* **12**, 94-8.

Zini A. & Libman J. (2006) Sperm DNA damage: clinical significance in the era of assisted reproduction. *Cmaj* **175**, 495-500.

Zirbel R.M., Mathieu U.R., Kurz A., Cremer T. & Lichter P. (1993) Evidence for a nuclear compartment of transcription and splicing located at chromosome domain boundaries. *Chromosome Res* **1**, 93-106.

Zuccotti M., Garagna S., Merico V., Monti M. & Alberto Redi C. (2005) Chromatin organisation and nuclear architecture in growing mouse oocytes. *Mol Cell Endocrinol* **234**, 11-7.

10. Appendix

10.1. Publications and activities arising from work presented in this thesis

10.1.1. Publications (as 1st author)

Ioannou D, Tempest HG, Skinner BM, Thornhill AR, Ellis M, Griffin DK. (2009) Quantum dots as new-generation fluorochromes for FISH: an appraisal. Chromosome Research 17:519-530.

Ioannou D, Griffin DK. (2010) Nanotechnology and molecular cytogenetics: the future has not yet arrived Nano Reviews. Vol.1. http://www.nano-reviews.net/index.php/nano/article/view/5117

Ioannou D, Griffin DK. (2010) Male fertility, chromosome abnormalities, and nuclear organisation. Cytogenetic Genome Research. http://content.karger.com/ProdukteDB/produkte.asp?doi=10.1159/000322060

A hard copy of the manuscripts is included at the end of this Appendix.

10.1.2. Other publications (my contribution is specified under each paper)

Finch KA, Fonseka KG, Abogrein A, **Ioannou D**, Handyside AH, Thornhill AR, Hickson N, Griffin DK .(2008) Nuclear organization in human sperm: preliminary evidence for altered sex chromosome centromere position in infertile males. Hum Reproduction 23:1263-1270.
(Did the experiments to address reviewers' comments for publication)

Finch KA, Fonseka G, **Ioannou D**, Hickson N, Barclay Z, Chatzimeletiou K, Mantzouratou A, Handyside A, Delhanty J, Griffin DK. (2008) Nuclear organisation in totipotent human nuclei and its relationship to chromosomal abnormality. J Cell Science 121:655-663.
(Did the experiments to address reviewers' comments for publication)

Skinner BM, Robertson LBW, Tempest HG, Langley E, **Ioannou D**, Fowler K, Crooijman RPMA, Hall AD, Volker M, Grfffin DK. (2009) Comparative genomics in chicken and Pekin duck using FISH mapping and microarray analysis.BMC Genomics 10:357.
http://www.biomedcentral.com/1471-2164/10/357
(Assisted with probe preparation and microscopy)

Morris WB, Stephenson JE, Robertson LBW, Turner K, Brown H, **Ioannou D**, Tempest HG, Skinner BM, Griffin DK (2007) Practicable approaches to facilitate rapid and accurate molecular cytogenetic mapping in birds and mammals. Cytogenetic Genome Research 117: 36-42.

(Assisted with probe preparation and microscopy)

10.1.3.Published abstracts

Ioannou D, Ellis M, Tempest HG, Griffin DK .The use of quantum dots in place of organic fluorochromes for FISH: Prospects and pitfalls. Chromosome Research, Volume 15, Supplement 2, August 2007, Page S16.

Ioannou D, Vetter M, Thomas L, Finch K, Abogrein A, Thornhill AR, Handyside AH, Griffin DK. Multi-colour FISH in 17 minutes: Towards 24 chromosome aneuploidy screening in under 24 hours. European Journal of Human Genetics, Volume 16, Supplement 2, May 2008, Page 176. https://www.eshg.org/eshg2008/downloads/ESHG2008AbstractBook.pdf

Fonseka GL, **Ioannou D**, Skinner BM, Ellis M, Griffin DK. Manual vs. automated methods to assess nuclear organisation. Chromosome Research, Volume 16, Issue 7, October 2008, Page 1050.

Ioannou D, Tempest HG, Skinner BM, Thornhill AR, Ellis M, Griffin DK. Quantum dots as new-generation fluorochromes for FISH: an appraisal. Chromosome Research, Volume 17, Issue 4, August 2009, Page 572.

Griffin DK, **Ioannou D**, Gabriel AS, Tempest HG, Grigorova M, Taylor J, Dunmore B, Clemente E, Affara N, Handyside AH, Thornhill AR. Novel perspectives on 24 chromosome diagnosis in human preimplantation embryos. Chromosome Research, Volume 17, Issue 4, August 2009, Pages 561-562.

Ioannou D, Fonseka GL, Ellis M, Meershoek E, Handyside AH, Thornhill AR, Griffin DK. 24 chromosome PGS: Position not quantity. Reproductive BioMedicine Online Volume 20, Supplement 1, May 2010, Pages S23-24.

K.G.L. Fonseka, Tempest H, **Ioannou D**, Ellis, M, Handyside A, Thornhill A, Griffin DK**.** The organisation of the genome in sperm heads of men undergoing chemotherapy for testicular cancer and Hodgkin's lymphoma. Human Reproduction, Volume 25, Supplement 1, June 2010, Pages i71-i72.

10.1.4.Presentations & Prizes

Invited oral presentation, "Towards a QD-FISH system", QD Symposium, London, January 2007.

Invited seminar, "Imagine all 24", The London Bridge Fertility & Gynaecology Centre, London, February 2008.

Final Year PhD presentation, "Multicolour strategies for assessing nuclear health: Questions and applications in reproductive medicine", University of Kent, Postgraduate Symposium, June 2009.

Best pitching for investment in a Dragon's Den template presentation (with D.K. Griffin). "Diagnosis of 24 chromosomes in 24 hours in IVF embryos", University of Kent, February 2008.

10.1.5. Conferences (nature of presentation)

- International Chromosome Conference (ICC) XVI, August 2007 (Amsterdam, the Netherlands).

Ioannou D, Ellis M, Tempest HG, Griffin DK .The use of quantum dots in place of organic fluorochromes for FISH: Prospects and pitfalls. (Poster Presentation)

- International Chromosome Conference (ICC) XVII, June 2009 (Boone, USA).

Ioannou D, Tempest HG, Skinner BM, Thornhill AR, Ellis M, Griffin DK. Quantum dots as new-generation fluorochromes for FISH: an appraisal. (Poster Presentation)

- European Human Genetics Conference, May 2008 (Barcelona, Spain).

Ioannou D, Vetter M, Thomas L, Finch K, Abogrein A, Thornhill AR, Handyside AH, Griffin DK. Multi-colour FISH in 17 minutes: Towards 24 chromosome aneuploidy screening in under 24 hours. (Oral presentation by DK Griffin)

- International Congress Preimplantation Genetic Diagnosis (10^{th}), May 2010 (Montpellier, France).

Ioannou D, Fonseka GL, Ellis M, Meershoek E, Handyside AH, Thornhill AR, Griffin DK. 24 chromosome PGS: Position not quantity. (Poster Presentation)

10.1.6. Other Activities

- Kreatech Diagnostics Newsletter, October 2009. Promotional flyer to advertise the 24-probe panel which was developed, validated and used in this Thesis (Chapter 4). http://www.kreatech.com/LinkClick.aspx?fileticket=gRdqfcCTFio%3d&tabid=1775

- Active member since April 2008 in the PGS diagnostic team at the London Bridge, Fertility & Gynaecology Clinic. Performed FISH-based PGS (>100 cases), provided diagnosis and reported back to clinics.

Chromosome Research
DOI 10.1007/s10577-009-9051-0

Quantum dots as new-generation fluorochromes for FISH: an appraisal

Dimitris Ioannou · Helen G. Tempest · Benjamin M. Skinner · Alan R. Thornhill · Michael Ellis · Darren K. Griffin

Received: 24 January 2009 / Revised and Accepted: 23 March 2009

Abstract In the field of nanotechnology, quantum dots (QDs) are a novel class of inorganic fluorochromes composed of nanometre-scale crystals made of a semiconductor material. Given the remarkable optical properties that they possess, they have been proposed as an ideal material for use in fluorescent in-situ hybridization (FISH). That is, they are resistant to photobleaching and they excite at a wide range of wavelengths but emit light in a very narrow band that can be controlled by particle size and thus have the potential for multiplexing experiments. The principal aim of this study was to compare the potential of QDs against traditional organic fluorochromes in both indirect (i.e. QD-conjugated streptavidin) and direct (i.e. synthesis of QD-labelled FISH probes) detection methods. In general, the indirect experiments met with a degree of success, with FISH applications demonstrated for chromosome painting, BAC mapping and use of oligonucleotide probes on human and avian chromosomes/nuclei. Many of the reported properties of QDs (e.g. brightness, 'blinking' and resistance to photobleaching) were observed. On the other hand, signals were more frequently observed where the chromatin was less condensed (e.g. around the periphery of the chromosome or in the interphase nucleus) and significant bleed-through to other filters was apparent (despite the reported narrow emission spectra). Most importantly, experimental success was intermittent (sometimes even in identical, parallel experiments) making attempts to improve reliability difficult. Experimentation with direct labelling showed evidence of the generation of QD-DNA constructs but no successful FISH experiments. We conclude that QDs are not, in their current form, suitable materials for FISH because of the lack of reproducibility of the experiments; we speculate why this might be the case and look forward to the possibility of nanotechnology forming the basis of future molecular cytogenetic applications.

Keywords quantum dot · nanotechnology · FISH · chromosome painting · semiconductor

Responsible Editor: Herbert Macgregor.

Electronic supplementary material The online version of this article (doi:10.1007/s10577-009-9051-0) contains supplementary material, which is available to authorized users.

D. Ioannou · H. G. Tempest · B. M. Skinner · A. R. Thornhill · D. K. Griffin (✉)
Department of Biosciences, University of Kent,
Canterbury CT2 7NJ, UK
e-mail: d.k.griffin@kent.ac.uk

H. G. Tempest · A. R. Thornhill
The London Bridge Fertility, Gynaecology and Genetics Centre and Bridge Genoma,
London SE1 9RY, UK

M. Ellis
Digital Scientific UK Ltd,
Sheraton House, Castle Park,
Cambridge CB3 0AX, UK

Published online: 31 July 2009

Abbreviations

BAC(s)	bacterial artificial chromosome(s)
BSA	bovine serum albumin
DAPI	4′,6-diamidino-2-phenylindole
ddH_2O	double-distilled water
DS	dextran sulfate
DOP	degenerate oligo primed
DTT	dithiothreitol
dUTP	2′-deoxyuridine 5′-triphosphate
FA	formamide
FISH	fluorescence in-situ hybridization
FITC	fluorescein isothiocyanate
HFEA	human fertilization and embryology authority
MAA	mercaptoacetic acid
NIR	near infrared
PBS	phosphate-buffered saline
QD	quantum dot
QD-FISH	quantum dot fluorescence in-situ hybridization
RT	room temperature
PCR	polymerase chain reaction
SERT	serotonin transporter protein
SSC	saline sodium citrate
UV	ultraviolet

Introduction

Traditionally associated with engineering and physical science (e.g. in computer chips), 'nanotechnology' is a research field that manipulates and creates structures of particles with dimensions smaller than 100 nm (Chan 2006). Within the last decade, however, there has been a growing interaction between nanotechnology and biology (Parak et al. 2003), particularly in fluorescence microscopy. One novel class of inorganic fluorophores arising from nanotechnology and useful in fluorescent microscopy are 'quantum dots' (QDs) (Miller and Chemla 1986; Reed et al. 1986). QDs are composed of nanocrystals of a semiconductor material (e.g. either cadmium sulfide (CdS), cadmium selenide (CdSe), indium phosphate (InP) or lead selenide (PbSe)) at the core (Lipovskii et al. 1997). This is coated with a (usually zinc sulfide, ZnS) shell that improves the optical properties (Michalet et al. 2005; Invitrogen 2006); plus an extra polymer coating that serves as a site for conjugation with biomolecule moieties. This brings the total size of the nanocrystal to 10–20 nm. The core material is chosen according to the emission wavelength range that is targeted (e.g. CdS for ultraviolet-blue, CdSe for the visible spectrum and CdTe for the far red and near infrared (Quantum Dot Corporation 2006); thus fluorophore colour is size-dependent and controlled during synthesis (Chan et al. 2002).

A unique property of QDs is their broad excitation and narrow symmetric emission spectra. The full spectral width of QDs at half maximum is 12 nm and leads to less overlap between absorption and emission spectra (Chan and Nie 1998). Thus different QDs can be excited by a single wavelength shorter than their emission wavelength (Green 2004; Alivisatos et al. 2005; Arya et al. 2005). Such an approach cannot be achieved with classical organic fluorophores because they have narrow excitation and broad emission that often results in spectrum overlap or red tailing (Dabbousi et al. 1997). QDs produce significantly brighter fluorescence (2–11 times) (Larson et al. 2003) because of the large molar extinction coefficients (10–50 times larger than those of organic fluorophores) (Gao et al. 2005). Due to their inorganic composition they are more resistant to photobleaching than organic fluorophores (Alivisatos 1996; Bruchez et al. 1998; Michalet et al. 2001; Jaiswal et al. 2003; Parak et al. 2005) and have a longer fluorescence half-life than typical organic dyes (Lounis et al. 2000).

There are many *in vitro* applications using QDs reported in the literature. For instance: detection of the cancer marker Her2 on the surface of fixed and live cancer cells (Wu et al. 2003), targeting the serotonin transporter protein (SERT) in transfected HeLa cells and oocytes (Rosenthal et al. 2002), and identifying the erbB/HER family of transmembrane receptor tyrosine kinases that mediate cellular responses to epidermal growth factor (Lidke et al. 2004). QDs have been used as cellular markers because they can be internalized by cells using a receptor (Chan and Nie 1998; Zheng et al. 2006) or by non-specific endocytosis (Parak et al. 2002). QD cell markers have been used in cell–cell interaction studies by creating unique colour tags for individual cell lines (Mattheakis et al. 2004). In addition, QD resistance to photobleaching has enabled 3D optical sectioning studies of the vascular endothelium

(Ferrara et al. 2006), applications in cell motility assays for studying actomyosin function (Mansson et al. 2004), and phagokinetic tracking of small epithelial cells responsible for 90% of cancers (Parak et al. 2002).

The optical properties of QDs have also been exploited for *in vivo* uses. For instance, as a means to deliver drugs to target molecule sites after injection (Akerman et al. 2002) and to study the behaviour of specific cells during early stage embryogenesis in *Xenopus* and Zebrafish embryos by microinjection of micelle-encapsulated QDs (Dubertret et al. 2002; Rieger et al. 2005). Gao et al. (2004) reported *in vivo* cancer targeting and imaging using antibody-conjugated QDs for human prostate cancer and QDs have been used as contrast agents during surgery to map sentinel lymph nodes in the pig and the mouse (Kim et al. 2004).

Given the potentially much-vaunted properties of QDs, they seem as ideal candidates for the study of chromosomes through adaptations of FISH protocols. Since its inception, FISH has continuously evolved but, as with all experiments involved in fluorescent microscopy, faces limitations imposed from the use of organic fluorophores. The number of available fluorochromes and their broad emission spectra make multicolour experiments difficult to resolve due to overlapping and the rapid photobleaching of organic fluorochromes. Published work related to QD-FISH is currently limited. Xiao and Barker (2004b) utilized biotinylated total genomic DNA on human metaphase chromosomes detected using streptavidin-conjugated QDs. Comparisons between detection with QDs and organic fluorochromes (Texas Red–streptavidin and FITC-streptavidin) showed that QD probes were significantly more photostable and 2–11 times brighter than organic fluorochromes. Furthermore, they applied this technique to detect the Her2 locus in low-copy human breast cancer cells, demonstrating that QD-FISH has the potential to become a medical diagnostic tool. A similar indirect labelling approach has been used on plant chromosomes (Muller et al. 2006) with limited success. Chan et al. (2005) developed a direct labelling approach to target specific mRNAs in mouse brain sections. Biotinylated labelled oligonucleotides were conjugated with QD-streptavidin in the presence of biocytin to block excess streptavidin sites that could result in oligonucleotide cross-linking. Bentolila and Weiss (2006) using a biotin–streptavidin strategy, labelled oligonucleotide probes with QDs; in this case complexes were analysed using gel electrophoresis and the optimum molar ratio of QD-DNA was used against the major (γ) family of mouse satellite DNA in both interphase and metaphase preparations. In addition they also used oligonucleotides labelled with different coloured QDs to target two classes of repetitive DNA in the centromeric region. Their results showed that QD-based probes are more efficient at hybridization than organic fluorochromes and have great potential in multicolour assays. Furthermore, Jiang et al. (2007) generated QD-genomic DNA probes to visualize gene amplification in lung cancer cells, while the most recent study involving direct labelling of maize chromosomes was published by Ma et al. (2008), in which QDs were solubilized with an MAA (mercaptoacetic acid) monolayer and then a thiol-DNA to create probes. Apparently, with this method, the probes were small enough to hybridize with the DNA sequences. This study also highlights the problem of steric hindrance regarding QDs and that pH (Xiao et al. 2005), ionic strength and formamide (FA) could affect the affinity of QD-probes for chromosomal targets (Ma et al. 2008).

Given the potential of QD-FISH, it is puzzling how few studies (notwithstanding the above) there are in this area. Clearly more studies are required to explore the use of QD-FISH. For instance, we are aware of no published data using QD-labelled probes to target whole chromosomes (chromosome painting) either in two dimensions or in 3D nuclear organization studies. The overall aim of this study was to therefore to explore the use QDs in the place of organic fluorochromes, specifically with a view to using QDs in multiplex experiments (i.e. to target multiple regions simultaneously).

The specific aims of the current study were thus as follows: (a) to ask whether streptavidin-QD conjugates could be used for the detection of biotinylated (or digoxigenin) labelled probes in 'indirect' FISH labelling experiments under a range of conditions; and (b) to develop strategies for the direct coupling of QDs to biotinylated probes (including oligonucleotides and chromosome paints) for use in 'direct' FISH experiments (with the ultimate goal of performing multiplex experiments).

Materials and methods

Biological material

Lymphocytes from peripheral blood cultures and sperm from freshly ejaculated semen samples formed the basis of target material for most of the experiments. Both cell types were obtained after written consent from a chromosomally normal male donor. Research was approved by the Research Ethics Committees of the University of Kent and carried out under the auspices of the treatment licence awarded by the Human Fertilization and Embryology Authority (HFEA). Whole blood was cultured in PB Max™ Karyotyping Medium (12557-013 Gibco/BRL, Invitrogen UK) arrested in metaphase using colcemid (D1925, Sigma, St Louis, MO, USA) then swelled and fixed to glass slides using 75 mM KCl and three changes of 3:1 methanol–acetic acid. Fresh ejaculate was washed in 10 mM NaCl/10 mM Tris pH 7.0 sperm wash buffer and then centrifuged for 7 min at 1900 rpm. The supernatant was removed and resuspended up to 5 times depending on the pellet size and colour. The sample was then fixed in a drop-wise fashion using 3:1 methanol–acetic acid to final volume of 5 ml. The process was repeated up to 5 times (pellet dependent) and 5–20 μl of the sample was spread on a poly-L-lysine-coated slide (631-0107, VWR, West Chester, PA, USA) (for better fixation of cells) and air dried at room temperature (RT). In addition, cultured embryonic fibroblasts from chicken and turkey were used; cells were suspended in metaphase using colcemid, trypsinized, swelled and fixed for cytogenetic analysis by standard protocols. For all experiments performed with avian samples or human lymphocytes, superfrost glass slides (AG00008232E, Menzel-Glaser, Braunschweig, Germany) were used.

QD-streptavidin conjugates

Two suppliers were used for these experiments, Invitrogen, Carlsbad, CA, USA (QD525 and QD585) and Evident Technologies, Troy, NY, USA (QD520, QD600 and QD620).

Source of probes

In early experiments, a commercially available pan-centromeric probe (1695-B-02, Cambio, Cambridge, UK) was utilized, as were bacterial artificial chromosomes (BACs) from chicken labelled with biotin by nick translation. Also, in-house chromosome paints were generated from flow-sorted human and chicken chromosomes (a kind gift from the Department of Pathology, University of Cambridge). The degenerate primer 6MW (5′→ 3′ CCG ACT CGA GNNN NNN ATG TGG) was used in a standard DOP-PCR experiment to generate sufficient material, which was then labelled with biotin or digoxigenin via nick translation and used in indirect FISH experiments. A custom-made DOP-PCR primer labelled with biotin (through a C6 linker; Invitrogen, personal communication 2009) was used to generate DOP-PCR products with a single biotin on each length of DNA for direct QD conjugation experiments (Invitrogen). In addition, for direct labelling experiments (and for indirect FISH), an oligonucleotide probe specific for a region on chromosome 12 with a single biotin molecule attached to the 5′ end was used. The biotin was incorporated during synthesis through biotin phoshoramidite by linking the 5′ OH to the phosphorus atom (Sigma Genosys, personal communication 2009).

The following protocol (Bentolila and Weiss 2006) was used to couple streptavidin-conjugated QDs to biotinylated oligonucleotides and chromosome paints labelled with a single biotin molecule. Direct coupling requires probes to have a single biotin (per primer binding site) to prevent QD aggregation and therefore unspecific signals. PCR products were purified using a QIAquick spin column (Qiagen, Valencia, CA, USA) following the manufacturer's instructions. QD:DNA constructs (i.e. FISH probes labelled with QDs) were made by mixing 1 μl of 500 nM QD with 1 μl of 50 ng/μl biotinylated probe. These were gently vortexed for 5 s, allowed to incubate at room temperature for a minimum of 30 min and stored on ice until ready for use. The QD:DNA construct was purified (from unbound probe) using S300 columns (GE Healthcare UK S-300 HR) following the manufacturer's instructions. In order to establish that the QD-DNA complex still had fluorescent activity, the tube was checked for fluorescence under a UV transilluminator. To test for QD:DNA construct formation, standard 2% agarose gel electrophoresis was used under the premise that 'naked' DNA has greater mobility than QD-conjugated DNA and than QD alone.

For all experiments, 100–200 ng/μl of probe was dissolved in standard hybridization buffer (50% formamide (20% for oligonucleotide probe), 2×SSC, 10% dextran sulfate, 60–200 μg of salmon sperm DNA). For direct FISH experiments, formamide was reduced to 25%, dextran sulfate was removed, and 5× Denhardt's solution together with 50 mM phosphate buffer, 1 mM EDTA were included. For the commercial pancentromeric probe, the manufacturer's standard hybridization buffer was used and the probe was denatured at 85°C prior to use according to the manufacturer's guidelines.

FISH

Slides containing metaphase preparations were dehydrated in an ethanol series, air dried and treated with 100 μg/ml RNase under a coverslip (Menzel-Glaser) at 37°C for 1 h, then washed twice in 2× SSC for 5 min each, before a second ethanol series and air drying. Slides bearing sperm preparations were washed in 0.1%DTT, 0.1% Tris-HCl (pH 8.0) at room temperature for 20–30 min to swell the sperm heads and then rinsed in 2× SSC. This was followed by pepsin treatment in a pre-warmed at 39°C Coplin jar with 49 ml of ddH_2O, 0.5 ml of 1 N HCl, 0.5 ml of 1% pepsin for 20 min. Slides were subsequently washed in ddH_2O followed by rinsing in 1× PBS before incubation in 4% paraformaldehyde/PBS (pH 7.0) at 4°C for 10 min; slides were then rinsed with 1× PBS followed by ddH_2O at room temperature and another ethanol series was carried out at RT for 2 min each and slides were air dried.

The cells were then denatured at 70°C in 70% formamide/2× SSC (pH 7.0) for 2 min (8–10 min for sperm) before washing with 70% ice-cold ethanol for 2 min followed by 80% and 100% ethanol for 2 min each prior to air drying.

Labelled probe in hybridization buffer (10 μl) was denatured at 65–85°C for 1–10 min, then added to a specified marked area under a 18×18 mm coverslip, which was sealed with rubber cement and hybridized at 37°C overnight. For direct labelling experiments, the slides were heated at 80°C for 3 min to prevent any reannealing of the DNA strand after denaturation. The rubber cement was removed and slides were washed in 2× SSC to remove the coverslips. Slides were then washed in 37°C 50% formamide–2× SSC solution for 20 min (2×5 min in 20% formamide–2× SSC solution at 37°C for oligonucleotide probes), then for 1 min in 2× SSC, 0.1% Igepal (v/v) at RT. For indirect FISH, slides were incubated in storage buffer (4× SSC, 0.05% Igepal (v/v)) for 15 min, then in blocking buffer (4× SSC, 0.05% Igepal (v/v), 3% BSA (w/v)) for 25 min at RT. The detection mix (QD-conjugated streptavidin for experiments and Cy3-conjugated streptavidin for controls) was prepared at 4°C for 20–25 min before use, centrifuged at 1300 rpm for 5 min, then applied to the slide under coverslip and incubated for 35 min at 37°C. For QD conjugates the detection mix consisted of 1 μl of QD in 99 μl of TNB buffer (pH 7.5) (0.1 M Tris-HCl, 0.15 M NaCl, 0.5% BSA (w/v)) per slide; for controls, the detection mix was Cy3-streptavidin in blocking buffer diluted 1:200. The coverslip was then removed and slides were washed in fresh storage buffer (in the dark) for 10 min, followed by a brief rinse with ddH_2O. Slides were then air-dried and counterstained using Vectashield with DAPI (Vector Laboratories, Burlingame, CA, USA). Direct FISH experiments had post-hybridization washes of 2× 10 min in TST buffer (0.1 M Tris, 0.15 M NaCl, 0.05% Tween 20 (v/v), 2× SSC pH 7) at 37°C then proceeded straight to the ddH_2O stage following post-hybridization washes.

Variations to protocol

In order to improve the efficacy and reliability of the QD experiments, various FISH conditions were altered, including removal of the block buffer step and changing the temperature and time of the post-hybridization washes.

To test the hypothesis that the presence or absence of dextran sulfate in the hybridization mix affected subsequent binding of QD conjugates in indirect FISH experiments (the direct QD FISH hybridization mix did not contain dextran sulfate), controlled experiments with and without dextran sulfate in the hybridization mix were performed.

To minimize steric hindrance of the biotin, biotin-21-dUTP was used in place of biotin-16-dUTP in both direct and indirect experiments. Also, the effects of different ratios of biotin labelled and unlabelled probes were assessed to minimize steric hindrance.

To determine whether there was a hapten-specific effect (i.e. whether biotin per se, was the best hapten to use) we attempted to detect digoxigenin-

labelled probes with mouse anti-digoxigenin antibody followed by a layer of QD-conjugated goat anti-mouse antibody.

To test the hypothesis that QD conjugates were aggregating and adhering to the sides of the tube, we performed controlled experiments sonicating the conjugates before use and using siliconized tubes and pipette tips.

To test the hypothesis that use of DAPI as a counterstain could affect visualization of the QDs, experiments were performed with and without DAPI.

Results

Indirect labelling

Use of streptavidin-conjugated QD525 and QD585 produced a degree of success in generating analysable preparations for FISH experiments. Figures 1, 2, 3, 4, 5 and 6 demonstrate successful experiments (some compared with Cy3 controls). We were successful in hybridizing chromosome paints from both human and birds to metaphases and interphases of the same species (Figs. 1, 2, 3 and 4); BAC clones for chicken chromosomes successfully hybridized (Fig. 5); and the oligonucleotide sequence specific for chromosome 12 gave a reproducible signal (Fig. 6).

By and large, when results were successful, the properties of QDs were apparent. Most notably, the preparations were significantly brighter by visual inspection than Cy3 preparations and were resistant to photobleaching. That is, when Cy3-labelled preparations were exposed continuously to light, photobleaching occurred after about 5 min. On the other hand, when QD preparations were exposed to light, no appreciable loss of signal was seen after one hour of exposure.

We also observed that preparations displayed the phenomenon known as 'blinking'; that is, when samples were visualized the fluorescent signal repeatedly appeared to switch 'on and off'. In general terms, QD preparations in these experiments had more background than was observed for Cy3 preparations. Also, there was a notable difference in the appearance in the fluorescent signal from QD compared to Cy3, which is perhaps best explained with an analogy: Cy3 signals gave the impression of examining fluorescent 'dust' compared the fluorescent 'rocks' impression given by the QDs. It was noticeable that, in many chromosome painting experiments, the QD signal was brighter around the periphery of the chromosome, giving the impression of a fluorescent 'sheath' (Fig. 3); moreover, in selected cases, a bright signal was visible in the interphases of the cell but not the metaphases. Another point of note was that the emission spectra of the QDs did not appear to be as narrow as the manufacturers claimed. That is, despite the use of narrow band-pass filters, QD525 and QD585 each showed a significant 'bleed-through' into the channel of the other. Most importantly, however, it was noticeable that, while the Cy3

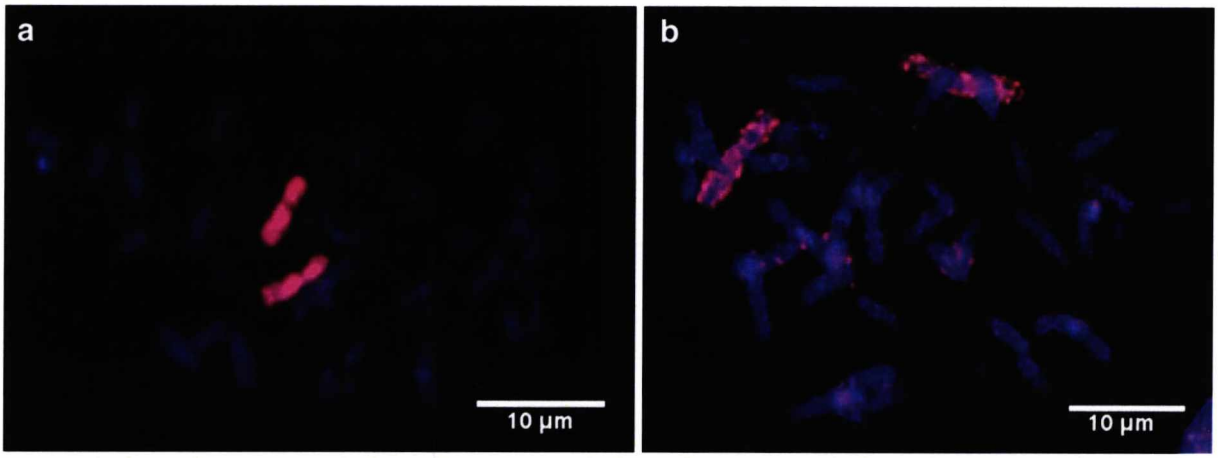

Fig. 1 Detection of biotinylated human chromosome paint 2 with **a** Cy3-conjugated streptavidin; **b** QD585-conjugated streptavidin. The Cy3-labelled probe gives a more specific signal with less background

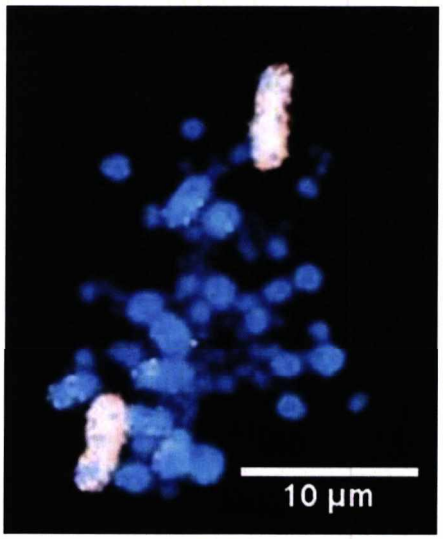

Fig. 2 FISH of turkey chromosome 1 paint to turkey chromosomes using QD525-conjugated streptavidin

controls worked successfully with rare exceptions, success from equivalent QD experiments was notably intermittent. In particular identical QD experiments could often be perfectly successful on one day but unsuccessful on the next or, even more confusingly, identical experiments run in parallel would work for one slide but not the other on a regular basis. As an overall estimate, indirect QD experiments were successful 25–35% of the time when controls gave an acceptable result (>95%).

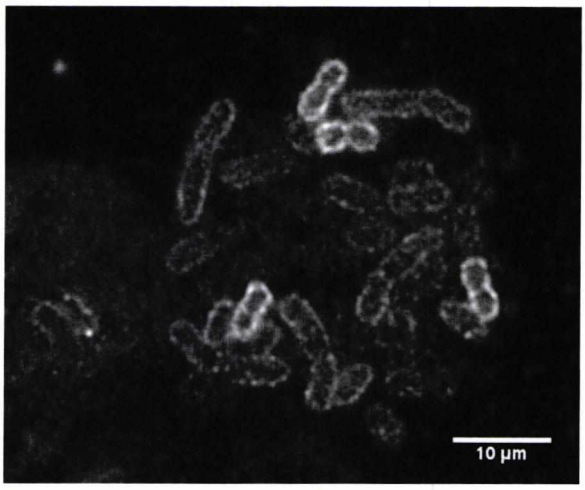

Fig. 3 FISH of chicken chromosome 2 paint to a chicken tetraploid chicken metaphase using QD525-conjugated streptavidin. Hybridization signals are brighter at the periphery of chicken chromosome 2 where the chromatin is less condensed

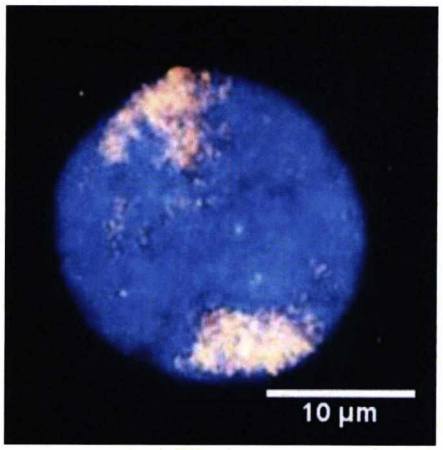

Fig. 4 Turkey nucleus showing hybridization of turkey chromosome 4 paint detected by QD525-conjugated streptavidin

In general terms, amidst this background of intermittent success, we were unable to identify any particular factor that would improve the success of the experiments. Controlled studies varying hybridization times and temperatures did not especially favour QD experiments on any occasion. There was no appreciable difference whether or not the blocking buffer and/or dextran sulfate in the hybridization mix and/or

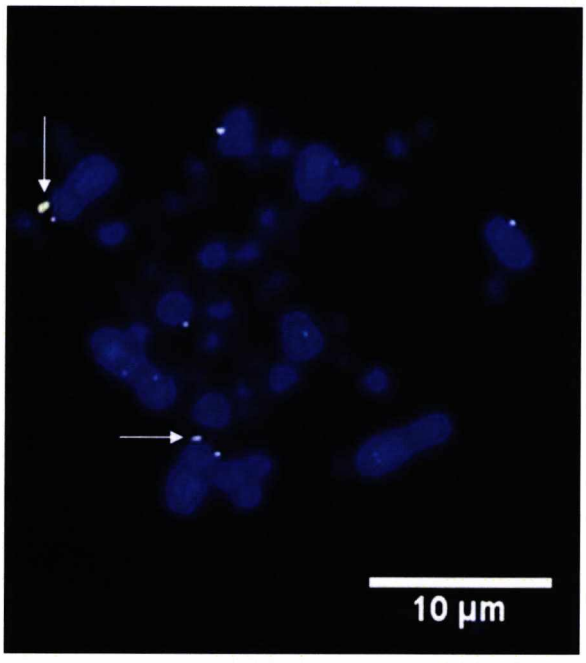

Fig. 5 Hybridization of a BAC probe to terminal chromosome 2p in chicken using QD525-conjugated streptavidin. Arrowheads indicate the specific hybridization sites (2p)

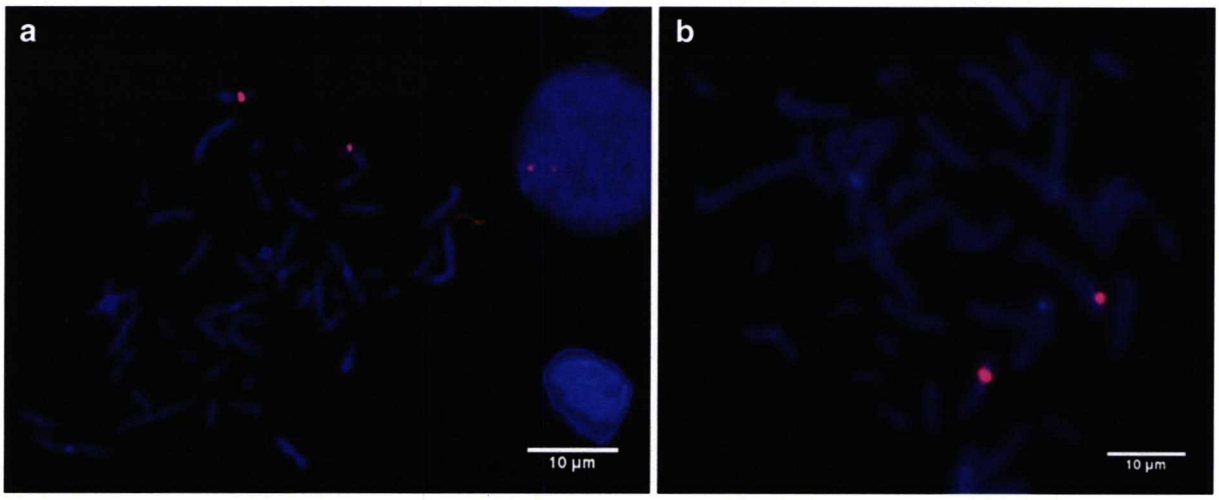

Fig. 6 FISH hybridization of an oligonucleotide probe for the centromere of human chromosome 12 on human metaphases detected by **a** QD585-conjugated streptavidin; **b** Cy3-conjugated streptavidin

DAPI in the mountant was used. We did observe good signals through the use of biotin-21-dUTP; however, this was, at least by visual inspection by a number of observers, not noticeably different from the use of biotin-16-dUTP, nor did our efforts to vary the relative concentrations of labelled versus unlabelled probes allow us to draw firm conclusions. The only intervention that we observed to demonstrate a degree of success was the use of silicon-coated Eppendorf tubes and sonication of the conjugate prior to use. In both scenarios we observed an improvement (albeit temporary) in the reliability of the results.

Direct FISH

Efforts to conjugate streptavidin-QDs to biotinylated DNA were initially encouraging. Figure 7 demonstrates a noticeable shift in the mobility of the DNA-QD

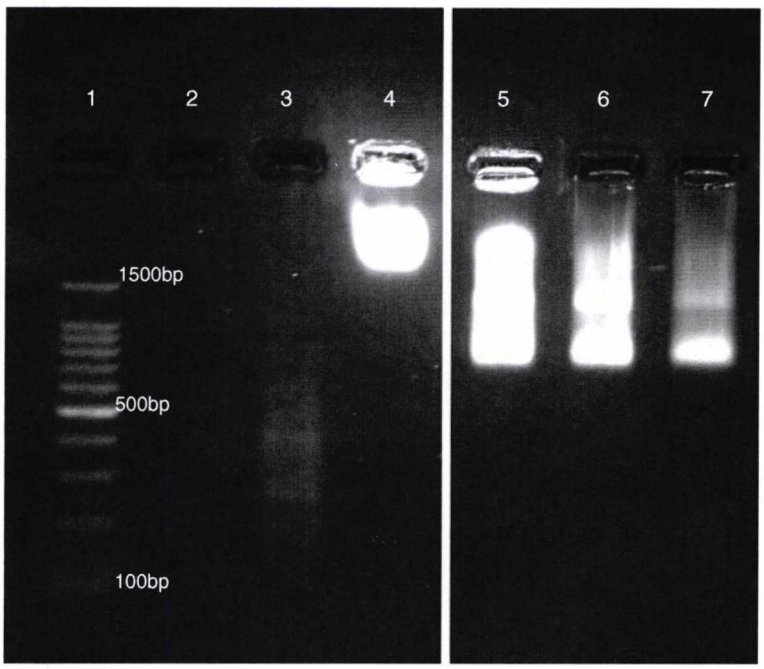

Fig. 7 Agarose gel (selected lanes from the same gel) showing differential motility of amplified biotinylated DNA (lane 3), QD alone (lane 4), and QD:DNA construct at varying concentrations (lanes 5–7). The differential motility seen in lanes 5–7 indicates that the construct was successfully generated. Lane 1 is a 100 bp ladder and lane 2 is blank

construct compared with either biotinylated DNA alone or streptavidin QD alone. These results were reproduced on approximately 20 occasions for both the oligonucleotide chromosome 12 probe and the chromosome paints; however, repeated attempts at subsequent FISH experiments (employing a range of different conditions of stringency, hybridization buffer, etc.) without exception ended in failure (despite known Cy3 conjugate controls working reliably).

Finally, it is worth noting that records from all QDs purchased were kept and results were obtained only through the use of Invitrogen samples (Lot 48184A, for QD585). In contrast, there were no results through the use of Evident samples.

Discussion

To the best of our knowledge, this is the first study to demonstrate a comprehensive appraisal of the utility of QDs for FISH experimentation. That is, while several studies have demonstrated the use of QDs in FISH, as with the majority of studies in the literature, there may be a tendency to present only the positive data. QD-based FISH studies are conspicuous mostly by their absence (Xiao and Barker 2004a; Bentolila and Weiss 2006; Ma et al. 2008); that is, if QDs had fulfilled their promise they would, at least in part, have replaced organic fluorochromes. One would expect orders of magnitude more QD-FISH papers in the literature and several companies marketing QD-labelled probes, which—at the time of writing—is simply not the case.

While we would not claim that we have explored every possible avenue with respect to QD-FISH, we have extensive experience in FISH over many years and have, for the last three or four of them, been running parallel QD-based experiments, mostly in avian and human cells. Put simply, lack of reproducibility appears to be the hallmark of QD-FISH in contrast to the more robust applications with antibody conjugates for cell labelling. This is possibly because of incomplete technical knowledge of the factors associated with penetration of a QD probe into a complex structure such as a chromosome or nucleus. Furthermore, in commercially available QD-streptavidin conjugates we are yet to understand many chemical and physical factors that are well understood for organic fluorophore conjugates (e.g. FITC, Texas red and the Cy dyes).

For these reasons we conclude that, for indirect FISH, QD-conjugated streptavidin (at least in its current form) is an unsuitable material compared with equivalent Cy3 conjugates. For direct labelling, despite recruiting the services of leading proponents involved in QD conjugation (L. A. Bentolila, personal communication 2007), we were unsuccessful in generating a single successful FISH preparation by this means. It seems reasonable to suggest that, had we continued our attempts, we would eventually have met with a degree of success; however, given the intermittent success of the simpler indirect approach, we are not confident that the experiments would have been reliable. In addition, we have gone to the lengths of canvassing like-minded groups who would benefit from the use of QDs and organized symposia to share knowledge and experience. Without exception, the message we have received from our colleagues is of a similar experience to our own. In addition, recent studies (Bruchez 2007) also hint at the unreproducible nature of QDs for FISH and stress the need for tailored protocols established by empirical means. If this were achieved, then the reliability might well improve and the benefits of QDs observed in this and other studies (e.g. increased brightness, resistance to photobleaching) might be properly realized.

It is of course appropriate to speculate why QDs lack reproducibility in FISH applications. One possible explanation is their size. QDs vary in size (this is the basis of the fluorescent colour that they emit) from 2 to 10 nm. A Cy3 molecule on the other hand is <2 nm in size (Bailey et al. 2004). This may explain in part why our successful FISH experiments gave the impression of larger fluorescent particles and why there was a greater degree of background for most experiments. It might also explain the fluorescent 'sheath' effect seen on some metaphases (Fig. 3) and why certain preparations were successful at interphase but not at metaphase (Fig. 4). That is, steric hindrance may have led to signals being brighter in areas where the chromatin is less compact (e.g. at the edge of the chromosomes and/or in the interphase nucleus). If this were the case, we might have expected to see an improvement when we reduced the ratio of labelled to unlabelled dUTPs and/or when we made use of a 'longer-arm' biotin dUTP; however, we did not. Again a general background of intermittent success may have masked any appreciable difference seen in any given

experiment. The steric hindrance problem was reported also by Muller et al. (2006) in their attempts to use streptavidin-conjugated QDs to target plant chromosomes.

It is not entirely clear how streptavidin is bound to the polymer site of the QD; the number of free streptavidin sites per QD varies from 10 to 15 and they are prone to de-conjugation for reasons not completely understood (L. A. Bentolila, personal communication 2007). We are also aware that QD streptavidin conjugates can be prone to degradation (a batch-specific attribute) and this can correlate with even subtle changes in temperature during storage. Additionally, we are given to understand that QDs are prone to adhere to tubes sides and tips (P. Chan, personal communication 2005). Our attempts to reduce this problem using siliconized tubes and regular sonication met with a degree of success (confirming this theory in part), but did not completely eliminate our technical problems.

A further complicating factor was that the emission spectrum of the QDs used appeared to be not as narrow as the manufacturers claimed, in that we observed 'bleed-through' from red to green channels and vice versa, despite using narrow band-pass filters. Anecdotal evidence suggests that this phenomenon is not uncommon (L. A. Bentolila, personal communication 2007) and could vary from batch to batch. As we understand it controlling the size of the core during synthesis (which will determine the colour that the QD will emit) is an imperfect process and can lead to QDs being smaller or larger than expected. Moreover, abnormalities in QD shape (failure of quality control) could result in the same effect (L. A. Bentolila, personal communication 2007). Such a phenomenon can potentially lead to a mixed population of QDs in any given batch. These findings are consistent with the work of Bawendi and colleagues who have tried to address monodispersity of QD preparations (Murray et al. 2000). Supplementary Fig. S1 illustrates this phenomenon in that the different colours seen represent individual QDs that emit at longer wavelengths (towards the red–large QDs) or shorter wavelengths (towards the blue–small QDs). All these technical features that were attributed to the chemical synthesis of the QDs possibly require more experimental attention in order to improve QD synthesis.

Another observed QD feature was 'blinking', which is not seen in conventional FISH (as shown in Supplementary Movie S2). Blinking is a phenomenon in which the QD alternates between an emitting (on) and non-emitting (off) state (Michler et al. 2000; Pinaud et al. 2006). This behaviour has been interpreted according to an Auger ionization model (Efros and Rosen 1997). Blinking affects single-molecule detection applications by saturation of the signal; however, one study suggests that this behaviour of the QD can be suppressed by passivating the QD surface with thiol groups (Hohng and Ha 2004). Photobrightening, wherein QD fluorescence intensity increases in the first stage of illumination and then stabilizes, can impose limitations on quantitative studies (Gerion et al. 2001). Both of these properties are associated with mobile charges on the surface of the QDs (Fu et al. 2005). It is also noteworthy that, although preparations often displayed blinking, they could go to an irreversible photodarkened state without easy explanation.

One possible explanation for the success of the groups that have published in this area (Xiao and Barker 2004a; Bentolila and Weiss 2006; Ma et al. 2008) is that they possessed the facility to synthesize and batch-test their own streptavidin QD conjugates (something that we, in common with most groups, do not currently have). In other words, they did not use commercially available streptavidin QDs. Ma (Ma et al. 2008) specifies that the QDs used were smaller than commercial ones, and that could help avoid steric hindrance and confer hybridization ability. Several authors (Xiao and Barker 2004a; Bentolila and Weiss 2006; Ma et al. 2008) used oligonucleotides to generate QD-DNA conjugates and highlight that, during the time of annealing of the QD-DNA probe to the target, steric hindrance has little effect but it may limit the QD's access to the target at the time of detection (Ma et al. 2008). This could also explain our negative results during direct FISH. A further complication of their application in biological environments is that QDs behave not as molecules but as nanocolloids (Resch-Genger et al. 2008).

Taking all of the above into consideration, the future of QD-FISH requires further research and interaction within the interested groups. Advances in nanomaterial synthesis (regarding uniformity and size control) and solubility will assist conjugation to biomolecules. Yao et al. (2006) described a new generation of nanocrystals called 'FloDots'. These are dye-doped silica nanoparticles that possess all QD

optical properties but, owing to the silica matrix that encompassed the dots, it is easier to make them water soluble and, according to the authors, the silica surface could be modified to contain functional groups for bioconjugation. In addition, a study by Choi et al. (2007) introduces a novel class of nanocrystals, 'C-dots', that could be 2–3 times brighter than QDs, less toxic and an ideal material for *in vivo* applications and cancer studies. Time will tell whether these or novel nanocrystals will be used robustly in FISH applications.

Nanotechnology has the potential to revolutionize the use of FISH in a wide range of molecular cytogenetic applications including gene mapping, clinical diagnostics, comparative genomics and microarray. The ability to multiplex much more effectively with a single excitation wavelength with bright, narrowly emitting fluorochromes that do not fade is highly desirable. QD-FISH will, in time, probably be seen as a significant stepping-stone towards this goal. Nanotechnology quite possibly holds the key to future of molecular cytogenetics. That future however, is not yet with us.

Acknowledgement The authors would like to thank Dr Laurent Bentolila for sharing important knowledge on QD synthesis and for his experimental expertise in direct QD experiments.

References

Akerman ME, Chan WC, Laakkonen P, Bhatia SN, Ruoslahti E (2002) Nanocrystal targeting in vivo. Proc Natl Acad Sci USA 99:12617–12621

Alivisatos AP (1996) Nanocrystals:building blocks for modern materials design. Endeavour 21:56–60

Alivisatos AP, Gu W, Larabell C (2005) Quantum dots as cellular probes. Annu Rev Biomed Eng 7:55–76

Arya H, Kaul Z, Wadhwa R, Taira K, Hirano T, Kaul SC (2005) Quantum dots in bio-imaging: revolution by the small. Biochem Biophys Res Commun 329:1173–1177

Bailey RE, Smith AM, Nie S (2004) Quantum dots in biology and medicine. Physica E 25:1–12

Bentolila LA, Weiss S (2006) Single-step multicolor fluorescence in situ hybridization using semiconductor quantum dot-DNA conjugates. Cell Biochem Biophys 45:59–70

Bruchez M (2007) Quantum dots for ultra-sensitive multicolor detection of proteins and genes. Paper presented at 16th International Chromosome Conference (16th ICC) Amsterdam

Bruchez M Jr, Moronne M, Gin P, Weiss S, Alivisatos AP (1998) Semiconductor nanocrystals as fluorescent biological labels. Science 281:2013–2016

Chan WC (2006) Bionanotechnology progress and advances. Biol Blood Marrow Transplant 12:87–91

Chan WC, Nie S (1998) Quantum dot bioconjugates for ultrasensitive nonisotopic detection. Science 281:2016–2018

Chan WC, Maxwell DJ, Gao X, Bailey RE, Han M, Nie S (2002) Luminescent quantum dots for multiplexed biological detection and imaging. Curr Opin Biotechnol 13:40–46

Chan P, Yuen T, Ruf F, Gonzalez-Maeso J, Sealfon SC (2005) Method for multiplex cellular detection of mRNAs using quantum dot fluorescent in situ hybridization. Nucleic Acids Res 33:1–8

Choi J, Burns AA, Williams RM et al (2007) Core-shell silica nanoparticles as fluorescent labels for nanomedicine. J Biomed Opt 12:064007

Dabbousi BO, Rodriguez-Viejo J, Mikulec FV et al (1997) (CdSe) ZnS core-shell quantum dots: synthesis and characterization of a size series of highly luminescent nanocrystallites. J Phys Chem B 101:9463–9475

Dubertret B, Skourides P, Norris DJ, Noireaux V, Brivanlou AH, Libchaber A (2002) In vivo imaging of quantum dots encapsulated in phospholipid micelles. Science 298:1759–1762

Efros AL, Rosen M (1997) Random telegraph signal in the photolyminescence intensity of a single quantum dot. Physical Rev Lett 78:1110–1113

Ferrara DE, Weiss D, Carnell PH et al (2006) Quantitative 3D fluorescence technique for the analysis of en face preparations of arterial walls using quantum dot nanocrystals and two-photon excitation laser scanning microscopy. Am J Physiol Regul Integr Comp Physiol 290:R114–R123

Fu A, Alivisatos AP, Gu W, Larabell C (2005) Semiconductor nanocrystals for biological imaging. Curr Opin Neurobiol 15:568–575

Gao X, Cui Y, Levenson RM, Chung LW, Nie S (2004) In vivo cancer targeting and imaging with semiconductor quantum dots. Nat Biotechnol 22:969–976

Gao X, Yang L, Petros JA, Marshall FF, Simons JW, Nie S (2005) In vivo molecular and cellular imaging with quantum dots. Curr Opin Biotechnol 16:63–72

Gerion D, Pinaud F, Williams SC et al (2001) Synthesis and properties of biocompatible water-soluble sillica-coated CdSe/ZnS semiconductor quantum dots. J Phys Chem B 105:8861–8871

Green M (2004) Semiconductor quantum dots as biological imaging agents. Angew Chem Int Ed Engl 43:4129–4131

Hohng S, Ha T (2004) Near-complete suppression of quantum dot blinking in ambient conditions. J Am Chem Soc 126:1324–1325

Invitrogen (2006) Qdot nanocrystal technology. Vol. 2006. Invitrogen Corporation, Carlsbad CA

Jaiswal JK, Mattoussi H, Mauro JM, Simon SM (2003) Long-term multiple color imaging of live cells using quantum dot bioconjugates. Nat Biotechnol 21:47–51

Jiang Z, Li R, Todd NW, Stass SA, Jiang F (2007) Detecting genomic aberrations by fluorescence in situ hybridization with quantum dots-labeled probes. J Nanosci Nanotechnol 7:4254–4259

Kim S, Lim YT, Soltesz EG et al (2004) Near-infrared fluorescent type II quantum dots for sentinel lymph node mapping. Nat Biotechnol 22:93–97

Larson DR, Zipfel WR, Williams RM et al (2003) Water-soluble quantum dots for multiphoton fluorescence imaging in vivo. Science 300:1434–1436

Lidke DS, Nagy P, Heintzmann R et al (2004) Quantum dot ligands provide new insights into erbB/HER receptor-mediated signal transduction. Nat Biotechnol 22:198–203

Lipovskii A, Kolobkova E, Petrikov V et al (1997) Synthesis and characterization of PbSe quantum dots in phosphate glass. Appl Phys Lett 71:3406–3408

Lounis B, Bechtel HA, Gerion D, Alivisatos PA, Moerner WE (2000) Photon antibunching in single CdSe/ZnS quantum dot fluorescence. Chem Phys Lett 329:399–404

Ma L, Wu SM, Huang J, Ding Y, Pang DW, Li L (2008) Fluorescence in situ hybridization (FISH) on maize metaphase chromosomes with quantum dot-labeled DNA conjugates. Chromosoma 117:181–187

Mansson A, Sundberg M, Balaz M et al (2004) In vitro sliding of actin filaments labelled with single quantum dots. Biochem Biophys Res Commun 314:529–534

Mattheakis LC, Dias JM, Choi YJ et al (2004) Optical coding of mammalian cells using semiconductor quantum dots. Anal Biochem 327:200–208

Michalet X, Pinaud F, Thilo DL et al (2001) Properties of fluorescent semiconductor nanocrystals and their application to biological labeling. Single Molecules 2:261–276

Michalet X, Pinaud FF, Bentolila LA et al (2005) Quantum dots for live cells, in vivo imaging, and diagnostics. Science 307:538–544

Michler P, Imamoglu A, Mason MD, Carson PJ, Strouse GF, Buratto SK (2000) Quantum correlation among photons from a single quantum dot at room temperature. Nature 406:968–970

Miller DAB, Chemla DS (1986) Mechanism for enhanced optical nonlinearities and bistability by combined dielectric - electronic confinement in semiconductor microcrystallites. Opt Lett 11:522-524

Muller F, Houben A, Barker PE, Xiao Y, Kas JA, Melzer M (2006) Quantum dots—a versatile tool in plant science? J Nanobiotechnol 4:5

Murray CB, Kagan CR, Bawendi M (2000) Synthesis and characterization of monodisperse nanocrystals and close-packed nanocrystal assemblies. Annu Rev Mater Sci 30:545–610

Parak WJ, Boudreau R, Le Gros MA et al (2002) Cell motility and metastatic potential studies based on quantum dot imaging of phagokinetic tracks. Adv Mater 14:882–885

Parak WJ, Gerion D, Pellegrino T et al (2003) Biological applications of colloidal nanocrystals. Nanotechnology 14: R15–R27

Parak WJ, Pellegrino T, Plank C (2005) Labelling of cells with quantum dots. Nanotechnology 16:R9–R25

Pinaud F, Michalet X, Bentolila LA et al (2006) Advances in fluorescence imaging with quantum dot bio-probes. Biomaterials 27:1679–1687

QDCorporation (2006) Qdot nanocrystals anatomy. Vol. 2006. Quantum Dot Corporation (QDC)

Reed MA, Bate RT, Bradshaw WM, Duncan WR, Frensley JWL, Shih HD (1986) Spatial quantization in GaAs-AlGaAs multiple quantum dots. J Vac Sci Technol B 4:358–360

Resch-Genger U, Grabolle M, Cavaliere-Jaricot S, Nitschke R, Nann T (2008) Quantum dots versus organic dyes as fluorescent labels. Nat Methods 5:763–775

Rieger S, Kulkarni RP, Darcy D, Fraser SE, Koster RW (2005) Quantum dots are powerful multipurpose vital labeling agents in zebrafish embryos. Dev Dyn 234:670–681

Rosenthal SJ, Tomlinson A, Adkins EM et al (2002) Targeting cell surface receptors with ligand-conjugated nanocrystals. J Am Chem Soc 124:4586–4594

Wu X, Liu H, Liu J et al (2003) Immunofluorescent labeling of cancer marker Her2 and other cellular targets with semiconductor quantum dots. Nat Biotechnol 21:41–46

Xiao Y, Barker PE (2004a) Semiconductor nanocrystal probes for human chromosomes and DNA. Minerva Biotec 16:281–288

Xiao Y, Barker PE (2004b) Semiconductor nanocrystal probes for human metaphase chromosomes. Nucleic Acids Res 32:e28

Xiao Y, Telford WG, Ball JC, Locascio LE, Barker PE (2005) Semiconductor nanocrystal conjugates, FISH and pH. Nat Methods 2:723

Yao G, Wang L, Wu Y et al (2006) FloDots: luminescent nanoparticles. Anal Bioanal Chem 385:518–524

Zheng J, Ghazani AA, Song Q, Mardyani S, Chan WC, Wang C (2006) Cellular imaging and surface marker labeling of hematopoietic cells using quantum dot bioconjugates. Lab Hematol 12:94–98

NANO REVIEWS

COACTION PUBLISHING

Review Article

Nanotechnology and molecular cytogenetics: the future has not yet arrived

Dimitris Ioannou and Darren K. Griffin*

Department of Biosciences, University of Kent, Canterbury, UK

Received: 4 March 2010; Revised: 1 April 2010; Accepted: 7 April 2010; Published: 3 May 2010

Abstract

Quantum dots (QDs) are a novel class of inorganic fluorochromes composed of nanometer-scale crystals made of a semiconductor material. They are resistant to photobleaching, have narrow excitation and emission wavelengths that can be controlled by particle size and thus have the potential for multiplexing experiments. Given the remarkable optical properties that quantum dots possess, they have been proposed as an ideal material for use in molecular cytogenetics, specifically the technique of fluorescent *in situ* hybridisation (FISH). In this review, we provide an account of the current QD-FISH literature, and speculate as to why QDs are not yet optimised for FISH in their current form.

Keywords: *quantum dot*; *nanotechnology*; *FISH*; *imaging*

Nanotechnology has to date been closely affiliated with engineering since nanomaterials became the major components of computer chips (1). Within the last 10 years or so, however, there has been a growing relationship between nanoscience and fluorescent biological imaging (2). Applications of fluorescent imaging have generated a tremendous drive to develop new probes for tagging molecules, enabling changes in their localisation, concentration and activities to be documented (3). However, traditionally used organic fluorochromes face limitations affecting imaging and multicolour detection.

A novel class of semiconductor nanocrystals, termed quantum dots (QDs) (4, 5), are inorganic fluorophores that provide a promising alternative to their organic counterparts. In this review, we will provide a brief account of QD properties and applications, then turn our focus on QDs and their applications for studying chromosomes – principally through the use of the technique 'FISH' (fluorescent (or fluorescence) *in situ* hybridisation). We appraise the current literature and offer possible explanations as to why QDs are not yet optimised for FISH in their current form.

Prof. Darren Griffin holds the chair in genetics at the University of Kent, Canterbury, UK. He is a graduate of the University of Manchester (BSc and DSc) and University College London (PhD). He is a Fellow of the Royal College of Pathology and of the Society of Biology. He has published over 100 papers on aspects related to chromosome research and runs a busy research laboratory.

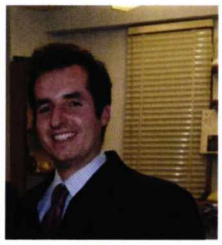

Dimitris Ioannou is a final year PhD student in the laboratory of Professor Griffin. He is a graduate of the University of Wales (BSc) and Nottingham (MPhil), and has performed original research work on applications of FISH including QD-FISH.

Quantum dots (QDs): core concepts

Synthesis

QDs are composed of a semiconductor core such as cadmium selenide (CdSe), indium phosphate (InP) or lead selenide (PbSe) (6, 7). This core is coated with a second semiconductor shell (usually zinc sulphide – ZnS) for the purpose of improving the optical properties of the nanocrystal (7, 8). To improve further the utility of QDs, an extra polymer coating is attached that serves as a site for conjugation with biomolecule moieties. This brings the total size of the nanocrystal to 10–20 nm (a few hundred to a few thousand atoms). Fig. 1 shows a diagram of the structural components of a QD conjugate.

Citation: Nano Reviews 2010, **1:** 5117 - DOI: 10.3402/nano.v1i0.5117

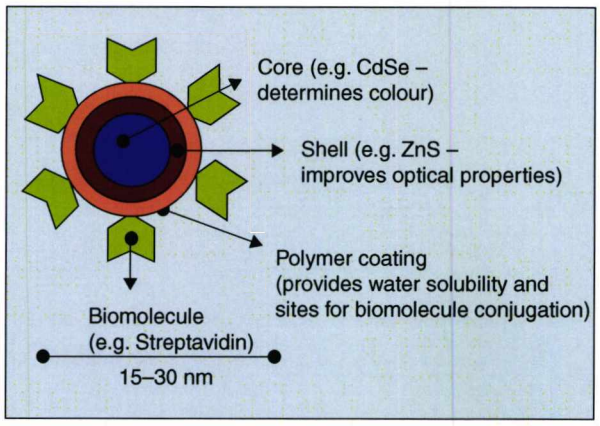

Fig. 1. Schematic representation of a QD conjugate.

The core material is chosen with respect to the required emission wavelength range (e.g. CdS for UV-blue, CdSe for the visible spectrum and CdTe for the far red and near infrared – NIR) (9), thus fluorophore colour is size dependent and controlled during synthesis (10). Synthesis occurs by injecting liquid precursors (dimethyl cadmium and selenium powder dissolved in tributylphosphione) in a hot organic solvent (trioctylphosphine oxide – TOPO) at temperatures reaching 300°C (11). Nanocrystals initiate formation immediately and the colourless starting mix becomes coloured. The size of the nanocrystals is adjusted by changing the amount of injected precursors and crystal growth time in the hot TOPO mix (2, 12). A variety of core shapes can be synthesised, but they require an extra shell of a high band gap semiconductor material, typically ZnS, to stabilise the core and increase the quantum yield [QY, ratio of the amount of light emitted from a sample to the amount of light absorbed by the sample (13)] up to 80% (10, 14). The surface layer of the ZnS shell is, however, hydrophobic and insoluble in aqueous solutions (8).

Optical properties

The most characteristic optical property of the QDs is that their colour is size dependent and thus controlled during synthesis (10). This arises as a result of the quantum confinement phenomenon (15), which refers to the spatial confinement of charge carriers (electrons and holes) within a semiconductor (16).

Because the physical size of the semiconductor nanocrystal is considerably reduced to be much smaller than the natural radius of the electron-hole pair, when a semiconductor is excited to emit light, the energy required to confine this excitation within the nanocrystal is higher, leading to a shift in emission in shorter wavelengths (i.e. towards the blue of emission) (13). To better understand this, an example of two different-sized CdSe QDs of 2.3 and 5.5 nm will be considered (Fig. 2).

Another unique property of QDs is their broad excitation and narrow symmetric emission spectra. The spectral width of QDs (full width at half maximum is 12 nm) (18) designate that multicolour nanocrystals of different sizes can be excited by a single wavelength (excitation source) that is shorter than their emission wavelength (14, 19, 20). This cannot be achieved with classical organic fluorophores because they have narrow

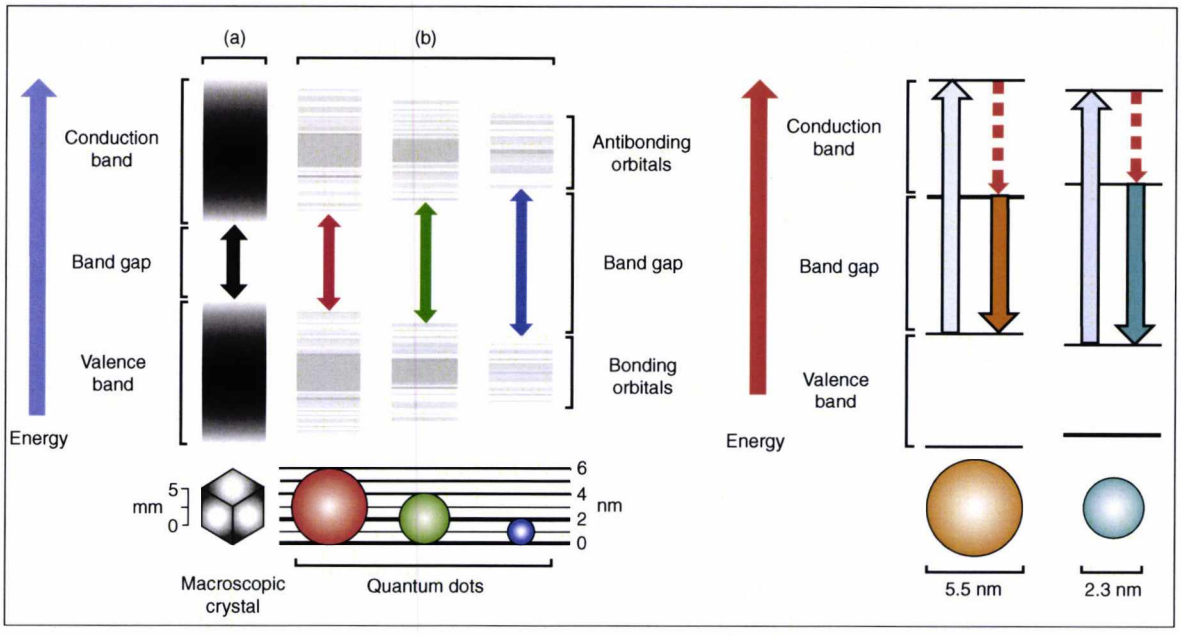

Fig. 2. The size-dependent luminescence of quantum dots. Larger QDs have narrow band gaps (red QD, b) comparing to small QDs (blue QD, b). In the example discussed, the 5.5 QD emits orange light (longer wavelength 590 nm), whereas the 2.3 QD emits turquoise light (shorter wavelength 500 nm). Adapted from Jonathan (17).

Citation: Nano Reviews 2010, **1**: 5117 - DOI: 10.3402/nano.v1i0.5117

excitation and broad emission that often results in spectrum overlap or red tailing (21). Fig. 3 compares excitation and emission spectra between an organic fluorophore and a QD.

QDs are reported to produce two to eleven times brighter fluorescence than organic fluorophores (23) because of the large molar extinction coefficients (10–50 times greater) (24) and, because QDs are inorganic, they are not prone to photo-bleaching (25, 26). Moreover, the two-photon action cross-section of QDs (linked to direct measure of brightness) is significantly higher compared with organic fluorophores (approximate value of 45,000 Goeppert–Mayer units, GM) (23). Moreover, QDs have a longer fluorescence lifetime (10–40 ns) (27) than typical organic dyes, which can decay after a few nanoseconds.

The aforementioned optical properties relate mostly to the inorganic nature of QD and provide great potential; however, some photophysical properties can impose limitations on QD use.

Blinking is a phenomenon where the QD alternates between an emitting (on) and non-emitting (off) state (28, 29). This behaviour has been interpreted according to an Auger ionisation model (30). Blinking affects single molecule detection applications by saturation of the signal. Hohng and Ha (31) carried out the first demonstration of blinking suppression by passivating the QD surface with thiol groups. Other strategies for blinking suppression are recently reviewed elsewhere (32). Photo-brightening, where QD fluorescence intensity increases at the first stage of illumination and then stabilises, can impose limitations on quantitative studies (33). Both these properties are associated with mobile charges on the surface of the QDs (13).

Water solubility

Synthesis of QDs renders hydrophobic nanocrystals as it occurs in non-polar organic solvents (8). However, for QDs to be useful in biological applications, they need to be soluble in aqueous buffers since all experiments involving cells require water-soluble conditions (34, 35). This essentially means that the surface of the QD needs to become hydrophilic. Several strategies have been employed to achieve this and most rely on exchanging the hydrophobic surfactant molecules with bifunctional molecules that are hydrophobic towards the ZnS shell of the nanocrystal and hydrophilic on the other end (8, 34).

Commonly, thiols (–SH) are used as the hydrophobic anchoring parts to ZnS and carboxyl (–COOH) as the hydrophilic (36, 37). The strategy of using mercaptohydrocarbonic acid to solubilise QDs has been applied in DNA immobilisation on the surface of the QD (38), FRET studies (39) and immunolabelling of proteins (40). Alternative approaches include surface silanisation (33, 41), coating the QD surface with amphiphilic polymers (42, 43), or polysaccharides (44), phospholipid micelles (45), non-charged molecules [i.e. dithiothreitol (36)], dendrons (46), peptides (phytochelatin-related) (47) and oligomeric ligands (oligomeric phosphines – OPs) (48). The effect of surface functionalisation on the optical properties of QDs is difficult to predict. In general, however, QY and decay behaviour respond to this effect whereas shape and spectral position of absorption and emission are hardly affected (49). These strategies allow QDs to be conjugated with a variety of biomolecules, including biotin (41), albumin (50), antibodies (51), avidin (52) and streptavidin (25, 53). Covalently linked avidin/streptavidin QDs are very popular amongst companies (e.g. Invitrogen, Evident Technologies); they take advantage of the strong affinity that avidin and streptavidin have for biotin, and the plethora of biotinylated reagents (e.g. antibodies, DNA probes) available (54).

Quantum dot (QD) applications in biology (*in-vitro* and *in-vivo*)

The robust optical properties alone of QDs make them powerful substitutes for organic fluorophores for a variety of biological applications. For the purposes of this review, we will refer to some of the *in-vitro* and *in-vivo* published applications of QDs. However, in order to

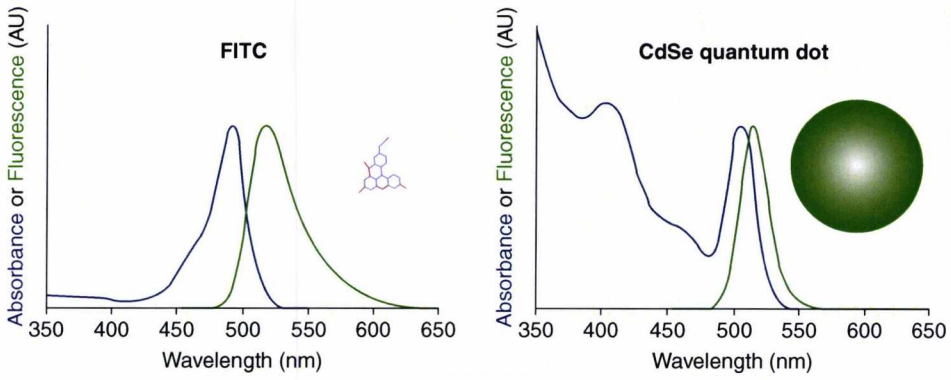

Fig. 3. Comparison of absorption and excitation spectra between FITC (Fluorescein isothiocyanate) (blue) and a CdSe QD (green). Adapted from Bailey et al. (22).

provide a broader aspect of their potential applications and limitations, we have summarised them in Table 1.

The first published study in a biological context was labelling of nanocrystals with F-actin using the biotin–streptavidin bridge (41). Tokumasu and Dvorak (55) used this approach to label human erythrocytes for immunocytochemistry purposes, Wu et al. (25) used QD–streptavidin probes linked with IgG to detect the cancer marker HER2 on the surface of cancer cells, whereas Rosenthal et al. (56) used serotonin-labelled nanocrystals (SNACs) to target the serotonin transporter protein (SERT) in transfected HeLa cells and oocytes *in-vitro*. The erbB/HER family of transmembrane receptor tyrosine kinases (RTKs) that mediate cellular responses to epidermal growth factor (EGF) were studied using a QD–EGF conjugate that was specific in activating the EGF receptor (57).

Additionally, QDs have found applicability as cellular markers given their inherent ability to be internalised by cells, using either a receptor (18, 58), non-specific endocytosis (59) or, for *in-vivo* injection, under the guidance of peptides (60). A more recent example of a peptide able to carry QDs in living cells is allatostatin, which was conjugated to streptavidin QDs and delivered without aggregation inside 3T3L1 and A431 cells (61). They can be employed for studies of cell–cell interaction by creating unique colour tags for individual cell lines (62), they can be encapsulated in micelles to track embryogenesis in frog or zebra fish embryos (45) for 3D optical sectioning investigations of the vascular endothelium (63), for cell motility assays of actinomyosin function (64) and for phagokinetic tracking of small epithelial cells that cause numerous cancers (65). In all these experiments, labelling of cells with QDs is apparently non-harmful to the cell (59).

The tunable size of QDs has allowed the use of NIR QDs as contrast agents during a surgical procedure to map sentinel lymph nodes (SLN) in pig and mouse (45, 66). Using this technique, the surgeon is provided with visual guidance during SLN mapping that minimises incision and dissection inaccuracies, enabling real-time confirmation of complete resection (67). Despite the challenges for QD technology, cancer research has already made extensive use of QD applications for *in-vivo* tumour cell imaging (68–71), surgical oncology (72) and metastasis detection (73).

Quantum dots (QDs) and their potential for molecular cytogenetics

The term 'cytogenetics' refers to the study of chromosomes. For both research and clinical applications, the recognition of specific chromosomal patterns has widespread applications. From the mid-1980s, cytogenetics entered the molecular era through the development of the technique known as FISH (74–76). FISH allowed for direct DNA sequences to be visualised on chromosomes, the principal application being gene mapping, but with many more besides, including chromosome painting, advanced diagnostics and comparative genomics. Most FISH experiments use biotinylated probes and (strept)avidin–fluorochrome conjugates for detection. Moreover, the use of coloured fluorophores allow for the detection of several DNA sequences in the same cell, culminating (with some judicious mixing of colours) with many multicolour applications. FISH techniques have thus continuously been adapted but, as with many fluorescence microscopy applications, face limitations imposed by the use of organic fluorophores. These include the number of available fluorochromes and their broad emission spectra that make multicolour experiments difficult to resolve because of spectrum overlapping and photo-bleaching. Thus, given the aforementioned properties of QDs, they are, potentially, most suitable candidates for the study of chromosomes through adaptations of FISH protocols, particularly as the conjugation of QDs and streptavidin is already widely reported. Indeed, QD-FISH has the potential to revolutionise FISH by overcoming many of the inherent difficulties from the use of organic fluorochromes. It is noteworthy however that a PubMed search using terms

Table 1. QD applications and limitations

QD applications	Target/application	Potential limitations for QDs (all categories)
In-vitro imaging	Fixed cells, tissues, intracellular organelles	• Cytotoxicity and how they are metabolised in the body (for use in human medical imaging)
In-vivo targeting	Cells, tissues, tumours in animals	• Size – QDs are bigger from organic fluorophores – imposes limitation on targeting for *in-vivo* and potentially *in situ* studies, plus on the success of multicolour experiments
Bioanalytical assays	Flow cytometry, microarrays	• Blinking suppression
Other applications (non-life sciences)	LEDs, telecommunications, quantum computers, cryptography, anti-counterfeit technologies	
Future applications	Gene/drug delivery, gene expression, biosensors	

Citation: Nano Reviews 2010, **1**: 5117 - DOI: 10.3402/nano.v1i0.5117

such as 'Quantum Dots FISH' or 'Quantum Dots Fluorescent *in situ* hybridisation' yields few results, of which only 11 are actually QD-FISH studies. Table 2 lists these studies from February 2004. The purpose of the current paper is to review these studies and provide insight, from our own experience, why they are so few in number, despite the enormous potential of QD-FISH.

A review of the quantum dot-fluorescent in situ hybridisation (QD-FISH) literature

In the initial study, Xiao and Barker (77) made use of biotinylated total genomic DNA as a probe on human metaphase chromosomes. The probe was detected using streptavidin-conjugated QD605 (infrared). Direct comparisons of detection with QDs and organic fluorochromes (Texas Red and Fluorescein) showed that QD-FISH was significantly more photostable and brighter than the more traditional approaches. More specifically, they noticed that after 2 h of continuous illumination there was a moderate loss of the QD signals (30%) compared to the more severe 73% and 89% loss for Texas Red and FITC, respectively. In addition, they made an initial observation regarding the pH and buffer used, as with a more alkaline pH (8.3) for the buffer used to dilute the QD conjugate, there was failure of signal detection in centromeres with QD probes. This did not seem to affect the organic fluorochromes. The importance of pH was further explored in a short correspondence by the authors, where signals from QD-FISH were at an optimum when the buffer pH was between 6 and 7 (78). Furthermore, they applied this technique to detect the clinically important locus of HER2 in low copy human cells and breast cancer cells, demonstrating that QD-FISH has the potential to become a medical diagnostic tool. They underlined the potential of QD probes stating that although expectations were raised, more evaluation of QDs was required entering a clinical setting (79).

Chan et al. (80) used direct labelling strategy to target specific mRNAs in mouse brain sections. This study raised the issue of the multiple streptavidin sites on the QD molecule that could interfere with hybridisation efficiency. For this reason, a competitive blocker of streptavidin, biocytin was used, in the presence of which they labelled their oligonucleotide probes. The authors reported that the use of QDs enabled them to observe the details of mRNA expression in the sub-cellular level because of the better image resolution. This study was the first to claim direct labelling of QDs with DNA (specifically oligonucleotides).

Table 2. The total number of QD-FISH studies to the best of the authors' knowledge

Authors	Type of study	Comment	PMID	Published Date
Xiao and Barker	Research	First FISH application in human metaphase spreads	14960711	February 2004
Xiao and Barker	Review	Review on QD-FISH potential and comments from their previous study	Not indexed for PubMed	December 2004
Chan et al.	Research	First direct labelling of QDs with DNA to detect mRNA targets in mice brain sections	16224100	October 2005
Xiao et al.	Correspondence	Importance of pH for QD-FISH	16179915	October 2005
Wu et al.	Research	QD-FISH application in *E. coli*	16625674	April 2006
Müller et al.	Research	QD-FISH attempt on plant chromosomes	16776835	June 2006
Tholouli et al.	Research	Application of QD-FISH on mRNA targets from clinical biopsies	16893519	September 2006
Bentolila and Weiss	Research	Direct labelling and first use of multicolour QD-FISH for mice satellite families	16679564	September 2006
Jiang et al.	Research	QD-FISH for the analysis of cancer-related genomic aberrations in basic research and clinical application	18283800	December 2007
Knoll	Book chapter	This chapter provided general protocols about slide preparation, probe labelling and a small amount on indirect detection of a chromosome loci using QDs	17237529	2007
Ma et al.	Research	Direct QD-FISH application in maize	18046569	December 2007
Choi et al.	Research	QD-DNA probes for direct localization and quantification of gene expression *in situ*	19517489	June 2009
Müller et al.	Research	Concurrent utilisation of QDs and organic fluorochromes for multiplex experiments in 4Pi microscopy	19556786	June 2009
Ioannou et al.	Research	An account of QD-FISH experiments (both indirect and direct labelling) with possible reasoning as to why QD-FISH is not fully optimised yet	19644760	July 2009

Wu et al. (81) were the first to report the successful application of QD-FISH without using the commercial streptavidin–QD conjugates, but by coating naked QDs (synthesised in their laboratory) with mercaptoacetic acid (MAA) to render them water soluble. This was followed by competitive displacing of QD-surface-confined MAA molecules with thiol single-stranded DNA complementary to their plasmid target of interest. By using this technique, they created highly monodisperse QD–DNA probes and because both the single-stranded DNA and the MAA coating were negatively charged, the generated repulsion between those molecules would keep the single-stranded DNA away from the QD surface, facilitating hybridisation in the *Escherichia coli* bacterium for the first time.

In 2006, Muller et al. (82) made the first attempts on plant chromosomes. An indirect approach to detect non-coding sequences in the plant *Allium fistulosum* was used, but with limited success. Although different strategies were employed to improve the performance of QDs (slide preparation, pepsin treatment to increase cell permeability), few results were forthcoming with either QD 605 streptavidin conjugate or by a QD 565 anti-Rabbit IgG conjugate. The offered explanation for the intermittent success was the phenomenon of steric hindrance owing to the large size of the nanocrystals (compared to the organic fluorophores).

The wide application of tissue staining by QDs was shown in another study where multiple mRNA targets in formalin-fixed bone marrow biopsies were targeted using QD–streptavidin conjugates, allowing quantitative characterisation of gene expression sites using non-bleaching fluorochromes (83). Testing different molar ratios between QD and oligonucleotide probes, the authors reported the highest signal intensity when a ratio of 1:2 (QD:probe) was used. Furthermore, there was evidence of QD signals still present in the bone marrow tissue even after 18 months of storage. This was not true for the control Cy3-stained tissue.

In September 2006, the first paper describing multicolour FISH using QDs was published by Bentolila and Weiss (84). Using analytical grade QD batches for a variety of QD–streptavidin conjugates, they formed QD–DNA complexes by incubating biotinylated oligonucleotides at various molar ratios at room temperature for 30 min. Complexes were run on an electrophoresis gel and the optimum molar ratio was established. At the same time this assay confirmed binding of the DNA to the nanoparticles because of the motility shift that is caused by the formation of this conjugant. These probes were used to recognise the major (γ) family of mouse satellite DNA. The novel feature in this study was the presentation of a dual colour QD-FISH using QD592 and 655 against centromere-associated sequences (satellites). Reading between the lines of this paper, however, data was presented from only two of the five different QDs that were tried, probably due to technical difficulties or hybridisation failure of the remaining constructs. Nevertheless, this was an important breakthrough for multicolour QD-FISH. Furthermore, QD525 was not used at all in the hybridisation experiments as it showed an irreversible spectral shift. The success of this study in detecting centromeric regions with QDs was in sharp contrast with the study by Xiao and Baker (77), where most of these regions could not be detected. The authors believed that this could be due to the variable steric hindrance effects during the FISH procedure. Another important aspect was the observation of partial loss of QD probes fluorescence over time. However, this was not an irreversible phenomenon as intensity could be fully restored after re-exposure to UV light. The clear message from this study was the great potential of QD-FISH probes to become a sophisticated toolbox that could be applied for high-resolution studies on chromosome binding through the use of spectrally distinguished QDs.

More recently, successful use of QD-FISH was reported by Jiang et al. (85). In this case, selected probes were used in lung cancer specimens to visualise gene amplification, offering another potential diagnostic tool for the study of genomic aberrations in cancer cells. Also in 2007, a methodology book was published entitled 'Quantum Dots' Applications in Biology, where Chapter 5 was dedicated to QD-FISH. It provided protocols for the preparation of human metaphase chromosomes, probe labelling by nick translation, standard FISH and indirect detection of a specific region on human chromosome 22 using anti-digoxigenin QD655 (86). Some key points from this chapter to enhance hybridisation efficiency included the importance of cell preparation (good chromosome spreading), formamide quality, temperature, pH and exposure of the probe to the denaturation solution.

In a more specialised investigation, QD-FISH was applied successfully on maize chromosomes (87). In contrast to the Muller et al. (82) study where the conclusion was that QD–streptavidin conjugates could not successfully detect plant chromosomes, successful hybridisation was indeed reported, albeit with QD probes prepared somewhat differently. That is, the nanoparticles were coated with MAA and the oligonucleotide was attached via a metal-thiol bond. The authors tried to address the possible steric hindrance problem by keeping the oligonucleotide probe further away from the QD surface using a homo-polymer of thymidine sequence. By doing this, it was claimed that modification of the hydrodynamic diameter of the bioprobes was small enough to penetrate into maize chromosomes. Moreover, the authors emphasise the improved impact of their own

Citation: Nano Reviews 2010, **1**: 5117 - DOI: 10.3402/nano.v1i0.5117

solubilisation strategy on these modified QD probes (MAA-coated) compared to the commercially available polymer-coated QD–streptavidin ones. Mirroring the report by Xiao and Barker (77), this study highlights the importance of pH, ionic strength and formamide to increase the affinity of QD probes to chromosomal targets. Although the report by Ma et al. (87) declared a preference for the MAA coating of QDs compared to the polymer-coated ones, Choi et al. (88) used polymer-coated QDs that maintained high QY and photostability in their FISH experiments. They coupled the DNA oligonucleotides via a 1-ethyl-3-(3-dimethylaminopropyl) carbodiimide hydrochloride (EDC) molecule and were able to visualise gene targets in *Drosophila*.

The only study that we are aware of to make use of both organic and inorganic fluorochromes in an attempt to increase the number of colours on a single cell was published by Muller et al. (89). One of the objectives of this report was to show the capability of QD probes in 4Pi microscopy, a technique that can push the resolution limits to 100 nm or even less, thereby requiring high photostable fluorophores. Although a combination of QDs and traditional fluorophores could be combined for the visualisation of chromosome painting probes (maximum multiplexing was achieved using three QDs and three traditional fluorochromes), there was some batch variability concerning QD conjugates that manifested as different signal intensity results even in parallel experiments. Thus, the authors argue that further progress is anticipated from the manufacturer's point of view to increase QD robustness and reliability.

Our own experience in quantum dot-fluorescent in situ hybridisation (QD-FISH)

Given the obvious potential of QD-FISH, we have been somewhat puzzled how few studies exist in this area. Around 2006, we began to explore the use of QDs in place of organic fluorochromes, specifically with a view to using QDs in multiplex experiments [i.e. to target multiple regions simultaneously, see Ioannou et al. (90)]. Our own research questions pertain to chromosome copy number and nuclear position of chromosome territories in human sperm (91) and preimplantation embryos (92) and possible links between aberrant nuclear organisation and infertility and/or aneuploidy. In preimplantation embryos specifically, cells are few in number and ethically sensitive; thus as much information as possible should be derived from them. Our other interests relate to genome organisation and evolution in birds (93–96) and fish (97–99), which have large numbers of small chromosomes that are not easily cytologically distinguishable. In all the above, clear bright signals amenable to multiplexing would be of great advantage in advancing our work, particularly if probes could be labelled directly with QDs. Some of our original work was published last year (90) and the following summarises aspects of it.

Our first clear observation was that the emission spectra of the QD samples (from both Invitrogen and Evident Technologies) appeared not to be narrow as the manufacturers claimed them to be. We established this by simply spotting diluted aliquots of the QD–streptavidin conjugates to a slide and observing them under the microscope. Indeed there appeared to be significant emission bleed-through into other filters (Fig. 4).

All QDs appeared to show significant bleed-through to other filters but, from visual inspection, QD585 appeared to have the narrowest emission. As a control, the Cy3–streptavidin (organic dye) also showed significant emission bleed-through to other channels, not dissimilar to some of the QDs. We therefore continued experiments mostly using QD585 (7).

Our initial results were very encouraging when biotinylated probes were detected using the QD585–strepavidin conjugate (7). Fig. 5 demonstrates this in chromosome painting experiment compared to a Cy3 control.

When results were successful, the reported properties of QDs were plain to see. In particular, preparations were noticeably brighter than Cy3 preparations and did not fade upon inspection. That is, when Cy3-labelled preparations were exposed continually to the fluorescent lamp, photo-bleaching occurred after about 5 min. By contrast, when QD preparations were exposed to UV light, no noticeable loss of signal was seen, even following 1 h of exposure. We also noticed that, in several chromosome painting experiments, the QD signal was brighter around the periphery of the chromosome – a sort

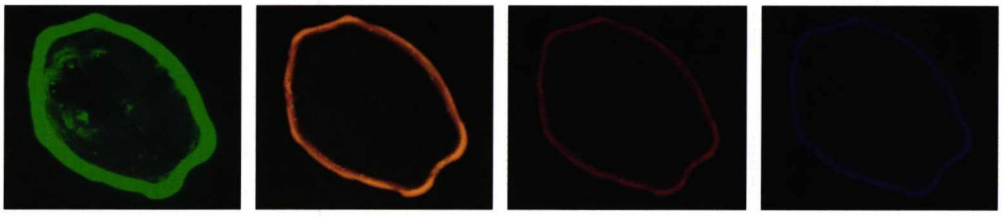

Fig. 4. QD520 (supplied by Evident) spotted on to a glass slide, excited by a UV filter and then detected with barrier filters at 525, 565, 585 and 605 nm, respectively. Although under the green barrier filter (525 nm) the brightest fluorescence is observed, significant bleed-through is seen on the other filters indicating that the emission spectrum is not as narrow as is usually purported for QDs.

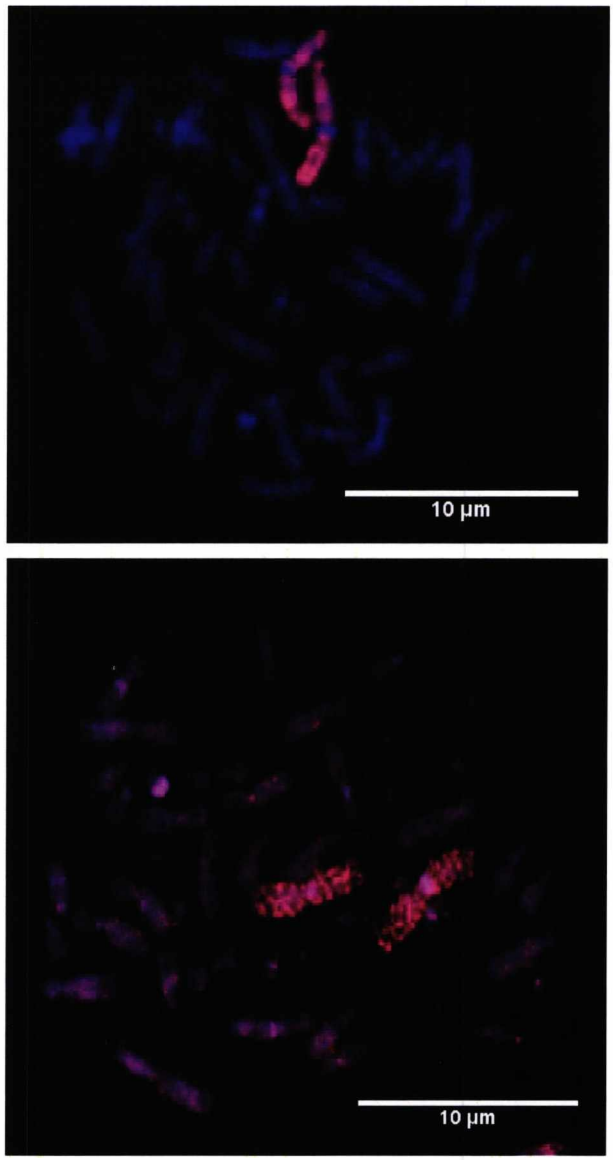

Fig. 5. Successful FISH experiments on human chromosome 1 using biotinylated chromosome 1 paint with Cy3–streptavidin conjugate control (upper) and QD585–streptavidin conjugate (lower). QD585 signals were brighter, though more 'patchy' and with a greater amount of background. Adapted from Ioannou et al. (90).

of fluorescent 'sheath' (Fig. 6). Moreover, in two or three cases, a bright signal was observed in the less condensed interphase nuclei of the cell, but not in the highly coiled metaphase chromosomes.

On the negative side, in general terms, QD preparations in these experiments had more non-specific background than were observed for Cy3 preparations and we can confirm a similar observation by Muller et al. (89) on identical experiments giving different levels of hybridisation efficiency. Even more confusingly, our experiment would regularly work on one slide but not the other identically processed in parallel. In general terms, indirect QD experiments were successful approximately 25–35% of the time, compared to Cy3 controls that worked reliably and consistently.

In attempts to improve the efficacy and reliability of our experiments, various FISH conditions were systematically altered. These included removal of a 'blocking' step prior to the addition of the conjugate and changing the temperature, pH and time of the post-hybridisation washes. These did not usually improve QD experiments and the same applied when controlled experiments were performed in the presence or absence of dextran sulphate (a component of hybridisation buffer used to chelate the hybridised probe and make the signal stronger). In an attempt to minimise steric hindrance, a longer carbon chain (biotin-21-dUTP) was used instead of 16-dUTP, and different ratios of biotin labelled and unlabelled probes were assessed. No noticeable difference was observed between the two biotins and there was no indication of more efficient hybridisation in any of the different ratios tested.

Several more alternative strategies were attempted with no increased efficacy of QD-FISH; these included trying numerous batches of chromosome preparations, labelling probes with digoxigenin (and attempting detection with anti-digoxigenin) and methods to increase cell permeability (fixation, pepsin). The only intervention that we did observe that had a degree of success was the use of silicon-coated plastic tubes and sonication of the conjugate prior to use. In both conditions, we observed an (albeit temporary) improvement in the reliability of the results. Notwithstanding the repeated efforts to increase

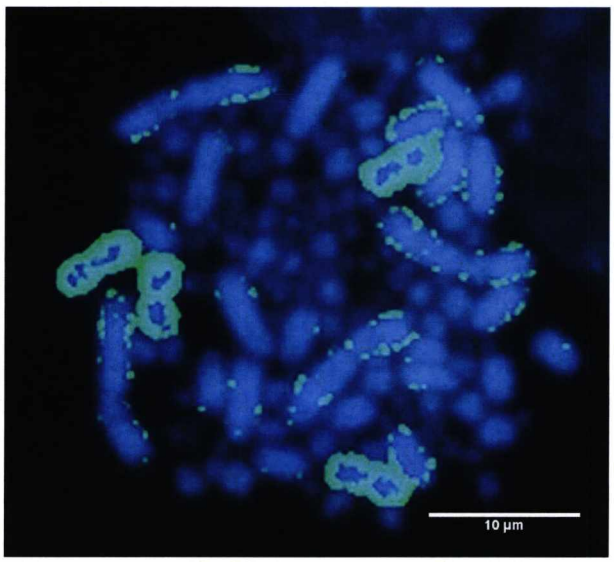

Fig. 6. Successful chromosome painting experiment (chromosome 2, tetraploid cell) in chicken, but with signals predominantly around the periphery of the chromosome, giving an impression of a fluorescent 'sheath'. Adapted from Ioannou et al. (90).

Citation: Nano Reviews 2010, **1**: 5117 - DOI: 10.3402/nano.v1i0.5117

the robustness of our approach, on the whole, outcomes were temperamental or unsuccessful. Fig. 7 shows some of our inglorious attempts.

This limited degree of success was, however, relatively encouraging compared to our attempts to conjugate QDs directly to FISH probes. Our direct conjugation strategy of DNA to QDs was based on recently published material (84) and, with the direct help of the authors, we were confident that we had made successful conjugates (established by mobility shifts on agarose gels). Such conjugates were generated for chromosome paints and oligonucleotide probes recognising the centromeres of chromosomes, however repeated attempts at subsequent FISH experiments (employing a range of different conditions of stringency, hybridisation buffer, QD:DNA concentration ratios and incubation times) without exception ended in failure (despite considerable success with Cy3 conjugate controls).

Quantum dot-fluorescent in situ hybridisation (QD-FISH): where does this leave us?

The message through our comprehensive appraisal of the utility of QDs for FISH has been that, in their current form, QDs are not suitable materials for FISH applications. If further evidence were needed, it can be found in the fact that traditional fluorochromes have not, for any application, been replaced by QDs, despite their great potential. There are few peer-reviewed studies pertaining to QD-FISH and we are unaware of any company marketing QD-labelled FISH.

In our experience (and following discussions with colleagues from other groups), lack of reproducibility appears to be a distinguishing feature of QD-FISH in contrast to the more robust applications with organic fluorophore–streptavidin conjugates. That is, while we would not claim that we have explored every possible avenue with respect to QD-FISH, we have nonetheless extensive experience in FISH over many years and have been (for the last three to four years) running parallel QD-based experiments (mostly in avian and human cells). Our collective experience paints a general picture of a non-reproducible approach when QDs are used in place of organic fluorochromes.

The unreliable nature of QDs (at least for FISH) is perhaps not totally unexpected as other colleagues have had similar experiences to our own (89, 100). There is clearly a challenging set of conditions pertaining to intracellular delivery of QDs and, since there are no reliable FISH protocols for this, individual adaptations need empirical establishment (49). If this was achieved then the reliability may well improve and the benefits of QDs observed in this and other studies (e.g. increased brightness, resistance to photo-bleaching) may be properly realised. With all this in mind, we can speculate about reasons for the lack of reproducibility of QD-FISH

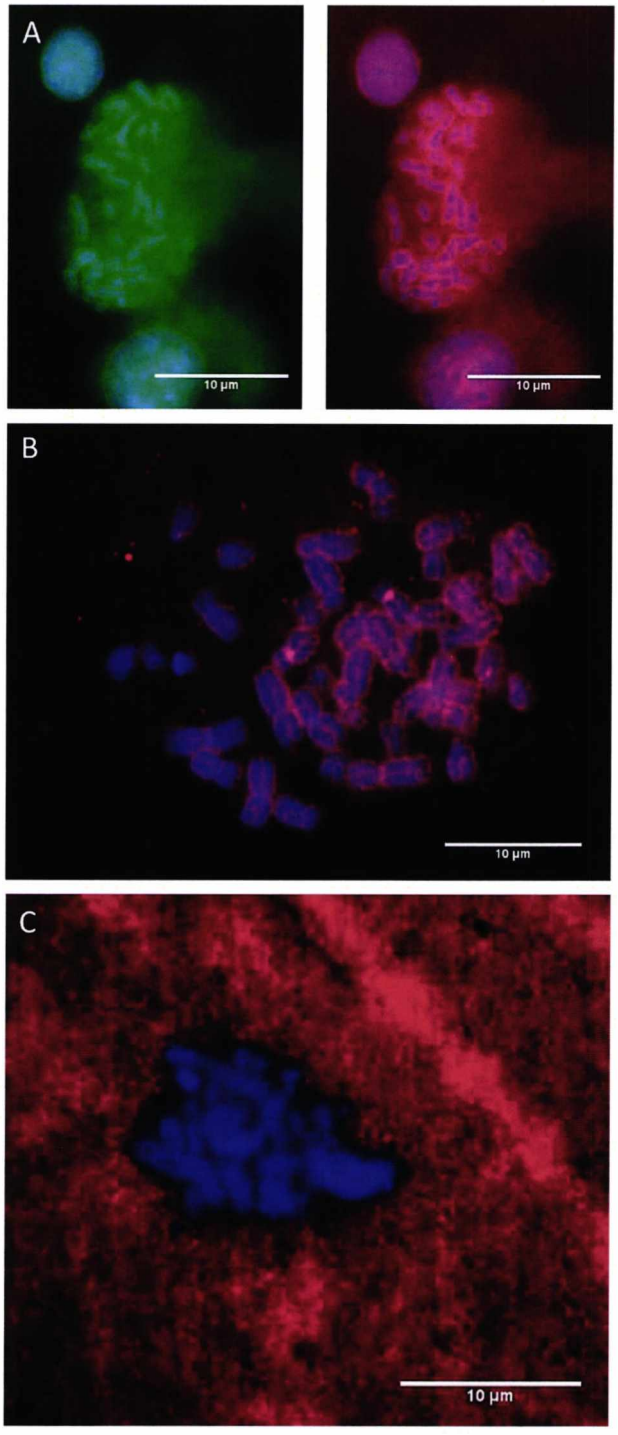

Fig. 7. (A) Chromosome painting attempt in human lymphocytes using QD520. No specific signal was seen and the area surrounding the chromosomes had a very high background (left), moreover the background signal bled through into the red channel (right). (B) Attempts to visualise the centromeres of human chromosome 12. There is some evidence of hybridisation and detection but the preparation has a very high background. (C) A bright red signal is seen on every part of the slide apart from the chromosomes! This was another attempt at human chromosome painting for chromosomes 1 and 2.

results. Clues about QD size and chemistry during synthesis may be a starting point.

QDs vary in size (this is the basis of the fluorescent colour that they emit) from 2 to 10 nm. A Cy3 molecule on the other hand is <2 nm in size (22). This may explain in part why our successful FISH experiments gave the impression of larger fluorescent particles and why there was a greater degree of background for most experiments. It might also explain an observed fluorescent 'sheath' effect seen on some metaphases (90) and why certain preparations gave bright signals in decondensed interphase nuclei, but not highly coiled metaphase chromosomes. That is, steric hindrance may have led to signals being brighter in areas where the chromatin is less compact (e.g. at the edge of the chromosomes and/or in the interphase nucleus), indeed steric hindrance has been an issue reported in many studies (82, 84, 87, 88). If this were true, we might have expected to see an improvement when we reduced the ratio of labelled to unlabelled dUTPs and/or when we made use of a 'longer-arm' biotin dUTP. This was not the case. Again, however, a general background of intermittent success may have masked any appreciable difference seen in any given experiment. Furthermore, as QD-streptavidin conjugates were used throughout these experiments, it is worth pointing out that it is not entirely clear how streptavidin binds on the actual polymer site of the QD. For this reason, the number of free streptavidin sites varies per individual QD (10–15). Incidentally, these sites can break off from the nanoparticle (for no reported reason) rendering the probe unstable or even detached, with immediate effect on the hybridisation signal (Bentolila, L *personal communication*). We are also informed that QD streptavidin conjugates can easily degrade (a batch-specific attribute) and this can be due to barely discernable temperature changes during storage. Additionally, we are given to understand that QDs are prone to adhere to tubes sides and tips (Chan, P *personal communication*). Our attempts to reduce this problem using siliconised tubes and regular sonication met with a degree of success; however it did not eliminate our technical issues completely.

Another confounding issue was that the emission spectra of the QDs did not appear to be as narrow as the manufacturers claimed, in that we observed 'bleed-through' between channels, despite making use of narrow band-pass filters. Apparently, this phenomenon is not as uncommon as the literature might suggest (Bentolila, L *personal communication*) and could vary from batch to batch. Controlling the size of the core during synthesis (that will tune the colour that the QD will emit) requires high technical skills and sometimes nanoparticles are larger than expected. Addressing the size control is critical in particular for multicolour detection or imaging and could hold the key to the success of multicolour experiments in QD-FISH. Also, abnormalities in their shape could result in the same effect (Bentolila, L *personal communication*). An additional possible explanation for this emission bleed-through to other channels was that QDs were not monodisperse. Simple spotting experiments confirmed this statement. Fig. 8 shows a QD605-conjugate dissolved in hybridisation mix where different QD populations could be observed under the different band-pass filters.

The different colours seen in Fig. 8 represent different-sized QDs that emit at longer (towards the red – large QDs) or shorter (towards the blue – small QDs) wavelengths. These findings are consistent with those of Murray and colleagues, who have tried to address the monodispersity of QD preparations (101). All these technical features that were attributed to the chemical synthesis of the QDs may require more experimental attention in order to improve QD synthesis. Of course, we cannot rule out the possibility that bleed-through and monodispersity are batch-specific problems; after all, we did not test more than three or four batches for each QD. However, we saw no evidence of batch-specific variance.

A further QD feature that we observed was 'blinking' – a phenomenon unknown in conventional FISH where the QD alternates between an emitting (on) and non-emitting (off) state (28, 29). Blinking has been explained according to an Auger ionisation model (30) and affects single molecule detection applications by saturation of the signal. It may, however, be suppressed by using thiol groups to passivate the QD surface (31, 84). A second phenomenon, photo-brightening, where the fluorescence

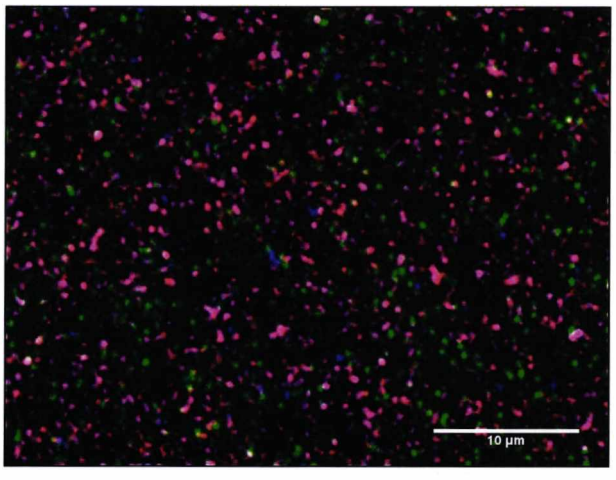

Fig. 8. QD605 dissolved in hybridisation mix and viewed directly under the microscope using four barrier filters: 525 nm (blue), 565 nm, 585 nm (red) and 605 nm (far red but pseudo-coloured purple for the purposes of this figure). The image represents a merge of all four filters. The QDs are predominantly purple (as would be expected), but a smaller number of green, blue and red QDs are seen. The discrete appearance of QDs of one or other of the colours indicates there is a mixed population of QDs. Adapted from Ioannou et al. (90).

Citation: Nano Reviews 2010, **1**: 5117 - DOI: 10.3402/nano.v1i0.5117

intensity increases rapidly at the first stage of illumination and then stabilises, can limit quantitative studies (33). Both these properties are associated with mobile charges on the surface of the QDs (13).

A likely reason to explain the positive results arising from groups that have published in this area (79, 84, 87) is that their laboratories were equipped with the ability to synthesise and batch-test their own conjugates (a luxury not afforded to most groups). Ma et al. (87) suggested that the QDs that they used were significantly smaller than those available commercially and may thus have reduced steric hindrance and increased hybridisation ability. Several laboratories (79, 84, 87), however, have generated QD-oligonucleotide conjugates and report that, during the time of annealing, steric hindrance has little effect but it may limit the QDs access to the target at the time of detection (84, 87). This may provide a possible explanation for our lack of success in generating usable conjugates. Furthermore, negative hybridisation was potentially caused by unbound QD left over after the incubation between QD and DNA (to generate a conjugant) that prevented the complex entering cells and hybridising (acted as a competitor). Excess cytoplasm around the chromosomes cannot solely be blamed as pepsin treatments were introduced to reduce it.

Taking all this into consideration, further research is essential. Advances in nanomaterials synthesis (regarding uniformity and size control) and solubility will assist conjugation to biomolecules. Moreover, a new generation of nanocrystals (FloDots, C-dots) has already been mentioned in the literature (102, 103). There may well be a future for a marriage between nanotechnology and molecular cytogenetics. Like all good marriages, however, a little patience may be required.

Acknowledgements

The authors would like to note the efforts of Dr Helen Tempest (formerly of our own group and now of the Florida International University) for her attempts on QD-FISH. We would also like to thank Mr. Michael Ellis (Digital Scientific UK) for his initial enthusiasm and funding for the project, and for assembling the image analysis hardware.

Conflict of interest and funding

There is no conflict of interest in the present study for any of the authors.

References

1. Chan WC. Bionanotechnology progress and advances. Biol Blood Marrow Transplant 2006; 12: 87–91.
2. Parak WJ, Gerion D, Pellegrino T, Zanchet D, Micheel C, Williams SC, et al. Biological applications of colloidal nanocrystals. Nanotechnology 2003; 14: R15–27.
3. Jaiswal JK, Simon SM. Potentials and pitfalls of fluorescent quantum dots for biological imaging. Trends Cell Biol 2004; 14: 497–504.
4. Reed MA, Bate RT, Bradshaw WM, Duncan WR, Frensley JWL, Shih HD. Spatial quantization in GaAs-AlGaAs multiple quantum dots. J Vac Sci Technol B 1986; 4: 358–60.
5. Miller DAB, Chemla DS, Schmittrink S. Absorption saturation of semiconductor quantum dots. J Opt Soc Am B 1986; 3: 42.
6. Lipovskii A, Kolobkova E, Petrikov V, Kang I, Olkhovets A, Krauss T, et al. Synthesis and characterization of PbSe quantum dots in phosphate glass. Appl Phys Lett 1997; 71: 3406–8.
7. Invitrogen. Qdot nanocrystal technology. Vol. 2006. Carlsbad, CA: Invitrogen Corporation; 2006.
8. Michalet X, Pinaud FF, Bentolila LA, Tsay JM, Doose S, Li JJ, et al. Quantum dots for live cells, in vivo imaging, and diagnostics. Science 2005; 307: 538–44.
9. Quantum Dot Corporation. Qdot nanocrystals. In: Anatomy. Vol. 2006. Hayward, CA: Quantum Dot Corporation (QDC); 2006.
10. Chan WC, Maxwell DJ, Gao X, Bailey RE, Han M, Nie S. Luminescent quantum dots for multiplexed biological detection and imaging. Curr Opin Biotechnol 2002; 13: 40–6.
11. Murray CB, Norris DJ, Bawendi MG. Synthesis and characterization of nearly monodisperse CdE (E = S, Se, Te) semiconductor nanocrystallites. J Am Chem Soc 1993; 115: 8706–15.
12. Michalet X, Pinaud F, Thilo DL, Dahan M, Bruchez MP, Alivisatos AP, et al. Properties of fluorescent semiconductor nanocrystals and their application to biological labeling. Single Mol 2001; 2: 261–76.
13. Fu A, Alivisatos AP, Gu W, Larabell C. Semiconductor nanocrystals for biological imaging. Curr Opin Neurobiol 2005; 15: 568–75.
14. Alivisatos AP, Gu W, Larabell C. Quantum dots as cellular probes. Annu Rev Biomed Eng 2005; 7: 55–76.
15. Alivisatos AP. Perspectives on the physical chemistry of semiconductor nanocrystals. J Phys Chem B 1996; 100: 13226–39.
16. Alivisatos P. The use of nanocrystals in biological detection. Nat Biotechnol 2004; 22: 47–52.
17. Jonathan C. A quantum paintbox. Chemistry World 2003: 1–8. Available from: http://www.rsc.org/chemistryworld/Issues/2003/September/paintbox.asp [cited 4 March 2010].
18. Chan WC, Nie S. Quantum dot bioconjugates for ultrasensitive nonisotopic detection. Science 1998; 281: 2016–8.
19. Arya H, Kaul Z, Wadhwa R, Taira K, Hirano T, Kaul SC. Quantum dots in bio-imaging: revolution by the small. Biochem Biophys Res Commun 2005; 329: 1173–7.
20. Green M. Semiconductor quantum dots as biological imaging agents. Angew Chem Int Ed Engl 2004; 43: 4129–31.
21. Dabbousi BO, Rodriguez-Viejo J, Mikulec FV, Heine JR, Mattoussi H, Ober R, et al. (CdSe)ZnS core-shell quantum dots: synthesis and characterization of a size series of highly luminescent nanocrystallites. J Phys Chem B 1997; 101: 9463–75.
22. Bailey RE, Smith AM, Nie S. Quantum dots in biology and medicine. Physica E 2004; 25: 1–12.
23. Larson DR, Zipfel WR, Williams RM, Clark SW, Bruchez MP, Wise FW, et al. Water-soluble quantum dots for multiphoton fluorescence imaging in vivo. Science 2003; 300: 1434–6.
24. Gao X, Yang L, Petros JA, Marshall FF, Simons JW, Nie S. In vivo molecular and cellular imaging with quantum dots. Curr Opin Biotechnol 2005; 16: 63–72.

25. Wu X, Liu H, Liu J, Haley KN, Treadway JA, Larson JP, et al. Immunofluorescent labeling of cancer marker HER2 and other cellular targets with semiconductor quantum dots. Nat Biotechnol 2003; 21: 41–6.
26. Jaiswal JK, Mattoussi H, Mauro JM, Simon SM. Long-term multiple color imaging of live cells using quantum dot bioconjugates. Nat Biotechnol 2003; 21: 47–51.
27. Lounis B, Bechtel HA, Gerion D, Alivisatos PA, Moerner WE. Photon antibunching in single CdSe/ZnS quantum dot fluorescence. Chem Phys Lett 2000; 329: 399–404.
28. Michler P, Imamoglu A, Mason MD, Carson PJ, Strouse GF, Buratto SK. Quantum correlation among photons from a single quantum dot at room temperature. Nature 2000; 406: 968–70.
29. Pinaud F, Michalet X, Bentolila LA, Tsay JM, Doose S, Li JJ, et al. Advances in fluorescence imaging with quantum dot bioprobes. Biomaterials 2006; 27: 1679–87.
30. Efros AL, Rosen M. Random telegraph signal in the photoluminescence intensity of a single quantum dot. Phys Rev Lett 1997; 78: 1110–3.
31. Hohng S, Ha T. Near-complete suppression of quantum dot blinking in ambient conditions. J Am Chem Soc 2004; 126: 1324–5.
32. Lee SF, Osborne MA. Brightening, blinking, bluing and bleaching in the life of a quantum dot: friend or foe? Chemphyschem 2009; 10: 2174–91.
33. Gerion D, Pinaud F, Williams SC, Parak WJ, Zanchet D, Weiss S, et al. Synthesis and properties of biocompatible water-soluble silica-coated CdSe/ZnS semiconductor quantum dots. J Phys Chem B 2001; 105: 8861–71.
34. Parak WJ, Pellegrino T, Plank C. Labelling of cells with quantum dots. Nanotechnology 2005; 16: R9–R25.
35. Yu WW, Chang E, Drezek R, Colvin VL. Water-soluble quantum dots for biomedical applications. Biochem Biophys Res Commun 2006; 348: 781–6.
36. Pathak S, Choi SK, Arnheim N, Thompson ME. Hydroxylated quantum dots as luminescent probes for in situ hybridization. J Am Chem Soc 2001; 123: 4103–4.
37. Gerion D, Parak WJ, Williams SC, Zanchet D, Micheel CM, Alivisatos AP. Sorting fluorescent nanocrystals with DNA. J Am Chem Soc 2002; 124: 7070–4.
38. Mitchell GP, Mirkin CA, Letsinger RL. Programmed assembly of DNA functionalized quantum dots. J Am Chem Soc 1999; 121: 8122–3.
39. Willard DM, Carillo LL, Jung J, van Orden A. CdSe–ZnS quantum dots as resonance energy transfer donors in a model protein-protein binding assay. Nano Lett 2001; 1: 469–74.
40. Sukhanova A, Devy J, Venteo L, Kaplan H, Artemyev M, Oleinikov V, et al. Biocompatible fluorescent nanocrystals for immunolabeling of membrane proteins and cells. Anal Biochem 2004; 324: 60–7.
41. Bruchez M Jr, Moronne M, Gin P, Weiss S, Alivisatos AP. Semiconductor nanocrystals as fluorescent biological labels. Science 1998; 281: 2013–6.
42. Pellegrino T, Manna L, Kudera S, Liedl T, Koktysh D, Rogach AL, et al. Hydrophobic nanocrystals coated with an amphiphilic polymer shell: a general route to water soluble nanocrystals. Nano Lett 2004; 4: 703–7.
43. Gao X, Cui Y, Levenson RM, Chung LW, Nie S. In vivo cancer targeting and imaging with semiconductor quantum dots. Nat Biotechnol 2004; 22: 969–76.
44. Osaki F, Kanamori T, Sando S, Sera T, Aoyama Y. A quantum dot conjugated sugar ball and its cellular uptake. On the size effects of endocytosis in the subviral region. J Am Chem Soc 2004; 126: 6520–1.
45. Dubertret B, Skourides P, Norris DJ, Noireaux V, Brivanlou AH, Libchaber A. In vivo imaging of quantum dots encapsulated in phospholipid micelles. Science 2002; 298: 1759–62.
46. Wang YA, Li JJ, Chen H, Peng X. Stabilization of inorganic nanocrystals by organic dendrons. J Am Chem Soc 2002; 124: 2293–8.
47. Pinaud F, King D, Moore HP, Weiss S. Bioactivation and cell targeting of semiconductor CdSe/ZnS nanocrystals with phytochelatin-related peptides. J Am Chem Soc 2004; 126: 6115–23.
48. Kim S, Bawendi MG. Oligomeric ligands for luminescent and stable nanocrystal quantum dots. J Am Chem Soc 2003; 125: 14652–3.
49. Resch-Genger U, Grabolle M, Cavaliere-Jaricot S, Nitschke R, Nann T. Quantum dots versus organic dyes as fluorescent labels. Nat Methods 2008; 5: 763–75.
50. Gao X, Chan WC, Nie S. Quantum-dot nanocrystals for ultrasensitive biological labeling and multicolor optical encoding. J Biomed Opt 2002; 7: 532–7.
51. Goldman ER, Balighian ED, Kuno MK, Labrenz S, Tran PT, Anderson GP, et al. Luminescent quantum dot-adaptor protein–antibody conjugates for use in fluoroimmunoassays. Phys Stat Sol B 2002; 229: 407–14.
52. Goldman ER, Balighian ED, Mattoussi H, Kuno MK, Mauro JM, Tran PT, et al. Avidin: a natural bridge for quantum dot–antibody conjugates. J Am Chem Soc 2002; 124: 6378–82.
53. Mason JN, Tomlinson ID, Rosenthal SJ, Blakely RD. Labeling cell-surface proteins via antibody quantum dot streptavidin conjugates. Methods Mol Biol 2005; 303: 35–50.
54. Dahan M, Levi S, Luccardini C, Rostaing P, Riveau B, Triller A. Diffusion dynamics of glycine receptors revealed by single-quantum dot tracking. Science 2003; 302: 442–5.
55. Tokumasu F, Dvorak J. Development and application of quantum dots for immunocytochemistry of human erythrocytes. J Microsc 2003; 211: 256–61.
56. Rosenthal SJ, Tomlinson A, Adkins EM, Schroeter S, Adams S, Swafford L, et al. Targeting cell surface receptors with ligand-conjugated nanocrystals. J Am Chem Soc 2002; 124: 4586–94.
57. Lidke DS, Nagy P, Heintzmann R, Arndt-Jovin DJ, Post JN, Grecco HE, et al. Quantum dot ligands provide new insights into erbB/HER receptor-mediated signal transduction. Nat Biotechnol 2004; 22: 198–203.
58. Zheng J, Ghazani AA, Song Q, Mardyani S, Chan WC, Wang C. Cellular imaging and surface marker labeling of hematopoietic cells using quantum dot bioconjugates. Lab Hematol 2006; 12: 94–8.
59. Parak WJ, Boudreau R, Le Gros MA, Gerion D, Zanchet D, Micheel CM, et al. Cell motility and metastatic potential studies based on quantum dot imaging of phagokinetic tracks. Adv Mater 2002; 14: 882–5.
60. Akerman ME, Chan WC, Laakkonen P, Bhatia SN, Ruoslahti E. Nanocrystal targeting in vivo. Proc Natl Acad Sci USA 2002; 99: 12617–21.
61. Biju V, Itoh T, Anas A, Sujith A, Ishikawa M. Semiconductor quantum dots and metal nanoparticles: syntheses, optical properties, and biological applications. Anal Bioanal Chem 2008; 391: 2469–95.
62. Mattheakis LC, Dias JM, Choi YJ, Gong J, Bruchez MP, Liu J, et al. Optical coding of mammalian cells using semiconductor quantum dots. Anal Biochem 2004; 327: 200–8.
63. Rieger S, Kulkarni RP, Darcy D, Fraser SE, Koster RW. Quantum dots are powerful multipurpose vital labeling agents in zebrafish embryos. Dev Dyn 2005; 234: 670–81.
64. Ferrara DE, Weiss D, Carnell PH, Vito RP, Vega D, Gao X et al. Quantitative 3D fluorescence technique for the analysis

Citation: Nano Reviews 2010, **1**: 5117 - DOI: 10.3402/nano.v1i0.5117

of en face preparations of arterial walls using quantum dot nanocrystals and two-photon excitation laser scanning microscopy. Am J Physiol Regul Integr Comp Physiol 2006; 290: R114–23.
65. Mansson A, Sundberg M, Balaz M, Bunk R, Nicholls IA, Omling P, et al. In vitro sliding of actin filaments labelled with single quantum dots. Biochem Biophys Res Commun 2004; 314: 529–34.
66. Bruchez MP. Turning all the lights on: quantum dots in cellular assays. Curr Opin Chem Biol 2005; 9: 533–7.
67. Kim S, Lim YT, Soltesz EG, De Grand AM, Lee J, Nakayama A, et al. Near-infrared fluorescent type II quantum dots for sentinel lymph node mapping. Nat Biotechnol 2004; 22: 93–7.
68. Takeda M, Tada H, Higuchi H, Kobayashi Y, Kobayashi M, Sakurai Y, et al. In vivo single molecular imaging and sentinel node navigation by nanotechnology for molecular targeting drug-delivery systems and tailor-made medicine. Breast Cancer 2008; 15: 145–52.
69. Ciarlo M, Russo P, Cesario A, Ramella S, Baio G, Neumaier CE, et al. Use of the semiconductor nanotechnologies 'quantum dots' for in vivo cancer imaging. Recent Pat Anticancer Drug Discov 2009; 4: 207–15.
70. Ballou B, Ernst LA, Andreko S, Fitzpatrick JA, Lagerholm BC, Waggoner AS, et al. Imaging vasculature and lymphatic flow in mice using quantum dots. Methods Mol Biol 2009; 574: 63–74.
71. Kang WJ, Chae JR, Cho YL, Lee JD, Kim S. Multiplex imaging of single tumor cells using quantum-dot-conjugated aptamers. Small 2009; 5: 2519–22.
72. Singhal S, Nie S, Wang MD. Nanotechnology applications in surgical oncology. Annu Rev Med 2010; 61: 359–73.
73. Mahmoud W, Sukhanova A, Oleinikov V, Rakovich YP, Donegan JF, Pluot M, et al. Emerging applications of fluorescent nanocrystals quantum dots for micrometastases detection. Proteomics 2009; 10: 700–16.
74. Pinkel D, Straume T, Gray JW. Cytogenetic analysis using quantitative, high-sensitivity, fluorescence hybridization. Proc Natl Acad Sci USA 1986; 83: 2934–8.
75. Ekong R, Wolfe J. Advances in fluorescence in situ hybridization. Curr Opin Biotechnol 1998; 9: 19–24.
76. Levsky JM, Singer RH. Fluorescence in situ hybridization: past, present and future. J Cell Sci 2003; 116: 2833–8.
77. Xiao Y, Barker PE. Semiconductor nanocrystal probes for human metaphase chromosomes. Nucleic Acids Res 2004; 32: e28.
78. Xiao Y, Telford WG, Ball JC, Locascio LE, Barker PE. Semiconductor nanocrystal conjugates, FISH and pH. Nat Methods 2005; 2: 723.
79. Xiao Y, Barker PE. Semiconductor nanocrystal probes for human chromosomes and DNA. Minerva Biotec 2004; 16: 281–8.
80. Chan P, Yuen T, Ruf F, Gonzalez-Maeso J, Sealfon SC. Method for multiplex cellular detection of mRNAs using quantum dot fluorescent in situ hybridization. Nucleic Acids Res 2005; 33: 1–8.
81. Wu SM, Zhao X, Zhang ZL, Xie HY, Tian ZQ, Peng J, et al. Quantum-dot-labeled DNA probes for fluorescence in situ hybridization (FISH) in the microorganism *Escherichia coli*. Chem Phys Chem 2006; 7: 1062–7.
82. Muller F, Houben A, Barker PE, Xiao Y, Kas JA, Melzer M. Quantum dots – a versatile tool in plant science? J Nanobiotechnol 2006; 4: 5.
83. Tholouli E, Hoyland JA, Di Vizio D, O'Connell F, Macdermott SA, Twomey D, et al. Imaging of multiple mRNA targets using quantum dot based in situ hybridization and spectral deconvolution in clinical biopsies. Biochem Biophys Res Commun 2006; 348: 628–36.
84. Bentolila LA, Weiss S. Single-step multicolor fluorescence in situ hybridization using semiconductor quantum dot–DNA conjugates. Cell Biochem Biophys 2006; 45: 59–70.
85. Jiang Z, Li R, Todd NW, Stass SA, Jiang F. Detecting genomic aberrations by fluorescence in situ hybridization with quantum dots-labeled probes. J Nanosci Nanotechnol 2007; 7: 4254–9.
86. Knoll JH. Human metaphase chromosome FISH using quantum dot conjugates. In: Bruchez MP, Hotz CZ, eds. Quantum dots applications in biology, vol. 374. Totowa, NJ: Humana Press; 2007, p. 55–66.
87. Ma L, Wu SM, Huang J, Ding Y, Pang DW, Li L. Fluorescence in situ hybridization (FISH) on maize metaphase chromosomes with quantum dot-labeled DNA conjugates. Chromosoma 2008; 117: 181–17.
88. Choi Y, Kim HP, Hong SM, Ryu JY, Han SJ, Song R. In situ visualization of gene expression using polymer-coated quantum-dot–DNA conjugates. Small 2009; 5: 2085–91.
89. Muller S, Cremer M, Neusser M, Grasser F, Cremer T. A technical note on quantum dots for multi-color fluorescence in situ hybridization. Cytogenet Genome Res 2009; 124: 351–9.
90. Ioannou D, Tempest HG, Skinner BM, Thornhill AR, Ellis M, Griffin DK. Quantum dots as new-generation fluorochromes for FISH: an appraisal. Chromosome Res 2009; 17: 519–30.
91. Finch KA, Fonseka KG, Abogrein A, Ioannou D, Handyside AH, Thornhill AR, et al. Nuclear organization in human sperm: preliminary evidence for altered sex chromosome centromere position in infertile males. Hum Reprod 2008; 23: 1263–70.
92. Finch KA, Fonseka G, Ioannou D, Hickson N, Barclay Z, Chatzimeletiou K, et al. Nuclear organisation in totipotent human nuclei and its relationship to chromosomal abnormality. J Cell Sci 2008; 121: 655–63.
93. Masabanda JS, Burt DW, O'Brien PC, Vignal A, Fillon V, Walsh PS, et al. Molecular cytogenetic definition of the chicken genome: the first complete avian karyotype. Genetics 2004; 166: 1367–73.
94. Robertson LB, Griffin DK, Tempest HG, Skinner BM. The evolution of the avian genome as revealed by comparative molecular cytogenetics. Cytogenet Genome Res 2007; 117: 64–77.
95. Skinner BM, Volker M, Ellis M, Griffin DK. An appraisal of nuclear organisation in interphase embryonic fibroblasts of chicken, turkey and duck. Cytogenet Genome Res 2009; 126: 156–64.
96. Griffin DK, Haberman F, Masabanda J, O'Brien PCM, Bagga M, Smith J, et al. Micro-and macro chromosome painting probes generated by flow cytometry and chromosome microdissection: tools for mapping the chicken genome. Cytogenet Cell Genet 1999; 87: 278–81.
97. Campos-Ramos R, Harvey SC, Masabanda JS, Carrasco LA, Griffin DK, McAndrew BJ, et al. Identification of putative sex chromosomes in the blue tilapia, *Oreochromis aureus*, through synaptonemal complex and FISH analysis. Genetica 2001; 111: 143–53.
98. Harvey SC, Masabanda J, Carrasco LA, Bromage NR, Penman DJ, Griffin DK. Molecular-cytogenetic analysis reveals sequence differences between the sex chromosomes of Oreochromis niloticus: evidence for an early stage of sex-chromosome differentiation. Cytogenet Genome Res 2002; 97: 76–80.
99. Griffin DK, Harvey SC, Campos-Ramos R, Ayling LJ, Bromage NR, Masabanda JS, et al. Early origins of the X

and Y chromosomes: lessons from tilapia. Cytogenet Genome Res 2002; 99: 157–63.
100. Bruchez M. Quantum dots for ultra-sensitive multicolor detection of proteins and genes. In: Jong H, Tanke H, Fransz P, eds. 16th International Chromosome Conference (16th ICC). Amsterdam, the Netherlands: Springer; 2007, pp. 1–108.
101. Murray CB, Kagan CR, Bawendi M. Synthesis and characterization of monodisperse nanocrystals and close-packed nanocrystal assemblies. Annu Rev Mater Sci 2000; 30: 545–610.
102. Yao G, Wang L, Wu Y, Smith J, Xu J, Zhao W, et al. FloDots: luminescent nanoparticles. Anal Bioanal Chem 2006; 385: 518–24.
103. Choi J, Burns AA, Williams RM, Zhou Z, Flesken-Nikitin A, Zipfel WR, et al. Core-shell silica nanoparticles as fluorescent labels for nanomedicine. J Biomed Opt 2007; 12: 064007.

***Darren K. Griffin**
Department of Biosciences
University of Kent
Canterbury CT2 7NJ, UK
Tel: +44 (0) 1227 823022
Fax: +44 (0) 1227 763912
Email: d.k.griffin@kent.ac.uk

Citation: Nano Reviews 2010, **1**: 5117 - DOI: 10.3402/nano.v1i0.5117

Cytogenetic and Genome Research

Cytogenet Genome Res
DOI: 10.1159/000322060

Published online: November 19, 2010

Male Fertility, Chromosome Abnormalities, and Nuclear Organization

D. Ioannou D.K. Griffin

School of Biosciences, University of Kent, Canterbury, UK

Key Words
Chromosome · DNA damage · Male infertility · Nuclear organization · Sperm

Abstract
Numerous studies have implicated the role of gross genomic rearrangements in male infertility, e.g., constitutional aneuploidy, translocations, inversions, Y chromosome deletions, elevated sperm disomy, and DNA damage. The primary purpose of this paper is to review male fertility studies associated with such abnormalities. In addition, we speculate whether altered nuclear organization, another chromosomal/whole genome-associated phenomenon, is also concomitant with male factor infertility. Nuclear organization has been studied in a range of systems and implicated in several diseases. For many applications the measurement of the relative position of chromosome territories is sufficient to determine patterns of nuclear organization. Initial evidence has suggested that, unlike in the more usual 'size-related' or 'gene density-related' models, mammalian (including human) sperm heads display a highly organized pattern including a chromocenter with the centromeres located to the center of the nucleus and the telomeres near the periphery. More recent evidence, however, suggests there may be size- and gene density-related components to nuclear organization in sperm. It seems reasonable to hypothesize therefore that alterations in this pattern may be associated with male factor infertility. A small handful of studies have addressed this issue; however, to date it remains an exciting avenue for future research with possible implications for diagnosis and therapy.

Male Infertility and Genetics

Infertility, the inability to conceive after at least a year of unprotected coitus, accounts for 1 in 6 couples wishing to start a family in the western world [Shah et al., 2003]. In around 20% of infertile couples male factor is the predominant cause, 38% originates from the female, both partners contributing in around 27% of cases, whereas the remaining 15% is unexplained [Seli and Sakkas, 2005; Ferlin et al., 2007]. The causes, however, can be classified as genetic, hormonal, age-related, lifestyle-related, a result of surgery or trauma, or associated with abnormalities in semen parameters [Shah et al., 2003]. Genetic causes account directly for at least 15% of male factor infertility and can be further subdivided to constitutional aneuploidy, structural abnormalities, single gene disorders, and multifactorial traits [Griffin and Finch, 2005]. More recently, associations with increased aneuploidy in the sperm heads and sperm DNA damage have also been made [Tempest and Griffin, 2004]. This study has a dual purpose: first, it reviews male fertility studies associated

KARGER

Fax +41 61 306 12 34
E-Mail karger@karger.ch
www.karger.com

1424–8581/11/0000–0000$38.00/0

Accessible online at:
www.karger.com/cgr

Prof. Darren K. Griffin
University of Kent
Canterbury CT2 7NJ (UK)
Tel. +44 1227 823 022, Fax +44 1227 763 912
E-Mail d.k.griffin@kent.ac.uk

with chromosomal abnormalities and DNA damage; second, it speculates whether altered nuclear organization, a further chromosomal/whole genome-associated phenomenon, is also related to male infertility.

Male Infertility and Constitutional Chromosome Abnormalities

Males with trisomy 21 are azoospermic or severely oligospermic and they do not usually reproduce due to physical and psychosocial limitations [Egozcue et al., 2000]. The most frequent constitutional aneuploidy relating to infertility in males, however, is Klinefelter's syndrome, present in 5% of severe oligospermic and in 10% of azoospermic males [Ferlin et al., 2007]. Klinefelter's syndrome causes arrest of spermatogenesis at the primary spermatocyte stage, although, occasionally, later stages of sperm development are observed. It exists in 2 forms: non-mosaic (47,XXY) and mosaic 47,XXY/46,XY [O'Flynn O'Brien et al., 2010]. The extra X chromosome originates in paternal meiosis I from non-disjunction of the XY bivalent (>50%) or from maternal meiosis I or II (40%) and post-zygotically in the remainder [Griffin and Finch, 2005]. The advent of ICSI has enabled Klinefelter patients to father children (54 normal births from 122 patients), but the risk of producing offspring with chromosome aneuploidies is significant due to elevated disomies in their sperm [Ferlin et al., 2007]. The chromosome constitution 47,XYY is present in 1 in 1,000 males, with fertility ranging from normozoospermia to azoospermia. The extra Y chromosome originates from paternal meiotic II non-disjunction and causes aberrant hormonal balance in the gonadal environment affecting normal chorionic gonadotropin function [Shah et al., 2003].

In terms of structural chromosome abnormalities that affect fertility, autosomal translocations are found 4–10 times more in infertile men compared to normals [O'Flynn O'Brien et al., 2010]. Robertsonian translocations occur when 2 acrocentric chromosomes fuse and can affect fertility by impairing gametogenesis or by producing gametes with an unbalanced combination of the parental rearrangement [Ferlin et al., 2007]. Similarly, in reciprocal translocations and inversions infertility can ensue through temporal impositions on the meiotic machinery caused by the formation of the pairing cross or loop, through reduced recombination in the pairing cross or loop, and/or through the production of chromosomally abnormal gametes [Griffin and Finch, 2005].

Microdeletions in the long arm of the Y chromosome are observed with a prevalence of 10–15% in non-obstructive azoospermic patients and 5–10% in severe oligospermic males [Ferlin et al., 2007; O'Flynn O'Brien et al., 2010]. A particular region of the Y chromosome that is involved in deletions associated with infertility is termed AZF (azoospermia factor) and contains vital genes for spermatogenesis [Shah et al., 2003]. AZF is comprised of 3 sub-regions (AZF a, b and c), and most deletions occur in AZFb and AZFc [Shah et al., 2003; Ferlin et al., 2007; O'Flynn O'Brien et al., 2010]. Most of the microdeletions are generated by intra-chromosomal homologous recombination between repeated sequence blocks that are organized as palindromic structures [Ferlin et al., 2007; Li et al., 2008]. Complete deletion of AZFc removes 8 gene families including DAZ (involved in spermatogenesis) which is the strongest candidate for the azoospermic phenotype of AZFc, whereas deletions in the AZFa region lead to Sertoli-cell-only syndrome, and complete deletions of AZFb or AZFb+c lead to azoospermia associated with Sertoli-cell-only syndrome or pre-meiotic spermatogenic arrest [Ferlin et al., 2007]. Several studies have tried to assess the infertility risk of a specific partial AZFc deletion termed gr/gr. The conclusion is not clear as out of the 15 studies 8 have shown an association with infertility or testicular cancer and 7 have failed to do so [Ravel et al., 2009]. Overall, studies of the assisted reproduction outcome in patients with an AZFc deletion suggest a tendency towards decreased fertilization rates but not a significant change in overall pregnancy and delivery rates compared to controls [Seli and Sakkas, 2005].

Sperm Disomy Levels and Infertility

Cumulative data from human hamster fusion assays [Martin et al., 1991] estimates that aneuploidy in spermatozoa in normal controls is 1–2% [Hassold et al., 1996]. However, structural abnormalities are higher, i.e., 6–7% [Martin, 2008]. With the advent of FISH technology, specific probes have assessed sperm chromosome disomy (nullisomy being indistinguishable from FISH failure) in larger numbers. These studies suggest that most autosomes have a disomy frequency of 0.1%, whereas there is a significant increase for disomy 21 (0.29%), 22 (0.25%), and sex chromosome disomy (0.43%) [Tempest and Griffin, 2004; Martin, 2006]. Thus, aneuploidy can occur for all chromosomes. However, there is a particular susceptibility of certain bivalents possibly due to the fact that they usually have a single chiasma. Indeed, non-disjunction of the sex chromosomes has been associated with reduced recombination in the pseudoautosomal region, both in paternally derived XXY patients [Hassold et al., 1991; Lorda-Sanchez et al., 1992] and XY disomic sperm [Shi et al., 2001; Martin, 2005, 2006, 2008].

Moosani et al. [1995] were the first to report a higher degree of chromosomal abnormalities in men with impaired fertility compared to controls. In a comprehensive review by Tempest and Griffin [2004], disomy results for all chromosomes studied are summarized (comparing normal and infertile males). The consensus, despite inter-study differences, is a correlation between sperm aneuploidy and male infertility. In general terms, most studies have observed an increase in the level of sperm disomy with increased severity of infertility; most chromosome pairs are affected, particularly the XY bivalent [Tempest and Griffin, 2004]. Since reduced recombination has been linked with increased aneuploidy in trisomic offspring, it seems reasonable to assume that the same principle would apply for a possible link between reduced recombination and infertility. To address this, Sun et al. [2005] used immunocytogenetic techniques that allow the analysis of recombination foci during prophase I in the synaptonemal complex. They reported reduced mean frequencies of recombination and increased frequencies of chromosomes without any recombination foci in infertile males.

A specific category of males studied with respect to the relationship between sperm disomy and infertility are OATs, i.e., patients with sperm concentration of less than 15 million per ml, motility of less than 40%, and normal morphology of less than 4% (OligoAsthenoTeratozoospermia). Pang and colleagues conducted one of the first FISH studies to compare aneuploidy for 12 autosomes and the sex chromosomes in OAT males undergoing ICSI. An increased level (up to 30-fold) of disomy for all chromosomes studied was found [Pang et al., 1999]. The observation of higher incidence of aneuploidy in OAT males has also been observed in other studies [Bernardini et al., 1997; Storeng et al., 1998; Pfeffer et al., 1999; Ushijima et al., 2000; Gole et al., 2001; Zhang and Lu, 2004]. The largest OAT cohort study was more recent [Durakbasi-Dursun et al., 2008]. Thirty OATs and 10 normal controls were studied for aneuploidy of 4 chromosome pairs (13, 18, 21, XY), and increased rates of disomy for 13, 21, XY, and YY were reported for OATs compared to controls. It has been suggested that non-disjunction of specific chromosome pairs may be associated with specific semen parameters [Tempest et al., 2004] and that screening for sperm aneuploidy could become a prognostic test for couples undergoing ICSI [Petit et al., 2005; Durakbasi-Dursun et al., 2008; Sanchez-Castro et al., 2009]. There may even be avenues for possible therapy [Tempest et al., 2008].

Sperm DNA Damage and Infertility

In addition to sperm aneuploidy, evidence of DNA damage is also apparent in association with male infertility. Liu et al. [2004] reported greater DNA fragmentation and mitochondrial dysfunction in OAT sperm, highlighting the importance of selecting good quality sperm in ICSI for oocyte injection. Moreover, Plastira et al. [2007] provided evidence for an age effect in OAT patients contributing to DNA fragmentation, poor chromatin packaging, as well as a decline in semen volume, morphology, and motility. A number of other studies also argue for possible links of sperm DNA damage and male infertility [Zini and Libman, 2006; Aitken and De Iuliis, 2007; Varghese et al., 2008; Delbes et al., 2010].

Three major mechanisms, which are not mutually exclusive, seem to be involved in DNA damage: chromatin remodeling by topoisomerase, oxidative stress, and abortive apoptosis [Tarozzi et al., 2007; Aitken and De Iuliis, 2010]. Normally during chromatin remodeling in sperm (histones to protamines), naturally occurring breaks by topoisomerase II relieve the torsional stresses as DNA is compacted and subsequently are resealed [Tarozzi et al., 2007]. Alteration to this machinery of break and repair can cause altered chromatin structure and residual breaks in the DNA of sperm [Tarozzi et al., 2007].

Sperm DNA damage has also been associated with high levels of reactive oxygen species (ROS) detected in the semen of 25% of infertile men [Zini and Libman, 2006]. The susceptibility to ROS damage stems from the presence of unsaturated fatty acids in the plasma membrane, necessary for membrane fluidity which is required in the acrosome reaction during fertilization [Aitken and De Iuliis, 2010]. The only defence mechanism against ROS is the antioxidant ability of the seminal plasma and the sperm chromatin compactness [Tarozzi et al., 2007]. However, free radicals can be produced both by defective spermatozoa and semen leukocytes, thus inducing sperm damage and conferring to male infertility [Zini and Libman, 2006; Tarozzi et al., 2007; Aitken and De Iuliis, 2010]. The point in time at which the damage occurs is still under debate, but it probably happens during epididymal maturation, as this is the longer exposure time that spermatozoa have to ROS [Tarozzi et al., 2007].

Sperm DNA damage has also been associated with a form of selective apoptosis. Under normal conditions, this regulates the production of abnormal sperm in spermatogenesis and limits the population of germ cells to a number that can be supported by the Sertoli cells [Zini and Libman, 2006; Tarozzi et al., 2007; Varghese et al., 2008]. Overexpression of this process could lead to oligo-

or azoospermia, whereas underexpression could give rise to abnormal sperm which could impair fertilization [Varghese et al., 2008]. Using a marker for apoptosis (Fas) it was found that less than 10% of apoptotic sperm exist in normospermic men whereas approximately 60% of oligospermic men have more than 10% of apoptotic sperm [Varghese et al., 2008]. It has also been postulated that advancing age and cancer therapies are associated with reduced apoptosis and increase of DNA damaged spermatozoa [Zini and Libman, 2006; Varghese et al., 2008].

Taken together, factors implicated in sperm DNA damage include age, obesity, smoking, and cancer treatment, i.e., those not dissimilar to factors causing increased sperm disomy [Aitken and De Iuliis, 2007].

The emerging message from clinical studies with regard to sperm DNA damage is that it has a detrimental effect on reproductive outcomes (i.e., lower intrauterine insemination pregnancy rates and higher pregnancy loss following IVF/ICSI) and that infertile men possess substantially more spermatozoa with DNA damage [Zini and Libman, 2006; Barratt et al., 2010]. Further examination is required to fully define the impact of sperm damage on reproductive outcomes and similarly to provide more information on the aetiology of infertility to be able to develop new treatments designed to help individuals with fertility problems.

Nuclear Organization

Correct chromosome copy number and absence of DNA damage are both indicators of a 'healthy' nucleus. Another marker of nuclear health is the appropriate spatio-temporal organization of the chromatin and associated proteins in the interphase nucleus (nuclear organization).

The nucleus of any eukaryotic cell is a highly complex and compartmentalized organelle that accommodates a wide spectrum of actions such as genome replication, transcription, splicing, and DNA repair. The level of organization can be considered with respect to chromatin (chromosome territories), the interchromatin compartment, and specialized structures (e.g., nucleolus, nuclear matrix).

Chromosome Territories and Nuclear Organization

Even when decondensed in the interphase nucleus, each chromosome occupies a nuclear distinct territory and, in most cells, this territory is preferentially located at a specific position within the nucleus [Cremer and Cremer, 2001; Parada and Misteli, 2002]. Indeed, measuring the relative position of chromosome territories is perhaps the best-known means of assaying for levels of nuclear organization, and perturbations in the normal patterns can be an indicator of a disturbed nuclear health [Croft et al., 1999].

The concept of the territorial organization of chromosomes in interphase nuclei originates from the late 19th century. It was Carl Rabl [1885] who first suggested it; however, it was Theodor Boveri [1909] who first proposed the term 'chromosome territory' (CT). Boveri argued that each chromosome occupied a distinct part in the nuclear space during interphase [Cremer and Cremer, 2006]. The first experimental evidence for the existence of CTs came in 1977 when fixed cells treated with acetic acid and high salt resulted in clumps of condensed chromatin reflecting interphase chromosomes [Stack et al., 1977]. With the advent of FISH, direct visualization of CTs was possible, and later a combination of 3D-FISH on intact nuclei and confocal microscopy allowed the spatial reconstruction of CTs [Cremer and Cremer, 2010]. Once CTs became easy to visualize and measure, researchers looked for patterns of proximity and organization. It became widely accepted that CT position in the interphase nucleus is non-random [Manuelidis, 1990; Cremer et al., 2001; Marshall, 2002; Oliver and Misteli, 2005; Khalil et al., 2007; Meaburn and Misteli, 2007], and 2 major models have been used to describe the radial position of chromosome territories: the gene-density model and the size model.

Croft et al. [1999], using paints for human chromosomes 18 and 19 in lymphoblasts and dermal fibroblasts, described observations best-fitting a gene density model (gene-rich chromosomes nearer the nuclear centre, gene-poor ones at the periphery). These observations were supported by Lukasova et al. [2002] for chromosomes 9, 17, 8, and 13 and by Cremer et al. [2003] using 3D studies. In a more recent study to support this model, Federico et al. [2008] studied chromosome 7 in lymphocytes which contains large blocks of both gene-dense and gene-poor regions. More gene-rich regions were located towards the interior, whereas the gene-poorest regions were aligned towards the periphery. This model has also been observed in primates where orthologous sequences to human chromosomes were used and occupied similar nuclear positions to humans [Tanabe et al., 2002, 2005]. The functional implications are that gene-rich chromosomes may be more associated with the transcriptional machinery. Moreover, the separation of the nucleus to transcriptionally active (gene-rich chromosome areas) and transcriptionally silent (gene-poor) regions may be important to enhance expression or repression [Foster and Bridger,

2005; Meaburn and Misteli, 2007]. Evidence for this model is supported from the movement of specific genes from the periphery to the interior upon their activation (e.g., β-globin during differentiation of mouse erythroid cells) [Takizawa et al., 2008]. Despite some evidence with regard to spatial position and gene activity, functional relevance still remains elusive as positional changes of any given locus are affected by more than one mechanism. Furthermore, different genes adopt different behaviors, thus prohibiting the application of universal rules [Takizawa et al., 2008]. A recent commentary by Misteli [2009] supports the use of more global approaches (rather than single-gene interrogations) to further understand the mechanisms of genome organization. In addition, it suggests that combined cytological and computational approaches point to the conclusion that genomes are self-organizing entities.

The alternative to the gene density model simply classifies chromosome territories according to their size, with the small chromosomes being close to the nuclear interior and large ones towards the nuclear periphery [Bolzer et al., 2005]. This model has been observed in fibroblasts with elliptoid nuclei, and recently Skinner et al. [2009] distinguished a size-based from a gene-density-based model in embryonic fibroblasts of chicken – a species previously reported as fitting both models [Foster and Bridger, 2005].

Foster and Bridger [2005] propose that these 2 models are not mutually exclusive but dependent on the status of the cell and/or chromosome. In a recent review, Cremer and Cremer [2010] argue that local gene density is a pivotal factor for the radial position of chromatin but also point that other parameters could be involved (e.g., replication timing). As will be discussed in a subsequent section, however, the nuclear organization of mammalian sperm is somewhat different to either of these models.

The space between the CTs is termed the interchromatin compartment [Cremer et al., 2006]. Active genes are thought to be located in the periphery of CTs near the interchromatin compartment in order to be accessible to transcription and splicing factors [Foster and Bridger, 2005; Branco and Pombo, 2007; Heard and Bickmore, 2007]. However, evidence suggests that genes can be transcribed both inside and outside the CTs necessitating the description of 'sponge-like' CTs permeated by intraterritorial interchromatin compartment channels [Cremer and Cremer, 2010].

Possibly separating the CTs and interchromatin compartment is the proposed 'perichromatic region' – a thin layer of decondensed chromatin thought to represent the subcompartment where transcription, co-transcriptional RNA splicing, and possibly DNA repair occurs [Cremer and Cremer, 2010]. If this is the case, one important assumption of this model is that small scale loops of 50–200 kb built up in the CTs whose configuration changes depending on the transcriptional status of its genes [Cremer et al., 2006]. An alternative model, however, is the lattice model that suggests that there is intermingling of 10–30-nm chromatin fibers between adjacent CTs [Branco and Pombo, 2007; Heard and Bickmore, 2007].

Nuclear Organization and Disease

Boyle et al. [2001] were, to the best of our knowledge, the first to investigate human chromosome repositioning associated with disease. They studied lymphoblasts from normal and X-linked Emery-Dreifuss muscular dystrophy (X-EDMD) males, where emerin protein is lacking, without observing significant changes in nuclear locations of specific CTs. Cremer et al. [2003] reported different patterns of CT position for chromosomes 18 and 19 in normal and in tumor cell lines. In a more recent study, Marella et al. [2009a] argued for a difference in CT association for chromosomes 4 and 16 in breast cancer lines compared to normal cells. In addition, several studies have highlighted that certain translocations could be generated due to close proximity of the chromosomes involved. Petrova et al. [2007] analysed the position of chromosome X and 1 in human cells having 1 copy and 4 copies of the X chromosome, respectively. In the polysomic cells (XXXY) the active X appears to be closer to the nuclear periphery than in normal XY cells. Also in XXXY cells the position of chromosome 1 appears to be more towards the nuclear periphery compared to normal XY cells. Another change in CT position was noticed for chromosome 17 upon infection of lymphocytes with Epstein-Barr virus (EBV) implying genome instability in host cells [Li et al., 2010]. Other diseases where a possible perturbed nuclear architecture may be involved are promyelocytic leukaemia (PML), X-linked mental retardation, and Huntington's disease [Misteli, 2005].

The most well-described involvement of a perturbed nuclear organization and disease is found in laminopathies [Foster and Bridger, 2005; Misteli, 2005]. Patients have a mutation in the *LMNA* gene, and phenotypes are associated with muscular dystrophy, lipodystrophies, neuropathies, and the premature aging disease Hutchinson-Gilford progeria [Bridger and Kill, 2004; Misteli, 2005]. Recently, it was shown that in patients with mutations in the *LMNA* gene positions of the territories of chromosomes 13 and 18 are more interior than in con-

trols [Elcock and Bridger, 2010]. Possible explanations for the causative mechanisms of the disease suggest that mutations in *LMNA* weaken nuclear integrity by exposing the nucleus (more specifically the nuclear matrix) to mechanical stress or that mutations cause misregulation of genes [Foster and Bridger, 2005; Misteli, 2005].

If a perturbed nuclear architecture is indeed manifested as altered CT (and thus gene) position, this could change the local gene environment and the availability of transcription factories thus leading to misregulation or even non-participation of some genes in transcription [Elcock and Bridger, 2010]. To the best of our knowledge, however, the association between nuclear organization and male infertility remains underexplored.

Nuclear Organization and Cell Differentiation

Changes in CT or individual locus position have been observed during differentiation in several systems. The immunoglobulin gene cluster repositions from the nuclear periphery (in non-lymphoid cells) to the nuclear center in pre-B cells, and a similar observation has been described for the *Mash1* locus during neural induction [Schneider and Grosschedl, 2007]. Furthermore, genes such as *HoxB1* in mouse embryos undergo a shift towards internal location upon activation [Takizawa et al., 2008]. The notion seems to be that loci in positions relative to the nuclear periphery or heterochromatin domains are linked with gene repression, whereas repositioning of loci from the nuclear periphery to the interior or away from heterochromatin is correlated with gene activation [Takizawa et al., 2008; Szczerbal et al., 2009]. This model may, however, well be an oversimplification and not universally applicable. Biallelically expressed genes occupy different radial position in the same nucleus, RNA polymerase II transcription sites are distributed throughout the nucleus (thus transcription is not only occurring internally), and moreover heterochromatin, which is largely transcriptionally silent, can be found throughout the nucleus [Takizawa et al., 2008]. Based on experiments with the β-globin gene, which during its inactive form is in the periphery and remains there until the early stages of activation and only then repositions to the interior, it seems that internal position is not a requirement for activity, and transcription alone does not drive the position of a gene [Francastel et al., 2000]. Chromosomal neighborhood seems to be another factor determining whether a locus changes its position. Certain loci show preferred contacts with their neighbors in a phenomenon termed 'chromosome kissing' implicated in both transcriptional activation and gene silencing [Cavalli, 2007].

Studies of differentiation are not limited to individual loci but have involved CTs, too. Kuroda et al. [2004] studied the relative positions of chromosomes 12 and 16 during adipocyte differentiation and found a close association of these 2 chromosomes. This proximity could influence their involvement in translocations such as t(12;16). Parada et al. [2004] studied the nuclear position of 6 chromosomes in 3 different tissues and found considerable differences indicating a tissue-specific genome organization. Szczerbal et al. [2009] found a correlation of gene expression and internal positioning for 6 porcine loci during adipogenesis, and Marella et al. [2009b] investigated the radial arrangement of the territories of chromosomes 18 and 19 during human epidermal keratinocyte differentiation. The latter found repositioning of chromosome 19 closer to the periphery (compared to chromosome 18) in the differentiated cells, plus a decrease in the interchromosomal association of these 2 chromosomes. Recently, a striking example of CT organization was shown by Solovei et al. [2009]. They demonstrated that the nuclear architecture of rod photoreceptor cells differs fundamentally in nocturnal compared to diurnal mammals. That is, the rods of retinas from diurnal mammals adopt a gene density model. Paradoxically, the rods of retinas from nocturnal mammal display a pattern that is inverted, i.e., the heterochromatin localizes towards the nuclear center, whereas the euchromatin lines the nuclear periphery. It is suggested that this adaptation occurs so that the nuclei can help the cell channel light efficiently toward the light-sensing rod outer segments. This example provides evidence that, under selective pressure, nuclear architecture can be modified to accommodate specific functionality [Cremer and Cremer, 2010].

Another striking example of chromosome repositioning in differentiation was provided by Foster et al. [2005] in porcine spermatogenesis. It was found that the sex chromosomes repositioned from the nuclear periphery to the interior during cell differentiation from spermatocytes to round spermatids. It was argued that this nonrandom position could have a functional significance in the future expression of the paternal genome during embryo development.

Nuclear Organization in Sperm Cells

Spermatogenesis can be divided into 3 main phases: the mitotic proliferation of spermatogonia to produce spermatocytes, the meiotic divisions to produce round spermatids, and spermiogenesis where the early spermatids are maturing to elongated spermatids. It is during the last stage, spermiogenesis, when reorganization and com-

paction of the sperm chromatin occurs. Histones are first replaced by transition proteins [Meistrich et al., 2003] and then by protamines [Balhorn, 1982] in a way that 15% of chromatin remains bound to histones whereas 85% is bound by protamines [Wykes and Krawetz, 2003]. Chromatin still associated with histones in sperm enriches important loci essential for embryo development (e.g., genes for key embryonic transcription factors) [Carrell and Hammoud, 2010].

The major component of protamines is arginine which is responsible for the abundance of positively charged $-NH_3^+$ groups [Bjorndahl and Kvist, 2010]. The functional implication of this is that $-NH_3^+$ groups neutralize the negative charges of the phosphate groups in the DNA backbone allowing a higher degree of compaction [Bjorndahl and Kvist, 2010]. This highly compacted DNA (10^{-6}-fold compared to 10^{-5}-fold offered by histones) provides an efficient packaging to facilitate proper delivery of the paternal genome to the egg [reviewed in Miller et al., 2010]. The cysteine residues of protamines confer extra stability in the sperm chromatin through intermolecular disulphide cross-links [Ward, 2010]. Ward also argues that sperm chromatin rearrangement by protamines functions to ensure proper fertilization (as a protective agent of the paternal genome) and not for embryonic development. It is also suggested that protamines serve as the silent agents of gene expression during spermiogenesis [Ward, 2010].

The nuclear organization in human sperm has been extensively studied and well defined [Haaf and Ward, 1995; Zalensky et al., 1995; Hazzouri et al., 2000; Tilgen et al., 2001; Mudrak et al., 2005]. The position of the chromosomes is non-random with the centromeres clustering in the nuclear center to form the 'chromocenter' and the telomeres exposed towards the periphery where they interact to form dimers [Zalensky et al., 1993, 1995; Luetjens et al., 1999; Solov'eva et al., 2004; Zalenskaya and Zalensky, 2004]. Similar spatial organization seems to be retained in other mammals as it is indicated by data from cattle [Zalenskaya and Zalensky, 2004], mouse [Haaf and Ward, 1995; Meyer-Ficca et al., 1998], pig, horse, and rat [Zalenskaya and Zalensky, 2004]. A recent study by Tsend-Ayush et al. [2009] argues for non-random positioning of 12 chromosomes in the sperm of chicken which is in contrast to some earlier observations made by Greaves et al. [2003] who suggested that the organization was random.

A chromocenter in human sperm was first visualized by CENP-A immunolocalization and FISH using an alpha-satellite probe for all chromosomes [Zalensky et al., 1993]. It seems that the chromocenter contains pericentric heterochromatin from different chromosomes and has the tendency to aggregate [Zalensky et al., 1995]. The fact that CENP-A is found in mature spermatozoa [Sullivan, 2001] indicates that centromeric DNA exists in both nucleosomal and protamine organization, and this suggests that these chromosomal regions may not need to undergo dramatic remodeling following fertilization [Zalensky and Zalenskaya, 2007].

With regard to the telomeres, dimers are formed between the p and q telomeres of each chromosome, conferring a hairpin loop structure [Solov'eva et al., 2004; Mudrak et al., 2005]. Zalensky and Zalenskaya [2007] argue that such a configuration could favor an ordered withdrawal of chromosomes via telomeres through their association with the sperm microtubule machinery. The importance of telomeres in fertilization has been shown in mice where telomerase knockout disrupts reproductive function [Lee et al., 1998].

In addition to the studies of the radial nuclear organization of chromosome territories, the polar nature of a sperm cell allows the position of chromosomes to be studied longitudinally. A combination of data from several studies [Luetjens et al., 1999; Hazzouri et al., 2000; Zalenskaya and Zalensky, 2004; Mudrak et al., 2005] arranges 11 chromosome territories in the following order head-tail: X, 7, [6, 15, 16, 17], 1, [Y, 18], 2, 5, where chromosome 13 seems to occupy a random position. The functional implication of this could be related to the order that chromosomes are being affected by the maternal cytoplasmic environment after fertilization [Zalensky and Zalenskaya, 2007]. This might also apply to the peripheral chromosomes being the first to be exposed to ooplasm that undergoes earlier remodeling [Zalensky and Zalenskaya, 2007]. It should also be emphasized that the positions of the sex chromosomes relative to the acrosome are similar in sperm of all mammals (but not birds), implicating a functional significance with regard to paternal X inactivation [Greaves et al., 2003]. The aforementioned studies were performed on flattened nuclei with the known disadvantage of having to compromise for the 3D nucleus shape to a 2D flattened object. Recent emerging evidence from Manvelyan et al. [2008], who studied 3D nuclear architecture in 30 sperm cells, argues for a possible correlation of chromosome position with size and gene density.

Nuclear Organization and Assisted Reproduction – Some Conclusions and Thoughts

If we accept that the non-random positioning of chromosomes in human sperm has functional significance and a possible impact on fertilization, then it follows that

men with altered nuclear organization in their sperm heads might have fertility problems. In other words, altered nuclear organization might be a measurable phenotype in the sperm of infertile men, perhaps explaining idiopathic (i.e., unexplained) infertility in some cases [Mudrak and Zalensky, 2006]. Relatively early evidence implicated the possible importance of nuclear organization in assisted reproduction and its possible association with aneuploidy [Luetjens et al., 1999]. The authors suggested that sperm used in ICSI that have not gone through the acrosomal reaction could impair chromatin decondensation located in the apical region and thus hinder progression to the first mitotic division of the zygote, hence causing non-disjunction errors (translated as aneuploidy) in ICSI offspring.

If we compare the above evidence with the well-established reports of perturbations in nuclear health associated with male infertility (i.e., increased levels of sperm disomy and compromised DNA repair as mentioned above), the indirect evidence to support the hypothesis of altered nuclear organization as a correlate of male infertility becomes more convincing. Indeed, it seems likely that altered nuclear organization would correlate with increased sperm disomy and/or altered DNA repair. Indeed, Zalensky and Zalenskaya [2007] argue for a different category of sperm chromosome abnormality related to atypical packing of CTs in sperm, aberrant positioning of chromosomes, or even disturbed telomere-centromere interactions. Furthermore, it has long been postulated that sperm with a chemically interrupted nuclear matrix (which mediates the attachment sites of compacted sperm chromatin) cannot produce viable offspring [Ward et al., 1999]. Direct evidence is, however, somewhat lacking and only a handful of studies have tried to establish this possible link.

Sbracia et al. [2002] investigated the longitudinal position of the sex chromosomes between normal and oligospermic males going through ICSI without finding a difference. Wiland et al. [2008] found inter-individual differences in centromere topology between normal males and reciprocal translocation carriers, and Olszewska et al. [2008] compared longitudinal positions for chromosomes 15, 18, X, and Y between control males and infertile patients without finding a difference in nuclear position. All these studies examined position in the longitudinal axis and argued that a larger number of individuals and more chromosomes were required. Thus far, the only study of which we are aware that examined the radial position for 3 chromosomes (centromeres of X and 18 and the long arm of the Y) is that of our own laboratory [Finch et al., 2008a]. It was suggested that all centromeres occupied central positions in normal males, but the sex chromosomes showed altered positions (a more random distribution) in some of the infertile patients. We are in the process of examining a larger number of chromosomes in a larger number of males [Ioannou and Griffin, unpublished results] and have extended these studies to human embryos in a further attempt to establish a link between non-disjunction and nuclear organization [Finch et al., 2008b]. The possible association between altered nuclear organization and male infertility remains an exciting area for further research with possible implications for improved screening, diagnosis, and therapy. Time will tell.

References

Aitken RJ, De Iuliis GN: Origins and consequences of DNA damage in male germ cells. Reprod Biomed Online 14:727–733 (2007).

Aitken RJ, De Iuliis GN: On the possible origins of DNA damage in human spermatozoa. Mol Hum Reprod 16:3–13 (2010).

Balhorn R: A model for the structure of chromatin in mammalian sperm. J Cell Biol 93:298–305 (1982).

Barratt CL, Aitken RJ, Bjorndahl L, Carrell DT, de Boer P, et al: Sperm DNA: organization, protection and vulnerability: from basic science to clinical applications – a position report. Hum Reprod 25:824–838 (2010).

Bernardini L, Martini E, Geraedts JP, Hopman AH, Lanteri S, et al: Comparison of gonosomal aneuploidy in spermatozoa of normal fertile men and those with severe male factor detected by in-situ hybridization. Mol Hum Reprod 3:431–438 (1997).

Bjorndahl L, Kvist U: Human sperm chromatin stabilization – a proposed model including zinc bridges. Mol Hum Reprod 16:23–29 (2010).

Bolzer A, Kreth G, Solovei I, Koehler D, Saracoglu K, et al: Three-dimensional maps of all chromosomes in human male fibroblast nuclei and prometaphase rosettes. PLoS Biol 3:e157 (2005).

Boyle S, Gilchrist S, Bridger JM, Mahy NL, Ellis JA, Bickmore WA: The spatial organization of human chromosomes within the nuclei of normal and emerin-mutant cells. Hum Mol Genet 10:211–219 (2001).

Branco MR, Pombo A: Chromosome organization: new facts, new models. Trends Cell Biol 17:127–134 (2007).

Bridger JM, Kill IR: Aging of Hutchinson-Gilford progeria syndrome fibroblasts is characterised by hyperproliferation and increased apoptosis. Exp Gerontol 39:717–724 (2004).

Carrell DT, Hammoud SS: The human sperm epigenome and its potential role in embryonic development. Mol Hum Reprod 16:37–47 (2010).

Cavalli G: Chromosome kissing. Curr Opin Genet Dev 17:443–450 (2007).
Cremer M, von Hase J, Volm T, Brero A, Kreth G, et al: Non-random radial higher-order chromatin arrangements in nuclei of diploid human cells. Chromosome Res 9:541–567 (2001).
Cremer M, Kupper K, Wagler B, Wizelman L, von Hase J, et al: Inheritance of gene density-related higher order chromatin arrangements in normal and tumor cell nuclei. J Cell Biol 162:809–820 (2003).
Cremer T, Cremer C: Chromosome territories, nuclear architecture and gene regulation in mammalian cells. Nat Rev Genet 2:292–301 (2001).
Cremer T, Cremer C: Rise, fall and resurrection of chromosome territories: a historical perspective. Part I. The rise of chromosome territories. Eur J Histochem 50:161–176 (2006).
Cremer T, Cremer M: Chromosome territories. Cold Spring Harb Perspect Biol 2:a003889 (2010).
Cremer T, Cremer M, Dietzel S, Muller S, Solovei I, Fakan S: Chromosome territories – a functional nuclear landscape. Curr Opin Cell Biol 18:307–316 (2006).
Croft JA, Bridger JM, Boyle S, Perry P, Teague P, Bickmore WA: Differences in the localization and morphology of chromosomes in the human nucleus. J Cell Biol 145:1119–1131 (1999).
Delbes G, Hales BF, Robaire B: Toxicants and human sperm chromatin integrity. Mol Hum Reprod 16:14–22 (2010).
Durakbasi-Dursun HG, Zamani AG, Kutlu R, Gorkemli H, Bahce M, Acar A: A new approach to chromosomal abnormalities in sperm from patients with oligoasthenoteratozoospermia: detection of double aneuploidy in addition to single aneuploidy and diploidy by five-color fluorescence in situ hybridization using one probe set. Fertil Steril 89:1709–1717 (2008).
Egozcue S, Blanco J, Vendrell JM, Garcia F, Veiga A, et al: Human male infertility: chromosome anomalies, meiotic disorders, abnormal spermatozoa and recurrent abortion. Hum Reprod Update 6:93–105 (2000).
Elcock LS, Bridger JM: Exploring the relationship between interphase gene positioning, transcriptional regulation and the nuclear matrix. Biochem Soc Trans 38:263–267 (2010).
Federico C, Cantarella CD, Di Mare P, Tosi S, Saccone S: The radial arrangement of the human chromosome 7 in the lymphocyte cell nucleus is associated with chromosomal band gene density. Chromosoma 117:399–410 (2008).
Ferlin A, Raicu F, Gatta V, Zuccarello D, Palka G, Foresta C: Male infertility: role of genetic background. Reprod Biomed Online 14:734–745 (2007).
Finch KA, Fonseka KG, Abogrein A, Ioannou D, Handyside AH, et al: Nuclear organization in human sperm: preliminary evidence for altered sex chromosome centromere position in infertile males. Hum Reprod 23: 1263–1270 (2008a).
Finch KA, Fonseka G, Ioannou D, Hickson N, Barclay Z, et al: Nuclear organisation in totipotent human nuclei and its relationship to chromosomal abnormality. J Cell Sci 121: 655–663 (2008b).
Foster HA, Bridger JM: The genome and the nucleus: a marriage made by evolution. Genome organisation and nuclear architecture. Chromosoma 114:212–229 (2005).
Foster HA, Abeydeera LR, Griffin DK, Bridger JM: Non-random chromosome positioning in mammalian sperm nuclei, with migration of the sex chromosomes during late spermatogenesis. J Cell Sci 118:1811–1820 (2005).
Francastel C, Schubeler D, Martin DI, Groudine M: Nuclear compartmentalization and gene activity. Nat Rev Mol Cell Biol 1:137–143 (2000).
Gole LA, Wong PF, Ng PL, Wang XQ, Ng SC, Bongso A: Does sperm morphology play a significant role in increased sex chromosomal disomy? A comparison between patients with teratozoospermia and OAT by FISH. J Androl 22:759–763 (2001).
Greaves IK, Rens W, Ferguson-Smith MA, Griffin D, Marshall Graves JA: Conservation of chromosome arrangement and position of the X in mammalian sperm suggests functional significance. Chromosome Res 11: 503–512 (2003).
Griffin DK, Finch KA: The genetic and cytogenetic basis of male infertility. Hum Fertil (Camb) 8:19–26 (2005).
Haaf T, Ward DC: Higher order nuclear structure in mammalian sperm revealed by in situ hybridization and extended chromatin fibers. Exp Cell Res 219:604–611 (1995).
Hassold TJ, Sherman SL, Pettay D, Page DC, Jacobs PA: XY chromosome nondisjunction in man is associated with diminished recombination in the pseudoautosomal region. Am J Hum Genet 49:253–260 (1991).
Hassold T, Abruzzo M, Adkins K, Griffin D, Merrill M, et al: Human aneuploidy: incidence, origin, and etiology. Environ Mol Mutagen 28:167–175 (1996).
Hazzouri M, Rousseaux S, Mongelard F, Usson Y, Pelletier R, et al: Genome organization in the human sperm nucleus studied by FISH and confocal microscopy. Mol Reprod Dev 55:307–315 (2000).
Heard E, Bickmore W: The ins and outs of gene regulation and chromosome territory organisation. Curr Opin Cell Biol 19:311–316 (2007).
Khalil A, Grant JL, Caddle LB, Atzema E, Mills KD, Arneodo A: Chromosome territories have a highly nonspherical morphology and nonrandom positioning. Chromosome Res 15:899–916 (2007).
Kuroda M, Tanabe H, Yoshida K, Oikawa K, Saito A, et al: Alteration of chromosome positioning during adipocyte differentiation. J Cell Sci 117:5897–5903 (2004).
Lee HW, Blasco MA, Gottlieb GJ, Horner JW 2nd, Greider CW, DePinho RA: Essential role of mouse telomerase in highly proliferative organs. Nature 392:569–574 (1998).
Li C, Shi Z, Zhang L, Huang Y, Liu A, et al: Dynamic changes of territories 17 and 18 during EBV-infection of human lymphocytes. Mol Biol Rep 37:2347–2354 (2010).
Li Z, Haines CJ, Han Y: 'Micro-deletions' of the human Y chromosome and their relationship with male infertility. J Genet Genomics 35:193–199 (2008).
Liu CH, Tsao HM, Cheng TC, Wu HM, Huang CC, et al: DNA fragmentation, mitochondrial dysfunction and chromosomal aneuploidy in the spermatozoa of oligoasthenoteratozoospermic males. J Assist Reprod Genet 21: 119–126 (2004).
Lorda-Sanchez I, Binkert F, Maechler M, Robinson WP, Schinzel AA: Reduced recombination and paternal age effect in Klinefelter syndrome. Hum Genet 89:524–530 (1992).
Luetjens CM, Payne C, Schatten G: Non-random chromosome positioning in human sperm and sex chromosome anomalies following intracytoplasmic sperm injection. Lancet 353:1240 (1999).
Lukasova E, Kozubek S, Kozubek M, Falk M, Amrichova J: The 3D structure of human chromosomes in cell nuclei. Chromosome Res 10:535–548 (2002).
Manuelidis L: A view of interphase chromosomes. Science 250:1533–1540 (1990).
Manvelyan M, Hunstig F, Bhatt S, Mrasek K, Pellestor F, et al: Chromosome distribution in human sperm – a 3D multicolor banding-study. Mol Cytogenet 1:25 (2008).
Marella NV, Bhattacharya S, Mukherjee L, Xu J, Berezney R: Cell type specific chromosome territory organization in the interphase nucleus of normal and cancer cells. J Cell Physiol 221:130–138 (2009a).
Marella NV, Seifert B, Nagarajan P, Sinha S, Berezney R: Chromosomal rearrangements during human epidermal keratinocyte differentiation. J Cell Physiol 221:139–146 (2009b).
Marshall WF: Order and disorder in the nucleus. Curr Biol 12:R185–R192 (2002).
Martin RH: Mechanisms of nondisjunction in human spermatogenesis. Cytogenet Genome Res 111:245–249 (2005).
Martin RH: Meiotic chromosome abnormalities in human spermatogenesis. Reprod Toxicol 22:142–147 (2006).
Martin RH: Meiotic errors in human oogenesis and spermatogenesis. Reprod Biomed Online 16:523–531 (2008).
Martin RH, Ko E, Rademaker A: Distribution of aneuploidy in human gametes: comparison between human sperm and oocytes. Am J Med Genet 39:321–331 (1991).

Meaburn KJ, Misteli T: Cell biology: chromosome territories. Nature 445:379–781 (2007).
Meistrich ML, Mohapatra B, Shirley CR, Zhao M: Roles of transition nuclear proteins in spermiogenesis. Chromosoma 111:483–488 (2003).
Meyer-Ficca M, Muller-Navia J, Scherthan H: Clustering of pericentromeres initiates in step 9 of spermiogenesis of the rat *(Rattus norvegicus)* and contributes to a well defined genome architecture in the sperm nucleus. J Cell Sci 111:1363–1370 (1998).
Miller D, Brinkworth M, Iles D: Paternal DNA packaging in spermatozoa: more than the sum of its parts? DNA, histones, protamines and epigenetics. Reproduction 139:287–301 (2010).
Misteli T: Concepts in nuclear architecture. Bioessays 27:477–487 (2005).
Misteli T: Self-organization in the genome. Proc Natl Acad Sci USA 106:6885–6886 (2009).
Moosani N, Pattinson HA, Carter MD, Cox DM, Rademaker AW, Martin RH: Chromosomal analysis of sperm from men with idiopathic infertility using sperm karyotyping and fluorescence in situ hybridization. Fertil Steril 64:811–817 (1995).
Mudrak O, Zalensky A: Genome architecture in human sperm cells: possible implication for male infertility and prediction of pregnancy outcome, in Kruger F, Kruger TF, Oehninger S: Male Infertility: Diagnosis and Treatment, pp 73–85 (Informa, London 2006).
Mudrak O, Tomilin N, Zalensky A: Chromosome architecture in the decondensing human sperm nucleus. J Cell Sci 118:4541–4550 (2005).
O'Flynn O'Brien KL, Varghese AC, Agarwal A: The genetic causes of male factor infertility: a review. Fertil Steril 93:1–12 (2010).
Oliver B, Misteli T: A non-random walk through the genome. Genome Biol 6:214 (2005).
Olszewska M, Wiland E, Kurpisz M: Positioning of chromosome 15, 18, X and Y centromeres in sperm cells of fertile individuals and infertile patients with increased level of aneuploidy. Chromosome Res 16:875–890 (2008).
Pang MG, Hoegerman SF, Cuticchia AJ, Moon SY, Doncel GF, et al: Detection of aneuploidy for chromosomes 4, 6, 7, 8, 9, 10, 11, 12, 13, 17, 18, 21, X and Y by fluorescence in-situ hybridization in spermatozoa from nine patients with oligoasthenoteratozoospermia undergoing intracytoplasmic sperm injection. Hum Reprod 14:1266–1273 (1999).
Parada L, Misteli T: Chromosome positioning in the interphase nucleus. Trends Cell Biol 12: 425–432 (2002).
Parada LA, McQueen PG, Misteli T: Tissue-specific spatial organization of genomes. Genome Biol 5:R44 (2004).
Petit FM, Frydman N, Benkhalifa M, Le Du A, Aboura A, et al: Could sperm aneuploidy rate determination be used as a predictive test before intracytoplasmic sperm injection? J Androl 26:235–241 (2005).
Petrova NV, Yakutenko II, Alexeevski AV, Verbovoy VA, Razin SV, Iarovaia OV: Changes in chromosome positioning may contribute to the development of diseases related to X-chromosome aneuploidy. J Cell Physiol 213: 278–283 (2007).
Pfeffer J, Pang MG, Hoegerman SF, Osgood CJ, Stacey MW, et al: Aneuploidy frequencies in semen fractions from ten oligoasthenoteratozoospermic patients donating sperm for intracytoplasmic sperm injection. Fertil Steril 72:472–478 (1999).
Plastira K, Msaouel P, Angelopoulou R, Zanioti K, Plastiras A, et al: The effects of age on DNA fragmentation, chromatin packaging and conventional semen parameters in spermatozoa of oligoasthenoteratozoospermic patients. J Assist Reprod Genet 24:437–443 (2007).
Ravel C, Chantot-Bastaraud S, El Houate B, Rouba H, Legendre M, et al: Y-chromosome AZFc structural architecture and relationship to male fertility. Fertil Steril 92:1924–1933 (2009).
Sanchez-Castro M, Jimenez-Macedo AR, Sandalinas M, Blanco J: Prognostic value of sperm fluorescence in situ hybridization analysis over PGD. Hum Reprod 24:1516–1521 (2009).
Sbracia M, Baldi M, Cao D, Sandrelli A, Chiandetti A, et al: Preferential location of sex chromosomes, their aneuploidy in human sperm, and their role in determining sex chromosome aneuploidy in embryos after ICSI. Hum Reprod 17:320–324 (2002).
Schneider R, Grosschedl R: Dynamics and interplay of nuclear architecture, genome organization, and gene expression. Genes Dev 21: 3027–3043 (2007).
Seli E, Sakkas D: Spermatozoal nuclear determinants of reproductive outcome: implications for ART. Hum Reprod Update 11:337–349 (2005).
Shah K, Sivapalan G, Gibbons N, Tempest H, Griffin DK: The genetic basis of infertility. Reproduction 126:13–25 (2003).
Shi Q, Spriggs E, Field LL, Ko E, Barclay L, Martin RH: Single sperm typing demonstrates that reduced recombination is associated with the production of aneuploid 24,XY human sperm. Am J Med Genet 99:34–38 (2001).
Skinner BM, Robertson LB, Tempest HG, Langley EJ, Ioannou D, et al: Comparative genomics in chicken and Pekin duck using FISH mapping and microarray analysis. BMC Genomics 10:357 (2009).
Solov'eva L, Svetlova M, Bodinski D, Zalensky AO: Nature of telomere dimers and chromosome looping in human spermatozoa. Chromosome Res 12:817–823 (2004).
Solovei I, Kreysing M, Lanctot C, Kosem S, Peichl L, et al: Nuclear architecture of rod photoreceptor cells adapts to vision in mammalian evolution. Cell 137:356–368 (2009).
Stack SM, Brown DB, Dewey WC: Visualization of interphase chromosomes. J Cell Sci 26: 281–299 (1977).
Storeng RT, Plachot M, Theophile D, Mandelbaum J, Belaisch-Allart J, Vekemans M: Incidence of sex chromosome abnormalities in spermatozoa from patients entering an IVF or ICSI protocol. Acta Obstet Gynecol Scand 77:191–197 (1998).
Sullivan KF: A solid foundation: functional specialization of centromeric chromatin. Curr Opin Genet Dev 11:182–188 (2001).
Sun F, Trpkov K, Rademaker A, Ko E, Martin RH: Variation in meiotic recombination frequencies among human males. Hum Genet 116:172–178 (2005).
Szczerbal I, Foster HA, Bridger JM: The spatial repositioning of adipogenesis genes is correlated with their expression status in a porcine mesenchymal stem cell adipogenesis model system. Chromosoma 118:647–663 (2009).
Takizawa T, Meaburn KJ, Misteli T: The meaning of gene positioning. Cell 135:9–13 (2008).
Tanabe H, Muller S, Neusser M, von Hase J, Calcagno E, et al: Evolutionary conservation of chromosome territory arrangements in cell nuclei from higher primates. Proc Natl Acad Sci USA 99:4424–4429 (2002).
Tanabe H, Kupper K, Ishida T, Neusser M, Mizusawa H: Inter- and intra-specific gene-density-correlated radial chromosome territory arrangements are conserved in Old World monkeys. Cytogenet Genome Res 108:255–261 (2005).
Tarozzi N, Bizzaro D, Flamigni C, Borini A: Clinical relevance of sperm DNA damage in assisted reproduction. Reprod Biomed Online 14:746–757 (2007).
Tempest HG, Griffin DK: The relationship between male infertility and increased levels of sperm disomy. Cytogenet Genome Res 107: 83–94 (2004).
Tempest HG, Homa ST, Dalakiouridou M, Christopikou D, Wright D, et al: The association between male infertility and sperm disomy: evidence for variation in disomy levels among individuals and a correlation between particular semen parameters and disomy of specific chromosome pairs. Reprod Biol Endocrinol 2:82 (2004).
Tempest HG, Homa ST, Routledge EJ, Garner A, Zhai XP, Griffin DK: Plants used in Chinese medicine for the treatment of male infertility possess antioxidant and anti-oestrogenic activity. Syst Biol Reprod Med 54:185–195 (2008).
Tilgen N, Guttenbach M, Schmid M: Heterochromatin is not an adequate explanation for close proximity of interphase chromosomes 1-Y, 9-Y, and 16-Y in human spermatozoa. Exp Cell Res 265:283–287 (2001).
Tsend-Ayush E, Dodge N, Mohr J, Casey A, Himmelbauer H, et al: Higher-order genome organization in platypus and chicken sperm and repositioning of sex chromosomes during mammalian evolution. Chromosoma 118:53–69 (2009).

Ushijima C, Kumasako Y, Kihaile PE, Hirotsuru K, Utsunomiya T: Analysis of chromosomal abnormalities in human spermatozoa using multi-colour fluorescence in-situ hybridization. Hum Reprod 15:1107–1111 (2000).

Varghese AC, du Plessis SS, Agarwal A: Male gamete survival at stake: causes and solutions. Reprod Biomed Online 17:866–880 (2008).

Ward WS: Function of sperm chromatin structural elements in fertilization and development. Mol Hum Reprod 16:30–36 (2010).

Ward WS, Kimura Y, Yanagimachi R: An intact sperm nuclear matrix may be necessary for the mouse paternal genome to participate in embryonic development. Biol Reprod 60: 702–706 (1999).

Wiland E, Zegalo M, Kurpisz M: Interindividual differences and alterations in the topology of chromosomes in human sperm nuclei of fertile donors and carriers of reciprocal translocations. Chromosome Res 16:291–305 (2008).

Wykes SM, Krawetz SA: The structural organization of sperm chromatin. J Biol Chem 278: 29471–29477 (2003).

Zalenskaya IA, Zalensky AO: Non-random positioning of chromosomes in human sperm nuclei. Chromosome Res 12:163–173 (2004).

Zalensky A, Zalenskaya I: Organization of chromosomes in spermatozoa: an additional layer of epigenetic information? Biochem Soc Trans 35:609–611 (2007).

Zalensky AO, Breneman JW, Zalenskaya IA, Brinkley BR, Bradbury EM: Organization of centromeres in the decondensed nuclei of mature human sperm. Chromosoma 102: 509–518 (1993).

Zalensky AO, Allen MJ, Kobayashi A, Zalenskaya IA, Balhorn R, Bradbury EM: Well-defined genome architecture in the human sperm nucleus. Chromosoma 103:577–590 (1995).

Zhang QF, Lu GX: Investigation of the frequency of chromosomal aneuploidy using triple fluorescence in situ hybridization in 12 Chinese infertile men. Chin Med J (Engl) 117:503–506 (2004).

Zini A, Libman J: Sperm DNA damage: clinical significance in the era of assisted reproduction. CMAJ 175:495–500 (2006).